

THE UNIVERSITY OF CHICAGO

FEEDING MECHANICS OF *TIKTAALIK ROSEAE*:
CONVERGENT MORPHOLOGY AND RECONSTRUCTED CRANIAL KINEMATICS OF A
TETRAPODOMORPH FISH AND MODERN ALLIGATOR GARS

A DISSERTATION SUBMITTED TO
THE FACULTY OF THE DIVISION OF THE BIOLOGICAL SCIENCES
AND THE PRITZKER SCHOOL OF MEDICINE
IN CANDIDACY FOR THE DEGREE OF
DOCTOR OF PHILOSOPHY
GRADUATE PROGRAM IN INTEGRATIVE BIOLOGY

BY
JUSTIN BRADLEY LEMBERG

CHICAGO, ILLINOIS

AUGUST 2018

In memory of those who are lost

TABLE OF CONTENTS

LIST OF FIGURES	vii
LIST OF TABLES	x
ACKNOWLEDGMENTS	xi
ABSTRACT	xiv
CHAPTER 1: INTRODUCTION TO TETRAPODOMORPH FEEDING DURING THE WATER-TO-LAND TRANSITION	1
CHAPTER 2: CRANIAL MORPHOLOGY OF <i>TIKTAALIK ROSEAE</i> REFLECTS SHIFTS IN FEEDING STRATEGIES PRIOR TO THE FIN-TO-LIMB TRANSITION.....	8
2.1 Abstract	8
2.2 Introduction.....	9
2.3 Materials and Methods	15
2.3.1 – Specimens of <i>Tiktaalik roseae</i>	15
2.3.2 – Computed tomography (CT) scanning of fossil specimens	16
2.3.3 – Reconstruction of digital anatomy	20
2.4 Results	22
2.4.1 – Chondrocranium and dermal skull roof	24
2.4.2 – Dermal cheek and lateral tooth row	36
2.4.3 – Endochondral and dermal palate	42
2.4.4 – Assessment of postmortem deformation	49
2.5 Discussion	58
2.5.1 – Functional implications of a platyrostral skull	58
2.5.2 – Functional implications of cranial consolidation	60
2.5.3 – Functional implications of cranial kinesis	63

2.6 Conclusion	67
CHAPTER 3: COMBINED USE OF JAW-RAM AND SUCTION GENERATION IN THE	
FEEDING MECHANISM OF ALLIGATOR GARS, <i>ATRACTOSTEUS SPATULA</i> . .	69
3.1 Abstract	69
3.2 Introduction	70
3.3 Materials and Methods	74
3.3.1 – Fish specimens and care	74
3.3.2 – High speed videography and digitizing	74
3.3.3 – <i>In situ</i> manipulation and preparation for imaging	79
3.3.4 – Contrast enhanced micro computed tomography (μ CT) and segmentation .	79
3.2.5 – Animation and kinematic model.	82
3.4 Results	84
3.4.1 – Kinematics of the feeding strike of <i>Atractosteus spatula</i>	85
3.4.2 – Osteology of specialized joints in the feeding system	92
3.4.3 – Myology and manipulation of the muscles of the feeding mechanism of <i>Atractosteus spatula</i>	101
3.5 Discussion	111
3.5.1 – Combined jaw-ram and suction in the feeding strike of <i>Atractosteus</i> <i>spatula</i>	111
3.5.2 – Specialized joints enabling expansive capabilities of the cranial linkage system	114
3.5.3 – Modulation of the feeding system with plesiomorphic hyoid musculature .	117
3.5.4 – Applications to paleontology and evolutionary biology.	121
3.6 Conclusions	123

CHAPTER 4: RECONSTRUCTED CRANIAL KINEMATICS OF <i>TIKTAALIK ROSEAE</i> , A PRECURSOR OF TERRESTRIAL-STYLE FEEDING MECHANICS	124
4.1 Abstract	124
4.2 Introduction	126
4.3 Materials and Methods	131
4.3.1 – Convergent features between lepisosteids and elpistostegids	132
4.3.2 – Phylogenetic bracketing of plesiomorphic feeding musculature	135
4.3.3 – Constraining models of <i>Tiktaalik</i> feeding kinematics	137
4.4 Results	140
4.4.1 – Assessment of a convergent cranial linkage system	140
4.4.2 – Estimation of cranial feeding musculature in <i>Tiktaalik roseae</i>	155
4.4.3 – Reconstructed feeding kinematics of <i>Tiktaalik roseae</i>	161
4.5 Discussion	168
4.5.1 – Maintenance of cranial expansion in a platyrostral system	168
4.5.2 – Jaw opening in <i>Tiktaalik</i> and insight into depressor mandibulae evolution.	172
4.5.3 – Evolution of terrestrial-style feeding kinematics	175
4.6 Conclusions	178
CHAPTER 5: CONCLUSIONS AND FUTURE DIRECTIONS	181
5.1 Feeding	181
5.2 Respiration and metabolism	183
5.3 Reproduction and locomotion	185
5.4 Skull mechanics of fossil fishes	186
REFERENCES	189

LIST OF FIGURES

2.1	Comparison of scanning parameters used for reconstructing internal cranial anatomy . .	19
2.2	External braincase and skull roof anatomy of <i>Tiktaalik</i> (NUFV 108)	23
2.3	Extent of internal ossification in the sphenethmoid region of <i>Tiktaalik</i> (NUFV 111)	24
2.4	Details of internal sutures and ossification of the anterior rostrum of <i>Tiktaalik</i> (NUFV 149)	33
2.5	Internal sutural anatomy of the frontal-nasal shield of <i>Tiktaalik</i> (NUFV 111)	34
2.6	Internal sutural anatomy of the skull roofing bones of <i>Tiktaalik</i> (NUFV 110) showing prevalence of interdigitating joints along the midline	35
2.7	Internal sutural anatomy of the dermal cheek and intracranial hinge of <i>Tiktaalik</i> (NUFV 108) highlighting differences between beveled sutures and scarf joints	40
2.8	Isolated dermal cheek bones of <i>Tiktaalik</i> (NUFV 108) showing extent of overlap between elements	41
2.9	Disarticulation of the cheek and palate from the braincase of <i>Tiktaalik</i> (NUFV 108) showing exposed areas of overlap with the skull roof	41
2.10	Disarticulation of the cheek and palate from the braincase of <i>Tiktaalik</i> (NUFV 108) showing exposed articulation points	47
2.11	Left palatoquadrate and associated dermal ossifications of <i>Tiktaalik</i> (NUFV 108)	48
2.12	Postmortem deformation of cranial elements of <i>Tiktaalik</i> (NUFV 108)	52
2.13	Postmortem deformation of cranial elements of <i>Tiktaalik</i> (NUFV 110)	54
2.14	Proposed retrodeformed proportions of the skull of <i>Tiktaalik</i>	55
2.15	Comparison of crushed, undeformed, and retrodeformed jaw-joint angles	56
2.16	Proposed retrodeformed proportions of the skull and pectoral girdle of <i>Tiktaalik</i>	57

3.1	Digitizing schema of anatomical landmarks for high-speed feeding videos	76
3.2	Averaged feeding kinematics of <i>Atractosteus spatula</i>	89
3.3	Representative feeding sequence of <i>Atractosteus spatula</i> showing suction and delayed hyoid depression	91
3.4	Points of articulation, axes of rotation, and primary muscular connections between elements of the braincase and suspensorium of <i>Atractosteus spatula</i>	97
3.5	Morphology of the hyoid constrictor sheath that assists in jaw opening	98
3.6	Morphology of jaw adductors and muscles of hyoid depression and suspensorial abduction	99
3.7	Morphology of the joint capsule containing the interhyal	100
3.8	Parasagittal cross section of the head-shoulder interface	101
3.9	Divisions of the sternohyoideus muscle	103
3.10	Adductor chamber of <i>Atractosteus spatula</i> showing multiple attachment areas for musculature	107
3.11	Small subdivision of the levator arcus palatini between the metapterygoid and hyosymplectic	109
3.12	Reconstructed gape cycle and feeding kinematics of <i>Atractosteus spatula</i>	110
4.1	Comparison of the rostral proportions of <i>Tiktaalik roseae</i> and <i>Atractosteus spatula</i>	131
4.2	Positions of analogous joints in <i>Atractosteus spatula</i> and <i>Tiktaalik roseae</i>	134
4.3	Comparison of the braincases of <i>Tiktaalik roseae</i> and <i>Atractosteus spatula</i>	149
4.4	Comparison of the suspensorial elements of <i>Tiktaalik roseae</i> and <i>Atractosteus spatula</i> .	151
4.5	Comparison of the jointed pectoral girdles of <i>Tiktaalik roseae</i> and <i>Atractosteus spatula</i>	152

4.6	Comparison of the vomer-dermopalatine articulations of <i>Tiktaalik roseae</i> and <i>Atractosteus spatula</i>	153
4.7	Comparison of the rostral scarf joints of <i>Tiktaalik roseae</i> and <i>Atractosteus spatula</i>	153
4.8	Comparison of the mandibular symphyses of <i>Tiktaalik roseae</i> and <i>Atractosteus spatula</i>	153
4.9	Evidence of soft tissue attachment to the posterior mandible of <i>Tiktaalik roseae</i>	154
4.10	Proposed configuration of feeding musculature for <i>Tiktaalik roseae</i>	160
4.11	Cranial linkage system of <i>Tiktaalik roseae</i>	165
4.12	Proposed mechanism of suspensorial abduction in <i>Tiktaalik roseae</i>	166
4.13	Reconstructed gape cycle and feeding kinematics of <i>Tiktaalik roseae</i>	167

LIST OF TABLES

2.1	Distribution of arguments for and against cranial kinesis in tetrapodomorph fishes	14
2.2	Scanning parameters used to document internal anatomy of the feeding apparatus of <i>Tiktaalik roseae</i>	17
2.3	Anatomical abbreviations for <i>Tiktaalik roseae</i> figures	21
3.1	Anatomical abbreviations for <i>Atractosteus spatula</i> figures.	82
3.2	Individual and aggregate means of <i>Atractosteus spatula</i> feeding kinematic.	88
4.1	Comparative osteichthyan feeding musculature and conditions inferred for <i>Tiktaalik</i> . . .	137

ACKNOWLEDGMENTS

This dissertation would not have been possible without the advice, support, and encouragement of my advisor, Neil Shubin, throughout the years. His belief in my abilities and constant enthusiasm for the project, helped me to forge onwards, even when times were rough. He pushed me to try techniques I never thought I could master, and he always assumed I would succeed. I am grateful and honored to have been a part of his lab.

Each of the members of my dissertation committee graciously shared their lab space, equipment, and experience, for which I am grateful. While graduate school sometimes made it difficult to keep track of why I wanted to study biology in the first place, Michael LaBarbera was always there to remind me of the joys of science and teaching. His guidance and mentorship encouraged me to explore the unknown, and his spirit of discovery was infectious. Mark Westneat was a constant source of support and advice for all phases of the project – from fish collection to manuscript preparation. He made me feel like an honorary member of his lab, and I would never have been able to learn as much about gars without being able to observe them firsthand in his facilities at the Field Museum and University of Chicago. Callum Ross gave me the first opportunity to truly work as a scientist when he welcomed me into his lab. It was thanks to the skills I learned early on as his laboratory technician that I was able to start and finish my Ph.D.

Other non-committee members of the University of Chicago faculty were similarly instrumental in my journey. Mike Coates was always interested in my project, and his wonderful insight and helpful discussions significantly improved the quality of this work. Zhe-Xi Luo and April Isch Neander gave me the amazing opportunity to learn CT scanning and provided me with countless hours of support when I was first getting started. Carol Abraczinskas was incredibly

helpful in teaching me techniques to combine art with science, and she taught me to always pay attention to the details. Laura Porro fatefully gave me my first tutorial using Amira almost a decade ago, which was a program I used for just about every aspect of this project. Finally, I never would have finished my dissertation if it weren't for Audrey Aronowsky, who helped organize me and keep me on track in those hectic final hours.

Support from outside the University came from many sources. Ted Daeschler gave me access to the *Tiktaalik* specimens housed at the Academy of Natural Sciences of Drexel University and helped me shuttle invaluable fossils to and from Chicago. Gar specimens were made possible through the generous assistance of the U.S. Fish and Wildlife Service. I would like to thank William Bouthillier, Carlos Echevarria, and Haile Macurdy at the Warm Springs National Fish Hatchery for supplying me with alligator gars. Outside funding support was provided through the National Science Foundation, and this work was supported under NSF IGERT Grant No. DGE-0903637, a Graduate Research Fellowship to Justin Lemberg, and Grant No. IOS-0818788 (Collaborative Research: the Late Devonian Tetrapodomorph, *Tiktaalik roseae*).

Cohort members, graduate students, undergraduates, and postdoc members of the numerous labs I associated with provided true friendship and made this process much less lonely than it could have been. In particular, I would like to thank Tom Stewart, Carrie Albertin, Laura Merwin, Aaron Olsen, Kristen Voorhies, Colin Kyle, Alice MacQueen, Courtney Orsbon, David Reed, Pepe Iriarte-Diaz, Tetsuya Nakamura, Natalia Taft, Andrew Gehrke, Joyce Pieretti, Gayani Senevirathne, Darcy Ross, Alexander Okamoto, Lu Yao, Brett Aiello, Charlie McCord, Andrew George, Kate Criswell, Haley Stinnett... and many, many more. This list is not exhaustive, and neither was the support you provided throughout the years. A special thanks is

reserved for Nora Loughlin, who was a wonderful and enthusiastic undergraduate assistant and contributed countless hours to all the projects of this thesis.

The Field Museum of Natural History was an important turning point in my life prior to graduate school. Inspired by Lance Grande, John Bolt, Pete Makovicky, and Ken Angielczyk, I learned it was possible to pursue my childhood dreams, and it was then that I decided I wanted to get a degree in paleontology. The Fossil Prep lab was a great source of comradery, and I am thankful for Connie Van Beek, Jim Holstein, Akiko Shinya, Lisa Herzog, and Debbie Wagner for teaching me the joys of working with fossils.

I am also grateful for the people that made my time as an undergraduate at the University of Chicago so memorable. I would like to thank Russ Tuttle, who taught all my favorite physical anthropology classes and gave me an appreciation for the application of biomechanics to extinct organisms. I am also indebted to Eric Lombard, who was a wonderful source of kindness to all the Lembergs at the University of Chicago. It was “Dr. L’s” early guidance and advice that made it possible for me to find a career in the fascinating world of early tetrapod research. I am incredibly fortunate to have been shaped by these individuals at an early age, and, years later, I still recognize the influence they had on my approach to paleontology.

My family encouraged a lifelong pursuit of knowledge and made it possible for me to attend the University of Chicago, a place that has shaped me in so many ways over the years. Most importantly, there I met the love of my life, Josh, when we were both undergraduates. No one else encouraged me to pursue my dreams as much as Josh, and I am so lucky to have had his love and support, as well as the love and support of our families, throughout this process.

Thank you.

ABSTRACT

The recreation of behavior in extinct fossil taxa is a difficult task, and many studies have attempted to analyze the feeding mechanics of early tetrapods on the basis of fragmentary elements or *a priori* assumptions of terrestrial selective pressures. The transitional fossil, *Tiktaalik roseae*, preserves exquisite details of many elements of the feeding apparatus of a derived, tetrapodomorph fish that existed right before the fin-to-limb transition. Here I present an in-depth study of the feeding mechanics of this important fossil on the basis of detailed internal anatomy, modern analogs, and cranial linkage reconstructions to attempt an all-data approach to reconstruct feeding behavior in this important taxon: Using micro computed tomography (μ CT) to visualize joint surfaces, deformation patterns, and internal feeding anatomy of the *Tiktaalik*, the first section of this work demonstrates the transitional nature of elpistostegid feeding anatomy. The cranium of *Tiktaalik* is shown to be platyrostral and consolidated in similar ways to more derived tetrapodomorphs, but the modified cheek and palate are shown to be kinetic and mobile. Each of these features represent a departure from assumed osteolepiform models of feeding, which is not reflected in the relatively plesiomorphic morphology of the lower jaws. On the basis on convergent features shared with lepisosteid gars, the second section of this work documents the feeding mechanism of the alligator gar, *Atractosteus spatula*, using high-speed videography, contrast-enhanced μ CT, and cranial linkage modeling. The feeding system of *Atractosteus spatula* incorporates elements of both jaw-ram and suction into the feeding strike, which is possible due to an unexpectedly expansive feeding mechanism and decoupling of kinematic events with plesiomorphic hyoid constrictors. The final section of this work demonstrates that the feeding mechanism of *Tiktaalik roseae* permitted a feeding strike similar to alligator gars, using a digitally reconstructed cranial linkage system, gar feeding kinematics, and

conservative estimates of tetrapodomorph muscular anatomy. Many of the elements of a terrestrial-style feeding system are demonstrated to be possible using the feeding apparatus of *Tiktaalik roseae*, which gars convergently evolved in an aquatic context. This suggests that components of the terrestrial-tetrapod feeding mechanism, such as delayed hyoid depression, predominantly biting-based prey capture, and a gape cycle capable of anterior-to-posterior movements, could have evolved first in water, without the need for a terrestrial stage. Many aspects of the feeding system of *Tiktaalik roseae* could have subsequently been exapted for use on land by the earliest terrestrial vertebrates.

CHAPTER 1 – INTRODUCTION TO TETRAPODOMORPH FEEDING DURING THE WATER-TO-LAND TRANSITION

The water-to-land transition is one of the greatest transitions in vertebrate history, of which over half of modern vertebrate species are descended from. It is a fascinating time period because over its course it required changes to essentially every vertebrate system. The colonization of land by vertebrates required changes to almost every originally aquatic locomotor, respiratory, reproductive, feeding, sensing, and physiological systems (Clack 2012). Terrestrial vertebrates had to find ways to support their weight (Clack 2001), transport their bodies (Pierce et al. 2012), prevent desiccation (Clack 2012), sense their surroundings (MacIver et al. 2017), dissipate CO₂, and uptake oxygen (Witzmann and Brainerd 2017). The reason for many of these changes is the drastically different properties of air and water, which require shifts in the ways animals regulate their bodies and interact with their environments (Vogel 1994)

Unfortunately, pinning down when the water-to-land transition occurred is problematic (Clack 2012). Some of the earliest signs of terrestrial-adapted axial anatomy are found in *Ichthyostega* (Ahlberg et al. 2005, Pierce et al. 2012, Pierce et al. 2013), and the earliest terrestrial autopodal adaptations are found in the whatcheeriid, *Pederpes* (Clack 2002b). These are both early limbed tetrapodomorphs; however, other limbed tetrapodomorphs, such as *Acanthostega*, do not exhibit these features (Clack 2002b, Ahlberg et al. 2005). Purported tetrapodomorph trackways with digits are found significantly earlier than any known body of limbed tetrapodomorphs (Warren and Wakefield 1972, Stössel 1995, Niedzwiedzki et al. 2010), but the morphology of the organisms that made those trackways are unknown and even limbed tetrapodomorphs with digits appear to be primarily or fully aquatic (Coates and Clack 1991,

Clack 2012). In terms of respiration, the operculum of tetrapodomorph fishes disappears among the elpistostegids (Daeschler et al. 2006), but internal gills persist into the tetrapod crown (Schoch and Witzmann 2010). The evolution of the amniotic egg is a definitive split with the aquatic needs of tetrapods for reproduction; however, this adaptation is only present in some descendants of terrestrial vertebrates. It is possible the water-to-land transition occurred during a time period during the early Carboniferous, known as Romer's Gap, when fossilized tetrapod remains are relatively uncommon (Clack 2002b). The problem with finding evidence of the water-to-land transition in the fossil record, is that it was essentially a change in behavior and, aside from aforementioned trackways (Warren and Wakefield 1972, Stössel 1995, Niedzwiedzki et al. 2010), behavior rarely leaves fossilized evidence.

In contrast, the fin-to-limb transition is a relatively discrete and well-documented transition (Coates et al. 2002, Clack 2009) accompanied by drastic morphological changes to the tetrapodomorph body plan both cranially and postcranially (Daeschler et al. 2006, Clack 2012). This transition likely happened in the rivers and estuaries surrounding the 'Old Red Sandstone' continent – Laurussia – close to the Frasnian-Famennian boundary (Vorobyeva 1980, Schultze 1996, Daeschler et al. 2006, Clack 2012). While the name implies postcranial changes, significant shifts to cranial anatomy occurred during this time period as well (Ahlberg et al. 1996, Daeschler et al. 2006, Ahlberg et al. 2008). Paleontologists typically rely on significant morphological changes to indicate a shift in ecology, and the evolution of limbed tetrapodomorphs from finned tetrapodomorphs is one such event. However, some of the key transitional taxa during this transition, such as *Eusthenopteron*, *Panderichthys*, *Elpistostege*, and *Ventastega* appear to occupy very similar environments – estuaries, deltaic, and nearshore marine environments (Vorobyeva 1980, Schultze 1984, Schultze 1996, Daeschler et al. 2006,

Ahlberg et al. 2008, Clack 2012). Many limbed tetrapodomorphs appear to have lived primary or exclusively aquatic lifestyles after this transition (Panchen 1985, Coates and Clack 1991), and the fin-to-limb transition appears to have occurred in water.

This study attempts to understand the issues related to feeding during the water-to-land transition. One of the reasons it is suspected that the earliest terrestrial vertebrates came onto land was to exploit terrestrial resources (Niedzwiedzki et al. 2010, Clack 2012, Heiss et al. 2018), but the way these primarily aquatic tetrapodomorphs fed is still very much a mystery (Clack 2012, Heiss et al. 2018). Like other physiological systems, the mechanics of feeding is significantly impacted by the physical context in which it occurs (Markey and Marshall 2007, Heiss et al. 2018). In terms of feeding, both prey capture and prey processing become more difficult in air, because most aquatic vertebrates use some form of suction to capture prey and hydraulic transport to swallow (Heiss et al. 2018). Suction-feeding is not an effective mechanism on land because air is approximately 800 times less dense and 50 times less viscous than water (Vogel 1994, Heiss et al. 2018). It is for these reasons that many researchers believe, that, in order to colonize land there had to be a suction-to-biting transition in addition to a water-to-land transition (Markey and Marshall 2007), and it would be expected that that transition had morphological indicators. However, studies of tetrapodomorph lower jaws indicate little to no shift in mandibular morphology between tetrapodomorph fishes and limbed tetrapodomorphs, including those believed to be at least partially terrestrial (Anderson et al. 2013, Neenan et al. 2014). This has led researchers to claim the earliest terrestrial vertebrates continued to feed similar to aquatic fishes, although interpretations of function in this context are inconsistent, with some claims that limbed tetrapodomorphs, such as *Acanthostega*, were well adapted for biting (Markey and Marshall 2007) and others saying they were suction feeders (Anderson et al. 2013,

Neenan et al. 2014, Porro et al. 2015b). The problem with studies entirely based on morphology is the inherent difficulty in inferring function from structure, particularly in the fossil record (Lauder 1995).

In order to infer the functional roles of fossilized morphology, paleontologists are limited to a handful of methods to interpret function from structure, each of which has inherent pitfalls (Lauder 1995). Phylogenetic inference allows a researcher to determine the probability that a structure may function in a certain way based on living in-groups and out-groups (Lauder 1995, Witmer 1995). This method is best when an extinct taxon is bracketed phylogenetically by close relatives that all use a unique morphology in the same unambiguous way (Lauder 1995, Weishampel 1995); however in the fossil record, that is rarely the case due to millions of years of evolution. For instance, the lower jaws of lungfish, the closest living outgroup of tetrapods, have lost the marginal teeth and instead evolved a crushing toothplate used for a durophagous diet (Bemis 1986, Bemis and Lauder 1986). The lower jaws of aquatic tetrapods can be used for either suction or biting, even in taxa with elongate slender jaws such as crocodilians and giant salamanders (Busbey 1989, Heiss et al. 2013). Furthermore, the extant in-group of tetrapodomorphs have particular soft-tissue adaptations, such as a muscular tongue, that cannot be inferred in fossils (Witmer 1995). Thanks to a depopulate out-group and an ambiguous in-group, the function of tetrapodomorph lower jaws (Anderson et al. 2013, Neenan et al. 2014) remains problematic using a phylogenetic method (Lauder 1995).

Alternatively, researchers concerned with feeding during the water-to-land transition can turn to biomechanical modeling. The paradigm modeling method does not require extant relatives, because it attempts to identify the optimal form for a function in an “ahistorical” approach, without regard for phylogenetic relatedness (Rudwick 1964, Lauder 1995). Because

structures are rarely “optimal” and often represent trade-offs between multiple functions (Liem 1980, Lauder 1995), researchers often limit such assumptions, such as feeding constraints at the water-to-land transition, to biological models, such as aquatic feeding salamanders or terrestrial feeding actinopterygians (Van Wassenbergh et al. 2006, Heiss et al. 2013, Michel et al. 2015, Van Wassenbergh et al. 2017). These approaches still require *a priori* assumptions of the functional demands of fossil morphology, but that does not mean that theoretical frameworks of optimal forms for specific functions cannot be illuminating (Kay and Cartmill 1977, Lauder 1995, Weishampel 1995). The drawback to these approaches, however, is that the feeding morphology of terrestrial-feeding teleosts (Van Wassenbergh et al. 2006, Michel et al. 2015) and even giant salamanders (Elwood and Cundall 1994) can be quite derived, and this morphology does not necessarily closely represent the known feeding morphology of extinct tetrapodomorphs (Jarvik 1980, 1996, Daeschler et al. 2006).

Biologists quite often overestimate the ability to estimate function from biological structures (Liem 1980, Lauder 1995); however, that does not mean that attempts to describe the physical constraints facing animals living in a physical world are valueless, and theoretical frameworks of optimal forms for specific functions have particular heuristic value (Lauder 1995, Heiss et al. 2018). The difficulty is that biomechanics allows you to easily rule out some possibilities (like sauropod flight), a “consequentialist” approach, but it is harder to make positive conclusions for fossils on the basis of morphology alone (Kay and Cartmill 1977). For these reasons, often the best alternative is to use as much data as is available, and see where different avenues of inquiry disagree (Weishampel 1995). With full knowledge that all biomechanical studies of fossils are essentially plausibility statements (Bryant et al. 1995) and that we are missing an important neuromuscular context (Lauder 1995), I propose to study

feeding mechanics of a tetrapodomorph fish that lived immediately prior to the fin-to-limb transition, *Tiktaalik roseae*, using a combination of phylogenetic inference, modeling based on likely extant analogs, and functional consequences of anatomy.

The first step involves building an in-depth understanding of the feeding anatomy of *Tiktaalik roseae*. While the lower jaws and external cranial anatomy of *Tiktaalik* have already been described (Daeschler et al. 2006, Downs et al. 2008, Hohn-Schulte et al. 2013), computed tomography (CT) has been increasingly used to detail the internal anatomy and joint surfaces of tetrapodomorphs (Markey and Marshall 2007, Pierce et al. 2013, Porro et al. 2015a, b, Sanchez et al. 2016). The first chapter will compare the anatomy of *Tiktaalik* to other tetrapodomorph taxa before and after the fin-to-limb transition in order to best understand the evolutionary context of its morphology. On the basis of CT data, some of the functional consequences of the derived morphology of *Tiktaalik roseae* will be described, and then cranial anatomy will be assessed for similarities to other potential modern analogs that could form the basis for productive biomechanical studies.

The next step involves studying the feeding anatomy of an unrelated, but potentially analogous, modern taxa. The alligator gar, *Atractosteus spatula*, shares many morphological similarities with elpistostegid tetrapodomorphs. While these similarities are entirely due to convergent evolution, convergent evolution is often the best test of adaptive evolution (Wake 1991). This chapter will attempt to understand the function of some of the more unusual specialized traits of the alligator gar, through the use of high-speed videography, soft-tissue reconstruction, and cranial linkage modeling based on CT data.

Finally, the last step combines the anatomical information of *Tiktaalik roseae* with functional modeling of the *Atractosteus spatula* feeding apparatus in order to recreate possible

scenarios of elpistostegid feeding mechanics. This approach combines phylogenetic inference of tetrapodomorph muscle configurations and modeling of the alligator gar feeding kinematics to determine some of the limitations and possibilities of the tetrapodomorph feeding mechanism. The benefit of using gars as a modern analog for understanding the water-to-land transition, is that they never experienced a terrestrial stage, and therefore demonstrate how some of the elements of a terrestrial style feeding mechanism could have evolved entirely in water, for the purposes of feeding in water.

CHAPTER 2 – CRANIAL MORPHOLOGY OF *TIKTAALIK ROSEAE* REFLECTS SHIFTS IN FEEDING STRATEGIES PRIOR TO THE FIN-TO-LIMB TRANSITION

2.1 – ABSTRACT

The fin-to-limb transition marks an important event in the evolution of terrestrial vertebrates during which a lineage of tetrapodomorph fishes, characterized by the elpistostegids, dramatically transformed in terms of cranial and postcranial morphology to arrive at the body plan of the earliest limbed tetrapodomorphs. Despite significant shifts in ecology suggested by this transition, lower jaw morphology is one aspect of the transition that lagged behind the rest, suggesting that the feeding ecology of these rapidly evolving animals remained relatively conserved. However, the discovery of articulated and well-preserved cranial material of the elpistostegid, *Tiktaalik roseae*, has opened new avenues of research into changes in upper jaw morphology of tetrapodomorph fishes just prior to the fin-to-limb transition. This study utilizes computed tomography (CT) data to reconstruct and interpret upper jaw morphology of numerous specimens of *Tiktaalik*, in order to assess shifts in feeding related to the evolution of a platyrostral, consolidated, but still kinetic skull. Postmortem deformation patterns of articulated specimens indicate the skull of *Tiktaalik* is almost twice as wide as it is tall, indicating a dramatic change in rostral proportions that have important ramifications for aquatic feeding. Assessment of sutural anatomy and ossification patterns from CT scans show that the skull of *Tiktaalik* exhibits some of the earliest signs of arriving at the consolidated condition of limbed tetrapodomorphs. Yet, despite these changes to cranial shape, articulation points, and mobility of the neurocranium, *Tiktaalik* still retains a mobile cheek and palate, suggesting this trait was not lost across the fin-to-limb transition. While cranial kinesis is likely plesiomorphic for

tetrapodomorph fishes, retention of cranial kinesis nevertheless would require significant changes to how that kinesis operated due to the rapidly evolving changes to the braincase that make previous models of osteolepidid and tristichopterid cranial kinesis difficult to apply. All these features indicate that the feeding system of elpistostegids was diverging from conditions found in plesiomorphic tetrapodomorph fishes in ways not suggested by stasis in lower jaw morphology.

Key words: sutural morphology, scarf joint, cranial consolidation, cranial modularity, platyrostral, tetrapodomorph, *Tiktaalik*

2.2 – INTRODUCTION

Feeding at the fin-to-limb transition:

The fin-to-limb transition was a key event in tetrapodomorph evolution during which the body plans of the earliest terrestrial vertebrates evolved from fish-like ancestors. This transition is documented through numerous fossils belonging to a diverse assemblage of tetrapod-like fishes, including rhizodonts, osteolepidids, megalichthyids, tristichopterids, and elpistostegids, as well as limbed stem-tetrapods, such as *Ventastega*, *Acanthostega*, *Ichthyostega*, whatcheeriids, *Crassigyrinus*, and colosteids (Coates et al. 2008, Clack 2012). Despite the name, changes during the fin-to-limb transition were distributed throughout the cranial and postcranial skeleton, affecting numerous physiological systems beyond just locomotion (Coates et al. 2008, Clack 2012). The result was sweeping changes to the body plans of tetrapodomorph fishes over the course of millions of years, from the Early to Late Devonian, which indicated drastic changes to the ecology and life-strategies of the ancestors of the earliest terrestrial vertebrates.

Most of what is known about feeding in tetrapodomorphs is based on their lower jaws which preserve comparatively well in the fossil record (Ahlberg 1995), are rich in phylogenetic characters (Ahlberg and Clack 1998), and are primarily used for feeding (Anderson et al. 2011). In contrast to otherwise major changes to the tetrapodomorph body plan during the fin-to-limb transition, lower jaws remain relatively conserved between tristichopterids, elpistostegids, and limbed tetrapodomorphs (Ahlberg and Clack 1998, Clack 2012), leading some researchers to conclude the earliest terrestrial vertebrates would have fed very similarly to tetrapodomorph fishes (Anderson et al. 2013, Neenan et al. 2014). While well-documented and significant, these conclusions do not reflect the rapid changes to upper jaw and cranial morphology that may also effect feeding ecology. Despite having lower jaws nearly identical to plesiomorphic tristichopterids, elpistostegids have numerous characters more similar to limbed tetrapodomorphs, including dorsoventrally compressed skulls, elongate rostra, horizontal palates, and reduced hyomandibulae (Brazeau and Ahlberg 2006, Daeschler et al. 2006). While hypothesized to affect feeding, it is uncertain how important these changes were to the overall feeding ecology of these animals or why the lower jaws are so conserved, and it is this gap in understanding, particularly for the derived-elpistostegid, *Tiktaalik roseae*, that guides the three aims of the research presented here.

Dorsoventral compression of the skull is a characteristic of both elpistostegids and early limbed tetrapodomorphs that results in far broader and flatter skulls than those seen in plesiomorphic osteolepidids and tristichopterids (Jarvik 1980). The cranium of *Tiktaalik* is reported to be dorsoventrally compressed as well (Daeschler et al. 2006, Downs et al. 2008), similar to the conditions seen in *Panderichthys* (Vorobyeva and Schultze 1991, Brazeau and Ahlberg 2006), *Elpistostege* (Vorobyeva and Schultze 1991), and *Acanthostega* (Clack 1994a,

Clack 1998); however, many of these fossils show signs of postmortem deformation that could affect our understanding of the overall cranial geometry of these animals. Rostral proportions have important implications for feeding because resistance to bending forces, hydrodynamics of the skull, and movements of cranial elements all rely on the relative geometry of the skull (Thomson 1967, Taylor 1987). Therefore, the first aim of this study is to determine the extent of postmortem deformation in the skull of *Tiktaalik roseae* using internal morphological data obtained from computed-tomography (CT) scans in comparison with archival photos of the specimens in various stages of preparation in order to recreate accurate cranial proportions for the purposes of understanding the effect it may have on feeding.

Cranial consolidation is another important trend in tetrapodomorph evolution first documented among elpistostegids and coinciding with dorsoventral compression of the skull (Ahlberg et al. 1996). The elpistostegid *Panderichthys* is noted for showing the earliest evidence of fusion of the intracranial hinge through interdigitating sutures between the parietal and postparietal shields of the dermal skull roof (Ahlberg et al. 1996). This hinge overlies the division between the sphenethmoid and otoccipital partitions of the braincase plesiomorphically found in sarcopterygians, but ultimately fused in limbed tetrapodomorphs (Clack 2012). While limbed tetrapodomorphs possess a fused intracranial fissure, they also lack ossification of the nasal capsule and the lateral wall of the otic capsule, the fenestra vestibulae, indicating a major shift in consolidation patterns of the chondrocranium across the fin-to-limb transition (Clack 1998). Furthermore, sutural diversity increases in later tetrapodomorphs, from simple scarf and butt joints in the tristichopterid *Eusthenopteron* to interdigitating and beveled tongue-in-groove joints in limbed tetrapodomorphs, such as *Acanthostega* (Markey and Marshall 2007). Although potentially indicating a shift in the way the skull is being loaded during feeding in

tetrapodomorph fishes, previously the only descriptions available of sutural anatomy or endocranial ossification in elpistostegids have been from surface details (Schultze and Arsenault 1985, Vorobyeva and Schultze 1991, Markey and Marshall 2007, Downs et al. 2008, Clack 2012). Therefore, a second aim of this study is to document the extent of cranial consolidation as it relates to feeding in *Tiktaalik roseae* by examining internal chondrocranial and dermatocranial anatomy obtained from CT scans.

Finally, whereas flattening of the skull and consolidation of the braincase was thought to represent shifts away from the cranial kinesis proposed for osteolepidid and tristichopterid tetrapodomorphs (Thomson 1967), various limbed tetrapodomorphs nevertheless possess evidence for either retained or re-evolved cranial kinesis (Panchen 1964). Cranial kinesis is common among aquatic feeding vertebrates that generate suction to capture prey, because it enables the buccal cavity to expand during feeding to draw in prey, and cranial kinesis has been proposed for osteolepidid and tristichopterid tetrapodomorphs (Thomson 1967) particularly due to their hinged braincases. Despite possessing fused braincases, cranial kinesis has also been proposed for limbed tetrapodomorphs and early crown-tetrapods, including *Acanthostega* (Clack 1989), colosteids (Romer 1969, Bolt and Lombard 2001), baphetids (Beaumont 1977), and anthracosaurs (Panchen 1964), on the basis of apparently mobile joints between the palate and braincase (see Table 1). In contrast, other limbed tetrapodomorphs, such as *Ichthyostega* (Jarvik 1996) and whatcheeriids (Lombard et al. 2006) appear to have fully consolidated and akinetic skulls. While researchers disagree on the extent and distribution of cranial mobility among tetrapodomorphs, many researchers assume that cranial kinesis in early tetrapods was inherited from fish-like ancestors (Iordansky 1990, Bolt and Lombard 2001), with some notable exceptions (Smithson 1982, Jarvik 1996). If cranial kinesis was maintained across the fin-to-

limb transition, there should be evidence of this in elpistostegids. Therefore, the third and final aim of this study is to document evidence of cranial kinesis, if present, using reconstructed joint morphology from CT scans of the last known tetrapodomorph fish prior to the fin-to-limb transition, *Tiktaalik roseae*.

Table 2.1. Distribution of arguments for and against cranial kinesis in tetrapodomorph fishes. While cranial kinesis appears to be plesiomorphic for both osteolepidid fishes and crown-group tetrapods, there is some uncertainty of the presence of cranial kinesis immediately before and after the fin-to-limb transition (see text). Phylogenetic groupings are based on (Coates et al. 2008).

Tetrapodomorpha					
Tetrapodomorph fishes			Limbed tetrapodomorphs		
	<u>Kinetic</u>	<u>Akinetic or limited</u>		<u>Kinetic</u>	<u>Akinetic or limited</u>
<i>Coelacanth</i> s (non-tetrapodomorph)		(Dutel et al. 2013)	<i>Ventastega</i>		
<i>Lungfish</i> (non-tetrapodomorph)		(Arratia and Schultze 1991)	<i>Acanthostega</i>	(Clack 1998) *uncertain	
<i>Kenichthys</i>			<i>Ichthyostega</i>		(Thomson 1967, Jarvik 1996)
<u>rhizodonts</u>			<u>whatcheerii</u> s		(Bolt and Lombard 2001, Lombard et al. 2006)
• <i>Gooloogongia</i>			• <i>Whatcheeria</i>		
• <i>Barameda</i>			• <i>Pederpes</i>		
<u>“osteolepidids” and megalichthyids</u>			<i>Crassigyrinus</i>	(Panchen 1985)	
• <i>Gogonaspis</i>		(Long et al. 1997)	<u>colosteids</u>	(Romer 1969, Bolt and Lombard 2001)	(Smithson 1982)
• <i>Osteolepis</i>			• <i>Colosteus</i>		
• <i>Medoevia</i>			• <i>Deltaherpeton</i>		
• <i>Gyropterygius</i>			• <i>Greerherpeton</i>		
• <i>Megalichthys</i> (megalichthyid)			• <i>Pholidogaster</i>		
• <i>Cladariosymblema</i> (megalichthyid)	(Fox et al. 1995)		<i>Eucritta</i> (stem-baphetid)		
• <i>Ectosteorhachis</i> (megalichthyid)	(Thomson 1967)		<u>baphetids + loxommatids</u>	(Beaumont 1977) *palate only	
			• <i>Megalocephalus</i>	(Bolt and Lombard 2001)	
			• <i>Loxomma</i>		
			• <i>Baphetes</i>		
			• <i>Spathicephalus</i>		
<u>tristichopterids</u>	(Hitchcock 1995)		<u>Temnospondyls</u>	(Romer 1969, Beaumont 1977)	(Beaumont 1977, Smithson 1982)? (Damiani 2001, Fortuny et al. 2012)
• <i>Eusthenopteron</i>		(Jarvik 1996, Long et al. 1997)	> <u>capitosaurs</u>		
• <i>Mandageria</i>			• <i>Wetlugasaurus</i>		
• <i>Spodichthys</i>			> <u>plagiosaurs</u>		(Witzmann and Schoch 2013)
• <i>Tristichopterus</i>			• <i>Gerrhotorax</i>		
• <i>Cabonnichthys</i>			<u>anthracosaurs + embolomeres</u>	(Panchen 1964, Thomson 1967)	
• <i>Platycephalichthys</i>			• <i>Eoherpeton</i>		
• <i>Mandageria</i>			• <i>Pholiderpeton</i>		
• <i>Eusthenodon</i>			• <i>Anthracosaurus</i>		
<u>“elpistostegids”</u>		(Brazeau and Ahlberg 2006, Downs et al. 2008)	• <i>Proterogyrinus</i>		
• <i>Panderichthys</i>			• <i>Paleoherpeton</i> (= <i>Palaeogyrinus</i>)		
• <i>Elpistostege</i>			• <i>Eogyrinus</i>		
• <i>Tiktaalik</i>			<u>seymouriamorphs</u>	(Thomson 1967)	
> <u>limbed tetrapodomorphs</u>	See next column				

Stem-Lissamphibia
Crown-group tetrapods
Stem-Amniota

2.3 – MATERIALS AND METHODS

2.3.1 – Specimens of *Tiktaalik roseae*

Tiktaalik roseae is known from articulated as well as isolated remains from approximately eighteen specimens (nineteen if you count NUFV 137 – an isolated rostral portion of a potentially unknown elpistostegid). Cranial material is known from fifteen of those specimens (NUFV 108, 109, 110, 111, 1158, 116, 119 122, 137, 142, 144, 149, 661, 666, 669), with articulated cranial material found in four specimens (NUFV 108, 109, 110, 149) forming the primary data for this study. Lower jaws referenced in this study used three of the best preserved and complete lower jaws (NUFV 109, left, 116, right, 122, right). While postcranial material is known from eight specimens (NUFV 108, 109, 110, 112, 113, 1155, 120, 149), these were not used for the purposes of this study except to ascertain the relative displacement of cranial elements due to postmortem deformation in two of the specimens (NUFV 108, 110). Multiple elements from each specimen were scanned to compose the computed tomography dataset collected for *Tiktaalik roseae*.

Cranial material:

- **Cheek and palatal material** – scans collected from 108, 109, 110, 111, 149
- **Chondrocranium and skull roof material** – scans collected from 108, 109, 110, 111, 119, 149, 169
- **Lower jaw material** – scans collected from 108, 109, 110, 1158, 116, 122, 137, 142, 144, 149, 661, 666
- **Hyobranchial material** – scans collected from 108, 109, 110, 669

Postcranial material:

- **Pectoral material** – scans collected from 108, 109, 110, 112, 113, 120, 149
- **Pelvic material** – scans collected from 108, and 1155,
- **Axial material** – scans collected from 108, 109

2.3.2 – Computed tomography (CT) scanning of fossil specimens

Computed tomography data was collected for the following specimens. Except for four scans completed at the University of Texas at Austin Scanning Facility (UTCT), all scans were collected by the author at the UChicago PaleoCT scanning facility using a GE Phoenix v|tome|x 240 kv/180 kv scanner (<http://luo-lab.uchicago.edu/paleoCT.html>) with the following scanning parameters:

Table 2.2. Scanning parameters used to document internal anatomy of the feeding apparatus of *Tiktaalik roseae*. In instances where multiple scans were conducted on the same cranial element, the last listed parameter set resulted in the greatest contrast of internal anatomy and sutures.

NUFV108	Voltage	Current	Filter	Timing	Total	Voxel Size	Resolution
<i>Skull (2005)</i> <i>*UTCT</i>	420 kV	1800 μ A	1 brass filter	NA	NA	$176.521 \times 176.521 \times 450 \mu\text{m}^3$	5.6650 pixels/mm
<i>Skull (2012)</i> <i>*UTCT</i>	350 kV	4200 μ A	1 brass filter	NA	NA	$178.711 \times 178.711 \times 300 \mu\text{m}^3$	5.5956 pixels/mm
<i>Skull (2015)</i>	100 kV	590 μ A	0.24 mm Cu	500 ms per image	1hr 26min	$(109.8660 \mu\text{m})^3$	9.1020 pixels/mm
<i>Skull table</i>	100 kV	580 μ A	0.24 mm Cu	500 ms per image	1hr 43min	$(66.4100 \mu\text{m})^3$	15.0580 pixels/mm
<i>Pectoral fin block (anterior)</i>	100 kV	570 μ A	0.24 mm Cu	500 ms per image	6hr 48min	$(122.4410 \mu\text{m})^3$	8.1672 pixels/mm

NUFV109	Voltage	Current	Filter	Timing	Total	Voxel Size	Resolution
<i>Basihyal</i>	130 kV	80 μ A	0.12 mm Cu	2000 ms per image	04hr 11min	$(40.4300 \mu\text{m})^3$	24.7341 pixels/mm
<i>Snout (2nd scan)</i>	130 kV	500 μ A	0.48 mm Sn & 0.50 mm Cu	2000 ms per image	16hr 15min	$(68.2370 \mu\text{m})^3$	14.6548 pixels/mm
<i>Urohyal</i>	70 kV	560 μ A	0.12 mm Cu	1000 ms per image	00hr 59min	$(47.6100 \mu\text{m})^3$	21.0040 pixels/mm
<i>Posterior palate (left)</i>	130 kV	500 μ A	0.48 mm Sn & 0.50 mm Cu	2000 ms per image	17hr 34min	$(68.2370 \mu\text{m})^3$	14.6548 pixels/mm
<i>Palate (right)</i>	130 kV	500 μ A	0.48 mm Sn & 0.50 mm Cu	2000 ms per image	06hr 10min	$(68.2370 \mu\text{m})^3$	14.6548 pixels/mm
<i>Anterior palate (left)</i>	130 kV	500 μ A	0.48 mm Sn & 0.50 mm Cu	2000 ms per image	03hr 03min	$(68.2370 \mu\text{m})^3$	14.6548 pixels/mm
<i>Temporal roofing bones (right)</i>	130 kV	500 μ A	0.48 mm Sn & 0.50 mm Cu	2000 ms per image	08hr 34min	$(68.2370 \mu\text{m})^3$	14.6548 pixels/mm
<i>Jaw left</i> <i>*UTCT</i>	215 kV	220 μ A	none	NA	NA	$74.707 \times 74.707 \times 80.15 \mu\text{m}^3$	13.3856 pixels/mm

Table 2.2, continued.

<i>NUFV110</i>	<i>Voltage</i>	<i>Current</i>	<i>Filter</i>	<i>Timing</i>	<i>Total</i>	<i>Voxel Size</i>	<i>Resolution</i>
<i>Palate (left)</i>	110 kV	95 μ A	none	1000 ms per image	13hr24min	(37.1720 μ m) ³	26.9020 pixels/mm
<i>Skull (2009)</i> <i>*UTCT</i>	300 kV	5000 μ A	none	NA	NA	130.311 \times 130.311 \times 450 μ m ³	7.6739 pixels/mm
<i>Skull (2015)</i>	90 kV	390 μ A	0.24 mm Cu	1000 ms per image	13hr 18min	(59.3900 μ m) ³	16.8379 pixels/mm
<i>Pectoral fin</i> <i>(right)</i>	90 kV	280 μ A	0.12 mm Cu	1000 ms per image	12hr 56min	(54.1580 μ m) ³	18.4645 pixels/mm
<i>Skull table</i>	110 kV	450 μ A	0.24 mm Cu	500 ms per image	01hr 44min	(71.4240 μ m) ³	14.0009 pixels/mm

<i>NUFV111</i>	<i>Voltage</i>	<i>Current</i>	<i>Filter</i>	<i>Timing</i>	<i>Total</i>	<i>Voxel Size</i>	<i>Resolution</i>
<i>Snout</i>	105 kV	100 μ A	none	2000 ms per image	22hr 21min	(34.4720 μ m) ³	29.0091 pixels/mm

<i>NUFV116</i>	<i>Voltage</i>	<i>Current</i>	<i>Filter</i>	<i>Timing</i>	<i>Total</i>	<i>Voxel Size</i>	<i>Resolution</i>
<i>Lower jaws</i>	95 kV	110 μ A	none	2000 ms per image	17hr 17min	(54.3540 μ m) ³	18.3979 pixels/mm

<i>NUFV119</i>	<i>Voltage</i>	<i>Current</i>	<i>Filter</i>	<i>Timing</i>	<i>Total</i>	<i>Voxel Size</i>	<i>Resolution</i>
<i>Snout</i> <i>*(1st scan)</i>	130 kV	80 μ A	0.12 mm Cu	2000 ms per image	05hr 06min	(31.8900 μ m) ³	31.3578 pixels/mm
<i>Snout</i> <i>*(3rd scan)</i>	80 kV	380 μ A	none	500 ms per image	01hr 07min	(32.3390 μ m) ³	30.9224 pixels/mm

<i>NUFV122</i>	<i>Voltage</i>	<i>Current</i>	<i>Filter</i>	<i>Timing</i>	<i>Total</i>	<i>Voxel Size</i>	<i>Resolution</i>
<i>Lower jaw</i> <i>(right)</i>	80 kV	130 μ A	none	2000 ms per image	19hr 55min	(31.8360 μ m) ³	31.4110 pixels/mm

<i>NUFV149</i>	<i>Voltage</i>	<i>Current</i>	<i>Filter</i>	<i>Timing</i>	<i>Total</i>	<i>Voxel Size</i>	<i>Resolution</i>
<i>Braincase</i> <i>with palate</i> <i>*(1st scan)</i>	90 kV	115 μ A	none	2000 ms per image	05hr 39min	(24.3080 μ m) ³	41.1387 pixels/mm
<i>Braincase</i> <i>with palate</i> <i>*(2nd scan)</i>	130 kV	80 μ A	none	1000 ms per image	03hr 00min	(24.3080 μ m) ³	41.1387 pixels/mm
<i>Rostrum</i> <i>*(1st scan)</i>	153 kV	60 μ A	0.54 mm Cu	4000 ms per image	13hr 33min	(48.7300 μ m) ³	20.5212 pixels/mm
<i>Rostrum</i> <i>*(2nd scan)</i>	110 kV	170 μ A	0.12 mm Cu	1000 ms per image	03hr 23min	(52.8280 μ m) ³	18.9294 pixels/mm

Internal contrast

Scanning parameters were adjusted to maximize internal contrast of the specimens. While lower voltages tended to increase contrast between matrix, bone, and internal bone structures, lower voltages also increased scanning artifacts due to higher dispersal of lower energy X-rays as they pass through the specimen. For accurate surface reconstructions of fossils, higher voltages resulted in sufficient penetration of the fossil without “beam-hardening” (brighter exterior and darker internal surfaces). For sutures and joints, however, lower voltages and higher resolutions resulted in greater internal detail.

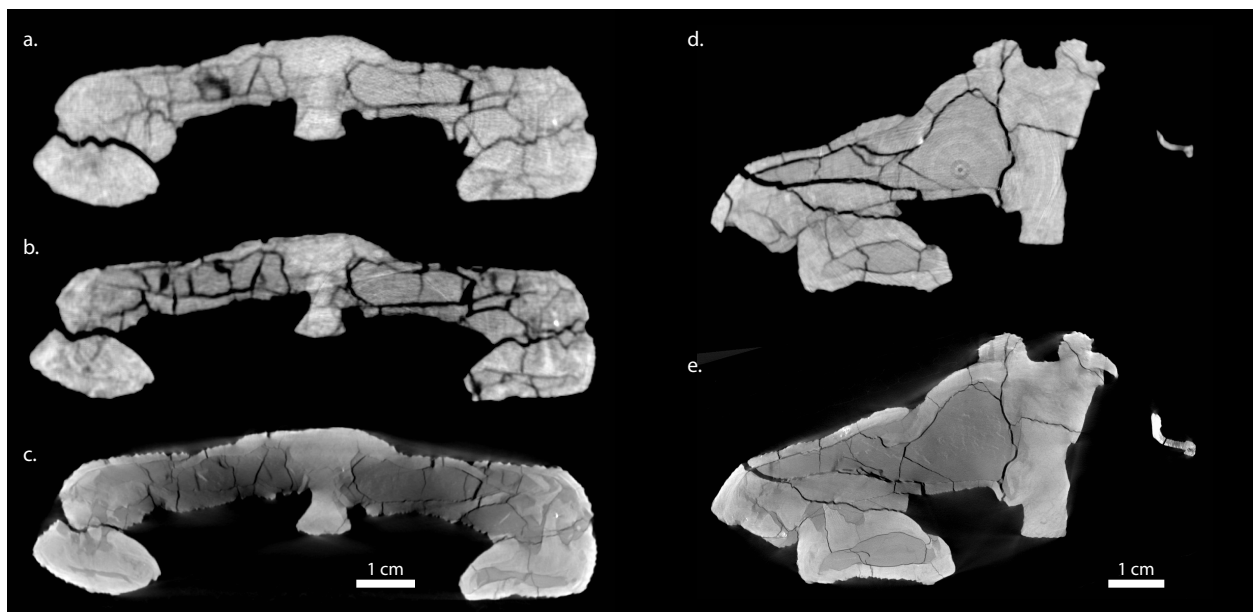


Figure 2.1. Comparison of scanning parameters used for reconstructing internal cranial anatomy. Decreasing voltage resulted in increased contrast for two *Tiktaalik* specimens (NUFV 108: *a-c*, 110: *d-e*). (*a*) 2005 scan at 420kV. (*b*) 2012 scan at 350kV. (*c*) 2015 scan at 100kV. (*d*) 2009 scan at 300kV. (*e*) 2015 scan 90kV. Each scan used a single copper or brass filter except *d*. (see table). While lower voltage resulted in greater contrast between matrix and bone, there was also an increase in “beam-hardening” artifacts that affected the relative greyscale values of internal and external surfaces. Increased resolution (see table) also aided visualization of thin joints between bones.

2.3.3 – Reconstruction of digital anatomy

Amira segmentation

Computed tomography data were analyzed using Amira 6.4 and 6.5 (FEI Software). Boundaries between bones were segmented to isolate individual elements of the cheek and palate. Regions of bones were segmented based on internal differences between endochondral and dermatocranial ossification. Beveled sutures and scarf joints were individually segmented, whereas fine interdigitations between cranial bones were not separated. Three dimensional reconstructions of bones enabled joint mobility and sutural morphology to be ascertained.

Analysis of postmortem deformation

Articulated cranial material is known from at least four individuals of *Tiktaalik roseae* (NUFV 108, 109, 110, 149). Two specimens (NUFV 108, 110) were also preserved *in-situ* with both pectoral and hyobranchial material, allowing comparisons of relative positions of pectoral, hyobranchial, and cranial elements. CT scans of cranial material from each specimen were first overlaid with archival photos of the specimens in various stages of preparation in order to recreate the post-deformation positions of elements. Anatomical midlines of the specimens were assessed using the orientation of the sphenethmoid. In cases where the sphenethmoid was not visible in specimen photos, the repositioned CT data revealed the orientation of the sphenethmoid relative to superficial elements. The angle between superficial elements and anatomical midline was then measured. Next, posterior angles of the jaw joints were measured using cranial reconstructions of the jaws. This angle was compared with the articular facet angles measured from the best preserved lower jaws (NUFV 109, left, 116 right). Next, measurements of the angle of the palate at its thickest portions were taken relative to the horizontal plane and

relative to surrounding elements of the cheek and tooth row. Cases of both breakage and displacement of bones relative to each other was documented for each specimen.

Table 2.3. Anatomical abbreviations for *Tiktaalik roseae* figures

ap, autopalatine;	mr, median rostral;
art. bpt, basipterygoid articulation with palate;	mx, maxilla;
art. dpt, articulation with dermopalatine;	n, nasal;
art. hyo, articulation with hyomandibula;	occ, occipital region;
art. jj; jaw joint articulation;	ot, otic capsule;
art. po, articulation with postorbital;	p, parietal;
at, anterior tectal;	pf, prefrontal;
bo, basioccipital;	pmx, premaxilla;
bs, basisphenoid;	po, postorbital;
clm, commissural lamina;	pop, preopercular;
dpt, dermopalatine;	pp, postparietal;
ect, ectopterygoid;	pq, palatoquadrate;
ent, entopterygoid;	pro, prootic process;
eth, ethmoid;	ps, parasphenoid;
f, frontal;	ptf, postfrontal;
f. ap, fossa apicalis;	q, quadrate;
f. spt, suprapterygoid fossa;	qj, quadratojugal;
hyo, hyomandibula;	sph; sphenoid
icf, intracranial fissure;	sq, squamosal;
j, jugal;	st, supratemporal;
l, lacrimal;	tab, tabular;
lat, lateral commissure;	vo, vomer
mpt. metapterygoid;	

2.4 – RESULTS

Summary Paragraph:

The cranium of *Tiktaalik roseae* is easily separable along anatomical divisions between the chondrocranium, dermal skull roof, dermal cheek, lateral tooth row, and palate. The braincase retains the primitive partition between the sphenethmoid and otoccipital; however, it also shows some of the earliest signs of consolidation by the anterior advancement of the prootic process, which spans the intracranial fissure and fuses elements of both the parietal and postparietal shields. Sutures in the skull roofing bones are complex and varied, with sutures along the midline showing the same degree of interdigitation as terrestrial tetrapods. Towards the periphery, dermal joints are generally broad and overlapping, with particularly loose connections between the skull roof and dermal cheek likely indicating some degree of mobility in life. The palate also retains a loose, fish-like, and probably mobile connection with the braincase, despite being dorsoventrally compressed. While the skull shows signs of postmortem deformation, consistent displacement patterns, joint angles, and localized fractures between individuals enable the cranium of *Tiktaalik* to be reliably reconstructed as a platyrostral structure.

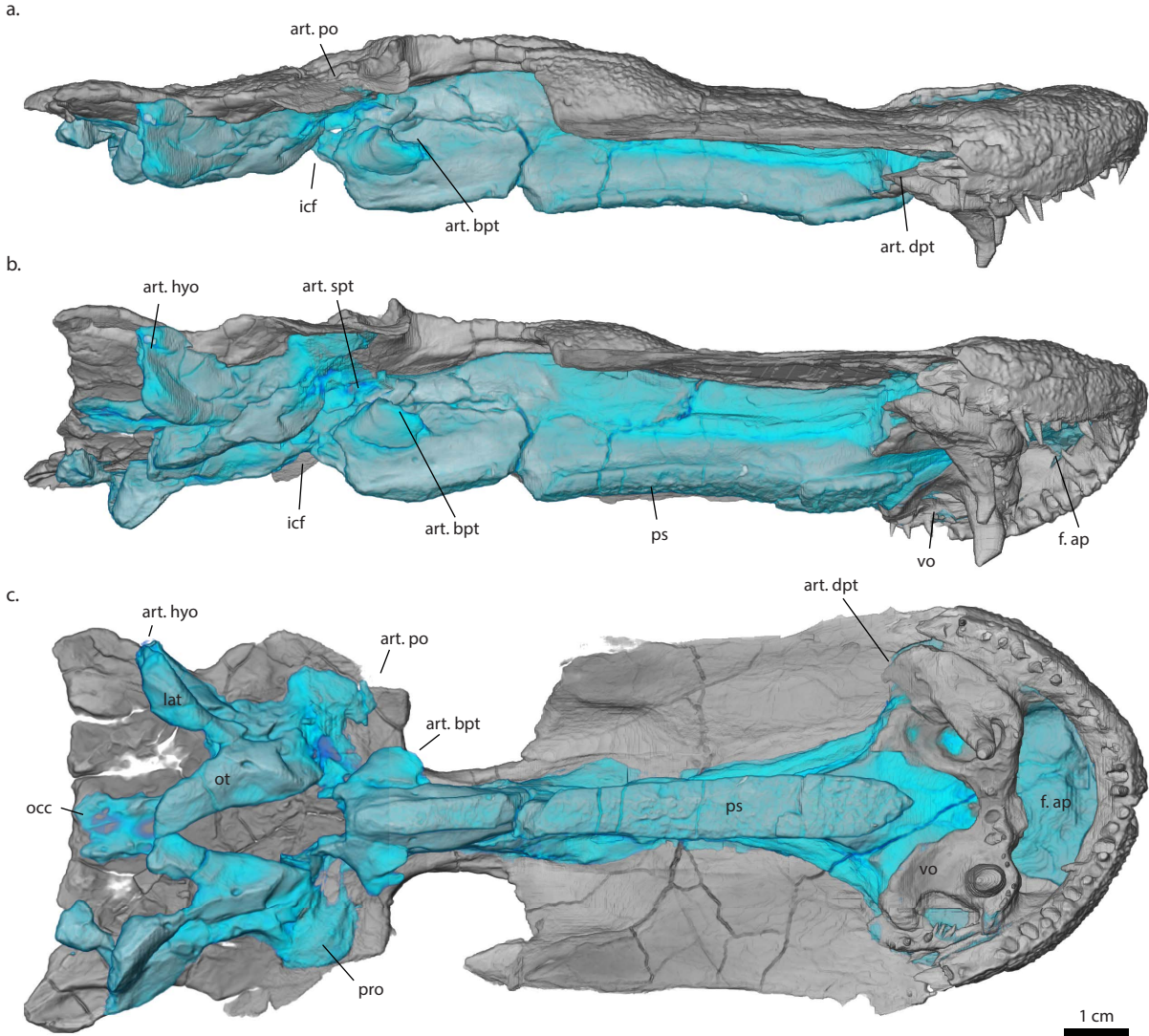


Figure 2.2. External braincase and skull roof anatomy of *Tiktaalik* (NUFV 108). Isolated braincase with the palate and cheek digitally removed, seen in (a) right lateral, (b) right ventrolateral oblique, and (c) ventral views. Blue corresponds to the ossified chondrocranium, whereas grey corresponds to associated dermal bones. While the intracranial fissure (icf) is still open, anterior advancement of the prootics (pro) that spans dorsolateral to the basipterygoid process (art. bpt). Due to dorsoventral compression of the skull, the suprapterygoid and basipterygoid articulations (art. spt and art. bpt) of the palatoquadrate have converged into close proximity with each other, in contrast to the condition seen in *Eusthenopteron* (Jarvik 1980).

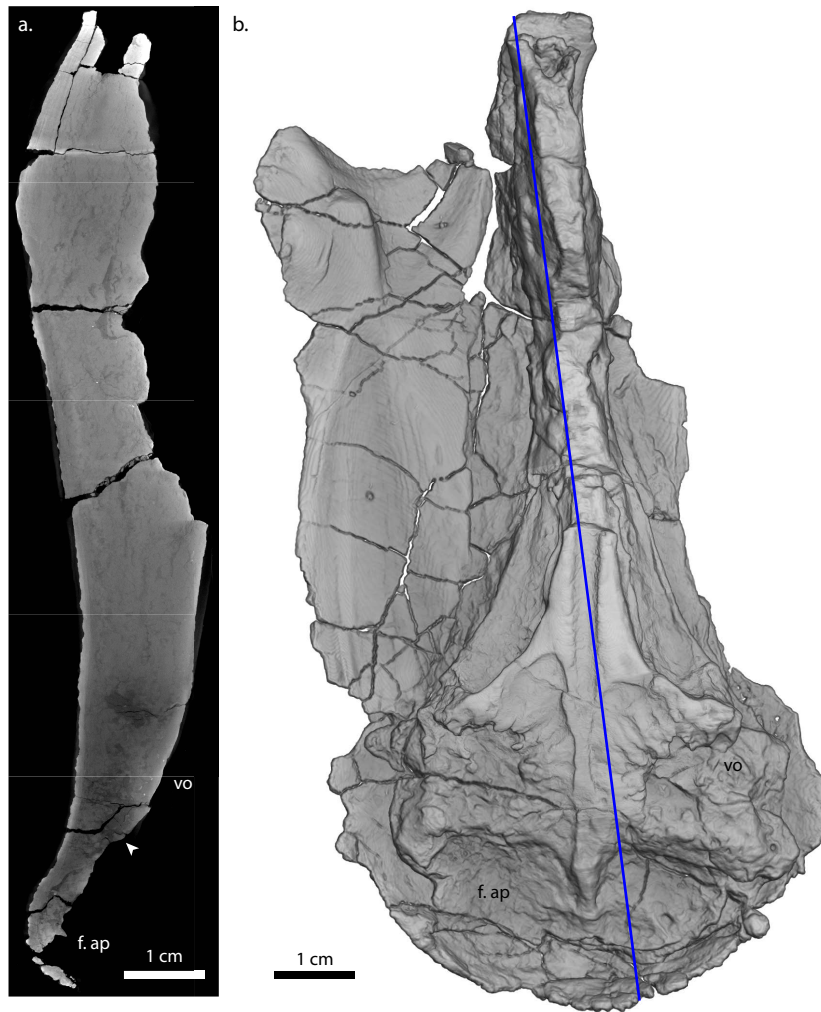


Figure 2.3. Extent of internal ossification in the sphenethmoid region of *Tiktaalik* (NUFV 111). The oblique-sagittal cross section (left) shows a gradient of ossification from well-ossified posteriorly (top) to weakly ossified (bottom). Ventral view of the sphenethmoid (right) shows that this weakly ossified portion corresponds to the sphenethmoid dorsal to the fossa apicalis and vomers, medial to the nasal capsule.

2.4.1 – Chondrocranium and dermal skull roof

Sphenethmoid

The sphenethmoid forms the anterior ossification of the chondrocranium, as in all sarcopterygians (Fig. 2.2). However, the derived sphenethmoid of *Tiktaalik* is extremely elongate, compared with other tetrapodomorph fishes, including *Panderichthys*. Unlike early

limbed tetrapodomorphs, such as *Acanthostega* (Clack 1998) and *Ventastega* (Ahlberg et al. 2008), the sphenethmoid of *Tiktaalik* is well-ossified. While most specimens appear to show complete ossification of the sphenethmoid all the way to the distal tip, two specimens (NUFV 111, NUFV 149) indicate that the distal-most tip may be less densely ossified than the rest, representing the earliest example of an unossified portion of the ethmoid more typically found in early limbed tetrapodomorphs (Figs. 2.3 and 2.4). Despite this, the nasal capsule and sphenoid portions of the braincase remain well ossified, even allowing the course of blood vessels and the olfactory canal to be traced through the sphenoid and nasal capsule of *Tiktaalik* in detail not available for later limbed tetrapodomorphs. While not directly pertinent to feeding, the circular cross section of these canals indicates the anterior braincase region is relatively well ossified and has remained largely undistorted during the fossilization process (see section on retrodeformation).

The well-ossified sphenethmoid of *Tiktaalik* also forms an important component of the dorsal roof of the mouth along with the vomers and parasphenoid. Unlike in later limbed tetrapodomorphs (Clack 1994a, Ahlberg et al. 2008), where the paired entopterygoids abut at the midline, the sphenethmoid and parasphenoid of *Tiktaalik* completely divide the left and right palates. The paired vomers completely surround the ventral surface of the nasal capsules and bear large pits for the development of vomerine fangs. Anterior to the vomers, an indentation between the vomers and premaxilla provides space for the symphyseal fangs of the lower jaws. This concavity, the fossa apicalis (Jarvik 1980), is roofed by a particularly weakly ossified portion of the ethmoid (Fig. 2.4). Otherwise, the sphenethmoid forms a robust, well-ossified, midline strut running along the dorsal roof of the mouth.

The sphenethmoid articulates with the palate in several places. The largest of these articulations is the basipterygoid process, which in *Tiktaalik*, has two articular facets: one for the metapterygoid facing posterodorsally and one corresponding to an unossified portion of the palate anterodorsally. This recess of the palate is seen in limbed tetrapodomorphs as well, but in larger *Tiktaalik* specimens this portion is ossified. The basipterygoid of *Tiktaalik* (Downs et al. 2008) is enlarged compared with that of *Panderichthys* (Ahlberg et al. 1996) or *Eusthenopteron* (Jarvik 1980), and it is proportional to the basipterygoid process in limbed tetrapodomorphs, such as *Acanthostega* (Clack 1998, Clack 2012). Unlike tristichopterids (Jarvik 1980), the basipterygoid, suprapterygoid, and prootic articulations have converged close together due to dorsoventral shortening of the skull (Fig. 2.2). The suprapterygoid fossa immediately dorsal to the basipterygoid receives the metapterygoid. Anteriorly, the palate articulates with the posterior wall of the nasal capsule by means of a small anterior prong of the dermopalatine that inserts into a facet formed by the vomer ventrally and the nasal capsule anteriorly. The crista suspensoria of the braincase articulates with a weakly ossified portion of the palatoquadrate, the commissural lamina. This articulation shows evidence of being loose and is disarticulated in many specimens. There does not appear to be a direct bony articulation between the autopalatine and ethmoid, although a weakly ossified autopalatine does appear to reach as far as the posterior wall of the nasal capsule.

Otoccipital

Ossification of the otoccipital region of the braincase is varied, with the otic region of *Tiktaalik* being well-ossified, whereas the occipital region is less ossified. There is no sign of reduction of the lateral wall of the otic capsule that could be interpreted as early signs of a fenestra ovalis. The basioccipital of larger *Tiktaalik* specimens is pronounced, bulbous, and

innervated by numerous foramina radiating from the foramen magnum, but in the smaller holotype specimen (NUFV 108), the basioccipital is reduced and, similar to *Acanthostega* (Clack 1994a), is only loosely attached to the rest of the endocranium (Downs et al. 2008). In cross section it possesses a thickened ring of bone surrounding the insertion for the notochord and the foramen magnum, with small foramina extending from the center and radiating outwards (Fig. 2.12g). While the occipital bones, where present, are well-ossified, it is impossible to rule out that some unossified portion of the posterior braincase could have collapsed dorsoventrally, shortening the skull in that region. In particular, there is little space for a posttemporal fossa in *Tiktaalik roseae*, which seems to indicate some collapse of the posterior braincase. However, overall the chondrocranium of *Tiktaalik* is more consistently ossified, similar to *Eusthenopteron*, compared to the chondrocrania of early limbed tetrapodomorphs, such as *Acanthostega* or *Ventastega*.

The lateral commissure of the otic capsule projects posterolaterally providing articular surfaces for the hyomandibula immediately ventral to a concave surface of the overlying tabular (Fig. 2.2). The articular surface is vertically oriented with a slight ventromedial slant, and corresponds to both the hyomandibula, as well as the suprapharyngeal element of the first branchial arch. Similar to the convergence of the basipterygoid and suprapterygoid articulations in the sphenethmoid, the lateral commissure of the otic region is dorsoventrally compressed compared to those found in *Eusthenopteron* (Jarvik 1980).

Intracranial fissure, intracranial hinge, and the prootic process

As in other sarcopterygians (Ahlberg et al. 1996), the otoccipital is separated from the sphenethmoid by a clear intracranial fissure; however, *Tiktaalik roseae* shows the earliest signs of closure of that fissure. In addition to interdigitations along the hinge line between the parietal-

postparietal shields known from other elpistostegids (Ahlberg et al. 1996), the prootic process of *Tiktaalik* extends anterior to the intracranial fissure, resting lateral to the sphenethmoid and integrating with the overlying dermal bones that lie anterior to the intracranial hinge (Fig. 2.2). In doing so, the prootic buttress immobilizes any movement between the parietal and postparietal shields. The prootic buttress also supports a boney shelf formed by the supratemporal and intertemporal, which underlaps the postorbital. As such the prootic is an important integrating support structure between the two elements of the chondracanium, as well as between the dermal cheek and dermal skull roof.

Postparietal

The postparietals of *Tiktaalik* are the posterior-most paired bones along the midline of the skull table. They lie immediately posterior to the intracranial hinge line, which is still apparent from surface views despite minor interdigitations along their contact with the parietals. In contrast, these bones are tightly interdigitated with each other along the midline (Fig. 2.6b), similar to *Acanthostega* (Markey and Marshall 2007), and they rest on top of the paired exoccipital bones of the underlying braincase. Laterally they overlap the tabular and supratemporal bones.

Tabular

The tabular is an elongate bone that runs laterally along most the length of the postparietal, which it underlaps in a beveled scarf joint (Fig. 2.6c). Similar to the supratemporal, it houses the postotic lateral line canal, but it also appears to have several canals that descend ventrally into the underlying chondrocranium. The tabular has a concave surface on its posterior ventral surface that articulates with the hyomandibula.

Supratemporal

The supratemporal of *Tiktaalik* lies immediately lateral to both the parietal and postparietal bones. While typically associated with the postparietal shield in osteolepidid and tristichopterid fishes, the supratemporal bones extend anterior to the intracranial hinge (Fig. 2.9), suturing with the posterior margins of the parietals and intertemporal bones (Fig. 2.7c). In cross section, these sutures are more tightly integrated than the parietal-postparietal suture, and therefore the supratemporal can be considered the primary dermatocranial element that immobilized the intracranial hinge. Supported by the underlying prootic buttress, the supratemporal and intertemporal bones form a short boney shelf that underlaps the postorbital (Fig. 2.7b). The postotic lateral line canal runs from the intertemporal posteriorly through the supratemporal to the tabular.

Intertemporal

The intertemporal of *Tiktaalik* is a small, scale-shaped bone on the dermal skull roof. It lies immediately medial to the postorbital, posterior to the postfrontal, lateral to the parietal, and anterior to the supratemporal. While dorsal exposure of the intertemporal is small, it has a significant component that is overlapped by the postorbital (Fig. 2.9). This boney shelf lies immediately anterior to the boney shelf of the supratemporal and the prootic buttress (Fig. 2.7b). It lies posterior to the postfrontal and lateral to the parietal. The presence of this bone was inferred by its presence in phylogenetically close taxa, such as *Ventastega*, *Acanthostega*, and *Panderichthys*; however, the intertemporal is also missing in other taxa, such as *Elpistostege* and *Ichthyostega*. When present this bone joins together the infraorbital, supraorbital, and postotic lateral lines, which appears to be the case in *Tiktaalik roseae*.

Parietal

The parietal bones are a pair of midline bones that lie just posterior to the frontal bones. The parietals interdigitate with the frontal bones approximately midway along the length of the postfrontals. Posteriorly, the hinge line between the parietal and postparietal is visible from surface views whereas, in cross section, some interdigitations are visible (Fig. 2.7a). Lateral to this joint, the parietal contacts the supratemporal in a more tightly integrated joint than the parietal-postparietal joint. The transition between these bones is difficult to make out in cross sections, likely due to sutural interdigitations finer than the scanning resolution.

Frontal

The frontal extends mid-length down the rostrum, medial to the prefrontals and postfrontals. The suture between the parietals and frontals are difficult to make out, but the frontal-nasal joint is a clear scarf joint, with the nasal overlapping the frontal (Fig. 2.5c). The paired frontals contact each other at the midline, and an interdigitating suture can be seen running between the two (Fig. 2.5b, 2.6e-f), a derived trait more similar to what is reported for the terrestrial temnospondyl, *Phonerpeton*, than for *Eusthenopteron* (Markey and Marshall 2007).

Postfrontal

The postfrontal bone of *Tiktaalik* forms the medial rim of the orbit. This bone has a distinct raised ridge dorsomedial to the orbits similar to other elpistostegids and, to a lesser extent, *Ventastega* (Ahlberg et al. 2008). Similar to *Acanthostega* and *Elpistostege*, the postfrontals of *Tiktaalik* are smaller than the condition reported in *Panderichthys* (Ahlberg et al. 2000). The postfrontal briefly overlaps the prefrontal, and posteriorly it overlaps the intertemporal (Fig. 2.6d).

Prefrontal

The prefrontal of *Tiktaalik* is an elongate bone running parallel to the lacrimal, extending from the orbit to the external nares. Like *Elpistostege* and *Acanthostega* (Ahlberg et al. 2000), the prefrontal of *Tiktaalik* is enlarged compared to earlier taxa, such as *Eusthenopteron* (Jarvik 1980) or *Panderichthys* (Ahlberg et al. 2000). This bone is characterized by significant beveling of its contact with the lacrimal laterally, which overlaps the prefrontal for most of its length (Figs. 2.6g, 2.7h). Where the jugal-lacrimal-prefrontal all converge, the lacrimal-prefrontal contact still remains overlapping, but the jugal sends a small flange that appears to underlap the prefrontal. Medial to this contact with the jugal, the prefrontal has a dorsally deflected ridge that rises to contact the postfrontal and frontal. The contact between the prefrontal-frontal is more rounded and less beveled than the lacrimal-prefrontal joint, and the prefrontal is overlapped by the frontal and postfrontal.

Nasals and the rostral mosaic

As in *Acanthostega* (Markey and Marshall 2007), the nasals overlap the frontal bones in an elongate scarf joint (Fig. 2.5d). Anterior to this joint, however, the mosaic of small fragmented bones becomes difficult to discern and compare between taxa (Figs. 2.5e-h, 2.6h-i). Similar to the rostral bones of *Panderichthys* and *Elpistostege*, the mosaic pattern of these bones in *Tiktaalik* appears to vary between specimens. Where this shield overlays the well ossified nasal capsule, these bones tend to be thin and difficult to discern from the underlying endochondral bone. Where the rostrals overlie the weakly ossified portion of the ethmoid, they tend to be broken, fragmentary, and occasionally missing (Fig. 2.4). The condition of these anterior bones becomes slightly more robust close to their contacts with the anterior tectals and premaxilla.

Anterior tectal and premaxilla

The anterior tectal bone lies immediately anterior to the prefrontal and is overlapped slightly by the anterior tip of the lacrimal. Similar to the premaxilla, it is overlapped dorsally by a canal bearing nasal or rostral bone (Fig. 2.4b).

The premaxilla forms an anterior continuation of the marginal tooth row from its posterior contact with the maxilla. This tooth row extends anterior to the apical fossa of the sphenethmoid and it is overlapped dorsally by the rostral bones (Fig. 2.4f). Compared to the elongate maxilla, the premaxilla only forms about one third of the marginal tooth row. Where it meets the maxilla posteriorly, the break in the dental arcade forms the lateral wall of the choana.

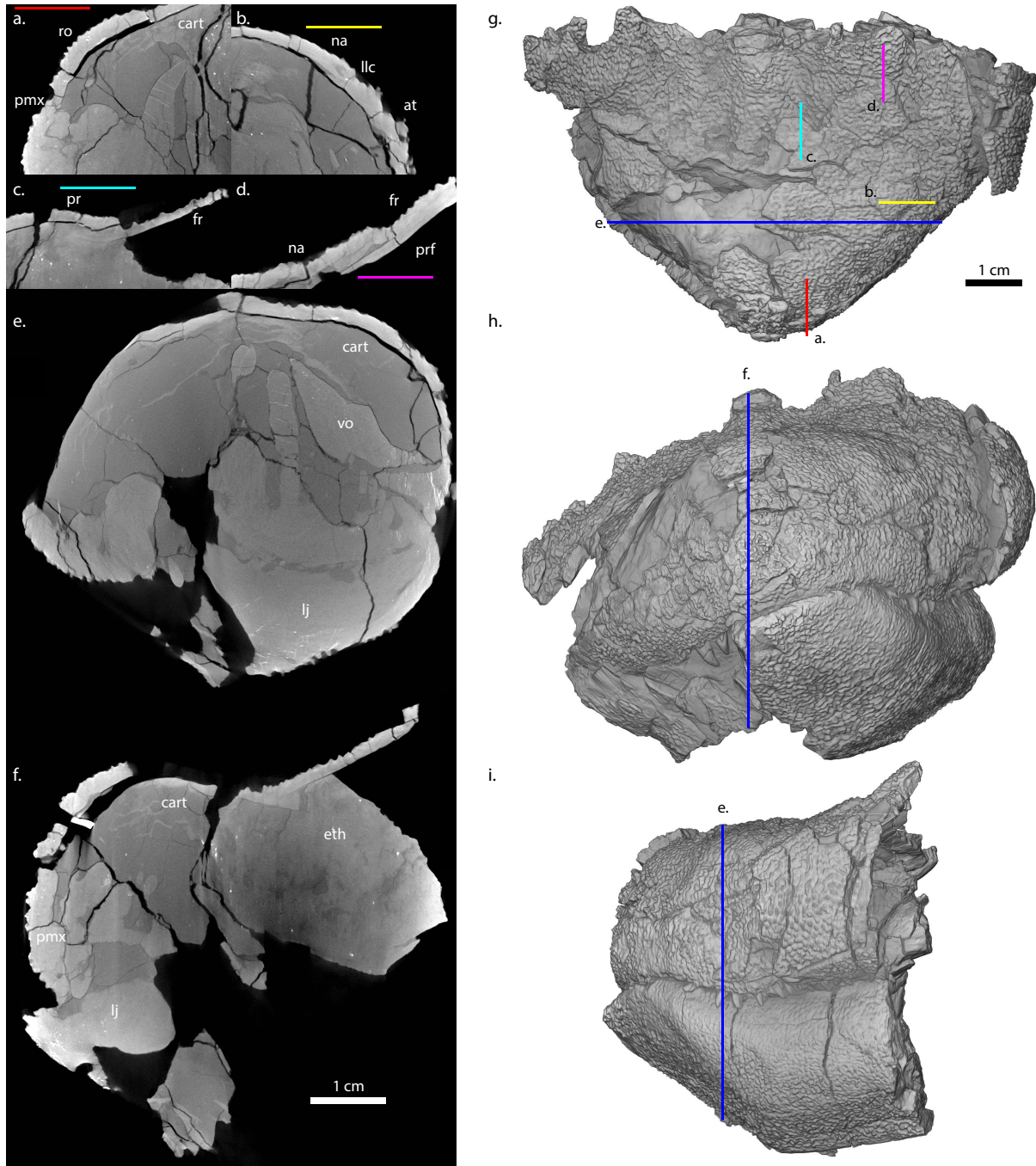


Figure 2.4. Details of internal sutures and ossification of the anterior rostrum of *Tiktaalik* (NUFV 149). (a) Parasagittal section showing the weakly ossified cartilage at the roof of the fossa apicalis. (b) Transverse section showing overlap of the anterior tectal by a canal bearing nasal bone; (c) Parasagittal section showing overlap of the frontal by a posterior rostral. (d) Parasagittal section showing complex overlapping patterns of the nasal bone over the frontal, both of which overlap the prefrontal. (e) Transverse cross section showing weakly ossified anterior cartilage at the roof of the fossa apicalis. (f) Parasagittal (slightly oblique) cross section

Figure 2.4, continued. showing the corresponding ossified and weakly ossified cartilaginous portions of the ethmoid. (g) Dorsal exterior view detailing remnants of the rostral shield and exposed ethmoid cartilage. (h) Anterior exterior view. (i) Left lateral exterior view. Reference color bars and scale bars each correspond to 1 cm.

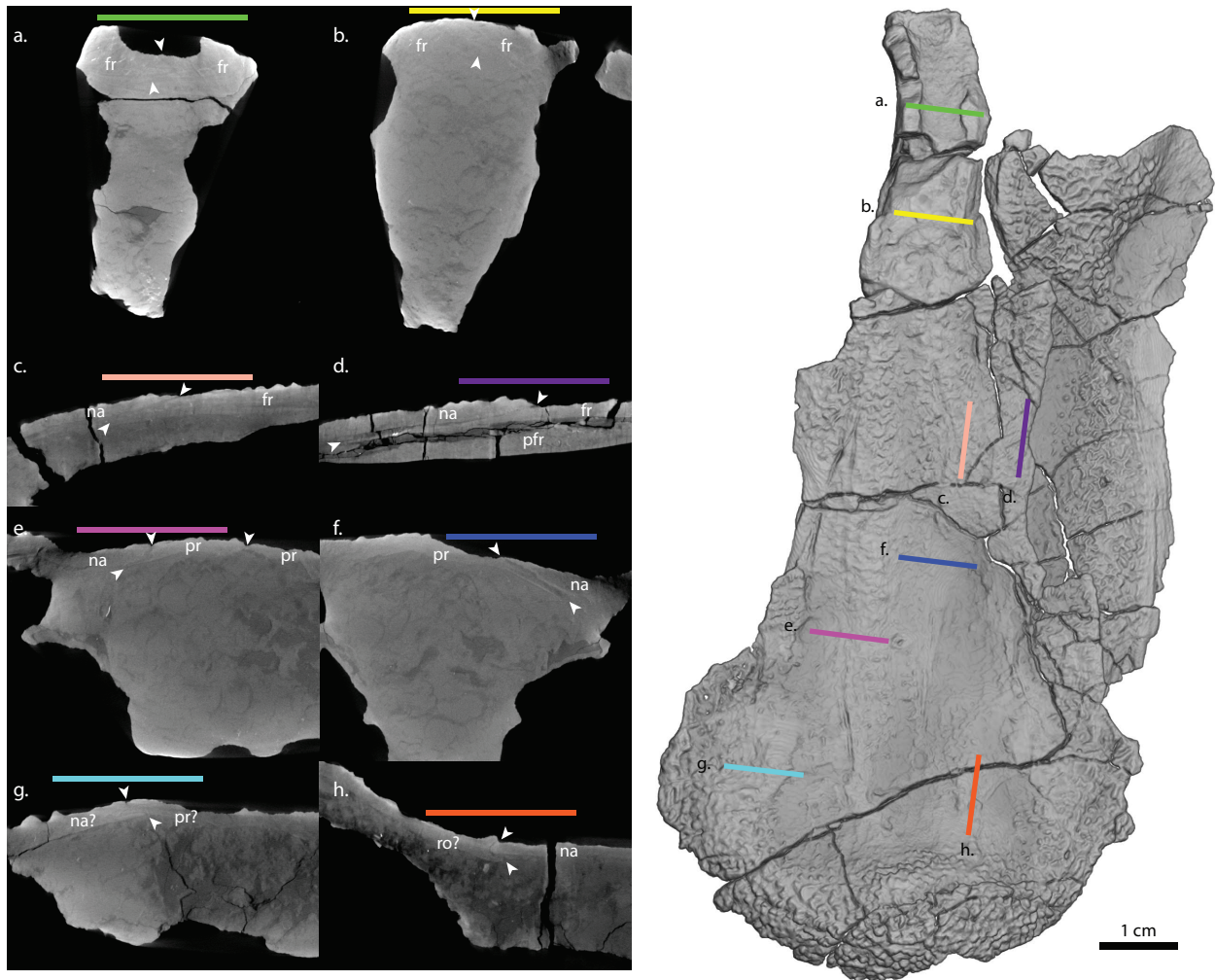


Figure 2.5. Internal sutural anatomy of the frontal-nasal shield of *Tiktaalik* (NUFV 111). (a) Inter-frontal suture. (b) Inter-frontal suture. (c) Beveled suture of nasal overlapping the frontal. (d) Detail of the beveled suture between the nasal and frontal bones which both overlap the prefrontal. (e-f) Details of the beveled and slightly interdigitating joints between the lateral nasals overlapping the postrostrals medially. (g-h) Beveled and slightly interdigitating sutures between the nasals and rostrals / postrostrals in the anterior region of the snout. Colored reference bars and scale all correspond to 1 cm.

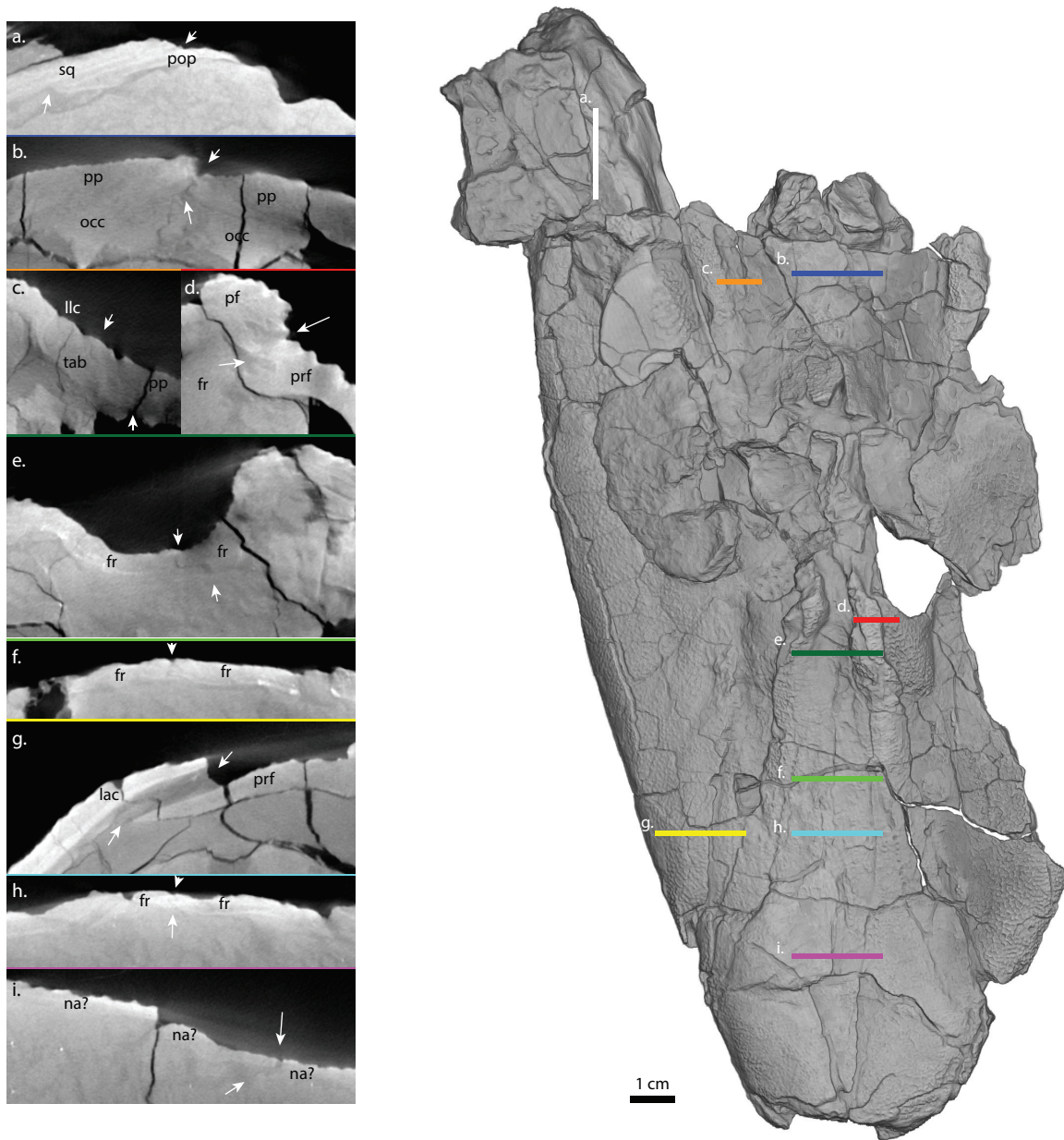


Figure 2.6. Internal sutural anatomy of the skull roofing bones of *Tiktaalik* (NUFV 110) showing prevalence of interdigitating joints along the midline. Shown are cross sections and an external dorsal view of skull. (a) Beveled suture between squamosal (overlap) and preopercle (underlap). (b) Interdigitating inter-postparietal suture dorsal to the occipital region of the braincase. (c) Postparietal overlapping the tabular in a beveled suture. (d) Complex interlocking joint between the postfrontal, prefrontal, and frontal. (e) Interdigitating inter-frontal suture. (f) Slightly interdigitating inter-frontal suture. (g) Loose overlapping scarf joint between the lacrimal and prefrontal. (h) Interdigitating sutures between frontals. (i) Slightly beveled sutures between nasal and/or rostral bones. **Figure 2.6, continued.** Colored reference bars are 2 cm except for c. and d, which are 1 cm.

2.4.2 – Dermal cheek and lateral tooth row

Lacrima

The lacrima of *Tiktaalik* extends from the external opening of the nares to the anterolateral margin of the orbit (Figs. 2.8 and 2.9). The bone is chevron shaped and covered in small, tubercular dermal sculpting (Witzmann et al. 2010), which obscures the external appearance of its suture with the jugal. In previous reconstructions, a prominent visible line interpreted to be the lacrima-jugal suture was depicted extending posteriorly to make contact with the postorbital (Daeschler et al. 2006) similar to the reconstructions for *Elpistostege* (Schultze and Arsenault 1985); however, this line is identified from CT scans to be the infraorbital lateral line canal. The actual suture between the lacrima-jugal runs nearly parallel and slightly anterior to it (Figs. 2.7g, 2.9). This suture is broadly beveled in cross section, but it develops a slight tongue-in-groove architecture closer to its articulation with the maxilla.

A prominent joint runs from the orbit to the nares, between the lacrima and prefrontal bones (Fig. 2.6g, 2.7h), and the comparisons between multiple specimens confirm this scarf joint to be non-sutural. Beveled sutures, although broadly overlapping, remain in articulation despite localized postmortem crushing. In contrast, the lacrima-prefrontal joint is loosely articulated and filled in with sediment when compared beveled sutures found throughout the dermal cheek and skull table. In specimens where the palate has been displaced medially (NUFV 110), this joint shows further pronounced overlap between the two bones (Fig. 2.13c). In specimens where the skull has been dorsoventrally crushed (NUFV 108), the joint remains patent, although posteriorly, where it integrates with the jugal, the joint has buckled dorsolaterally. The surface of the prefrontal that is overlapped by the lacrima is smooth and free of dermal sculpting.

The infraorbital lateral line canal runs the length of the lacrimal, joining with the canal running through the jugal posteriorly. This canal is immediately dorsal to the joint of the lacrimal with maxilla, which takes the form of a longitudinal overlapping joint.

Jugal

The jugal is a one of the largest bones in the external cheek. It is a large plate like bone that forms a portion of the orbit and articulates with the lacrimal, postorbital, squamosal, quadratojugal, and maxilla (Fig. 2.8). Anteriorly, the bone is overlapped by the lacrimal. Whereas the lacrimal primarily overlaps the prefrontal, close to the orbit, a small portion of the jugal is overlapped by the prefrontal in a complex, tongue-in-groove joint with the lacrimal. An extensive portion of the jugal is overlapped by the postorbital and the scarf joint appears to be looser than in other joints between dermal cheek elements. The jugal has a tongue-in-groove joint with the squamosal (Fig. 2.7e), where the squamosal is both overlapped and underlapped by ridges of the jugal. The jugal also overlaps the maxilla and an anterior extension of the quadratojugal.

The infraorbital and preopercular-mandibular lateral line canals meet at a junction within the jugal. The infraorbital canal ventral to the postorbital leaves a clear line of indentation on its dorsal surface that could be mistaken for a suture with the lacrimal (see above). The infraorbital lateral line extends dorsally to insert into the postorbital. The preopercular-mandibular lateral line extends posteriorly to insert into the squamosal.

Postorbital

The postorbital is the dorsal-most bone of the dermal cheek, and it overlaps all the surrounding bones (Fig. 2.8). The overlap with the jugal is extensive, and the scarf joint here is slightly disarticulated and appears somewhat loose (Fig. 2.7f). The posterior overlap with the

squamosal is less extensive. Similar to the lacrimal, the postorbital also articulates with the dermal skull roof. The skull roof articulation is intricate and includes a minimum of three bones, the postfrontal, intertemporal, supratemporal, and perhaps the prootic process itself. These components of the skull roof compose a boney shelf supported by the prootic buttress that the postorbital overlaps and rests upon. Unlike the condition reported for *Acanthostega*, none of these bones interdigitates directly with the postorbital (Fig. 2.7b), and instead, the postorbital maintains a clear division from the dermal skull roof. Similar to the prefrontal-lacrimal scarf joint, this articulation is loose, slanted, and somewhat disarticulated.

Squamosal

The squamosal lies posterior to the postorbital and jugal, and it bears the posterior branch of the preopercular-mandibular lateral line canal. It overlies a portion of the palatoquadrate, and where the palatoquadrate has been crushed upwards, a break can be seen in the squamosal as well. The squamosal slightly overlaps the preopercular (Fig. 2.6a) and overlays the quadratojugal (Fig. 2.7d). Where it articulates with the jugal, it sends a ridge of bone anteriorly that is both overlapped and underlapped by the jugal in a tongue-in-groove joint.

Preopercular

The preopercular is a small rectangular bone on the posterior edge of the dermal cheek. It is overlapped slightly by the squamosal (Fig. 2.6a), and it rests on top of the quadrate. Its ventral edge overlaps the quadratojugal as well. The preopercular also houses a canal for the lateral line proximal to where it inserts into the mandible.

Quadratojugal

The quadratojugal is peculiarly large in *Tiktaalik*. The main portion of the quadratojugal lies ventral to and is overlain by the squamosal; however, a long, anterior prong of the

quadratojugal extends anteriorly (Fig. 2.8). This prong lies medial to the jugal and dorsal to the maxilla. It tapers as it reaches anteriorly, and its articulation with parallel bones appears to be smooth with no interdigitations. While this appears to be the case in multiple specimens (NUFV 108 and 110), this is an unusual characteristic and may represent a broken and disarticulated portion of the maxilla.

Maxilla

The maxilla is an elongate tooth-bearing bone that runs from the choana to the lateral rim of the adductor chamber. This bone is overlapped by the lacrimal and jugal and the articulation with those bones takes the form of a smooth, longitudinal suture. While this bone is expected to lie ventral to the lacrimal and jugal, in several *Tiktaalik* specimens examined, it appears to have been twisted inwards, so that instead of being arranged vertically, the teeth are facing inwards (Figs. 2.12 and 2.13). The tooth row extends the entire length of the maxilla, and multiple teeth can even be found lateral to the adductor chamber.

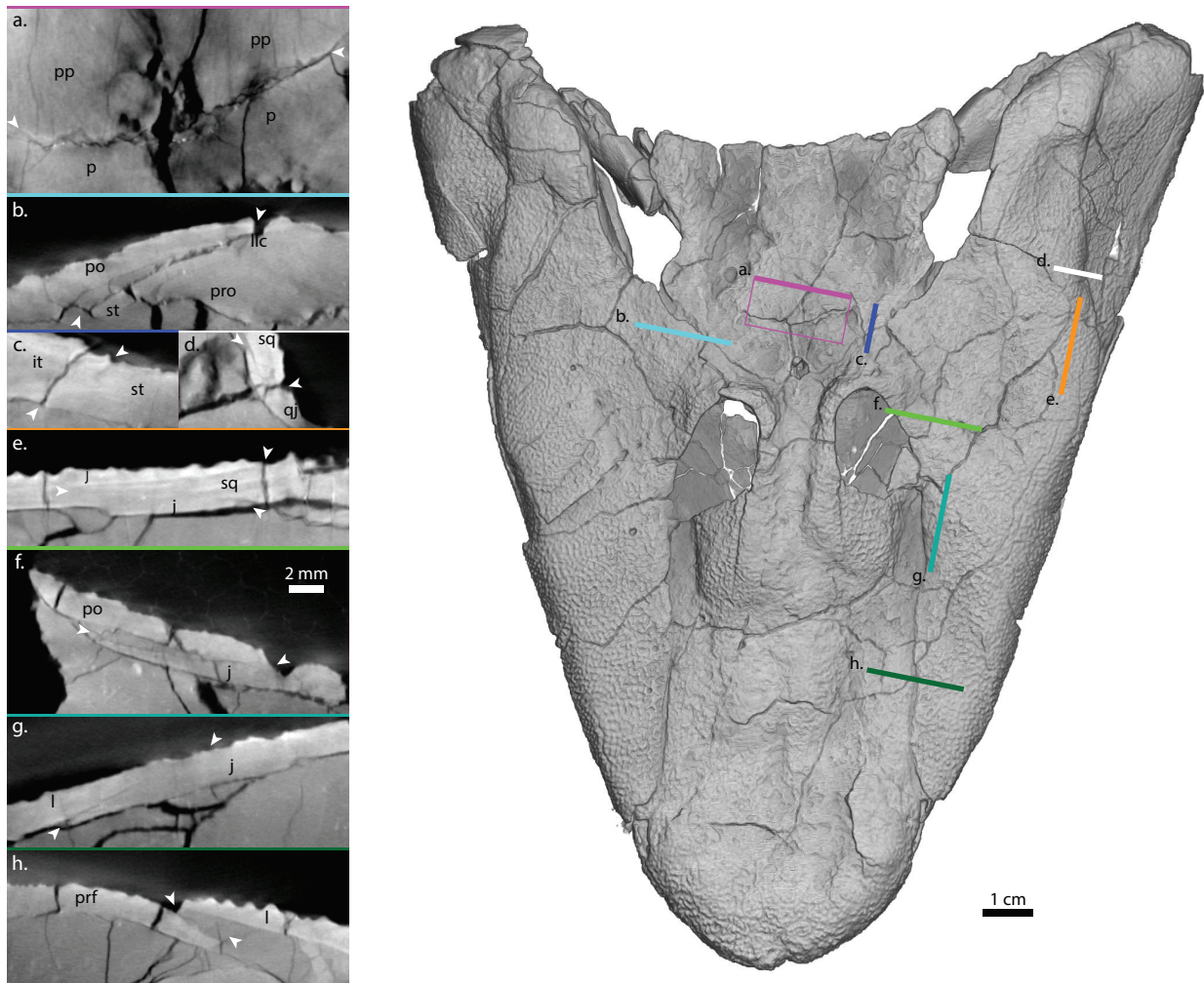


Figure 2.7. Internal sutural anatomy of the dermal cheek and intracranial hinge of *Tiktaalik* (NUFV 108) highlighting differences between beveled sutures and scarf joints. Shown are cross sections and an exterior dorsal view of skull. (a) Dorsal view of the intracranial hinge showing slight interdigitations between the parietals and postparietals. (b) Loose overlapping scarf joint between the postorbital and underlying supratemporal supported by the prootic. (c) Interdigitations between the intertemporal and supratemporal. (d) Beveled suture between the squamosal and the underlying quadratojugal. (e) Tongue-in-groove joint between the squamosal and the surrounding posterior flanges of the jugal. (f) Scarf joint between the postorbital and the jugal. (g) Beveled suture between the lacrimal and jugal. (h) Loose scarf joint between the prefrontal and the overlapping lacrimal. All colored reference bars are 2 cm, except c. and d. (1 cm).

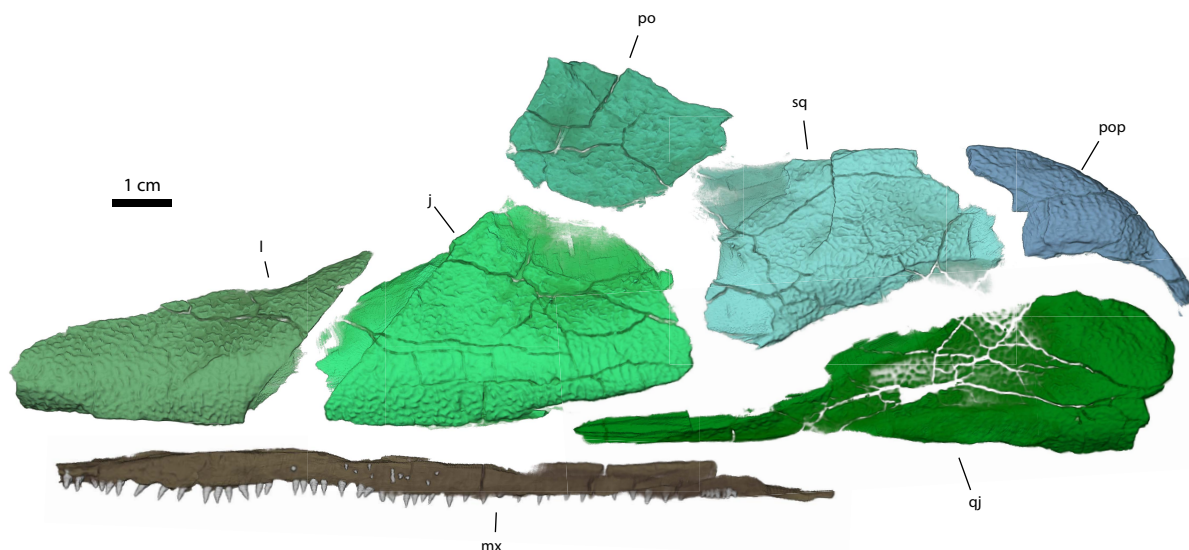


Figure 2.8. Isolated dermal cheek bones of *Tiktaalik* (NUFV 108) showing extent of overlap between elements. Exploded left-lateral view of dermal cheek bones and maxilla. Overlaps exist between the lacrimal-jugal, jugal-postorbital, squamosal-postorbital, squamosal-preopercle, and squamosal-quadratojugal (see Figs. 2.6a, 2.7d-g for internal detail). Due to postmortem deformation, the maxilla has been crushed inwards and is covered externally by the lacrimal and jugal (Fig. 2.12d).

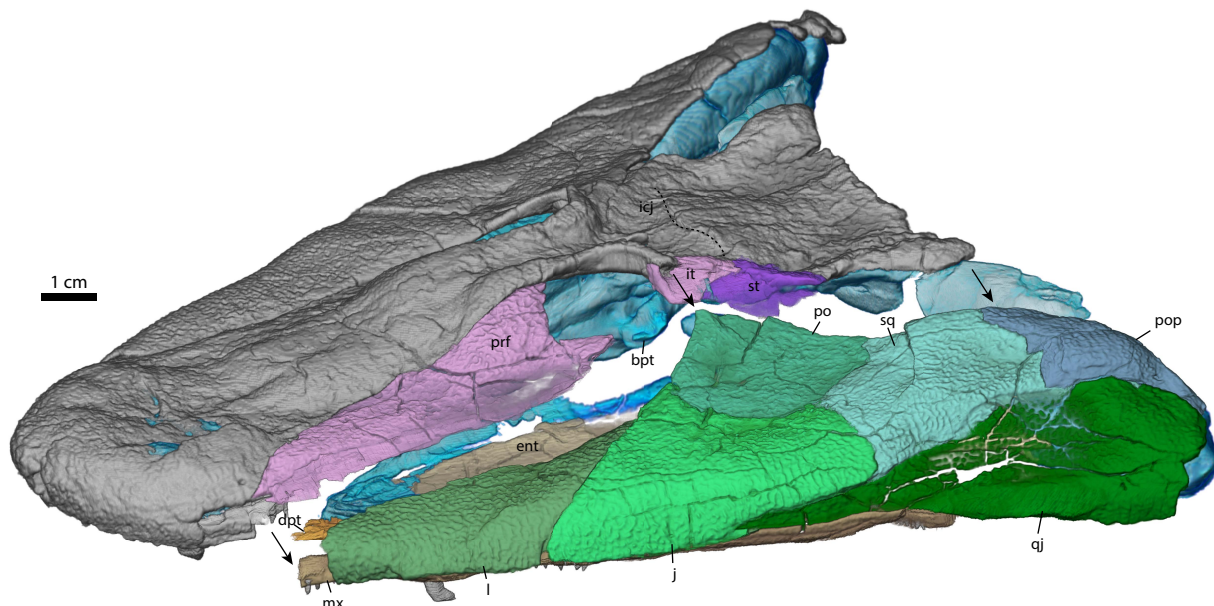


Figure 2.9. Disarticulation of the cheek and palate from the braincase of *Tiktaalik* (NUFV 108) showing exposed areas of overlap with the skull roof. Shown is an oblique dorsolateral view of the skull with the left cheek and palate digitally isolated and displaced relative to their

Figure 2.9, continued. articulations with the braincase. Loose scarf joints are found between the lacrimal-prefrontal and postorbital-supratemporal-intertemporal (see Figs. 2.6g, 2.7b, 2.7h for internal detail). These scarf joints differ in morphology from other beveled sutures (compare with Figs. 2.5d, 2.6a, 2.7g) and are found along the anatomical division between the dermal cheek and skull roof of other tetrapodomorph fish (Jarvik 1980).

2.4.3 – Endochondral and dermal palate

Quadrate

The quadrate of *Tiktaalik roseae* is the largest endochondral ossification of the palatoquadrate (Fig. 2.11). Posteriorly it has a bicondylar articulation with the jaw joint, with the medial condyle resting lower than the lateral condyle. This is similar to the condition reported for other limbed tetrapodomorphs, including *Acanthostega*, temnospondyls, and modern crocodilians. Similar to *Panderichthys* (Brazeau and Ahlberg 2006), the medial surface of the quadrate is grooved, presumably for articulation with the distal, unossified portion of the hyomandibula (Downs et al. 2008). The ventral surface of the quadrate is covered by and partially fused with the entopterygoid. Dorsally, the quadrate is covered by the squamosal and preopercle, which appear to have a loose, overlapping articulations with the dorsal surface of the quadrate. Anteriorly, the quadrate co-ossifies with the metapterygoid, and the boundary between these bones is hard to make out. There is a seam, however, that runs through this co-ossification, and in some specimens, it appears to have broken in some places (see postmortem deformation section).

Metapterygoid (= epipterygoid)

The metapterygoid (= epipterygoid) of *Tiktaalik roseae* is the primary contact of the palatoquadrate with the chondrocranium (Fig. 2.10). The ascending process of the metapterygoid is a relatively thin stylus that fits into the suprapterygoid fossa, an indentation on the lateral wall of the sphenethmoid. The metapterygoid is bounded ventrally by the basipterygoid process of the

sphenethmoid and dorsally by the anterior extension of the prootic (Fig. 2.9). While these articulations leave clear corresponding facets on the metapterygoid of tristichopterid fishes (Jarvik 1980), in *Tiktaalik* the metapterygoid primarily articulates with the suprapterygoid fossa. Along its distal length, the metapterygoid is surrounded and co-ossified with the entopterygoid, similar to *Acanthostega* (Clack 1994a). Although co-ossified with the quadrate, the metapterygoid and quadrate show some indication of separation along the midshaft (Fig. 2.12b).

Autopalatine and commissural lamina

The endochondral palate of *Tiktaalik roseae* also includes the autopalatine and commissural lamina portions (Fig. 2.11). While absent in limbed tetrapodomorphs (Rosen et al. 1981), these anterior extensions of the endochondral palate form a significant portion of palate in tetrapodomorph fishes, such as *Eusthenopteron* (Jarvik 1980). The anterior endochondral palate of *Tiktaalik* is present but thin and weakly ossified. The autopalatine of *Tiktaalik* runs along the lateral length of the palate just dorsal to the dermopalatine and ectopterygoid. While posteriorly the autopalatine co-ossifies with the entopterygoid to form a thickened, robust portion just dorsal to the ectopterygoid (Figs. 2.11, 2.12e-f), as it extends anteriorly, the autopalatine tapers into a thin lamina that covers the dorsal surface of the dermopalatine and medial surfaces of the jugal and lacrimal. Although in *Eusthenopteron*, the autopalatine has a prominent articulation with the ethmoid (Jarvik 1980), in *Tiktaalik* it tapers into a thin lamina just posterior to the ethmoid and does not reach its posterior wall. While present, the reduced autopalatine of *Tiktaalik* appears to represent an intermediate condition between tetrapodomorph fishes and limbed tetrapodomorphs.

The commissural lamina spans the dorsal surface of the palate to connect the autopalatine with the metapterygoid-quadrate endochondral ossifications. This thin lamina is only intermittently ossified, and disappears completely at times; however, closer to the midline, the

medial margin of the endochondral bone thickens into a rounded edge that abuts the sphenoid immediately ventral to the crista suspendens, a ridge formed by a lateral expansion of sphenoid that houses the olfactory nerve. Just anterior to the basipterygoid process, the medial margin of the palate forms a small recess that corresponds with the dorsoanterior articular facet of the basipterygoid process (Fig. 2.10). In life, this articulation may have been cartilaginous. Although loss of the autopalatine also reduces the commissural lamina in limbed tetrapodomorphs, the commissural lamina is still present, albeit thin and weakly ossified, in *Tiktaalik*.

Entopterygoid (= pterygoid)

The entopterygoid (= pterygoid) of *Tiktaalik* is the largest element of the palate (Fig. 2.11). It is a large, horizontal plate of bone that spans between the ethmoid anteriorly and the quadrate and metapterygoid posteriorly. Similar to *Acanthostega* and *Panderichthys*, its orientation relative to the braincase appears to be horizontal (Clack 1994a, Brazeau and Ahlberg 2006). Posteriorly, it fuses and underlaps the endochondral components of the palatoquadrate and forms a ventral margin of the spiracular canal, similar to *Panderichthys* and *Acanthostega* (Clack 1994a, Brazeau and Ahlberg 2006) (Figs. 2.10 and 2.11). The shape and orientation of the entopterygoid is the primary derived feature of the palate of *Tiktaalik*, more similar to limbed tetrapodomorphs than earlier tetrapodomorph fishes.

The entopterygoid of *Tiktaalik* also has plesiomorphic features. Similar to *Eusthenopteron* (Jarvik 1980), the entopterygoid is covered dorsally by a thin commissural lamina (Fig. 2.11). Anterior to the adductor chamber, it appears to co-ossify with the autopalatine to produce a thickened horizontal portion just above the ectopterygoid, which abuts the medial surface of the jugal (Fig. 2.11). Unlike *Acanthostega* (Clack 1994a), the left and right entopterygoids are fully separated at the midline by the parasphenoid and sphenethmoid (Fig.

2.10), and, instead, the autopalatine and entopterygoid have a co-ossified medial margin that connects with the braincase similar to *Eusthenopteron* (Jarvik 1980). Unlike *Eusthenopteron*, however, this lamina is short and does not exhibit a dorsally deflected portion relative to the rest of the palate. Anteriorly, the entopterygoid abuts, but does not form a distinct articulation with the posterior wall of the nasal capsule, instead it curves gently anterolaterally (Fig. 2.10), following the shape of the posterior wall of the ethmoid and gradually overlays the dermopalatine. Laterally, it has a flange that rests above the dermopalatine and ectopterygoid. Along its border with the ectopterygoid and dermopalatine, it bears an additional row of teeth (an internal third tooth row), and where it is exposed in the roof of the mouth (Fig. 2.11), it bears an extensive tooth plate, covered in denticles. As a result, the entopterygoid of *Tiktaalik* is a mixture of plesiomorphic and derived features.

Ectopterygoid

The ectopterygoid is a large tooth-bearing bone that, along with the dermopalatine and vomer, forms the second of three parallel tooth rows in the upper jaws of *Tiktaalik roseae*. The most prominent feature of the ectopterygoid is a deep excavation that houses one or two of the enlarged palatal fangs of the medial tooth row. Dorsal to this excavation, the ectopterygoid is thin or unossified and opens into the chamber for soft tissue between the external cheek and palate. The ectopterygoid lies medial to the maxilla, quadratojugal, and jugal. Along its articulations with these bones, it forms simple longitudinal butt joints with those bones. It lies lateral to the entopterygoid and some portion of the adductor chamber (Fig. 2.10). Its articulation with the entopterygoid is a butt joint medially; however, where the entopterygoid forms a thickened portion co-ossified with the autopalatine posteriorly, the joint becomes overlapping along most of the dorsal surface of the ectopterygoid. Posteromedial to the ectopterygoid, the

palate opens into the space for the jaw adductor muscles. The most posterior teeth of the tooth row even extend lateral to the adductor chamber (Fig. 2.10). Anteriorly, the ectopterygoid sends interdigitating fingers to integrate with the posterolateral margin of the dermopalatine.

Dermopalatine

The dermopalatine is the anterior-most bone of the palate that forms the primary anterior connection of the palate to the braincase. This connection is in the form of a forward-projecting prong that fits into a socket in the posterior wall of the nasal capsule formed by the vomer and ethmoid (Figs. 2.10 and 2.11). The dermopalatine has a tooth row continuous with that of the vomer (anteriorly) and the ectopterygoid (posteriorly), and similar to the ectopterygoid it has a deep excavation for the formation of the palatal fangs. Between the dermopalatine and ectopterygoid, a fossa receives a corresponding coronoid fang pair of the lower jaws. The dermopalatine is overlapped by the weakly ossified anterior extent of the autopalatine, and, where the excavation for the fang pair exists, the dorsal surface of the dermopalatine opens into the matrix filled cavity between the cheek and palate that in life would have been filled with soft tissue. Laterally, the dermopalatine is bounded by the lacrimal and maxilla, which it forms longitudinal butt joints with, and medially, it abuts and is slightly overlapped by the entopterygoid. Although only a small element of the palate, due to its prominent anterior position, the dermopalatine forms an important juncture between the braincase, endochondral palate, dermal palate, and lateral tooth row.

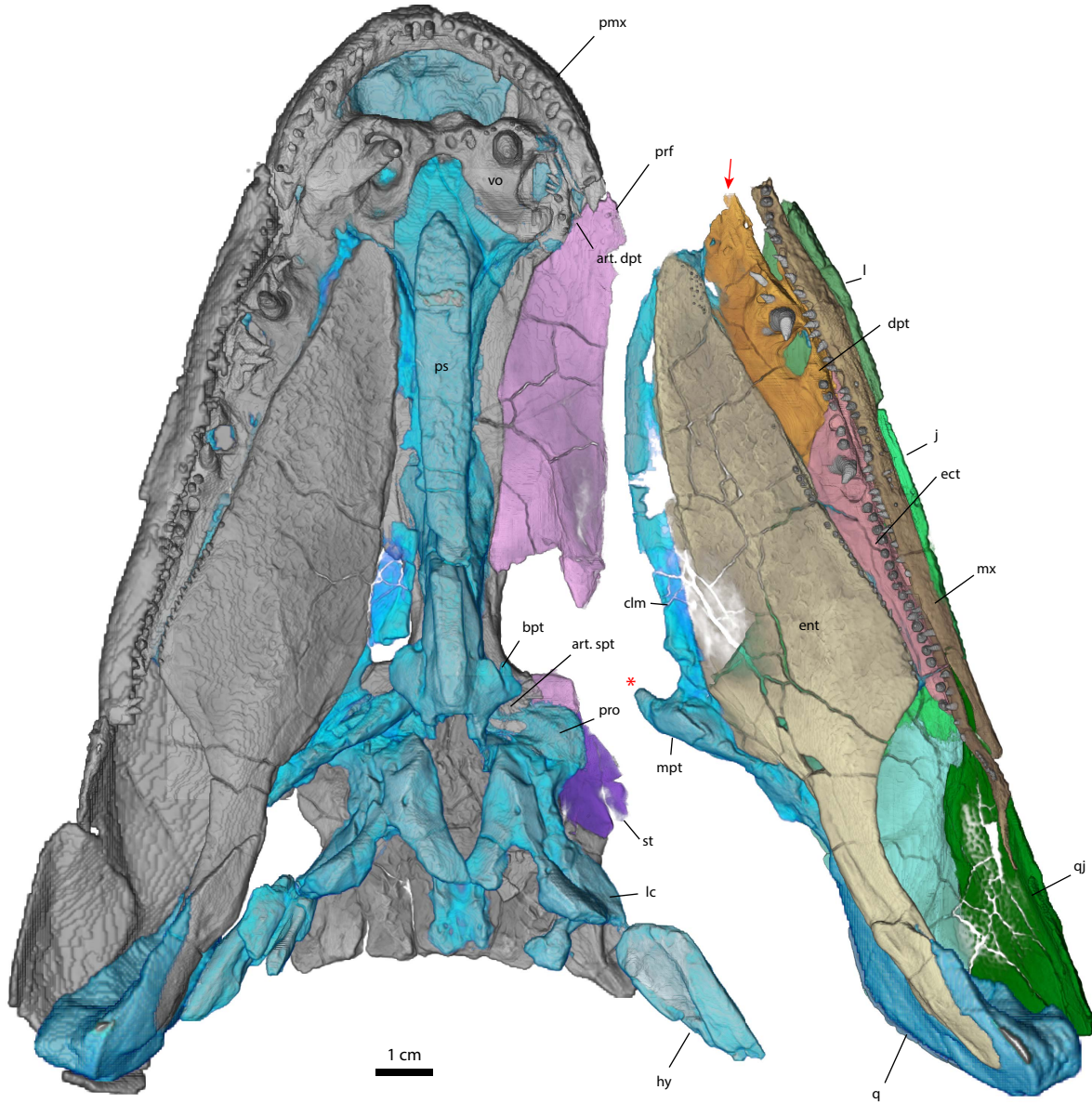


Figure 2.10. Disarticulation of the cheek and palate from the braincase of *Tiktaalik* (NUFV 108) showing exposed articulation points. Shown is a ventral view of the skull with the left cheek and palate digitally isolated and displaced relative to their articulations with the braincase. The most anterior articulation of the palate with the braincase is found on the dermopalatine (dpt), which has a forward facing prong (red arrow) that sockets above the vomer (art. dpt). The ascending process of the metapterygoid (red asterisk) that fits into the suprapterygoid fossa (art. spt).

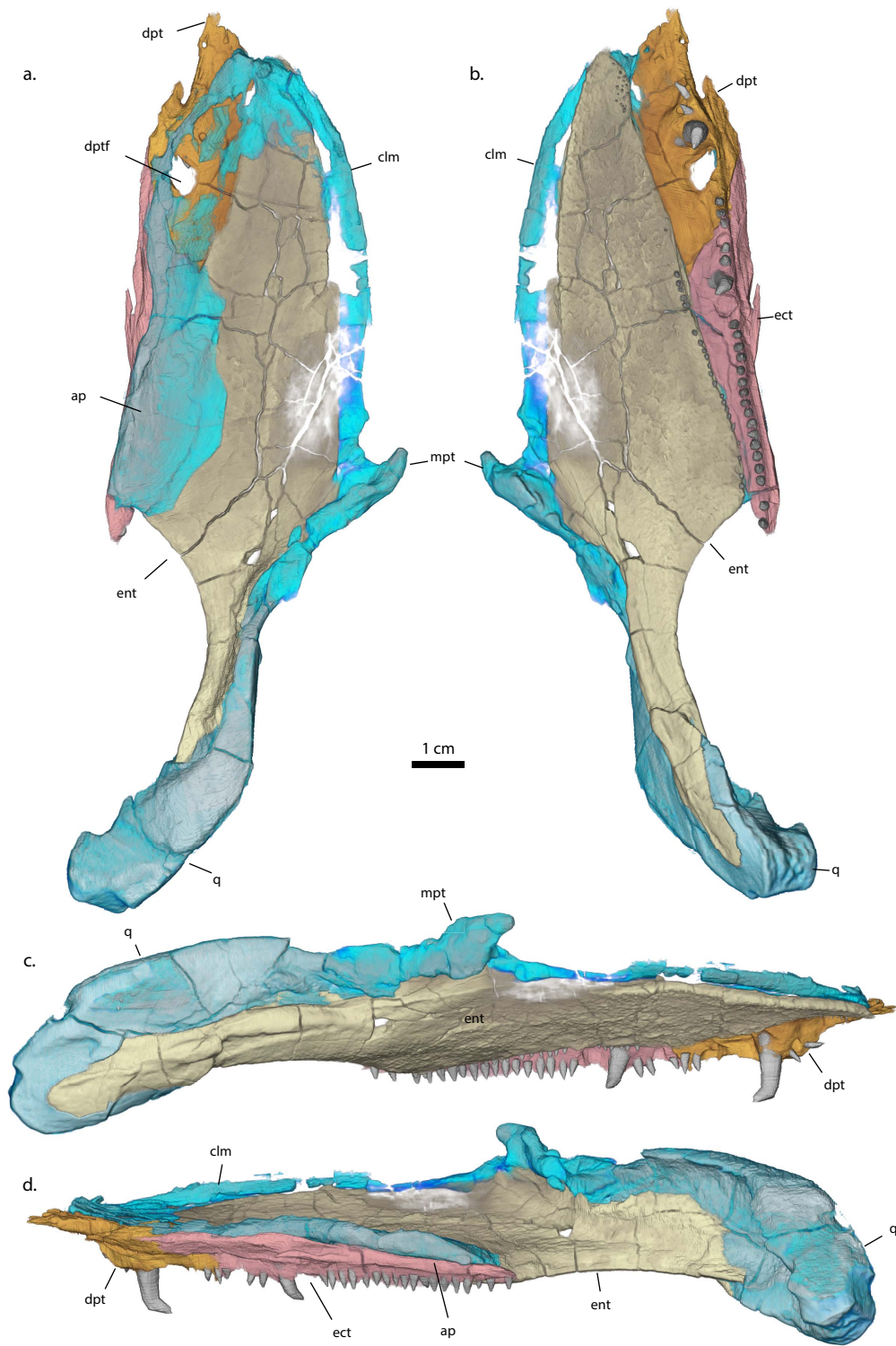


Figure 2.11. Left palatoquadrate and associated dermal ossifications of *Tiktaalik* (NUFV 108). Shown are (a) dorsal, (b) ventral, (c) medial, and (d) lateral views of the left palate, which has been digitally isolated from the rest of the skull. Blue coloration indicates ossifications of the

Figure 2.11, continued. palatoquadrate or co-ossification of the entopterygoid (ent) with the endochondral palate. While the autopalatine (ap) forms a distinct articulation with the braincase in other tetrapodomorph fish (Jarvik 1980), it tapers anteriorly and does not reach as far as the anterior projection of the dermopalatine (*a*, *dpt*).

2.4.4 – Assessment of postmortem deformation

Deformation patterns in the two most articulated specimens of *Tiktaalik roseae* (NUFV 108 and 110) are subtly different, providing an opportunity to reconstruct an averaged, retrodeformed model of life-like proportions. Using internal morphology based on CT scans, it appears that the holotype (NUFV 108) is primarily dorsoventrally crushed with the skull having settled further back relative to the pectoral girdle, whereas the E-specimen (NUFV 110) shows signs of having been laterally compressed when the splanchnocranium and pectoral elements settled approximately 9° to the left of the midline.

NUFV108

The holotype specimen of *Tiktaalik* was preserved in articulation with cranial, hyobranchial, and pectoral girdle elements all in articulation; however, these elements have been displaced relative to each other during postmortem settling in a manner suggesting that the skull is dorsoventrally compressed (Fig. 2.12). Surface inspection of cranial elements shows that the skull has been pushed posteriorly onto the pectoral girdle. In ventral view, the basihyal and urohyal lie ventral to the right clavicle in a manner that would not be possible prior to decay of connective tissue. The right clavicle has also been displaced medially over the anatomical midline to lie on the left side of the body, while the left scapulocoracoid has been displaced posteromedially. Although both the cleithra remain in upright position, the anocleithra have each slumped ventromedially and disarticulated with the cleithra (Fig. 2.14).

Although the cranium itself appears relatively symmetrical, with little signs of deformation during the fossilization process, cranial elements were still displaced during postmortem deposition. Olfactory canals running through the sphenoid are circular and undistorted, while the cavity dorsal to the palate has plenty of space that has been infilled with matrix. This suggests geological processes have had little effect in warping the specimen, whereas most deformation occurred during the settling process.

The fine-grained matrix that has filled in the spaces between bones allows interpretations of how the bones may have settled relative to each other. The lower jaws appear to have been splayed laterally during dorsoventral crushing, and the palate has been forced dorsally into the cavity immediately below the cheeks. Where the lateral and medial tooth rows would be expected to be in alignment, the maxillary tooth row has inverted – at some points almost 45° - and the medial tooth has rotated outward in contrast. This suggests that the palate has been displaced dorsally relative to the cheek and lateral tooth row. While the thickened shelf of the posterior portion of the entopterygoid might be expected to be orthogonal to the cheek, as it is in three dimensionally preserved *Eusthenopteron* specimens (Jarvik 1980), these shelves in *Tiktaalik* instead have been rotated dorsolaterally approximately 17° (Fig. 2.12e,f). Similarly, the angle of the paired condyles of the quadrate appear to be over-extended dorsolaterally, with an eversion angle greater than 31° . In contrast, isolated and uncrushed lower jaws (NUFV 109 and 116) had shallower inclined glenoid angles (only 19° and 14° respectively). While displaced bones remained in relative articulation with each other, the patterns of deformation throughout the cranium are consistent with an interpretation that the holotype specimen was slightly dorsoventrally crushed after the animal died.

The E specimen of *Tiktaalik* was also preserved in articulation with cranial, hyobranchial, and pectoral material *in-situ*, and upon initial inspection the specimen appears to be more three dimensionally preserved than the holotype specimen. However, comparing CT scans of the skull with specimen photos prior to disarticulation of the branchials and pectoral girdle show that elements of the splanchnocranium have been laterally displaced during postmortem deposition (Fig. 2.13). In ventral view, the lower jaws, urohyal, basihyal, and cleithrum show a similar pattern of being displaced 9° relative to the anatomical midline (confirmed by CT scans) of the braincase. This is highly suggestive that these viscerocranial elements were suspended below the braincase by at least 9°. As a result, although the prepared specimen appears largely three dimensional, it simply shows a medial displacement pattern of the right-side cranial elements, whereas the holotype specimen is primarily dorsoventrally crushed.

The specimen appears three dimensionally preserved in part because the chondrocranium is very well preserved. The nasal capsule of NUFV 110 preserves numerous canals running through it that are circular in cross section and undistorted by geological processes that could have warped the specimen. Similar to the holotype specimen, spaces between bones have been infilled by fine sediment that allow interpretations of displacement patterns.

Examination of the bones in cross section appears to corroborate the surface interpretations. The right lower jaw has rotated inwards, in contrast to eversion of the holotype's lower jaws, and as a result the angle of the articular condyles of the quadrate is much lower than that seen in the holotype. Similar to the holotype specimen, the maxillary tooth row has rotated inwards, likely due to the palate shifting dorsomedially relative to the cheek. The medial tooth row is dorsally depressed relative to the lateral tooth row and dermal cheek. This has resulted in

severe crushing of the right prootic process and postorbital articulation with the skull roof, as well as displacement of the right basipterygoid process. Furthermore, the lacrimal-prefrontal joint shows a greater degree of overlap than the holotype specimen. These features all suggest that the E-specimen has been laterally compressed and would have been more platyrostral in life.

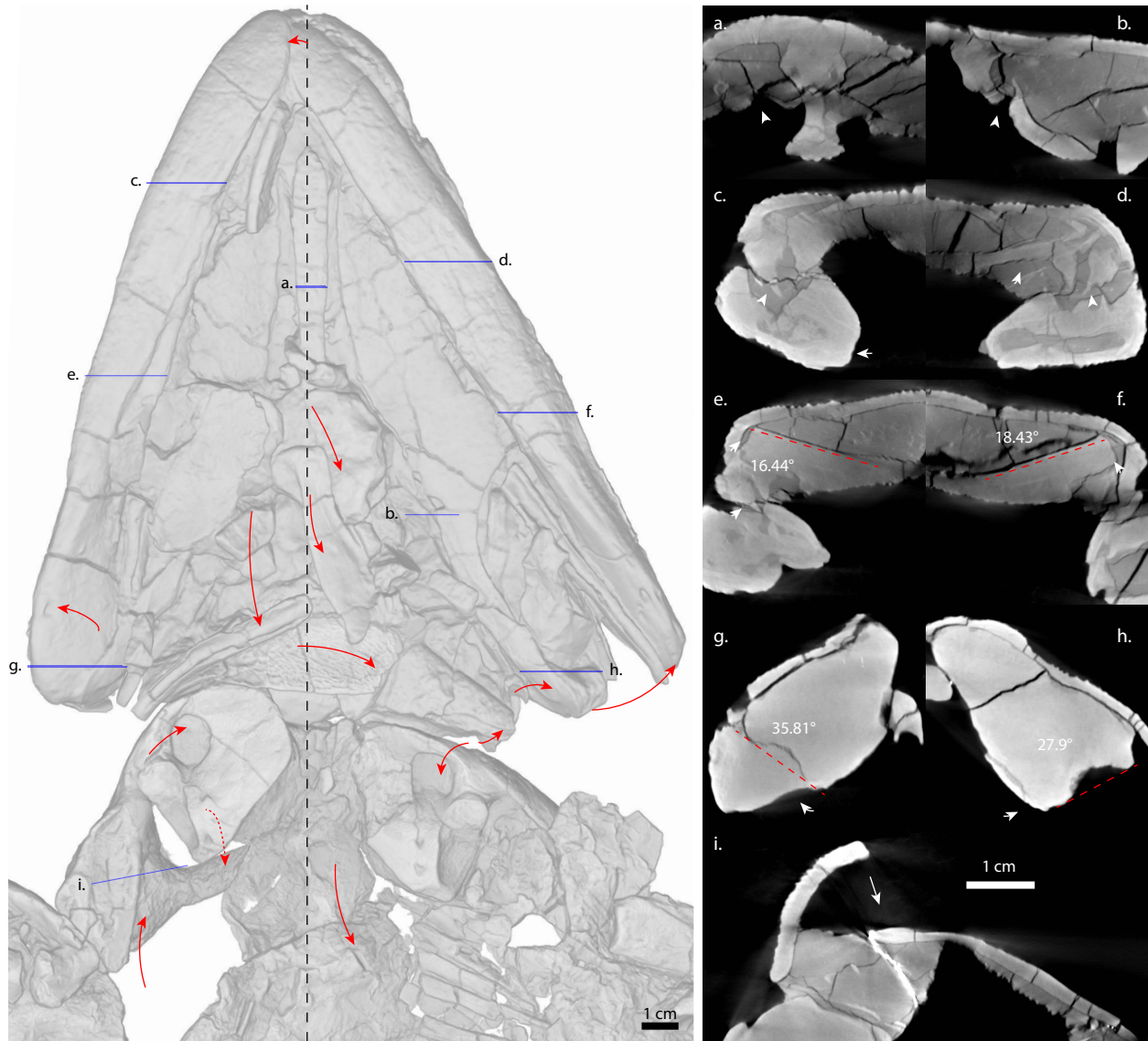


Figure 2.12. Postmortem deformation of cranial elements of *Tiktaalik* (NUFV 108). Shown is a ventral view of articulated holotype specimen (left) prior to removal of branchials. Red arrows indicate proposed displacement of cranial and pectoral elements due to postmortem deformation. Blue lines correspond to cross sections from high resolution scans (*a-i*). (*a*) Midsection of sphenoid showing loose connection of palate under the olfactory canals as well as

Figure 2.12, continued. dorsal displacement of the palate. (b) Dorsal displacement and disarticulation of entopterygoid relative to the palatoquadrate. (c) Anterior section of the tooth row showing relatively minor displacement of tooth bearing elements. (d) Midsection of the tooth row showing dorsal displacement of palate relative to the cheek and inversion of the maxillary teeth. (e) Posterior section of tooth row showing dorsal displacement of autopalatine and inversion of the maxillary teeth even though the lower jaws are laterally splayed. (f) Corresponding posterior section of the left tooth row showing similar pattern of displacement as the right side. In both instances the angle of the autopalatine relative to the jugal appears to be elevated by an average of 17.4° . (g) Cross section of the jaw joint showing lateral rotation of the lower jaw relative to the quadrate. (h) Cross section of the jaw joint showing lateral rotation of the quadrate. (i) Cross section of the right pectoral girdle showing ventral displacement of the anocleithrum relative to the vertically standing cleithrum.

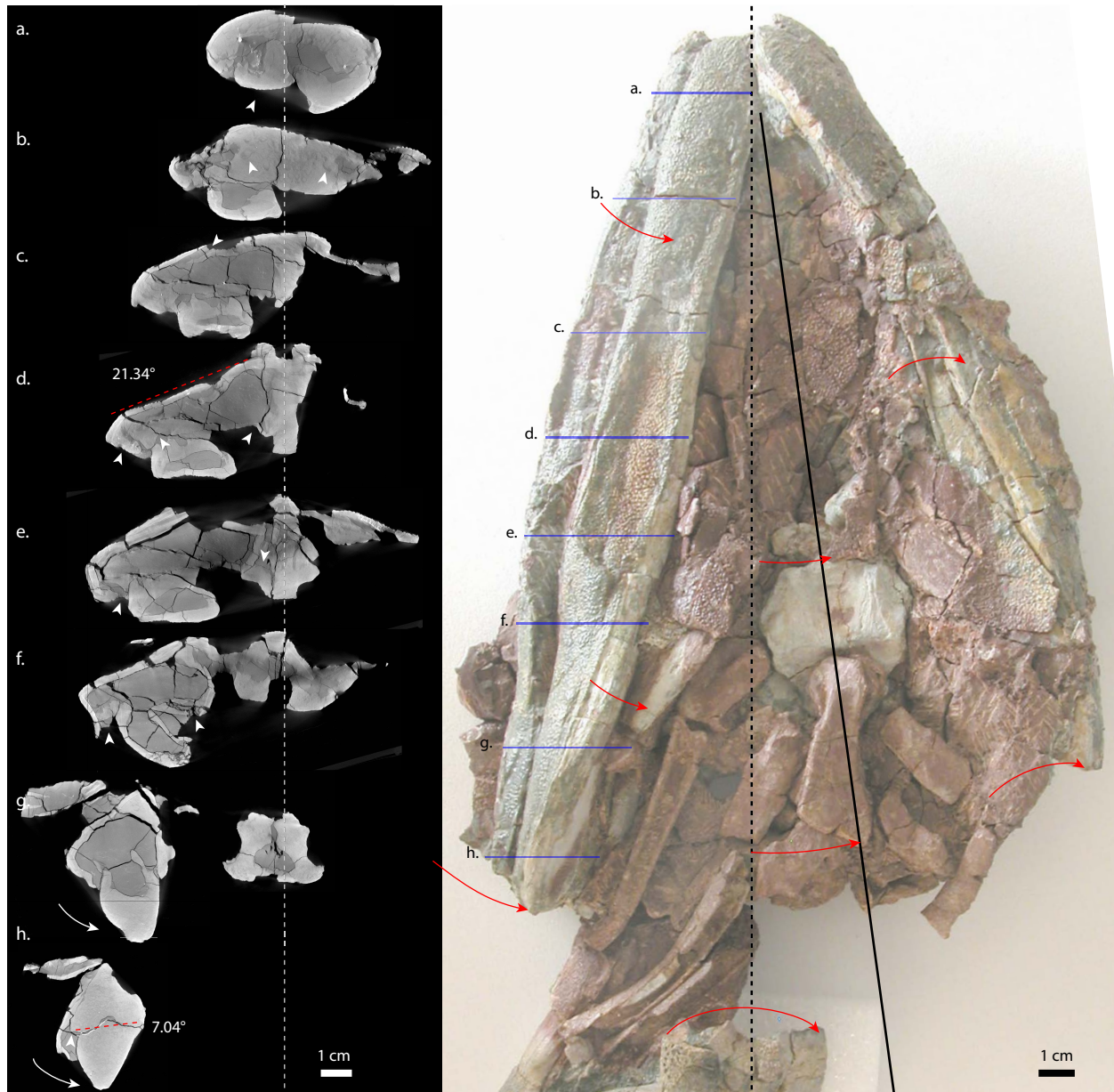


Figure 2.13. Postmortem deformation of cranial elements of *Tiktaalik* (NUFV 110). Shown is a ventral view of articulated E specimen (right) prior to removal of branchials, left palate, and left lower jaw. Blue lines correspond to section details from high-resolution CT scan (a-h). (a) Medial displacement of right lower jaws at the symphysis. (b) Circular cross sections of the olfactory canals. (c) Loose overlapping scarf joint at the prefrontal-lacrimal. (d) Medial displacement of the jugal and dorsal displacement of the palate with the lower jaw medially displaced. Red dashed line indicates slope of the dermal cheek relative to the palate in this specimen. (e) Inversion of the lateral tooth row and crushing of the palate onto the basiptyergoid process. (f) Inversion of the lateral tooth row and breakage of the palatoquadrate due to dorsal displacement of lower jaw. (g) medial displacement of lower jaw. (h) dorsal displacement of the quadrate relative to the dermal cheek and inversion of the jaw joint due to medial displacement

Figure 2.13, continued. of the ventral cranial elements. Red arrows show proposed shift of cranial elements due to uniform rotation of the viscerocranial and pectoral girdle elements (midline indicated by solid black line) relative to the braincase (midline indicated by dashed line) by an angle of 8.76° .

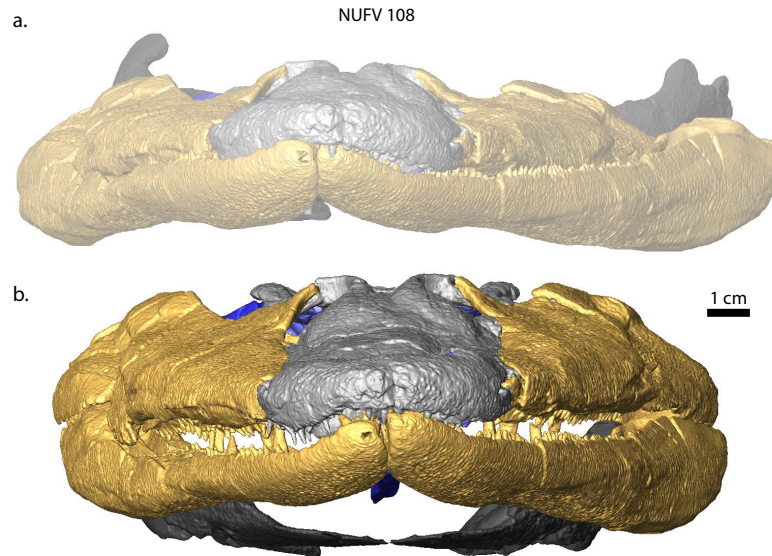


Figure 2.14. Proposed retrodeformed proportions of the skull of *Tiktaalik*. Shown are the proportions of the skull before (a) and after (b) rotating cranial elements into their approximate reconstructed positions. Deformation patterns indicate the skull of NUFV 108 was primarily dorsoventrally crushed and posteriorly displaced relative to the pectoral girdle (see Fig. 2.12), whereas the skull of NUFV 110 experienced lateral compression (see Fig. 2.13). Even after repositioning cranial elements, the cheek and palate are still horizontally oriented, indicating limited lateral expansion capabilities due to dorsolateral rotation.

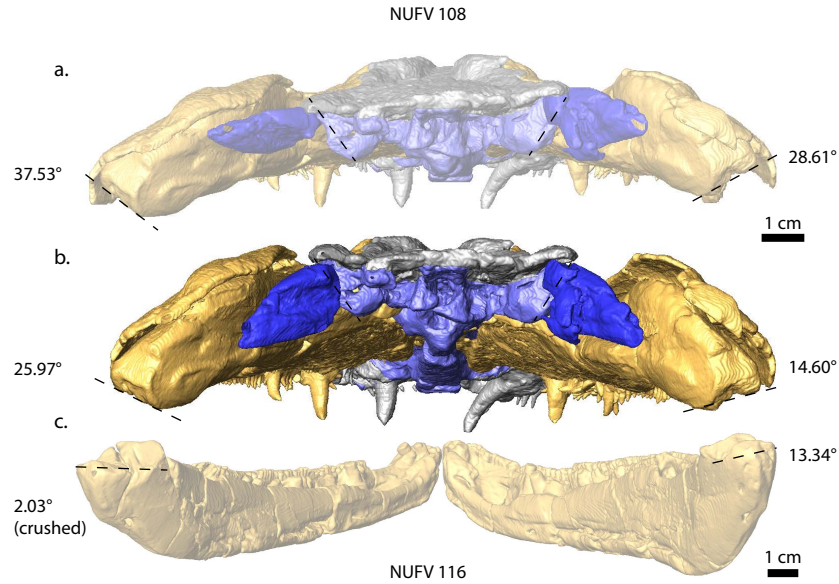


Figure 2.15. Comparison of crushed, undeformed, and retrodeformed jaw-joint angles. Shown in posterior view is the skull of the holotype specimen (NUFV 108) both before (*a*) and after (*b*) repositioning of cranial elements with the lower jaws digitally removed. The hyomandibulae (dark blue) were rotated back into articulation with the lateral commissure (interior dashed lines). The quadrates were rotated to correspond to the angle of the jaw joint in an uncrushed specimen (NUFV 116, right lower jaw) (*c*).

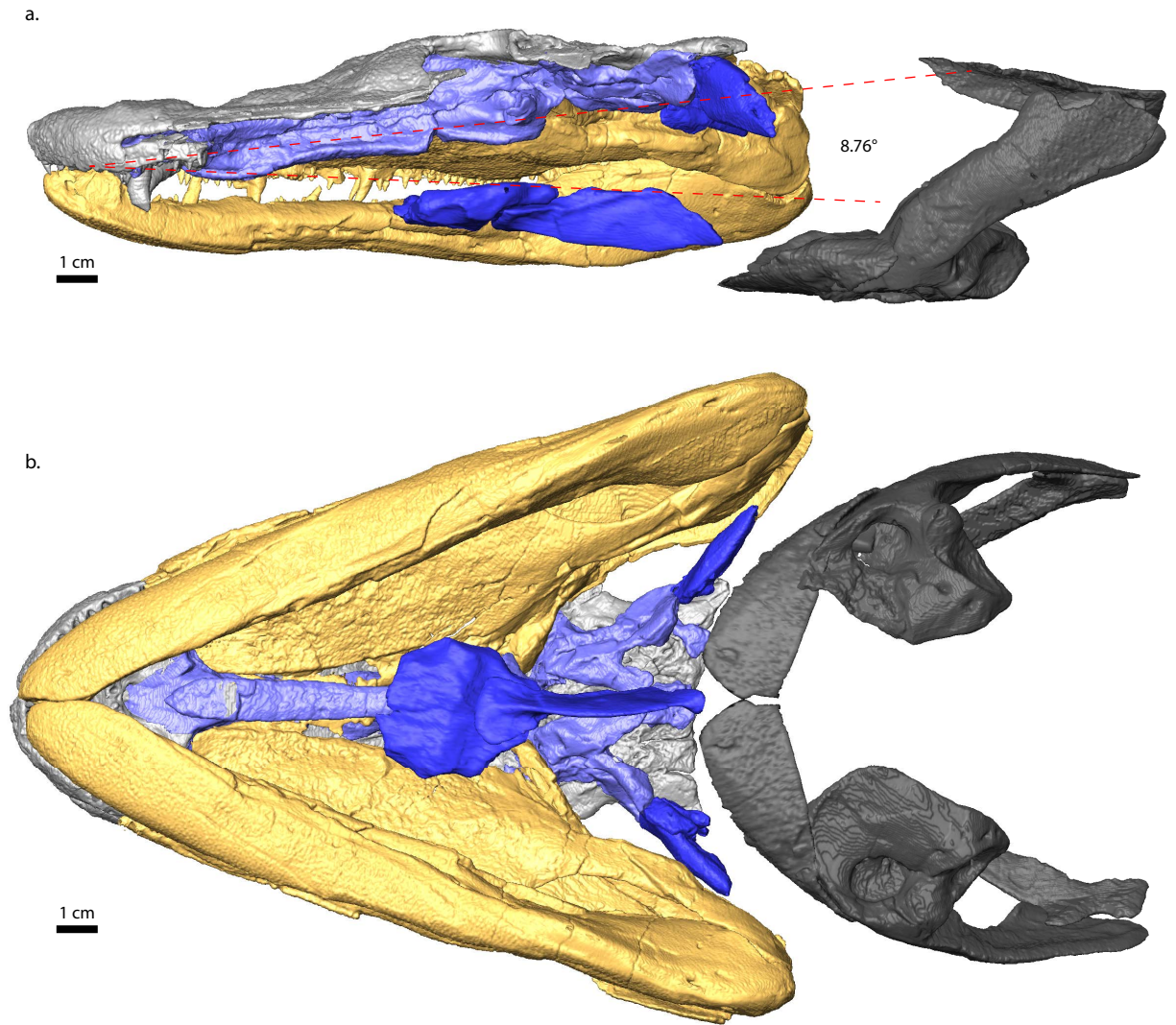


Figure 2.16. Proposed retrodeformed proportions of the skull and pectoral girdle of *Tiktaalik*. Shown are the lateral and ventral reconstructions of the skull and pectoral girdle of *Tiktaalik roseae* based on deformation patterns documented in NUFV 108 and 110 (Figs. 2.12 and 2.13). The left clavicle is a mirrored replicate of the right clavicle, but all other bones are original elements.

2.5 – DISCUSSION

2.5.1 – Functional implications of a platyrostral skull

Tiktaalik roseae appears to be platyrostral, similar to the condition reported for other elpistostegids and early tetrapods (Schultze and Arsenault 1985, Ahlberg et al. 1996, Brazeau and Ahlberg 2006, Daeschler et al. 2006, Clack 2012). Although that may not be too surprising, other close relatives, such as *Ventastega* and *Acanthostega* were not reported to be platyrostral to quite the same degree (Clack 1994a, Ahlberg et al. 2008). While there is some clear indication of limited postmortem deformation in the *Tiktaalik* cranial material examined for this study (see above), conservative restorations of rostral proportions show a skull that is approximately twice as wide as it is tall (Fig. 2.14). In comparison to the tall and narrow skulls of osteolepidids (Long et al. 1997) and plesiomorphic tristichopterids (Jarvik 1980), the platyrostral proportions found in elpistostegids represent a significant departure from ancestral conditions. This allows us to explore some of the functional implications of the evolution of a platyrostral feeding apparatus in *Tiktaalik* and other elpistostegids.

The evolution of a dorsoventrally compressed skull would have significant implications for the feeding ecology of elpistostegids. While the fusiform body and comparatively tall skulls of *Eusthenopteron* could indicate a pursuit-based predation strategy similar to pikes (Porro et al. 2015a), the flattened morphology of the upper jaws in later tetrapodomorphs would incur substantial drag if swimming at prey open-mouthed (Taylor 1987, Damiani 2001). Platyrostral skulls are more susceptible to dorsal bending forces when compared with taller, narrower skulls (Taylor 1987, Rayfield and Milner 2008) and are additionally problematic for lacking an effective mechanical advantage for powerful jaw musculature (Taylor 1987, Busbey 1995). Horizontal palates theoretically limit the ability of the cheeks to swing laterally (Alexander

1970), limiting suction potential. Furthermore, elongate jaws with unoccluded tooth rows are less conducive to suction feeding, which favors short, broad jaws (Taylor 1987, Schoch and Milner 2000, Hohn-Schulte et al. 2013, Witzmann and Schoch 2013). These tradeoffs for evolving a platyrostral skull indicate that other selective pressures, perhaps changing feeding ecology, may have driven evolution of the unique rostral proportions of elpistostegids.

Cranial changes likely indicated a shift in feeding strategies for elpistostegids, and there are several theories for how the broad flat jaws of *Tiktaalik* and other elpistostegids were used. With reduced ability to generate suction (Downs et al. 2008), some researchers suggest it indicated a shift towards biting. In many aquatic tetrapods, elongate and flattened jaws are used to laterally snap at prey like crocodilians (Taylor 1987, Johanson et al. 2003, Hohn-Schulte et al. 2013). However, although rostral elongation is a derived feature that arises with elpistostegids (Ahlberg et al. 1996, Daeschler et al. 2006), extreme specializations in the form of pincer-like, narrow jaws similar to gharials or long-nosed gars do not appear until much later among the crown-group tetrapod radiation (Clack 2012). This has led other researchers to propose the broad flat jaws of elpistostegids could have also been used to engulf prey, much like giant salamanders (Clack 2012, Heiss et al. 2013).

Whether a lateral snapper or an unspecialized gulper, both hypotheses suggest a radical shift in the way prey capture occurs relative to the pursuit based, pike-like prey capture method suggested for *Eusthenopteron* (Clack 2012, Porro et al. 2015a). The evolution of a platyrostral skull is accompanied by significant postcranial changes as well (Daeschler et al. 2006), suggesting a shift in the overall feeding ecology of these animals. Parallel evolution of large, predatory fish, with reduced midline fins and dorsoventrally-compressed bodies, occurs in several other groups of tetrapodomorph fishes (Ahlberg and Johanson 1998), particularly

rhizodonts and derived-tristichopterids, such as *Mandageria* (Johanson et al. 2003), indicating convergent evolution towards a particular ecological niche among Middle to Late Devonian sarcopterygians (Ahlberg and Johanson 1998, Johanson et al. 2003). While that niche appears to involve a greater degree of lateral snapping (Ahlberg and Clack 2006, Hohn-Schulte et al. 2013), more information is needed to assess how cranial and postcranial changes interact to influence the feeding ecology of tetrapodomorph fishes.

Despite the changes to cranial and postcranial anatomy of elpistostegids relative to tristichopterids, the lower jaws of elpistostegids remain curiously similar to *Eusthenopteron* and other tristichopterids (Ahlberg and Clack 1998, Clack 2012, Anderson et al. 2013, Neenan et al. 2014). This suggests that the lower jaws of tetrapodomorph fishes may not be the best indicator for shifts in feeding strategies, and more information about the upper jaws is necessary to understand how the feeding strategies changed across the water-to-land transition.

2.5.2 – Functional implications of cranial consolidation

Tiktaalik roseae maintains the plesiomorphic divide between the sphenotic and otoccipital partitions of the braincase (Downs et al. 2008), but otherwise the braincase is fully consolidated in a manner that is both transitional (in terms of de-ossification of the nasal capsule and lateral wall of the otic capsule) and derived (in terms of sutural morphology, see below). The derived condition of endocranial consolidation among tetrapodomorphs is characterized by fusion of the otoccipital and sphenethmoid regions, as represented by *Ventastega* (Ahlberg et al. 2008) and *Acanthostega* (Clack 1994b, Ahlberg et al. 1996). In both these taxa, the intracranial fissure is already fused, but the nasal capsule and lateral otic wall have de-ossified (Clack 1994b, Ahlberg et al. 2008). *Tiktaalik* shows some of the earliest signs of these processes by the anterodorsal extension of the prootic buttress, which spans the intracranial fissure, and evidence

of de-ossification of the anterior-most tip of the sphenethmoid immediately dorsal to the fossa apicalis. While not derived from a character-state point of view, these changes have interesting implications for the function of the feeding apparatus.

First, while the prootics do not directly articulate with the sphenethmoid, they articulate with the bones of the dermatocranium anterior to the intracranial hinge, thereby immobilizing the joint between the parietal and postparietal shields. By spanning the intracranial fissure, and supporting dermatocranial elements anterior to that fissure, the prootics enable the braincase to operate as a single unit. The well-ossified sphenethmoid forms a solid strut running down the midline of the skull that takes the form of an I-beam, reinforcing the neurocranium in a way that may suggest it was capable of resisting bending forces incurred during biting that might otherwise be problematic for a platyrostral skull (Rayfield and Milner 2008). The process of interdigitation and fusion of the intracranial hinge, begun in the early elpistostegid, *Panderichthys* (Ahlberg et al. 1996), appears to have been further reinforced in *Tiktaalik*. If intracranial kinesis affected the feeding kinematics of tristichopterids and other tetrapodomorph fishes, then immobilization of this hinge would indicate a large departure of elpistostegid feeding mechanics from the plesiomorphic condition.

An increase in interdigitating sutures and sutural complexity throughout the skull roof of *Tiktaalik* is further indicative of a shift toward biting-based prey capture. Dermal sutures are frequently used as proxies for understanding the predominant loading regimes incurred between dermal bones in fossil taxa (Bolt 1974, Markey and Marshall 2007). While simple butt joints are thought to resist tension, more complex beveled and interdigitating joints are thought to resist torsion and compression respectively (Bolt 1974, Markey and Marshall 2007). An increase in the diversity and complexity of sutures is found throughout the dermatocranium in limbed

tetrapodomorphs in comparison to tetrapodomorph fishes, which has been hypothesized to indicate a shift from fish-like suction feeding to terrestrial-style biting (Markey and Marshall 2007, Clack 2012). However, now we now know a similar pattern of sutures can be found in an elpistostegid as well. *Tiktaalik* possesses interdigitating sutures along the midline, between the paired frontal bones as well as the paired postparietal bones in much the same way as terrestrial temnospondyls, such as *Phonerpeton*, which was thought to be resisting compressive forces due to biting as well (Markey and Marshall 2007). The prevalence of interdigitating sutures along the skull roof of *Tiktaalik* indicates biting-based prey capture evolved in tetrapodomorph fishes prior to the fin-to-limb transition.

In *Tiktaalik*, a pattern of overlapping bones lateral to the midline may suggest a shift towards biting as well, but caution must be taken when interpreting their function. Throughout the cheek and dermal skull roof of *Tiktaalik*, a range of sutural types can be found, including beveled (Fig. 4.7g) and tongue-in-groove sutures (Fig. 4.7e). These same overlapping sutures in *Acanthostega*, have been interpreted as resisting torsional forces incurred during twist feeding, similar to crocodilians (Busbey 1995, Clack 2002a), and the broad flat scarf joints found in analogous positions in *Tiktaalik*, *Acanthostega*, and crocodilians have been taken as evidence that these tetrapodomorphs engaged in unilateral bites and twist feeding similar to crocodilians (Busbey 1995, Clack 2002a, Hohn-Schulte et al. 2013). However, unlike crocodilians, tetrapodomorphs lack a consolidating secondary palate that reinforces and immobilizes the primary palate (Rayfield and Milner 2008), and important consideration must be given to the loose, overlapping scarf joints that lie along the anatomical division of the cheek and skull roof (Fig. 4.6g, 4.7b, 4.7h). These scarf joints may not be sutural at all and correspond to a presumably kinetic hinge in plesiomorphic tetrapodomorph fishes (see below). While the specific

pattern of overlapping, bone-to-bone contact in the cheek of *Tiktaalik* is more similar to limbed tetrapodomorphs, indicating a shift in feeding strategies, more information is needed to understand how that pattern of beveled sutures and scarf joints was used in a platyrostral skull with a consolidated braincase that nevertheless shows some signs of kinesis.

2.5.3 – Functional implications of cranial kinesis

Tiktaalik exhibits evidence of a both a mobile cheek and palate, suggestive of maintained cranial kinesis up to the fin-to-limb transition. Although beveled sutures, which are prevalent throughout the cheek and braincase of *Acanthostega* and *Tiktaalik*, were interpreted to resist torsional forces incurred during biting similar to crocodilians (Bolt 1974, Busbey 1995, Clack 2002a, Markey and Marshall 2007), in *Tiktaalik* some of these sutures do not appear to be sutural at all, and instead may have allowed movements between the dermal cheek and skull roof. Furthermore, although the neurocranium shows signs of consolidation that would immobilize any form of intracranial kinesis between the partitioned braincase, the easily separable articulations between the palate and braincase may have retained some degree of mobility. Here we go through the evidence for that mobility, and some of the implications for interpretations of homology of cranial kinesis between tetrapodomorph fishes and limbed tetrapodomorphs.

The dermal cheek of *Tiktaalik* is identifiable as a separate region from the skull roof in much the same way as *Eusthenopteron* (Jarvik 1980) and other tetrapodomorph fishes. Although the trend in limbed tetrapodomorph evolution is to integrate the postorbital into the skull roof through interdigitating sutures (Clack 2012), the postorbital of *Tiktaalik* appears to be more directly a part of the dermal cheek. It rests upon a slanting dermal shelf formed by the intertemporal and supratemporal, supported by the prootic, and this shelf is smooth and likely allowed some sliding. No interdigitating sutures form between the postorbital of *Tiktaalik* and

the intertemporal or postfrontal, as in *Acanthostega* (Clack 2002a, Porro et al. 2015b). Furthermore, the postorbital has broad overlapping articulations with the jugal and squamosal. Unlike other beveled sutures, these articulations are not as tightly integrated with the postorbital and show some signs of separation from the ventral surface of the postorbital, which may suggest an intermediate state between the conditions found in *Eusthenopteron* (Jarvik 1980) and *Acanthostega* (Clack 2002a). Similar to *Acanthostega* (Clack 1994a), *Tiktaalik* possesses a broad overlapping scarf joint between the prefrontal and lacrimal (Fig. 4.6g, 4.7h), and in *Tiktaalik* this joint is smooth, often slightly disarticulated and filled in with matrix, implying it was less tightly bound in life than other beveled sutures found throughout the cheek, such as the lacrimal-jugal suture (Fig. 4.7g). Again, these joints follow the same anatomical divisions of tetrapodomorph fishes with presumed mobile cheeks (Thomson 1967, Jarvik 1980) and seem to suggest mobility between the cheek and palate in ways that would have accommodated movements of the underlying palate relative to the braincase.

Mobile joints of the dermal skull roof correspond to underlying joints between the palate and braincase in a way that suggest the entire cheek and palate could move relative to the braincase. Anteriorly, the dermopalatine forms the anterior most articulation with the braincase by means of a small anterior facing prong that articulates with the vomer in a small socket at the back of the nasal capsule. Posteriorly, the ascending process of the palatoquadrate takes the form of a thin tapering point that inserts into the suprapterygoid fossa just dorsal to an enlarged basipterygoid process. The basipterygoid is large, with both anterior and posterior facing articular facets. The anterior facet corresponds to a small recess of the palate immediately anterior, which could correspond to a cartilaginous articular surface. Similar to *Acanthostega* and *Crassigyrinus* (Panchen 1985, Clack 1994a, Clack 1998), this joint of the basipterygoid appears

to have an unfinished surface that may correspond to a mobile synovial joint. Posteriorly, the basipterygoid process bounds the metapterygoid ventrally, whereas the prootic bounds the metapterygoid dorsally. While an enlarged basipterygoid process has been interpreted to restrict movements of the palate by some researchers (Downs et al. 2008), others have interpreted it to be the point of rotation, particularly for *Crassigyrinus*, colosteids, baphetids, and anthracosaurs (Thomson 1967, Romer 1969, Beaumont 1977, Panchen 1985, Bolt and Lombard 2001).

Although it is not possible to say for certain what degree of cranial kinesis was possible at these various joints between the palate and braincase, evidence of palatal mobility does appear to be present in *Tiktaalik*, which has interesting implications for feeding ecology in tetrapodomorph fishes immediately prior to the fin-to-limb transition.

Despite evidence of cranial kinesis in *Tiktaalik*, due to significant changes between the anatomy of elpistostegids and more plesiomorphic tetrapodomorph fishes, there were likely changes to how that cranial kinesis occurred in taxa with platyrostral and consolidated skulls. Osteolepidid and tristichopterid models of cranial kinesis (Thomson 1967, Hitchcock 1995) assume rotation of the palate around its articulation with the suprapterygoid articulation; however, in taxa with an enlarged basipterygoid process, it is assumed the metapterygoid is pivoting on its articulation with the basipterygoid instead (Thomson 1967, Romer 1969, Beaumont 1977, Panchen 1985, Bolt and Lombard 2001). *Tiktaalik* likely represents an intermediate stage, where the articular points of the metapterygoid with the braincase are converging due to dorsoventral compression of the skull and anterior attachment of the palate, the dermopalatine-vomerine joint, is diverging due to rostral elongation. The shifting of these articulations would have changed the kinematics of elpistostegid cranial kinesis and made it more difficult to laterally expand the skull. Due to the horizontal orientation of the palate (less

than 20°), dorsolateral rotation of palate would only result in a meager lateral expansion of $<6\%$ ($\cos(20^\circ)$). Furthermore, reduction of the size of hyomandibula, an important component of osteolepidid cranial kinesis (Thomson 1967), also suggests a reduction in the amount of lateral expansion possible. Despite maintaining “fish-like” palatal mobility up until the fin-to-limb transition, implying homology of tetrapodomorph fish cranial kinesis and palatal mobility in limbed tetrapodomorphs, *Tiktaalik* nevertheless represents a major departure from the kinetic systems proposed for early tetrapodomorph fishes.

For these reasons, cranial kinesis in elpistostegids and limbed tetrapodomorphs suggest the feeding system is experiencing functional tradeoffs during the fin-to-limb transition. On the one hand, a platyrostral and consolidated skull with interdigitating sutures implies a shift toward biting, whereas maintained cranial kinesis suggests suction generation is still important. As a transitional taxon, the feeding system of *Tiktaalik* offers insight into how early tetrapods might have retained cranial kinesis from fish-like ancestors, but more information is needed to assess how cranial kinesis was used by elpistostegids. How does lateral expansion occur with a horizontal palate and reduced hyomandibula? What is the function of cranial kinesis in a presumably lateral snapping specialist? In order to answer these questions, we need a modern analog that helps us understand what function kinesis performs in a platyrostral fish. While multiple potential modern analogs for elpistostegids exist, one particular taxon, the lateral-snapping, broad and blunt snouted lepisosteid genus, *Atractosteus*, may represent the best analog for interpreting these conditions due to its extensive convergent morphology with elpistostegid tetrapodomorph fishes.

2.6 – CONCLUSIONS

Through the use of computed tomography (CT) data from numerous specimens, the internal anatomy of the upper jaws of *Tiktaalik roseae* was evaluated for evidence of shifts in feeding ecology related to the fin-to-limb transition. While still a tetrapodomorph fish, with lower jaws very similar to plesiomorphic tristichopterids, *Tiktaalik* otherwise exhibits many derived traits in terms of functional feeding system morphology that represents a departure from that of earlier tetrapodomorph fishes. Through analysis of postmortem deformation, new estimates of rostral proportions are provided, indicating that *Tiktaalik* was a significantly platyrostral fish that shared many traits found in other convergently evolved taxa with dorsoventrally compressed skull, such as elongate jaws, horizontal palate, and numerous scarf joints. CT scans confirmed the presence of a broad diversity of sutural types in the skull of *Tiktaalik* that is on par with sutural morphology found in terrestrial feeding tetrapods. Interdigitating sutures, as well as an anterior advancement of the prootic fuse the intracranial hinge of *Tiktaalik*, enabling the neurocranium and skull roof to operate as a single unit during feeding, in contrast to models proposed for earlier osteolepidid fishes. However, despite significant restructuring of the cranium in the evolution of an elongate, dorsoventrally compressed, and consolidated skull, the dermal cheek and palate of *Tiktaalik* show numerous indications of retaining cranial kinesis. Each of these changes represent a broad departure from the feeding morphology of plesiomorphic osteolepidid and tristichopterid fishes that, while not reflected in lower jaw morphological changes, likely reflects shifts in ecological niches suggested by postcranial anatomy changes across the fin-to-limb transition. With this new information, we should examine the rest of the feeding apparatus to better understand how it all

works together as a feeding system, using modern analogs, where available, to interpret some of the functional implications of the unusual feeding features seen in *Tiktaalik*.

CHAPTER 3 – COMBINED USE OF JAW-RAM AND SUCTION GENERATION IN THE FEEDING MECHANISM OF ALLIGATOR GARS, *ATRACTOSTEUS SPATULA*

3.1 – ABSTRACT

Lepisosteid gars are a small clade of seven species and two genera that occupy an important position on the actinopterygian phylogenetic tree as members of the Holostei (*Amia* + gars), the sister group to the teleost radiation. Sometimes termed “living fossils” they preserve many of the plesiomorphic characteristics of the basal osteichthyan feeding mechanism, thus providing important insight into the functionality of that system. Studies of feeding kinematics in gars have focused exclusively on *Lepisosteus*, and here I expand that dataset to a sister-genus and the largest species of gar, *Atractosteus spatula*, the alligator gar. Through the use of high-speed videography, contrast enhanced micro computed-tomography (μ CT), and manual manipulation of fresh specimens, I document comparative feeding kinematics, details of the cranial linkage system, and muscle anatomy of the feeding apparatus of *A. spatula*. Although all gars specialize in capturing elusive prey through rapid lateral snapping, high-speed videography reveals the unexpected result that the feeding strike of *A. spatula* combines elements of jaw-ram and suction to capture prey. The feeding mechanism of *A. spatula* is capable of expanding rapidly from anterior-to-posterior during feeding to maintain a unidirectional flow of water into the mouth throughout the feeding strike, precisely timed and mediated by an unspecialized complement of hyoid constrictor muscles plesiomorphically found in all osteichthyans. Although the cranial kinematics of *A. spatula* are unlike those seen in teleosts, the alligator gar feeding system maintains all the basic mobile elements of the osteichthyan feeding mechanism and demonstrates one of the many ways the basal osteichthyan feeding mechanism has been modified for prey

capture. The complexity and versatility seen in the feeding system of *A. spatula* greatly expands the known repertoire of feeding strategies available among osteichthyans before the predominance of teleosts.

KEY WORDS: ram-suction, decoupling, cranial linkage, jaw-opening mechanism, platyrostral, flat-plate suction, cleithral rotation

3.2 – INTRODUCTION

It is difficult to overstate the scientific importance of information on lepisosteid gars for understanding the early osteichthyan condition. Due to their phylogenetic placement at the base of modern teleosts, they form an important outgroup for inferring the ancestral condition for approximately half of vertebrate diversity (Grande 2010, Near et al. 2012). Additionally, lepisosteid gars exhibit uniquely low rates of speciation and morphological evolution (Rabosky et al. 2013), preserving many plesiomorphic osteichthyan conditions that were independently lost in other groups and allowing researchers to study how those features function in extant organisms. Described as “living fossils” (Darwin 1859, Wiley 1976, Grande 2010, Wright et al. 2012, Rabosky et al. 2013), gars have helped to bridge our understanding of the evolution of modern forms to the distant past: e.g. biomechanical studies have used similarities between gars and other non-teleost, non-tetrapod osteichthyans to determine the plesiomorphic conditions of the early osteichthyan feeding mechanism (Lauder 1980a, b, Bemis and Lauder 1986, Wilga et al. 2000, Carroll and Wainwright 2003), developmental studies use their conserved gene sequences to identify homologous regions of genetic code between teleosts and tetrapods (Braasch et al. 2016, Nakamura et al. 2016), and systematic studies use their conserved

morphological and molecular patterns to inform plesiomorphic conditions of the Neopterygii (Grande 2010, Near et al. 2012).

Although their phylogenetic position and often plesiomorphic trait retention is useful, it is important to note that, since diverging from the rest of Neopterygii approximately 300 million years ago (Near et al. 2012), gars have accumulated numerous specializations, many presumably related to their unique method of capturing prey using rapid lateral strikes. These specializations include platyrostral and elongate upper jaws, enlarged and horizontally oriented palates, a uniquely enlarged basipterygoid-metapterygoid articulation, dorsally exposed ectopterygoid, extremely-low mechanical advantage of the lower jaws, numerous plicidentine teeth, tooth-bearing lacrimomaxillary bones, and fusiform bodies with posteriorly placed midline fins (Wiley 1976, Lauder 1980a, Jollie 1984, Arratia and Schultze 1991, Webb et al. 1992, Porter and Motta 2004, Kammerer et al. 2006, Grande 2010). While gars are typically characterized as representing morphological “extremes” towards biting-based, ram-feeding prey capture (Muller 1989, Porter and Motta 2004), they are consistently outliers in comparison with other ram-feeding, ambush predators that appear convergently evolved with gars, such as barracuda, needlefish, and pike (Webb et al. 1992, Porter and Motta 2004) as well as other non-teleost actinopterygians (Lauder 1980a) in terms of feeding kinematics. Despite their scientific importance, there is still much we do not know about how gars use these specialized features in feeding.

To further expand our understanding of feeding kinematics within lepisosteid gars, this study focuses on a gar with unique anatomy and ecology, the alligator gar, *Atractosteus spatula*. As the species of gar with the largest adult body size and bluntest snout (Kammerer et al. 2006, Grande 2010), *A. spatula* differs from other gars for which feeding kinematics are available

(*Lepisosteus oculatus* (Lauder 1980a, Lauder and Norton 1980), *L. platyrhinchus* (Porter and Motta 2004), and *L. osseus* (Webb et al. 1992)), both in terms of diet – stomach contents include fish, smaller gars, invertebrates, birds, and scavenged material (Raney 1942, Kammerer et al. 2006, Robertson et al. 2008, Grande 2010) – as well as feeding morphology (Kammerer et al. 2006, Grande 2010). While many extinct gar species were blunt-snouted, such as *Cuneatus*, *Masillosteus*, and *Nhanulepisosteus* (Grande 2010, Brito et al. 2017) and, while rostral proportions vary greatly between sympatric species of gars (Kammerer et al. 2006, Robertson et al. 2008, Grande 2010, Wright et al. 2012), it is uncertain how varying snout shape affects the overall pattern of feeding kinematics in gars. Therefore, the first aim of this study is to quantify feeding kinematics in *A. spatula*, using high-resolution, high-speed videography, to compare with other living species of gars and examine if the unique shape of the alligator gar feeding apparatus also reflects changes to prey capture and feeding strategy.

Although suspensorial abduction, one of the key components of volumetric expansion in osteichthyans, was previously thought to be limited in gars (Lauder 1980a, Lauder and Norton 1980, Porter and Motta 2004), preliminary observations suggest that suspensorial mobility may be an important component of the feeding strike of *Atractosteus spatula*. In *Amia* and most teleosts, suspensorial abduction occurs around the long axis of the suspensorium, laterally abducting the jaw-joints, which are suspended vertically below this axis (Liem 1978, Lauder 1980a), but, in gars and other platyrostral taxa, the jaw-joints are already laterally displaced due to the horizontal inclination of the palate (Alexander 1970, Lauder 1980a, Adriaens and Verraes 1994). Gars possess several derived features, such as the patent sulcus between the ectopterygoid and the skull roofing bones, as well as a unique sliding articulation between the metapterygoid and basipterygoid process of the neurocranium (Wiley 1976, Jollie 1984, Arratia and Schultze

1991, Grande 2010) that may aide in suspensorial abduction. However, with tight connections between the palate and a fixed premaxilla (Grande 2010), the mechanism driving cranial movements is not fully understood. Therefore, a secondary aim of this study is to document the mechanism of cranial expansion in *A. spatula*, using manipulations of fresh specimens and detailed anatomical reconstructions of soft tissue anatomy through contrast enhanced micro-computed tomography (μ CT).

Although gars were instrumental in identifying key plesiomorphic features of the early osteichthyan feeding mechanism (Lauder 1980a, Lauder and Norton 1980, Lauder 1982), they appear to depart from this feeding mechanism in one key area, the timing of hyoid depression. The osteichthyan feeding mechanism relies on muscular input from the pectoral girdle, the sternohyoideus (= coracohyoideus), to rotate the hyoid posterodorsally, which also transmits posterodorsal forces to lower jaws by means of the mandibulohyoid ligament (Lauder 1980a, Lauder and Shaffer 1993, Wilga et al. 2000). Prior to the evolution of secondary jaw opening mechanisms, such as opercular rotation in *Amia* and teleosts, or a depressor mandibulae muscles in lepidosiren lungfish and tetrapods, jaw opening in basal groups is mechanically coupled with these posterodorsal movements of the hyoid (Lauder 1980a, Lauder 1982, Lauder 1985, Wilga et al. 2000). However, feeding studies of gars report a distinct delay of hyoid depression until close to peak gape (Lauder 1980a, Lauder and Norton 1980, Porter and Motta 2004). While intermandibular musculature may contribute to jaw-opening in *Amia*, these muscles are ruled out as contributing to jaw-opening in other actinopterygians due to their line-of-action (Lauder 1980a). With no other known muscular contributions to jaw-opening in gars (Lauder 1980a, Lauder and Norton 1980, Lauder 1982) and gars having also lost the ancestral gnathostome coracomandibularis coupling (Wilga et al. 2000), the jaw opening mechanism in gars is not fully

understood. A third aim of this study is to examine the surrounding musculature of the feeding apparatus of *Atractosteus spatula* for distinct subdivisions using contrast enhanced micro-computed tomography (μ CT). With new insights on cranial kinesis gained from modelling the cranial linkage system, additional details of the myology of *A. spatula* may also provide information on changing muscle function during the feeding strike.

3.3 – MATERIALS AND METHODS

3.3.1 – Fish specimens and care

Atractosteus spatula specimens were obtained from the U.S. Fish and Wildlife Service Warm Springs National Fish Hatchery (trip number 14-023), with all aquarium maintenance and care performed at The University of Chicago under Institutional Animal Care and Use Committee protocol 72365. The fish were trained to feed on pieces of freeze dried krill held in forceps in the presence of bright lights to acclimate fish for later high-speed videography. Although primarily piscivorous, invertebrates form a portion of the diet of young gars in the wild (Buckmeier 2008). The gars were enticed to feed in midwater to enhance their visibility during feeding. Specimens were fed three times a week, with a fasting period of 48-72 hours observed before filming.

3.3.2 – High speed videography and digitizing

A cohort of five of the most actively feeding *Atractosteus* juveniles (1.5 years old) were selected for high-speed videography. A mirror submerged in the tank and angled at 45° provided simultaneous lateral and dorsal views. Strike videos were recorded at 500 frames per second using a Photron FASTCAM SA7 color high-speed video camera with a shutter speed of 1/1000th of a second. A total of 101 feeding strikes was recorded. Strikes were screened for clarity and

positioning of the fish relative to both views of the camera, and 25 of the best videos were selected for digitization, with five videos per individual forming the basis of the kinematics dataset.

Videos were digitized using the StereoMorph R package version 1.5.1 (Olsen and Westneat 2015). Seven landmarks in dorsal view and eleven landmarks in lateral view were digitized in each frame from the onset of the feeding strike to the completion of the reset phase. In instances when a landmark was occluded (i.e. by the forceps, prey item, or moving out of the field of view), the landmark's position was interpolated from the position of surrounding markers or discarded until it could be tracked again.

The known width and inter-tine spacing (0.083 cm) of the forceps provided a reliable scale in each feeding video. The number of pixels per centimeter was measured in the clearest frame of each video, where the forceps were held perpendicular in the field of view. An arbitrary point in the center of the prey item was used at the beginning of the prey strike to establish the starting position of the prey.

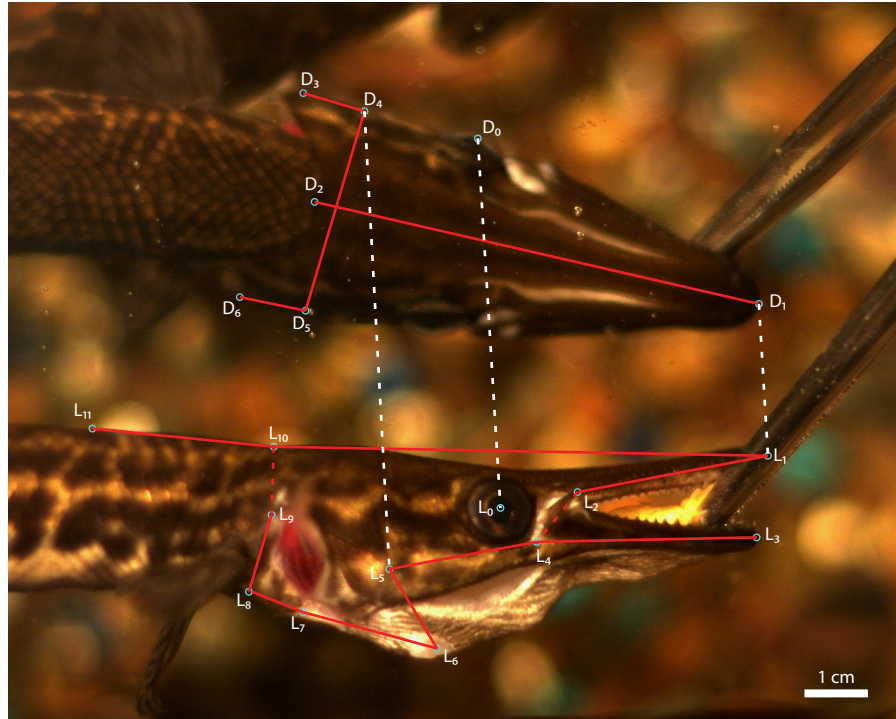


Figure 3.1. Digitizing schema of anatomical landmarks for high-speed feeding videos. Seven dorsal and eleven lateral points were tracked continuously in StereoMorph throughout the feeding sequence. Dorsal points: center of orbit (D0), tip of the upper jaws (D1), back of the skull (D2), right opercular flap (D3), right subopercle-preopercle joint (D4), left subopercle-preopercle joint (D5), left opercular flap (D6) (note the inversion of left and right because the dorsal view is a mirrored view). Lateral points: center of the orbit (L0), tip of upper jaws (L1), base of upper jaws (L2), tip of lower jaws (L3), jaw joint (L4), right subopercle-preopercle joint (L5), anterior tip of the hyoid (L6), anterior tip of cleithrum (L7), base of right pectoral fin (L8), cleithral-supracleithral joint (L9), inflection point of neck (L10), fixed dorsal body point (L11). Other points such as the starting position of the food item in dorsal and lateral views were measured once to establish prestrike starting conditions. The in-frame scale for distance measurements was established by measuring the pixels between thirteen tines on the forceps (= 1 cm).

Measuring kinematic variables

Landmarks first were rotated into a global coordinate system. The center of the eye facing the camera was used as a marker for the global vertical axis by measuring its position in dorsal and lateral views throughout the sequence ($\overrightarrow{D_0L_0}$, Fig. 3.1). The angle between this vector ($\overrightarrow{D_0L_0}$, Fig. 3.1) and the global vertical axis was averaged throughout the feeding sequence, and

then all landmarks were rotated by that averaged global offset. This aligned all landmarks shared between the dorsal and lateral views in the global vertical axis (Fig. 3.1) and created a horizontal global axis that is perpendicular to the reflection of the mirror between dorsal and lateral views.

After establishing a global coordinate system, yaw angle was measured and calculated as the offset angle between the midline of the skull in dorsal view ($\overrightarrow{D_1D_2}$) and the global horizontal axis. Yaw greater or less than 0° in dorsal view foreshortens angles in the lateral view by the cosine of its angle (i.e. $\cos(15^\circ) = 96.59\%$), so a correction factor, $(1/\cos(\text{yaw}^\circ))$, was applied to horizontal distance measurements in lateral view to account for this distortion.

Gape angle was measured as the angle between the upper tooth row ($\overrightarrow{L_1L_2}$), and the tip of the lower jaws to the jaw joint ($\overrightarrow{L_3L_4}$) in lateral view. Peak gape was set as time zero in the feeding strike, as it was often associated with other kinematic variables, such as onset of suspensorial abduction and peak lateral-snapping speed (Fig. 3.2).

Hyoid depression was measured as the change in angle (relative to the beginning of the feeding strike) between the jaw joint, the bottom of the opercular joint, and the bulge indicating the hypohyals ($\angle L_4L_5L_6$, Fig. 3.1). The bottom of the opercular joint (marked by the intersection of the subopercle, preopercle, and adjacent suborbital), while not the exact location of the interhyal-ceratohyal joint, was a consistently clear landmark in the feeding videos and an effective proxy for its location between individuals.

Neurocranial elevation was measured as the change in angle (relative to the beginning of the feeding strike) between the inclination of the skull ($\overrightarrow{L_1L_{10}}$) and the body axis ($\overrightarrow{L_{10}L_{11}}$). Similarly, pectoral girdle retraction was measured as the change in angle (relative to the beginning of the feeding strike) between the cleithrum ($\overrightarrow{L_8L_9}$) and body axis ($\overrightarrow{L_{10}L_{11}}$).

Suspensorial abduction was measured as the width of the skull at the preopercle-opercle hinge ($\overline{D_4D_5}$) divided by the resting width of the skull in dorsal view. Initially, the preopercle-opercle hinge is not visible in dorsal view, so the widest point of the skull is measured at the sphenotics for the initial values of skull width. This produces a value between 1.0 and 1.7, equal to 0% and 70% expansion of cranial width due to suspensorial abduction respectively.

Opercular abduction was measured in the same way as suspensorial abduction except, in order to isolate the component of cranial expansion due to opercular abduction alone, the concurrent width of the preopercle-opercle hinge ($\overline{D_4D_5}$) was subtracted from total interopercle width ($\overline{D_3D_6}$). This value was then divided by the resting width of the skull, producing values between 0.82 (opercular adduction) and 1.23 (opercular abduction), equal to 18% constriction and 23% expansion of resting cranial width respectively due to opercular movements independent of suspensorial movements.

Lateral-snapping speed was calculated by first measuring the perpendicular distance of the midline axis of the skull in dorsal view ($\overline{D_1D_2}$) to the initial coordinates of a point in the center of the prey item at the beginning of the prey strike (marked by an 'x' in Fig. 3.3). The distance traversed frame-by-frame in centimeters was multiplied by 500 to get lateral snapping speed $\left(500 \frac{\text{frames}}{\text{second}} \times \frac{\text{cm}}{\text{frame}} = \text{speed} \left(\frac{\text{cm}}{\text{s}}\right)\right)$. Note that negative values for speed indicate that the center line of the jaws had passed the starting coordinates of the prey.

Forward-lunging speed was measured the same way as lateral snapping speed, except only the distance between the back of the skull in dorsal view (D_1) and the same initial prey item point was used. The distance traversed frame-by-frame in centimeters was multiplied by 500 to get forward-lunging speed (see above).

3.3.3 – *In situ* manipulation and preparation for imaging

Individual “D” from the feeding experiments was sacrificed for contrast-enhanced computed tomography (CT). The specimen was euthanized in a solution of tricaine methanesulfonate (MS222), 200 mgL⁻¹ buffered with 200 mg sodium bicarbonate (NaHCO₃) (Cho and Heath 2000).

Before fixation, *in situ* manipulations were performed to test the full range of cranial kinesis in a fresh specimen. A stainless-steel wire was threaded through the connective tissue directly anterior to the pectoral girdle allowing the pectoral girdle to be retracted, simulating sternohyoideus muscle force. Hyoid constrictor muscle forces were simulated by holding the hyoid in an elevated position and holding the preopercles in an adducted position. The action of the jaw adductors was mimicked by holding the jaws shut.

After manipulation experiments, the gar was fixed in a solution of 10% formalin in water (weight/volume). The specimen was fixed with fully abducted palates and depressed hyoid by filling the pharyngeal cavity with folded paper towel that could easily be removed after the fixation process. No additional method was needed to hold the jaws closed at peak hyoid depression, suggesting the mandibulohyoid ligament is not tensed due to hyoid rotation alone. A period of 1 week in 10% formalin was followed by washing and soaking the specimen in water for another week with the pharyngeal cavity empty before preparation for micro computed tomography scanning.

3.3.4 – Contrast enhanced micro computed tomography (μCT) and segmentation

A reference scan established the position of bones in the specimen. Prior to scanning, the specimen was rehydrated in a 20% solution of sucrose in water (weight/volume) for 48 hours. The reference scan was collected using the UChicago PaleoCT (GE Phoenix v|tome|x 240

kv/180 kv scanner) (<http://luo-lab.uchicago.edu/paleoCT.html>) with the following scanning parameters: voltage = 70 kV, current = 150 μ A, timing = 333 ms, voxel width = 25 μ m, resolution = 40 pixels/mm, no filter.

Next, the specimen was immersed in a 2.5% solution of phosphomolybdic acid (PMA) in water (weight/volume) for a period of 12 days. During this time, the specimen and solution were set to mix on an orbital shaker, kept at room temperature, and covered with foil to prevent photoreaction. PMA is a contrast agent used to enhance micro computed-tomography scans (μ CT) (Pauwels et al. 2013) allowing distinction between a variety of tissues including muscle, bone, ligament, and nervous tissue. The PMA-enhanced CT scan used the following scanning parameters: voltage = 70 kV, current = 300 μ A, timing = 200 ms, voxel width = 25 μ m, resolution = 40 pixels/mm, no filter. Some shrinkage occurred between the reference scan and the PMA-enhanced scan, which could pose a problem for measuring muscle volumes, but anatomical structures were readily distinguishable. A preliminary scan after only five days in the PMA solution indicated that PMA had penetrated everywhere except the densest portions of the axial musculature and neural cavity. Twelve days in the PMA solution was sufficient time for the PMA to diffuse throughout the entire body.

Digital segmentation

Atractosteus μ CT scans were segmented using Amira 6.2.0 (FEI). To speed segmentation, an 8 bit, down sampled version of the dataset was used to make the initial segmentation at a resolution of 20 pixels/mm. The higher resolution (40 pixels/mm, 16 bit) dataset and reference scan were used to confirm any ambiguous segmentation made in the lower resolution scan.

Atractosteus has a long dividing sulcus separating dermal bones associated with the suspensorium (palatoquadrate and hyomandibula) from bones associated with the neurocranium. This division spans the entire length of the skull from the nasal capsule all the way to the gills (Fig. 3.4). Functional units of the skull were identified along this anatomical division. The ectopterygoid underlaps the lateral flanges of the premaxilla and frontal bones, forming a broad sliding scarf joint. Beginning just anterior to the orbit, the supraorbitals slightly overlap the frontal before the scarf joint transitions to a simple hinge between the dermosphenotic and the frontal. This hinge continues dorsal to the suborbitals, ventral to the sphenotic, dorsal to the dermohyal, and finally dividing the operculum from the lateral most extrascapular (terminology after Grande 2010).

The digital dissection emphasized bones, muscles, and cartilage of interest for elucidating the feeding mechanism. Visualization incorporated volume renderings of the individually segmented elements, with color-coding based on the region of the braincase the element belonged to: muscles were given a red-to-yellow-to-white color scheme, dermal bones were colored grey-to-white, while endochondral bones and closely associated dermal bones (such as the lacrimomaxillas, and dermal bones of the lower jaws) were given a blue-to-cyan-to-grey-to-white color scheme. Ligaments were left white. Application of these color transitions was made to emphasize the anatomical structures of cranial elements, not strictly to show the distinction between bone and cartilage.

Table 3.1. Anatomical abbreviations for *Atractosteus spatula* figures

Muscles and ligaments	Bones and cartilage
AHY, adductor hyomandibulae;	ap, pars autopalatina;
AM, adductor mandibulae;	art, articular;
AOP, adductor operculi;	bhy, basihyal;
DO, dilatator operculi;	bpt, basipterygoid process;
EP, epaxial musculature;	ch, ceratohyal (posterior);
GA, gill arch adductor;	cl, cleithrum;
HH, hyohyoideus;	dpo, dermopterotic;
HYP, hypaxial musculature;	dpt, dermopalatine;
IH, interhyoideus;	ect, ectopterygoid;
IM, intermandibularis;	eth, ethmoid;
LAP, levator arcus palatini;	es, extrascapular;
MHL, mandibulohyoid ligament;	fr, frontal;
OM, opercular membrane;	ga, gill arch;
PM, palatomandibularis;	hh, hypohyal;
PMm, palatomandibularis minor;	hyo, hyosymplectic;
POs, preorbitalis superficialis;	ihy, interhyal;
POp, preorbitalis profundus;	l, lacrimal;
SDL, supradorsal ligament;	lmx, lacrimomaxilla;
SH, sternohyoideus;	mpt, metapterygoid;
	op, opercle;
	pmx, premaxilla
	pop, preopercle;
	pq, palatoquadrate cartilage;
	psp, parasphenoid;
	q, quadrate;
	rhy, rostrorhinal;
	scl, supracleithrum;
	so, subopercle;
	spo, sphenotic;
	sop, subopercle;
	sph, sphenoid;
	suo, suborbital;
	v, vomer;

3.3.5 – Animation and kinematic model

In order to recreate the cranial movements seen in the high-speed videos, individually segmented elements of the cranial skeleton were rotated in Amira 6.2.0 (FEI) into four successive kinematic states: resting-state, jaw-opening prior to hyoid-depression, hyoid-

depression prior to jaw-closing, and peak suspensorial-abduction/hyoid-depression. In Amira, each segmented element can be rotated relative to surrounding cranial elements, and the resulting rotation is exported as a (4×4) transformation matrix which defines its position during one of the four kinematic states. During animation, cranial elements are able to smoothly transition between these four states as the Amira software interpolates between each of the four transformation matrices.

Because the CT scanned individual was fixed in a state of suspensorial-abduction and hyoid-depression close to the maximum values observed in high-speed videos, the *in situ* fixed positions of the cranial elements were used for the later stage. This meant that only three other kinematic stages needed to be recreated: resting-state, jaw-opening prior to hyoid-depression, and hyoid depression prior to jaw-closing.

First, in order to recreate the resting-state position, each palate was fully adducted along its sliding articulation with the basipterygoid process, keeping its anterior process in articulation with the vomer. The hyomandibula, along with the dermal cheek, was rotated to rearticulate its connection with the palatoquadrate while maintaining articulation with the neurocranium. The jaws were rotated into fully closed position and the mandibulohyoid ligaments protracted to articulate with retroarticular process. The ceratohyals were repositioned to fit snugly under the palate without intersecting the preopercles, while maintaining the ceratohyal's connection with the mandibulohyoid ligaments. The interhyals were then rotated to match the new orientation between the ceratohyals and the hyosymplectics.

To position the cranial elements into jaw-opening prior to hyoid depression, the jaws were rotated from resting position into gape similar to the gape angles recorded in the high-speed videos. Some long axis rotation of the jaws occurs during jaw opening to prevent the medial

flanges of the prearticular from intersecting with the ventrolateral wing of the palatoquadrate that lies anteromedial to the jaw joint. The mandibulohyoid ligament was retracted to match the new orientation of the retroarticular processes, and the ceratohyal was retracted to follow the mandibulohyoid ligament. The interhyal was then pivoted posteriorly in its articular socket with the hyosymplectic to follow the new position of the ceratohyal.

To recreate hyoid-depression prior to jaw-closing, the neurocranium was elevated to the peak angle seen in high-speed videos. Then the pectoral girdle was retracted by half the amount observed. By maintaining distance between the hypohyals and pectoral girdle, the hyoid was similarly rotated by approximately half its full observed value from high-speed videos. Prior to jaw-closing, the jaws were set to their maximum value, which was only a slightly higher gape angle compared to the previous stage. Although the ceratohyals were being depressed in this stage, the interhyals were kept at their maximum posterior rotation relative to the preopercle.

3.4 – RESULTS

The feeding apparatus of *Atractosteus spatula* is capable of rapidly unfolding, much like a piece of origami, from a tightly compacted resting state to a massively expanded volume in under 41 ms. High-speed videos document the timing of this expansion, which occurs in an anterior-to-posterior sequence and incorporates suction throughout the feeding strike. The feeding apparatus of *A. spatula* functions as a cranial linkage system which binds many separate mobile elements into a single expansive mechanism using muscles and ligaments. Specialized joints, found throughout the feeding apparatus of *A. spatula* (visualized using μ CT), increase the range of motion of the linkage system and enable the multiple configurations of the feeding apparatus seen during feeding. Control of this feeding system is modulated by a plesiomorphic

complement of osteichthyan feeding musculature. Although unspecialized, many of these muscles nevertheless are found to serve dual roles within the feeding mechanism, necessary for driving the anterior-to-posterior expansion of the linkage mechanism seen in feeding videos.

3.4.1 – Kinematics of the feeding strike of *Atractosteus spatula*

Phase I: Jaw opening and lateral snapping

Jaw opening in *Atractosteus spatula* was rapid, lasting 17.4 ± 0.7 ms (Table 1), just under 9 frames at 500 fps. As lateral axial bending swept the jaws into position around the prey item, the neurocranium elevated slightly, about 10 degrees relative to the pectoral girdle and body (Table 1). As the lower jaws rotated ventrally, the ligamentous maxilla swung anteriorly and the medial wings of the prearticular flared laterally, exposing the unpigmented tissue underneath (Fig. 3.3). Slight, bracing movements of the pectoral girdle could be seen at this stage, although pronounced onset of kinematic movements of this element did not begin until later during hyoid depression (Fig. 3.2).

During the initial stages of jaw opening, the floor of the buccal cavity could be seen buckling inwards, indicating negative pressure in the space between the expanding jaws prior to the initiation of hyoid depression (0 ms, Fig. 3.3). Although the prey item was held by the forceps, suction acted upon the floating portion of the prey item, drawing it towards the buccal cavity (Fig. 3.3). Lateral movements towards the prey continued until the jaws reached the prey item, at which point lateral movement of the jaws abruptly decelerated and the fish transitioned to anterior acceleration accompanied by hyoid depression (Figs. 3.2 and 3.3).

Phase II: Hyoid depression and forward lunging

Hyoid depression was variable in timing and its onset could occur at any time during jaw opening. The variation showed individual effect, with the two largest individuals in the study (A

and B) regularly opening their jaws fully prior to hyoid depression while the smallest individual (E) initiated hyoid depression and jaw opening at the same time (Fig. 3.2 and 3.3). On average, onset of hyoid depression was delayed an average of 9.1 ± 2.8 ms between individuals after initiation of jaw opening, at which point the jaws had already reached approximately half of peak gape (Fig. 3.2, Table 1).

The initiation of hyoid depression marked a distinct shift in the movement of cranial elements in high-speed videos. The folds of skin and musculature that were held in a constricted and elevated state in the initial phases of jaw opening could be seen distending ventrally to accommodate the hyoid bars and basihyal toothplate as they were depressed (10 ms, Fig. 3.3). Pronounced rotation of the pectoral girdle resulted in a posteroventral displacement of the tip of the cleithrum, and the isthmus connecting the cleithrum and hyoid could be seen retracting from underneath the branchiostegal membrane (Figs. 3.2 and 3.3, 20 ms). Lateral movement of the jaws decelerated, and anterior displacement toward the prey accelerated (Fig. 3.2). Suction continued to draw the prey item into the oral cavity (10 ms, Fig. 3.3). Movement of the prey into the oral cavity occurred throughout hyoid depression, even while anterior acceleration and/or jaw closing might have been expected to displace the water containing the prey item out of the jaws.

Phase III: Jaw closing and suspensorial abduction

While jaw closing typically marks the onset of the “compressive phase” in other actinopterygians (Liem 1978, Lauder 1980a), in *Atractosteus* jaw closing coincided with the greatest volumetric expansion of the oral cavity. Due to the late onset of hyoid depression, the majority of hyoid depression occurred after peak gape (Figs. 3.2 and 3.3). Furthermore, suspensorial abduction occurred exclusively during jaw closing (Table 1, Fig. 3.2). The jaws closed even as other elements, such as the neurocranium, cleithrum, suspensorium, and hyoid,

continued to rotate and abduct, making jaw closing an “expansive” kinematic event. At the moment of jaw closure (an average of 23.3 ± 3.3 ms after peak gape), the feeding apparatus was fully expanded, coinciding with both peak hyoid depression and peak suspensorial abduction (Table 1, Fig. 3.2).

Suspensorial abduction resulted in a large posterior expansion of the feeding apparatus during this phase, laterally flaring the jaw joints, cheeks, and opercular flaps. Suspensorial abduction was evident posteriorly as the dermal cheeks rotated dorsolaterally along their hinge with the braincase, which resulted in an average of $44.9 \pm 7.6\%$ lateral expansion of the cranium occurring at the cheek-opercular hinge by peak abduction (Table 1, Fig. 3.2). Anteriorly, the palate could be seen sliding laterally, exposing the underlying unpigmented skin of the ectopterygoid (Fig. 3.3). This portion of the ectopterygoid is normally covered by an overlapping scarf joint of the frontal and premaxilla (see below) but was clearly visible during suspensorial abduction as a longitudinal white line running the length of the rostrum in dorsal view (Fig. 3.3).

Phase IV: Compression and opercular abduction

Although the opercular flaps were laterally abducted during suspensorial abduction, distinct opercular abduction beyond movements of the cheeks was not apparent until the compressive phase of the feeding strike (Figs. 3.2), after the jaws had fully closed (30-50 ms, Fig. 3.3). During the reset phase, the hyoid elevated, the pectoral girdle protracted, the ventrolateral margins of the cheeks adducted, and the palate slid back beneath the frontal and premaxilla. This caused the opercular flaps to adduct medially as well; however, the dorsal portion of the opercular flaps were continually held open until all other elements were brought back into resting position, and water could be seen flowing posteriorly through the open gill

covers. The prey item was held in the feeding apparatus for an extended period of time prior to deglutition as the hyoid elevated and suspensorium slowly adducted (Table 1, Fig. 3.2).

Table 3.2. Individual and aggregate means of *Atractosteus spatula* feeding kinematics. Means of kinematic variables were calculated for all five individuals with standard deviations (\pm). [1] Timing is relative to peak gape at 0 ms. [2] Peak value is measured in degrees, except for suspensorial abduction (percent lateral expansion) and snapping/lunging (cm/s). [*] For hyoid depression, pectoral girdle retraction, and suspensorial abduction, duration only includes time from onset to peak, because the prey is held in the pharyngeal cavity for an extended period of time before prey processing. Sample size: individuals (n = 5), strikes per individual (n = 5).

Kinematic Variable	Onset (ms) ^[1]	Peak (ms) ^[1]	Value at Peak ^[2]	Duration (ms)
Jaw opening/closing	-17.4 \pm 0.7	NA	48.2 \pm 1.3°	40.7 \pm 3.3
Neurocranial elevation	-18.7 \pm 2.1	5.9 \pm 4.8	10.3 \pm 2.2°	53.2 \pm 6.9
Hyoid depression	-8.3 \pm 2.8	17.8 \pm 3.6	47.4 \pm 6.0°	26.2 \pm 5.1 [*]
Pectoral girdle retraction	-6.9 \pm 2.9	26.1 \pm 2.7	19.7 \pm 5.0°	32.9 \pm 2.4 [*]
Suspensorial abduction	1.0 \pm 2.9	22.4 \pm 2.9	44.9 \pm 7.6%	21.5 \pm 2.5 [*]
Lateral snapping	-13.5 \pm 1.5	-2.8 \pm 1.2	143.6 \pm 22.1 cm/s	24.4 \pm 0.8
Forward lunging	-5.7 \pm 2.2	10.2 \pm 1.7	66.1 \pm 14.1 cm/s	118.4 \pm 15.8

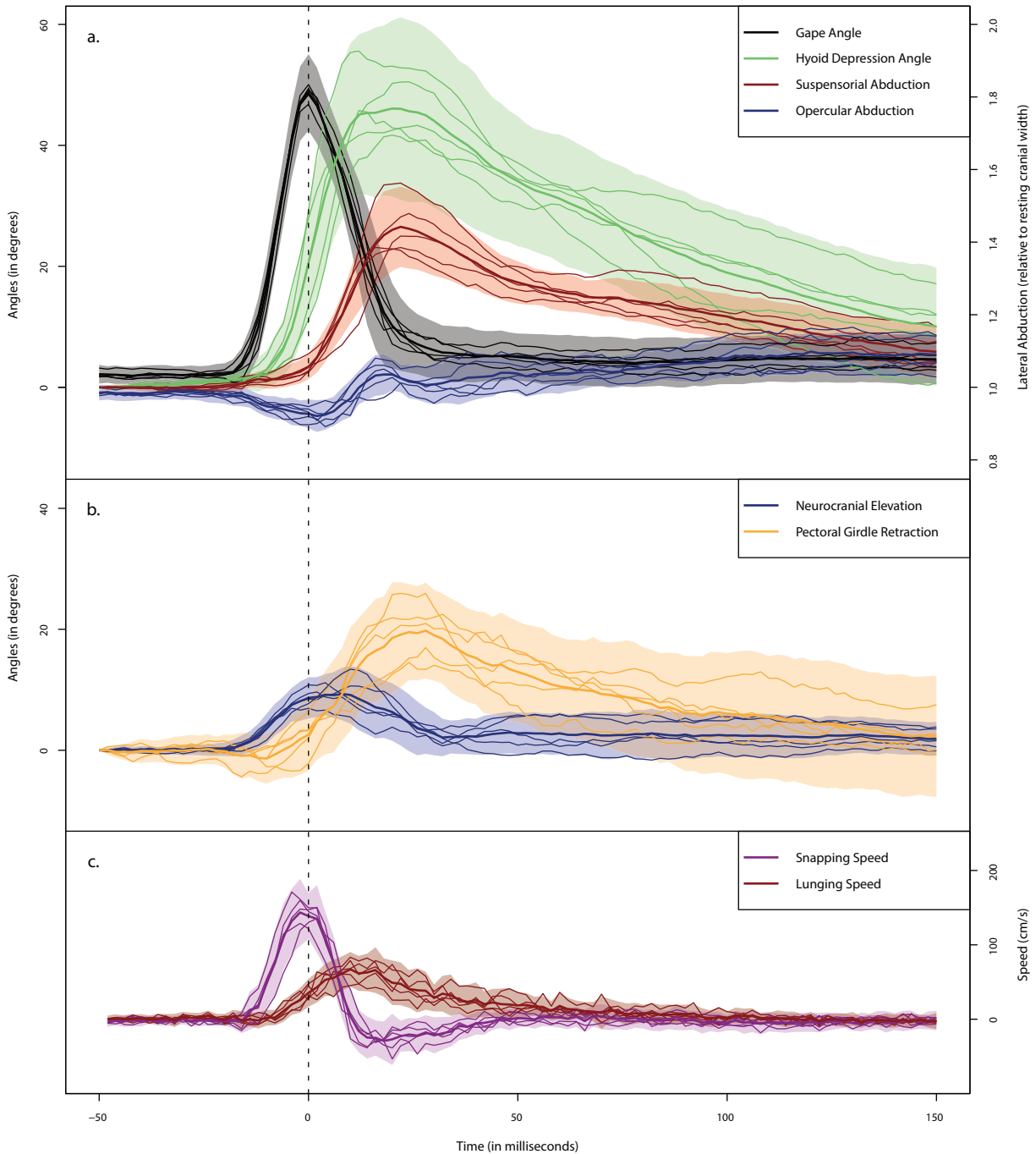


Figure 3.2. Averaged feeding kinematics of *Atractosteus spatula*. Graphs show the means of each measured kinematic variable. Shown are the individual means (thin lines) as well as the aggregate means for each variable (all individuals, thickened line). Standard deviations are indicated by the shaded area above and below each aggregate mean. All sequences are aligned with peak gape coinciding with time 0 ms. Kinematics show a clear anterior-to-posterior wave of expansion of cranial elements (a). Onset of hyoid depression is highly variable between individuals (a). The transition between jaw opening and hyoid depression is closely associated

Figure 3.2, continued. with pectoral girdle retraction (*b*). Lateral snapping speed promptly decelerates with the onset of hyoid depression (*c*).

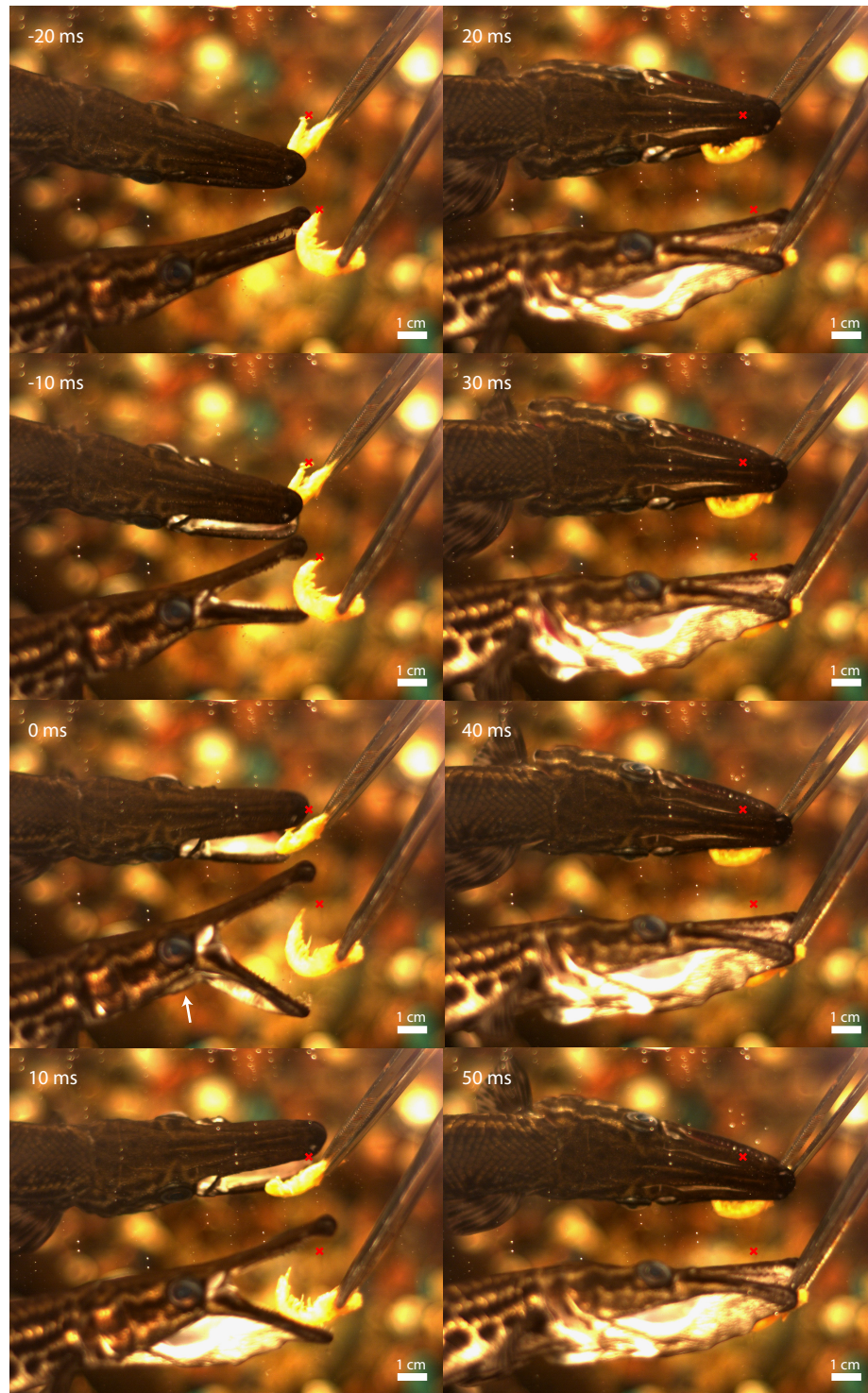


Figure 3.3. Representative feeding sequence of *Atractosteus spatula* showing suction and delayed hyoid depression. Shown are key frames from high-speed video indicating positioning of the animal prior to strike (-20 ms), jaw opening (-10 ms), peak gape (0 ms), hyoid depression (10 ms), suspensorial abduction just prior to peak (20 ms), peak pectoral girdle retraction (30

Figure 3.3, continued. ms), and kinematic recovery while the opercular flaps are held abducted (30-50 ms). The initial starting position of the prey item is marked by a red 'x' in both mirror and lateral views. The prey item is drawn into the buccal cavity prior to the onset of hyoid depression (-20 ms to 0 ms), which begins with peak gape (white arrow, 0 ms). Depression of the hyoid, accompanied by retraction of the pectoral girdle, draws the prey item further into the pharyngeal cavity just prior to jaw closure (10 ms). The scarf joint between the ectopterygoid and frontal bones can be seen as a distinct, white line along the length of the rostrum anterior to the orbits. Peak hyoid depression and suspensorial abduction occurs at 24 ms (not shown).

3.4.2 – Osteology of specialized joints in the feeding system

The feeding apparatus of *Atractosteus spatula* is a linkage mechanism composed of elements of the mandibular arch (palatoquadrate, dermal palate, and lower jaws), the hyoid arch (hyosymplectic, interhyal, and hyoid bar), and the pectoral girdle (supracleithrum and cleithrum), all suspended from the neurocranium and bound together into a single linkage system by muscles, ligaments, fibrous connective tissue, and synovial joints. Internal to each of the arches and pectoral girdle, specialized joints between individual elements increase the range of motion of each functional unit. The bones comprising these functional units have been described in detail for *Atractosteus* and *Lepisosteus* in other studies (Wiley 1976, Arratia and Schultze 1991, Grande 2010), so the following descriptions focus on new information on soft-tissue anatomy documented through contrasted-enhanced μ CT and in-situ manipulations.

Mandibular arch

The palatoquadrate and dermal palate form three distinct articulations with the braincase. Anteriorly, a small forward-facing process of the dermopalatine fits into a socket formed dorsally by the premaxilla and ventrally by the vomer (Fig. 3.4e). This joint is filled with dense connective tissue, allowing only slight mediolateral movement (Fig. 3.4e). Anterior to the jaw joint, a pair of cartilaginous processes extend dorsolaterally from the ethmoid cartilage to support lateral flanges of the overlying frontal bones. These processes correspond to a thickened,

anteriorly tapering portion of the palatoquadrate cartilage lying in a dorsal groove of the ectopterygoid, the pars autopalatina sensu (Konstantinidis et al. 2015) (Fig. 3.4c). This unusual ethmoid-autopalatine articulation allows mediolateral sliding, while restricting dorsolateral rotation of the palate. Posteriorly, the metapterygoid ossification of the palatoquadrate articulates with an enlarged basipterygoid process. This joint is unique in gars (Wiley 1976, Arratia and Schultze 1991, Grande 2010) and provides a broad expanded surface for mediolateral excursions of the metapterygoid. Unlike the hyosymplectic, movements of the palate pivot around a vertically oriented axis of rotation through the dermopalatal-vomerine joint (Fig. 3.4e, black dashed line) (see below).

Specialized joints of the lower jaws of *Atractosteus spatula* correspond with mediolateral movements of the palate. As reported for *Lepisosteus* (Haines 1942, Askary et al. 2016), the quadrate-articular joint is synovial, and the convex, rounded condyle of the quadrate allows a wide range of dorsoventral as well as mediolateral motion. This joint is exclusively suspended from the palatoquadrate without any support from the hyoid arch (Wiley 1976, Grande 2010) (see below). In contrast to the condition in *Lepisosteus* (Grande 2010), the mandibular symphysis of *A. spatula* is short and flexible, allowing mediolateral wish-boning of the lower jaws. In gars, the symphysis does not contain Meckel's cartilage (Jollie 1984, Grande 2010). Instead, in *A. spatula*, it is filled with cartilage both continuous with and of a similar composition as the rostrhyal sensu (Hilton et al. 2014), forming a discrete anterior buccal floor (Fig. 3.5).

Gars have a distinct retroarticular process ventral to the jaw joint where the mandibulohyoid ligament attaches (Fig. 3.5) (see below). There is no evidence for an interoperculomandibular ligament in *Atractosteus spatula*, despite the clear presence of other ligaments in contrast-enhanced μ CT (Fig. 3.4d). No other ligament or muscle attaches to the

retroarticular process, which makes retraction of the mandibulohyoid ligament, by means of hyoid retraction due to sternohyoideus, the sole input responsible for depression of the lower jaws (Lauder 1980a).

Hyoid arch

The hyosymplectic is suspended from the spheno-pterotic ridge (sensu (Allis 1919)) of the auditory capsule, directly ventral to the dermopterotic (Grande 2010). In ontogeny the hyosymplectic fuses to the medial surface of the preopercle, and its movements are directly linked to movements of the dermal cheek. Contact between the hyosymplectic and palatoquadrate is limited to a small overlap between the posteroventral angle of the palatoquadrate cartilage and the anterior portion of the symplectic (Grande 2010). Gars are unusual in that the hyoid arch does not contact any ossifications of the palatoquadrate directly (Wiley 1976, Arratia and Schultze 1991, Grande 2010). Unlike in *Amia*, there is no direct contact between the metapterygoid and the hyosymplectic (Wiley 1976, Arratia and Schultze 1991, Grande 2010). As a result, it is possible for hyosymplectic-palatoquadrate joint to twist during suspensorial abduction. As the palate slides mediolaterally, the hyosymplectic-cheek complex rotates dorsolaterally. Rotation of the hyosymplectic-cheek complex is centered around a horizontal, anteromedially oriented axis of rotation through the hyomandibular-otic joint (Fig. 3.4). Unlike the ectopterygoid-frontal scarf joint, the joint between the dermal cheek and skull roof is a simple hinge which remains articulated during suspensorial abduction (Fig. 3.3).

The interhyal rests in a synovial joint on the medial wall of the preopercle, bounded dorsally by the hyosymplectic (Fig. 3.7). In contrast-enhanced μ CT, this joint shares similar histology to the quadrate-articular joint, which is a known synovial joint (Haines 1942, Askary et

al. 2016) (Fig. 3.10). The interhyal is capable of a wide range of motion upon the dorsal process of the posterior ceratohyal, which is large, rounded, and acts as a ball-in-socket joint.

Due to the mobility of the interhyal-ceratohyal joint and the hypohyal-basihyal joint, the hyoid bar is capable of retraction relative to the hyosymplectic, rotation relative to the interhyal, and abduction relative to the sagittal plane. The mandibulohyoid ligament originates on the neck of the dorsal process of the posterior ceratohyal, close to the point of rotation of the ceratohyal-interhyal joint and attaches to the retroarticular process of the lower jaws (see above). The mandibulohyoid ligament links hyoid retraction with jaw depression (Lauder 1980a), but it also causes hyoid protraction when the jaws are adducted. The sternohyoideus attaches to the hypohyals of the hyoid bar and serves to link movements of the hyoid apparatus and pectoral girdle.

Pectoral girdle

The supracleithrum attaches to the back of the dermatocranium by means of a small cup-shaped articulation that extends anterodorsally to the lateral extrascapular and posttemporal (Grande 2010). The supracleithrum is tightly bound to the dermatocranium by dense connective tissue through which the lateral line passes (Grande 2010). As a result, movement at this joint is restricted, although the neurocranium is capable of slight elevation relative to pectoral girdle.

The cleithrum is only loosely connected to the supracleithrum by connective tissue and a small, undescribed muscle originating on the medial surface of the supracleithrum (Fig. 3.8). The cleithrum is capable of large posteroventral rotation relative to the supracleithrum, and is easily disarticulated during manual manipulation. The cleithrum is the origin of the sternohyoideus, which acts as a contractile link between the pectoral girdle and hyoid arch. The cleithrum is also

the attachment point for powerful hypaxial musculature which drives the expansion of the cranial system due to posteroventral retraction of the sternohyoideus (see below).

Cranial Linkage

The interconnections of all these elements can be demonstrated on a fresh *Atractosteus* specimen via in-situ manipulations. By simply retracting the pectoral girdle, simulating input of the sternohyoideus and hypaxial musculature, the entire feeding system expands simultaneously. The hyoid depresses, the cheek-hyosymplectic rotates dorsolaterally, the palate slides laterally, and the jaws weakly open. Counterintuitively, closing the jaws in this state causes the cheek and suspensorium to expand further laterally, whereas pressing the cheeks together cause the jaws to open wider. Maximal jaw opening occurs when the cheeks are held adducted, the hyoid is restrained in an elevated position, and the pectoral girdle is retracted. This demonstrates that additional muscular input is needed – other than sternohyoideus and axial musculature – to produce the multiple configurations of the feeding apparatus seen in the high-speed videos throughout the feeding strike.

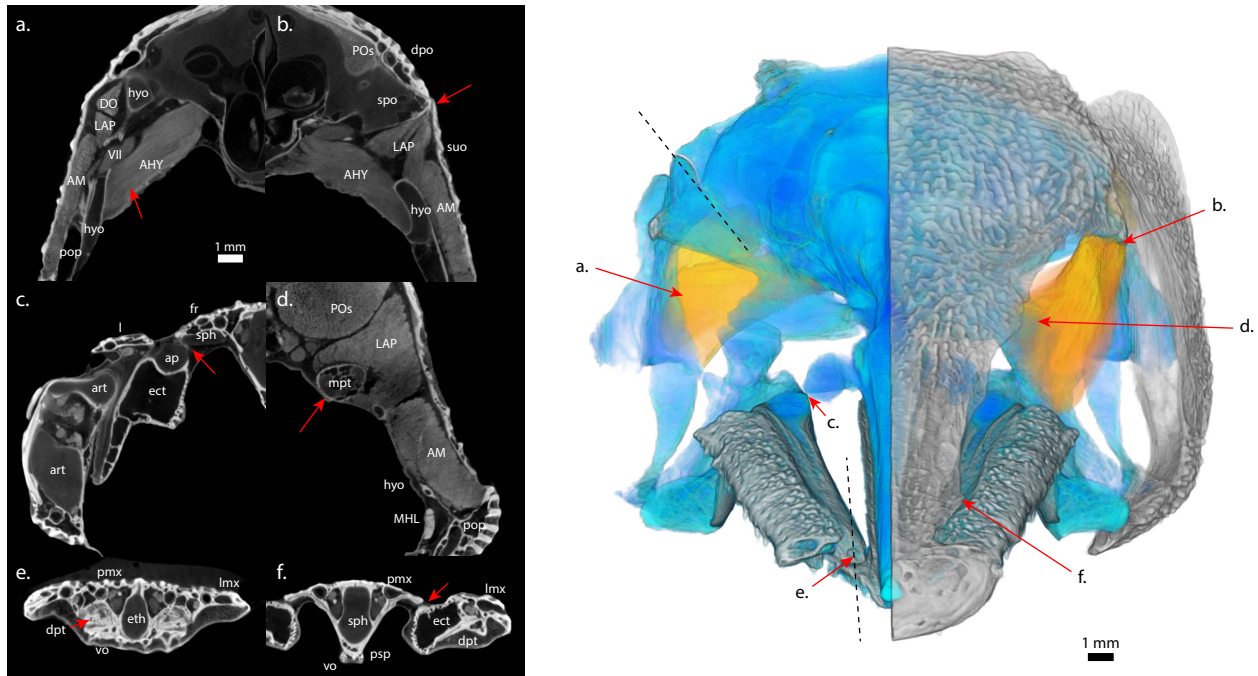


Figure 3.4. Points of articulation, axes of rotation, and primary muscular connections between elements of the braincase and suspensorium of *Atractosteus spatula*. (a) The hyosymplectic (hyo) has an oblique articular axis with the braincase, is intimately connected to the medial surface of the preopercle (pop), and has a broad attachment area of the adductor hyomandibulae (AHY) near the foramen for the hyomandibular trunk of facial nerve (VII). (b) The sphenotic (spo) is the origin for the levator arcus palatini (LAP). (c) Corresponding gliding cartilages exist between the pars autopalatina (ap) and specialized lateral projections of the sphenoid (sph). (d) The levator arcus palatini wraps around both the dorsal and ventral surfaces of the metapterygoid (mpt). (e) Rotation of the palate is around a vertical axis running through the dermopalatine-vomerine joint (dpt, vo). (f) Lateral sliding of the palate is possible due to the broad, overlapping scarf joint between the premaxilla (pmx) and ectopterygoid (ect) that lacks tightly binding connective tissue.

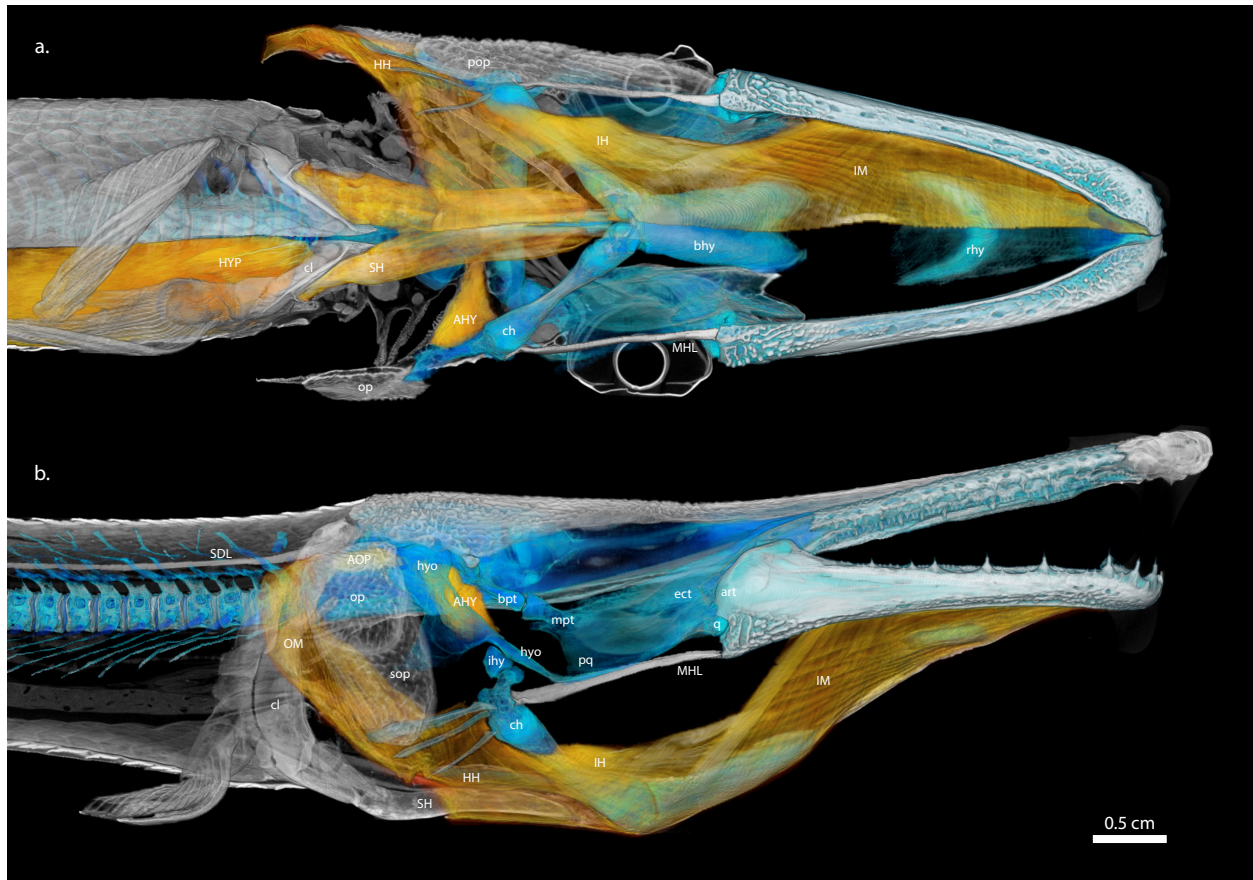


Figure 3.5. Morphology of the hyoid constrictor sheath that assists in jaw opening. (a) Ventral hyoid constrictors wrap around the sternohyoideus (SH) and elevate the hyoid apparatus (ch, bhy) enabling the hyoid to be retracted without depressing. This retracts the mandibulohyoid ligament (MHL) and opens the jaw. (b) After jaw opening, these muscles relax and allow the hyoid to depress and the suspensorium to flare laterally. See Fig. 3.6 for dorsal view of the adductor operculi (AOP).

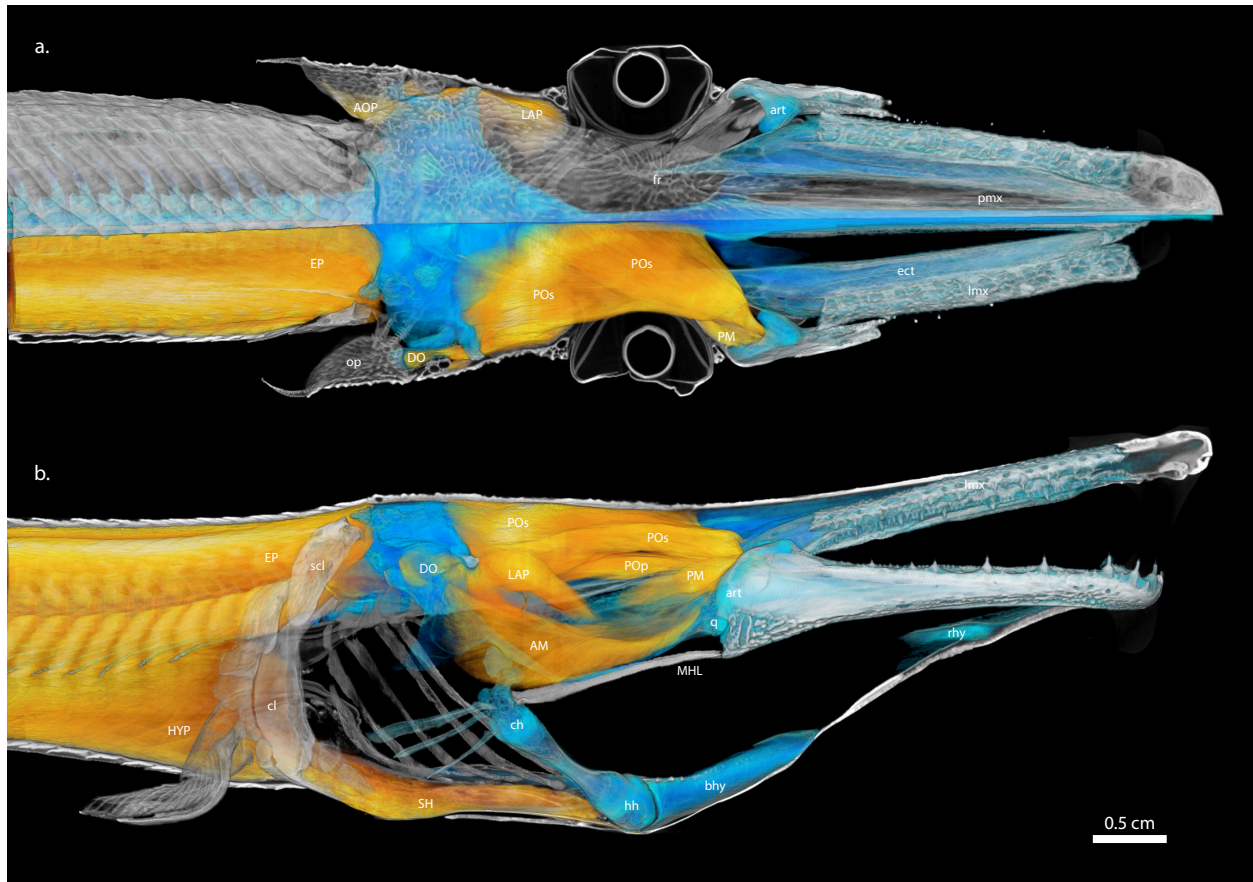


Figure 3.6. Morphology of jaw adductors and muscles of hyoid depression and suspensorial abduction. (a) Epaxials (EP) and jaw adductors (AM, PM, POs) shown in dorsal view. Jaw adductors can be seen entering into the adductor chamber of the lower jaw (see Fig. 3.10 for more detail). (b) Epaxials and hypaxials (HYP) are responsible for elevating the neurocranium and retracting the pectoral girdle (cl), which elevates the interhyal-ceratohyal (ch) joint relative to the line of action of the sternohyoideus (SH). Lateral rotation of the ceratohyal (ch) is mediated by the levator arcus palatini (LAP) and jaw adductors, which anterolaterally rotates the posterior ceratohyal while the sternohyoideus ventroposteriorly retracts the hypohyals (hh).

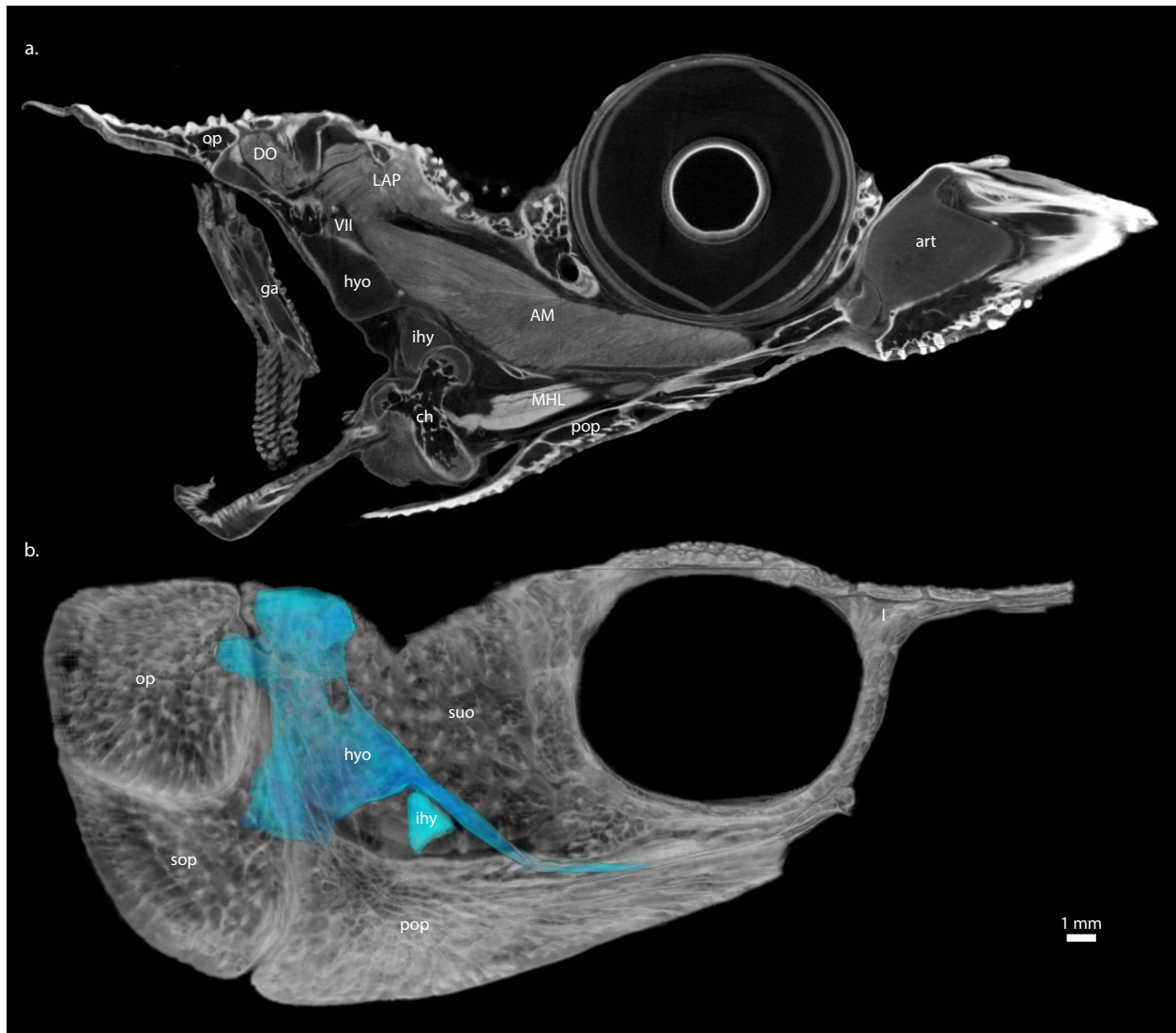


Figure 3.7. Morphology of the joint capsule containing the interhyal. Shown is the left joint capsule of the interhyal in (a) parasagittal cross section, and (b) medial view. This joint appears to be synovial, is bounded by the hyosymplectic (hyo) and preopercle (pop), and includes the posterior ceratohyal (ch), mandibulohyoid ligament (MHL), and branchiostegal rays.

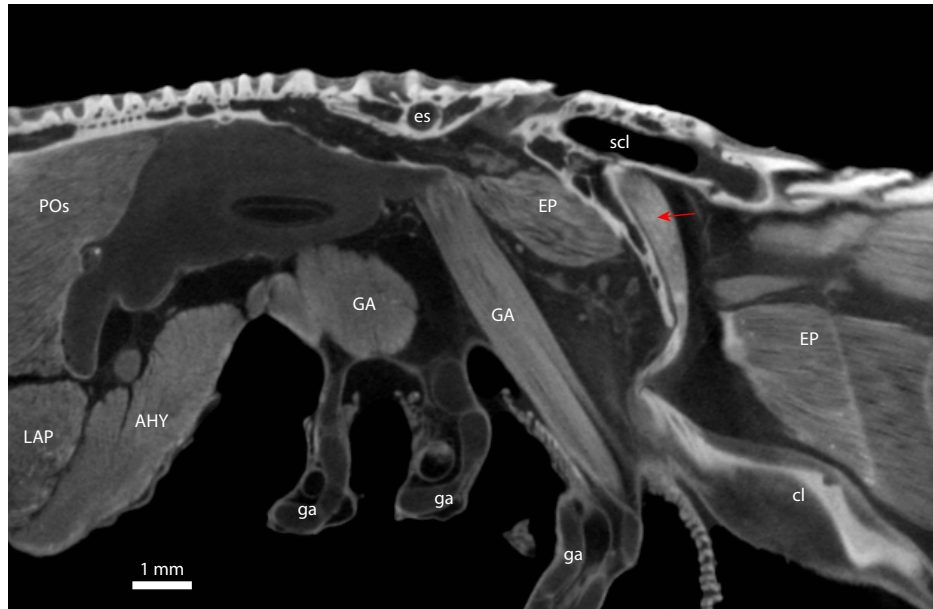


Figure 3.8. Parasagittal cross section of the head-shoulder interface. The supracleithrum (scl) is attached to the back of the skull (es); however, the cleithrum (cl) is only loosely connected to the supracleithrum by a flexible joint. A small slip of muscle on the medial surface of the supracleithrum (red arrow) inserts onto a small anterior prong of the cleithrum.

3.4.3 – Myology and manipulation of the muscles of the feeding mechanism of *Atractosteus spatula*

Manipulation of fresh specimens indicates that additional muscular input is necessary to create the multiple configurations of the feeding apparatus seen in high-speed videos. Gars maintain only a plesiomorphic complement of feeding musculature with which to modulate the anterior-to-posterior expansion of their cranial linkage system. However, many of these muscles appear to have secondary functions typically found only in more specialized muscles in derived actinopterygians. Emphasis is placed here on muscles with atypical morphology (sternohyoideus, levator arcus palatini, dilatator operculi) and potentially multiple roles driving cranial expansion during the feeding strike of *Atractosteus spatula*.

Sternohyoideus

The sternohyoideus connects the cleithrum to the hypohyals and basihyal toothplate (Figs. 3.5 and 3.6). This muscle is responsible for both hyoid retraction and rotation, which in gar are two separate kinematic events (Figs. 3.2 and 3.3). More than any other muscle, its function changes during the feeding strike due to repositioning of its origin and insertion. At rest, this muscle passes just below the point of rotation of the interhyal-ceratohyal joint (Fig. 3.12). During early activity, the sternohyoideus serves primarily to retract the hyoid. The ventral isthmus containing the sternohyoideus passes dorsally to and is separate and free from the ventral hyoid constrictor musculature (Farina et al. 2015), which allows the sternohyoideus to retract freely relative to those muscles (see below under hyoid constrictors). However, as the pectoral girdle rotates posteroventrally and the ventral hyoid constrictors relax, this line action falls well below the point of rotation of the interhyal-ceratohyal joint (Fig. 3.12). As a result, activity of the muscle results in rotation of the hyoid and retracting forces are lessened. Indeed, the posterior ceratohyal is able to protract even as the hyoid rotates ventrally (Fig. 3.5).

To serve as both rotator and retractor of the hyoid, the sternohyoideus has an atypical morphology. In *Polypterus* and *Amia*, the sternohyoideus is divided into three muscle blocks by two transverse septa (Allis Jr 1922, Edgeworth 1935, Lauder 1980a), but in *Atractosteus spatula*, these muscle blocks are deeply nested within each other (Fig. 3.9). This pennate morphology suggests the muscle is optimized for force transmission rather than displacement. To open the jaws fully requires very little displacement of the retroarticular process due to the low mechanical advantage of the jaws (Kammerer et al. 2006); however, hyoid rotation requires far more displacement than the sternohyoideus itself is capable of (Fig. 3.3). Due to its structure, the sternohyoideus is able to convey powerful posterior retracting forces to the hyoid over a short

distance, but any further retraction of the hyoid is likely conveyed through the sternohyoideus by hypaxial-driven pectoral girdle rotation.

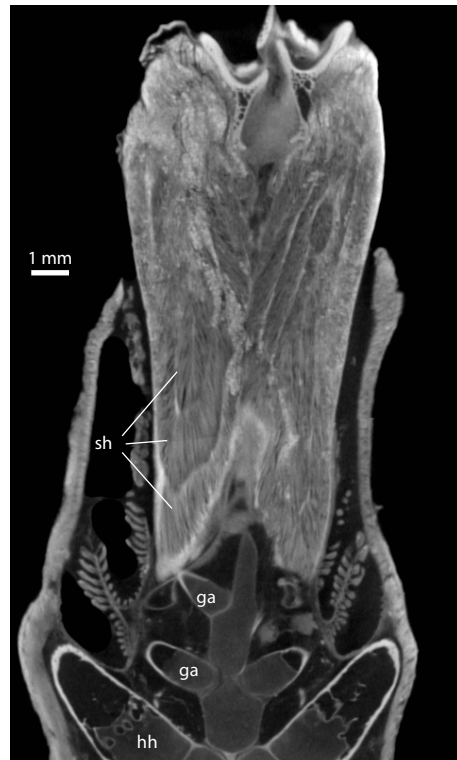


Figure 3.9. Divisions of the sternohyoideus muscle. Shown is a coronal section of the sternohyoideus muscle, which is separated into at least three deeply nested cones along its length by septa internal to the muscle.

Hyoid constrictors

An extensive, continuous sheath of hyoid constrictor musculature supports the ventral floor of the buccal, pharyngeal, and opercular cavities. From anterior to posterior, this muscular sheet is composed of the intermandibularis (originating from the paired Meckel's cartilages), interhyoideus (originating from the anterior ceratohyals), and hyohyoideus (inferioris/superioris) (spanning between the branchiostegal rays and originating from the medial surfaces of the subopercle). These muscles all intermingle fibers and join together at the midline to form a muscular sling that supports the rostrhyal, basihyal, hyoid, and sternohyoideus (Fig. 3.5). The

ventral constrictor sheet functions primarily to return the hyoid apparatus to its resting state after the feeding strike is complete (interhyoideus = protractor hyoideus sensu (Wiley 1976)). To serve this function, these muscles are capable of extreme extension during hyoid depression to accommodate hyoid depression (Figs. 3.3 and 3.5). However, along with the dorsal hyoid constrictors, these muscles may have a secondary role in jaw opening (see below)

A band of dorsal hyoid constrictors binds the dorsal and posterior edge of the opercular flap. These muscles include the adductor hyomandibulae (originating from the lateral wall of the otic capsule and inserting onto the medial surface of the hyosymplectic) and the adductor operculi (originating from the connective fascia just lateral to the otic capsule and inserting onto the medial surface of the opercle). Unlike *Lepisosteus* (Lauder 1980a, Konstantinidis et al. 2015), no distinct adductor arcus palatini muscle could be identified in *Atractosteus spatula*: the adductor hyomandibulae does not have any fibers that insert onto the palatoquadrate (Fig. 3.5). Like *Lepisosteus* (Lauder 1980a, Konstantinidis et al. 2015), the adductor operculi shows no sign of subdivision, and no specialized jaw opening muscle corresponding to the levator operculi in *Amia* could be identified.

The adductor operculi intermingles fibers with the opercular membrane, which also subsequently fuses with the hyohyoideus superior to form a complete opercular valve around the margins of the gills. The primary function of these muscles is to adduct the opercular valve, cheeks, and suspensorium. Along with the ventral hyoid constrictor sheet, these muscles remain constricted during the earliest phases of jaw opening (Fig. 3.3). It has been proposed that this constriction functions to prevent fluid from flowing anteriorly through the gills during jaw opening (Lauder 1980a); however, prior to suspensorial abduction or hyoid depression (due to

action of the ventral hyoid constrictors), negative pressure should not exist within the pharyngeal cavity during jaw opening to generate a flow of water.

Epaxials

Epaxial muscles attached to the back of the neurocranium are powerful elevators of the neurocranium. While neurocranial elevation has been a well-documented contributor to jaw opening in teleosts, it is less clear how this elevation would contribute to rapidly increasing the gape angle in gars without some mechanism for jaw protrusion. Neurocranial elevation persists well into jaw closing when the hyoid is depressed (Fig. 3.2). However, in maintaining elevation of the hyoid during jaw opening, ventral hyoid constrictors may provide a novel way for epaxial musculature to contribute to the force of jaw opening. By elevating the hypohyals during neurocranial elevation while the cleithrum remains stationary, ventral hyoid constrictors may work together with epaxial musculature to elevate the hyoid and extend the sternohyoideus muscle, even while the sternohyoideus is contracting to retract the hyoid apparatus. It is possible this mechanism increases the force and speed of jaw opening beyond what the sternohyoideus by itself would be capable of.

Hypaxials

The cleithrum rotates extensively during the later stages of the feeding strike of *Atractosteus spatula* (Figs. 3.2 and 3.3). While it is recognized that hypaxial musculature functions to stabilize the pectoral girdle during jaw opening in gars (Lauder 1980a), hypaxial musculature attaching to the posterior portion of the cleithrum may also drive posterolateral rotation of the shoulder girdle. Rotation of the pectoral girdle marks a kinematic shift in the feeding strike of *A. spatula* (Figs. 3.2 and 3.3), and corresponds to both the transition between hyoid retraction and hyoid rotation as well as the transition from flat-plate suction to hyoid-based

suction. Depression of the anterior portion of the cleithrum drops the origin of the sternohyoideus well below the interhyal-ceratohyal joint, and is likely responsible for the shift in the function of that muscle (see above). Furthermore, by driving rotation of the hyoid and expansion of the feeding apparatus, the hypaxials likely play an important role in generating most of the suction seen in the later stages of the feeding strike (Fig. 3.3).

Adductor mandibulae

The divisions of adductor mandibulae function primarily as jaw adductors during jaw closing. These muscles include the preorbitalis muscles, which originate on the neurocranium, as well as the adductor mandibulae and palatomandibularis muscles, which originate from the palate, preopercle and hyosymplectic. However, due to the attachment of the lower jaws to the posterior ceratohyal by means of the mandibulohyoid ligament, jaw closing has a secondary function of also protracting the dorsolateral portion of the hyoid bar while the sternohyoideus retracts and rotates the hypohyals. In this way jaw adductors contribute to rotation and abduction of the hyoid apparatus (Fig. 3.12f).

Additionally, depending on their attachment to the lower jaw, some muscles may play an important secondary role in joint stabilization by preventing disarticulation of the jaw joint during jaw opening. Attachments to the mandible can be categorized into at least three attachment areas (Fig. 3.10). The first is a broad attachment zone dorsolateral to the adductor chamber that provides insertion points for the adductor mandibulae tendon, the dorsal subdivision of preorbitalis superficialis, and the superficial palatomandibularis minor muscle (inserting just inside the adductor chamber). The next attachment zone lies deep within the adductor chamber, distal to the jaw joint, providing an insertion for preorbitalis superficialis (and perhaps some intermingled fibers of profundis). The last attachment zone lies deep within the

adductor chamber, proximal to the jaw joint, providing insertions for palatomandibularis major and a tendinous slip of the preorbitalis profundus. These last two muscles, which originate just medial and posterior to the jaw joint, also attach close to the center of rotation of the jaw joint, suggesting they may have a greater role in joint stabilization than the other jaw adductor muscles.

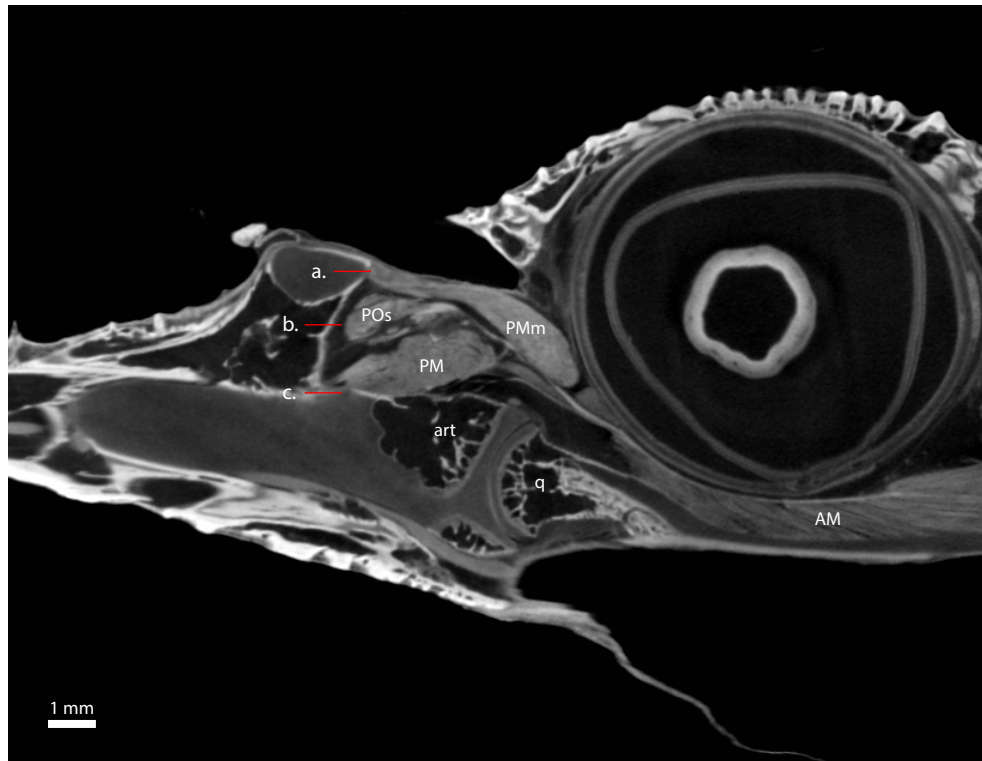


Figure 3.10. Adductor chamber of *Atractosteus spatula* showing multiple attachment areas for musculature. Jaw adducting musculature entering the adductor chamber attach to one of three areas of attachment: (a) dorsal, (b) middle, and (c) ventral (see text).

Levator arcus palatini

Levator arcus palatini (LAP) originates from the lateral most portion of the neurocranium, the sphenotic, and envelops the basipterygoid-metapterygoid joint where it inserts onto the dorsal and ventral surfaces of the metapterygoid. In this configuration it is able to act as

a powerful abductor of the palate relative to the braincase. However, LAP also originates partially on the suborbital bones of the cheek, although to a lesser degree than the condition reported for *Lepisosteus* (Lauder 1980a). LAP also has small subdivisions extending posteriorly, the protractor hyomandibulae sensu (Konstantinidis et al. 2015), and a portion extending directly between the metapterygoid and the hyosymplectic (Fig. 3.11), which in *Lepisosteus* is reported to be entirely ligamentous (Arratia and Schultze 1991). With these muscular connections between the palatoquadrate and hyosymplectic-cheek, it is possible that LAP also serves to connect movements of the palatoquadrate and hyosymplectic as these regions are particularly flexible relative to each other (see above). When the cheeks and hyomandibulae are powerfully abducted, as in the earliest stages of jaw opening, LAP may function to stabilize the basipterygoid-metapterygoid joint, and therefore the jaw joint, during jaw opening.

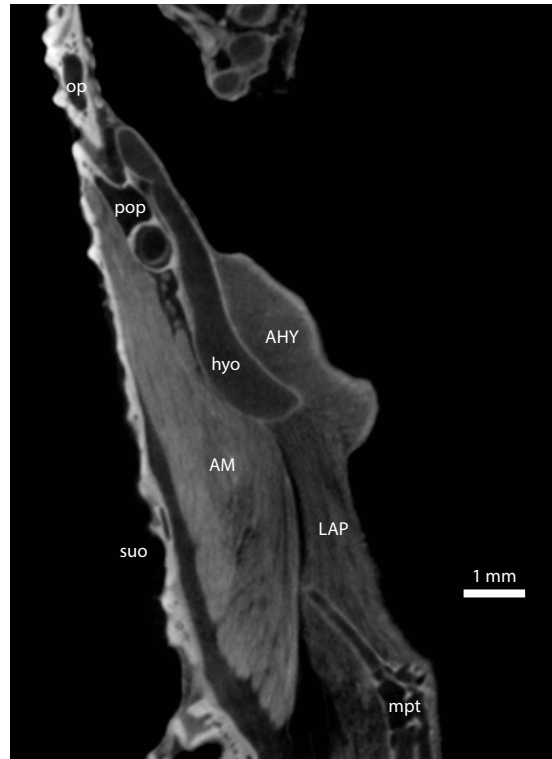


Figure 3.11. Small subdivision of the levator arcus palatini between the metapterygoid and hyosymplectic. The levator arcus palatini (LAP) originates on the sphenotic and primarily inserts onto the metapterygoid (mpt) with some fibers inserting onto the hyosymplectic. However, a small slip of this muscle directly connects the metapterygoid and hyosymplectic. Some muscle fibers of the adductor mandibulae (AM) also appears to originate from the hyosymplectic.

Dilatator operculi

The dilatator operculi is small and dwarfed by its likely antagonist, the adductor operculi muscle (Fig. 3.5). Opercular pumping during respiration may largely be due to suspensorial abduction/adduction rather than alternation of dilatator and adductor operculi activity. This suggestion is supported by observations of heavy respiration of gar in the lab, where suspensorial movements drive mediolateral movements of the operculum.

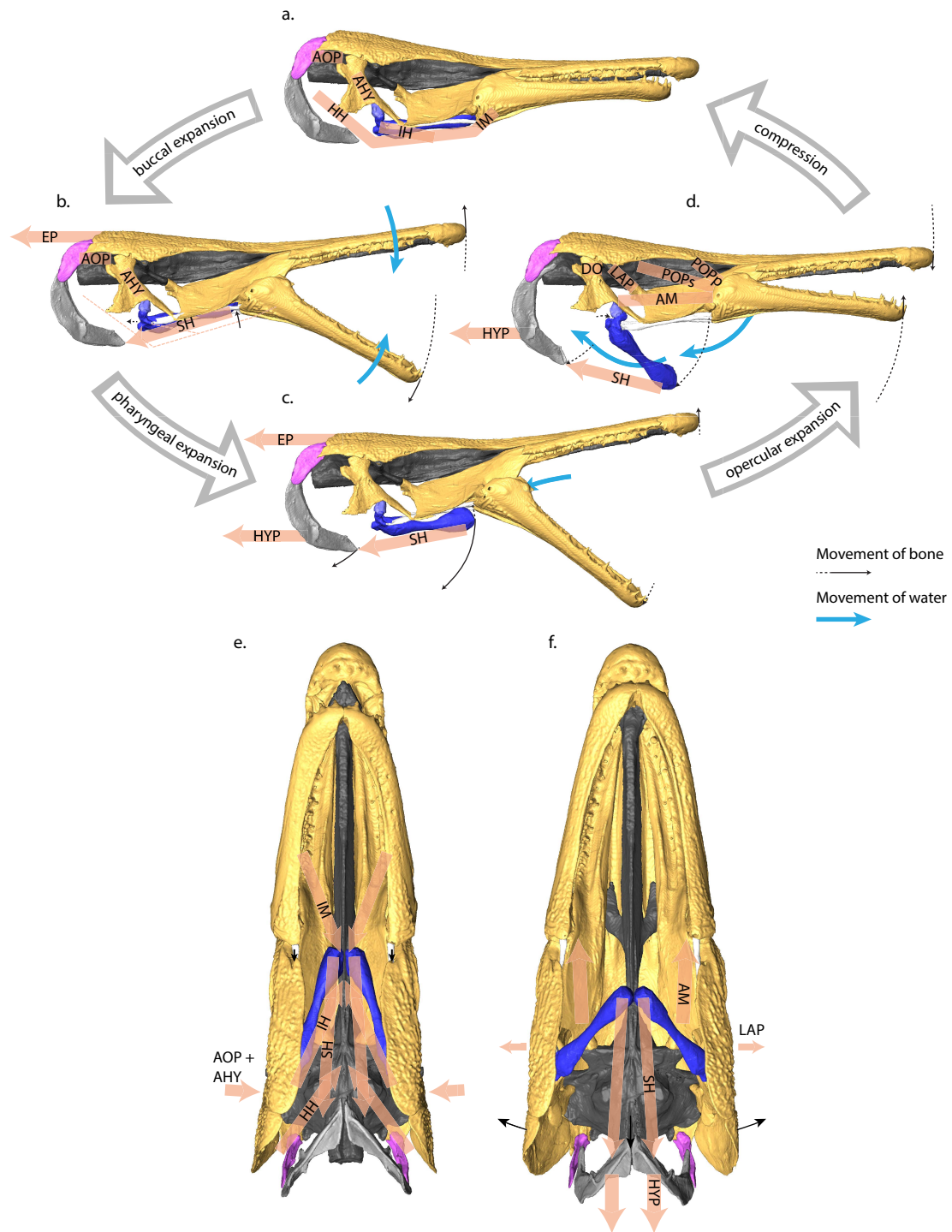


Figure 3.12. Reconstructed gape cycle and feeding kinematics of *Atractosteus spatula*. (a-d) The feeding apparatus of alligator gars is capable of successive expansions of the buccal, pharyngeal, and opercular cavities, modulated by hyoid constrictor musculature, which causes an anterior-to-posterior flow of water through the feeding apparatus (blue arrows). (a) At resting state, the ceratohyals and sternohyoideus are positioned within a sheath of hyoid constrictor

Figure 3.12, continued. musculature (IM, IH, HH, AOP, AHY). (b) Buccal expansion is caused by posterior retraction of the ceratohyals by the sternohyoideus (SH) while the hyoid elevation is maintained by ventral hyoid constrictors (IM, IH, and HH) and ceratohyal adduction is maintained by dorsal hyoid constrictor musculature (AOP, AHY). (c) A transition to pharyngeal expansion is enabled by relaxation of the ventral hyoid constrictors, which allows the sternohyoideus to ventrally rotate the ceratohyals as the pectoral girdle begins to rotate and depress the line-of-action of the sternohyoideus. (d) Opercular expansion is caused by further rotation of the pectoral girdle by hypaxial musculature while the jaws close due to jaw adductors (AM). (e) Suspensorial adduction is maintained in the early stages of jaw opening due to the hyoid constrictors. (f) Opercular expansion is the combined result of lateral rotation of the suspensorium and lateral rotation of the hyoid during jaw closing.

3.5 – DISCUSSION

An unexpected result of this study was the extent to which suction was involved in prey capture by *Atractosteus spatula*, and here I discuss the extent to which the continued need for suction generation has influenced evolution of the feeding kinematics, cranial morphology, and muscular function of the alligator gar. While gars are known for their characteristic, lateral snapping method of prey capture, *A. spatula* engages in a synergistic combination of jaw-ram and suction-feeding behaviors during the feeding strike. Suction generation relies on expansive cranial elements, and the skull of *A. spatula* has numerous modifications that enable continued lateral expansion despite being platyrostral. Finally, plesiomorphic musculature modulates cranial expansion for the combined jaw-ram and suction feeding strike of *A. spatula*, explaining the unusual firing patterns of lepisosteid cranial muscles during feeding, as well as the evolution of specialized jaw-opening musculature in other taxa.

3.5.1 – Combined jaw-ram and suction in the feeding strike of *Atractosteus spatula*

It was previously thought that gars only used suction during prey processing and respiration (Porter and Motta 2004, Werth 2006), but this study shows that *Atractosteus spatula* utilizes suction during prey capture as well. Suction appears to act on the prey throughout all

phases of the feeding strike of *A. spatula* to create a unidirectional flow of water into the oral aperture, complimenting the unique, lateral-snapping feeding strategy of lepisosteid gars. Feeding kinematics of *A. spatula* are largely comparable to those reported for *Lepisosteus oculatus* and *L. platyrhinchus* (Lauder 1980a, Porter and Motta 2004), but high-speed video of *A. spatula* feeding indicates that the function and timing of these kinematic events are also used to control the flow of water during the feeding strike. Most of the differences between gars and other, piscivorous, ram-feeding specialists (Porter and Motta 2004) are best explained by alligator gar's use of a synergistic combination of jaw-ram and suction generation.

We found that the alligator gar used flat plate suction during feeding, likely to avoid the loss of prey due to the bow wave induced by rapid jaw movements. One of the problems of feeding in water, whether by ram or suction, is that prey approach can generate substantial bow-wave-induced disturbances (Holzman and Wainwright 2009). Gars use surprise and rapid lateral acceleration to overcome prey (Porter and Motta 2004), but that behavior would still incur a proportionately large bow-wave (Holzman and Wainwright 2009), which has the potential to alert or even displace elusive prey (van Leeuwen and Muller 1984, Day et al. 2015). In high-speed videos of *Atractosteus spatula* feeding, however, the prey item shows no indication of being pushed away by a bow-wave (Fig. 3.2), and instead it is drawn towards the space between the opening jaws. It is likely the jaws of *A. spatula* act as diverging flat plates during jaw opening, which generates suction (Vogel 1994). Similar to the way body-ram predators precisely time hyoid depression to prevent a bow-wave from pushing prey away during their prey approach (van Leeuwen and Muller 1984), *A. spatula* appears to create negative pressure between the jaws through flat-plate suction, which draws the prey item in even prior to hyoid depression.

The observed delay in hyoid depression (due to hyoid constrictor muscle function) appears to be a mechanism for reducing the lateral drag profile of the head during the lateral strike. The platyrostral (dorsoventrally compressed) morphology of gars is recognized as an adaptation to reduce drag during lateral snapping (Porter and Motta 2004); however, this streamlined drag profile is only present prior to hyoid depression. The buccopharyngeal floor of *Atractosteus spatula* is massively expanded during hyoid depression, and its expansion coincides with rapid lateral deceleration (Fig. 3.2c). Pronounced delay of hyoid depression is a kinematic feature common to both *Lepisosteus spp.* (Lauder and Norton 1980, Porter and Motta 2004) and *A. spatula* (this study). It is likely that delayed hyoid depression is a strategy shared by all gar species for reducing drag during lateral snapping. However, in *A. spatula*, it is also useful for prolonging suction generation, because it saves hyoid-based suction for when it would be most effective.

It has been argued that the primary function of ram behavior is to move the oral aperture close enough to the prey for suction to be effective (Wainwright et al. 2001), and the feeding kinematics of *Atractosteus spatula* surprisingly support this suggestion. Effective suction drops precipitously beyond a distance of one mouth diameter (Wainwright et al. 2001, Day et al. 2005, Day et al. 2015, Wainwright et al. 2015). In gars, the oral aperture is positioned at the base of the jaws, formed by the lateral wings of the ectopterygoids, medial wings of the prearticulars, parasphenoid, and basihyal toothplate. During lateral snapping, the upper and lower jaws are swung around the prey item, but hyoid depression typically does not begin until the prey item is passing between the upper and lower jaws, in front of the oral aperture. During hyoid depression of *A. spatula*, the prey item is drawn further into the oral aperture even while the jaws begin to close (Fig. 3.3).

Suspensorial-opercular abduction during jaw closure completes an anterior-to-posterior wave of expansion of cranial elements in *Atractosteus spatula* (Fig. 3.2), and precisely timed anterior-to-posterior expansion is recognized as an important component of specialized suction feeding in actinopterygian fishes (Wainwright et al. 2015). In the case of *A. spatula*, suspensorial and opercular abduction occur exclusively during jaw closure and likely aide in directing fluid posteriorly as a counter to flat-plate compression, which might otherwise push the prey item out of reach of the jaws.

A central conclusion of this study is that jaw-ram and suction, combined with delayed hyoid expansion, operate synergistically to achieve prey capture in the alligator gar's unusual strike. By simultaneously mitigating the bow-wave, reducing drag, and precisely timing the expansion of cranial elements for when they are most effective – all within 42 ms – *Atractosteus spatula* demonstrates how jaw-ram and suction can be complementary feeding strategies. While gars are incapable of the jaw protrusion seen in many jaw-ram specialists (Porter and Motta 2004), their strategy of laterally sweeping the jaws over prey can be considered a form of jaw-ram. This paper joins a growing body of literature recognizing the potential synergism and overlapping feeding strategies that jaw-ram and suction share (Longo et al. 2016, Cooper et al. 2017).

3.5.2 – Specialized joints enabling expansive capabilities of the cranial linkage system

Atractosteus spatula maintains the expansive capabilities of its feeding apparatus despite dorsoventral compression of the cranium. While gars are noted for evolving a dorsoventrally compressed skull associated with lateral snapping (Porter and Motta 2004), these same modifications place significant barriers on the ability to produce suction within traditional models of teleost suction feeding (Liem 1978, Lauder 1980a, Muller et al. 1982, van Leeuwen

and Muller 1984, Muller 1989, Day et al. 2015, Wainwright et al. 2015). In particular, restricted dorsolateral rotation of the palate (Lauder 1980a), reduced hyoid to jaw length ratio (Muller 1989) due to rostral elongation, and relative reduction of the operculum (Hutchinson 1973) (Muller et al. 1982) are problematic for suction generation. There appears to be direct tradeoffs between effective suction generation and enhanced performance during ram-feeding (Norton and Brainerd 1993); however, *A. spatula* demonstrates that suction generation can be maintained despite ram-related modifications to the feeding system through the use of specialized joints that maintain a compact, streamlined profile during lateral snapping but allow rapid volumetric expansion for suction generation.

First, a specialized joint between the hyosymplectic and palatoquadrate portions of the suspensorium increases the range of motion of the palate by freeing it to rotate out the plane of the long axis of the suspensorium. Intrasuspensorial mobility is required for rotation of any element of the suspensorium relative to other elements; this decoupling enables the cheeks to rotate dorsolaterally while the palate slides mediolaterally. Flexible joints within the suspensorium have been identified in multiple groups of derived actinopterygians, which require separate movements of suspensorial elements. While typically these joints enhance the extreme jaw protrusion seen in jaw-ram specialists, such as the sling-jaw wrasse (Westneat and Wainwright 1989), several long-jawed chaetodontid species (Ferry-Graham et al. 2001), and several cichlid species (Waltzek and Wainwright 2003), they have also evolved within the dorsoventrally compressed crania of benthic fish that utilize suction to capture prey, such as catfish (Arratia 1990) and sturgeons (Carroll and Wainwright 2003). It is likely that intrasuspensorial mobility is more commonplace than previously thought and could be used to enhance the range of suspensorial movements within their respective cranial linkages. Among

gars, this enhanced range of motion of the cheek and palate enables gars to maintain suspensorial abduction despite dorsoventral compression of the cranium.

Additional specialized joints in the feeding apparatus of *Atractosteus spatula* directly facilitate its unique form of suspensorial abduction. The sliding scarf joint between the palate and dermal skull roof (Fig. 3.4f), the gliding cartilages between the ethmoid and pars autopalatina (Fig. 3.4c), and the enlarged basipterygoid-metapterygoid articulation (Jollie 1984), are derived features that support mediolateral rotation of the enlarged palate relative to the cheek. The continuing need to maintain functional suspensorial abduction within the cranial linkage system of *A. spatula* likely provided the selective pressure for these specialized joints to evolve. Mobile joints between the braincase and palate persist despite significant restructuring of the palate and elongation of braincase (Wiley 1976, Arratia and Schultze 1991) during the shift towards biting-based prey capture in gars.

In order to understand the function of suspensorial abduction we need to understand the limitations of the opercular pumping mechanism in dorsoventrally compressed taxa. The role of opercular abduction for both feeding and respiration is widely recognized (Hutchinson 1973, Muller et al. 1982); however, dorsoventral compression and elongation of the lepisosteid skull relegates the opercle and subopercle to a narrow posterior margin of the postorbital region of the skull (Fig. 3.5). In *Atractosteus spatula*, opercular abduction alone is only capable of expanding the resting width of the cranium by ~10% (Figs. 3.2 and 3.3). In contrast, suspensorial abduction in *A. spatula* expands the cranium more than 45% through lateral abduction of the cheeks (Figs. 3.2 and 3.3, Table 1). The ability of suspensorial movements to laterally expand the opercular cavity is the most likely hypothesis for the maintenance of suspensorial mobility in gars because opercular cavity expansion has multiple physiological purposes. Suspensorial movements were

observed not only in feeding (Fig. 3.3), but respiration as well (personal observation). These observations support a primarily hydrodynamic role of suspensorial abduction in gars over alternative hypotheses restricted to feeding, such as to permit taking larger prey items or extending the reach of the lateral tooth row during jaw closing.

Finally, an additional specialized joint between the cleithrum-supracleithrum enables the function of the sternohyoideus to change drastically throughout the course of the feeding strike. While at rest in a protracted state, the origin of the sternohyoideus on the cleithrum remains hidden behind the gill flaps, maintaining the streamlined profile of the body during lateral snapping. In this position, the primary component of sternohyoideus-generated forces would be posteriorly directed, with little torque component. However, pectoral girdle retraction depresses the origin of the sternohyoideus below the ventral plane of the body, drastically changing the line-of-action of the sternohyoideus, which would increase torque on the interhyal-ceratohyal joint (Fig. 3.12). Although the joint between the cleithrum-supracleithrum is likely a plesiomorphic feature of actinopterygians, in a dorsoventrally compressed taxon it takes on a new role of modulating the nature of sternohyoideus activity throughout the feeding strike.

3.5.3 – Modulation of the feeding system with plesiomorphic hyoid musculature

Modulation of the feeding apparatus in gars into an anterior-to-posterior sequence of expansion requires the input of auxiliary muscles not typically associated with jaw opening. Anterior-to-posterior expansion is characteristic of both *Lepisosteus spp.* (Lauder 1980a, Porter and Motta 2004) and *Atractosteus spatula* (this study), and it is hypothesized to be characteristic of gnathostomes as a whole (Lauder and Shaffer 1993); however, gars lack any of the specialized jaw-opening musculature, such as a levator operculi or depressor mandibulae muscle, thought to be necessary for decoupling jaw-opening from hyoid depression in their respective groups, as

well as the primitive coracomandibularis coupling of gnathostomes (Wilga et al. 2000). Without the input of additional musculature, the sternohyoideus causes the feeding apparatus to expand as a single unit, indicating additional muscular input is needed to match the distinct pattern of expansion seen in feeding (Fig. 3.2).

Variable timing of hyoid depression relative to jaw opening indicates that the decoupling of these kinematic events is controlled by muscles, rather a passive mechanism operating within the feeding apparatus. In this study I identified variation in timing of hyoid depression between sequences and individuals (Fig. 3.2), providing evidence of this modulation. I conclude that gars are capable of controlling when function of the sternohyoideus shifts from primarily jaw-opening (hyoid retraction) to one of hyoid depression (hyoid rotation). While decoupling hyoid depression from jaw opening is recognized to be an important adaptation for derived suction feeding specialists (Wainwright et al. 2015), it was assumed to require independent mechanical pathways for those separate kinematics (Lauder 1982). *Atractosteus spatula* demonstrates that this decoupling is possible utilizing only the basic elements of the early osteichthyan feeding mechanism.

Decoupling hyoid retraction and rotation is made possible through the use of a small but highly mobile interhyal working together with a continuous sheath of hyoid constrictor musculature. The interhyal of *A. spatula* is capable of a wide range of motion relative to the suspensorium and ceratohyal (this study, Fig. 3.12), and manipulation of fresh specimens demonstrates that the hyoid can be fully retracted despite forced hyoid elevation and adduction of the cheeks. The extensive hyoid constrictor sheath (Fig. 3.5) is the only musculature in position to constrain ventrolateral movements of the hyoid bars. While there are currently no EMG data available for *Atractosteus*, studies in other taxa have documented extensive

conservation in EMG patterns between closely related taxa (Wainwright et al. 1989), and EMG work on *Lepisosteus* documented a burst of hyoid constrictor activity (interhyoideus, hyohyoideus, and adductor operculi) during the earliest phases of jaw opening (Lauder 1980a). While it was assumed that activity of the opercular adductors prevented influx of water anteriorly through the gills during hyoid rotation, in gars the hyoid remains elevated during the earliest phases of jaw opening, which means these muscles are active even though negative pressure is not yet building in the pharyngeal cavity. While gill adductors and intermandibular muscles may not have the line-of-action to actively depress the lower jaws, by restricting movements of the hyoid solely to retraction (rather than lateral or ventral rotation) they nevertheless contribute to rapid and forceful jaw opening.

It is also possible that ventral hyoid constrictors provide a means of coupling the powerful epaxial musculature to jaw opening as well. By providing a rigid support for the hyoid apparatus during neurocranial elevation, ventral hyoid constrictors may actively lift the hyoid away from the cleithrum, extending the distance between the hyoid and the origin of the sternohyoideus. With the sternohyoideus contracting during extension and the pectoral girdle stabilized by hypaxial musculature (Lauder 1980a), it is possible the hyoid can retract relative to the lower jaws with minimal shortening of the sternohyoideus (Fig. 3.12). Brief hyoid elevation was noted in *Lepisosteus oculatus* (Lauder and Norton 1980), and a similar mechanism has been proposed in teleost fishes, where neurocranial elevation, pectoral girdle retraction, and adduction of the suspensorium results in jaw opening (Muller 1987) as well as in tongue raking fishes (Sanford and Lauder 1989). Powerful axial musculature is now recognized as contributing to hyoid-based suction generation in a wide array of fish (Camp et al. 2015), but *Atractosteus*

spatula demonstrates how maintaining hyoid elevation during hyoid retraction enables epaxial muscle forces to also contribute to forceful mandibular depression and flat plate suction.

Further modulation of the feeding apparatus is provided by the hypaxial musculature acting on the pectoral girdle. Through pectoral girdle rotation, function of the sternohyoideus is drastically altered during the course of the feeding strike, further decoupling the kinematics of hyoid retraction and hyoid rotation. Both the origin and line-of-action of the sternohyoideus drop below the interhyal-ceratothyal joint during pectoral girdle and hyoid rotation (Fig. 3.12), and, due to the increased cleithral-hypohyal-interhyal angle (Fig. 3.12), force components of the sternohyoideus necessarily shift as well (Aerts 1991). As a result, the primary action of the sternohyoideus shifts from retraction of the hyoid to rotation, and this helps to explain the characteristic dual firing pattern of the sternohyoideus recorded in *Lepisosteus*, in which the sternohyoideus is active during both jaw opening and closing, unlike *Amia* or *Polypterus* (Lauder 1980a). Cleithral rotation is the primary mechanism of expansion of the feeding apparatus in *A. spatula* (Fig. 3.12) and this study joins a growing body of evidence for the contribution of hypaxial musculature to the generation of suction in actinopterygians (van Leeuwen and Muller 1984, Muller 1987, Camp et al. 2015).

Following hyoid depression, opercular abduction is aided by jaw adductor muscles as part of the final phase of the feeding strike in *Atractosteus spatula*. Suspensorial abduction occurs during cleithral rotation in fresh specimens, even with no input of the levator arcus palatini. As a contractile link between the cleithrum and hyoid, the sternohyoideus is capable of transmitting the forces of cleithral rotation to the hyoid, which depresses and laterally abducts the hyoid bars in a manner similar to models described by (Muller 1989, Aerts 1991), with one small exception – peak suspensorial abduction coincides with jaw closure in *Atractosteus spatula*

rather than peak gape. While the hypohyals are retracted and held in place by cleithral rotation and the sternohyoideus, the posterior ceratohyals are held in place and *protracted* by the mandibulohyoid ligament when the jaws are shut. Maintenance of a fixed length mandibulohyoid ligament is recognized as playing a role in the unexpected movements of the lower jaws during jaw closing in sturgeons (Carroll and Wainwright 2003) as well. This is perhaps the first study to propose a link between a direct contribution of jaw adductors to suspensorial abduction, potentially powering posterior expansion of the feeding apparatus during jaw closing.

3.5.4 – Applications to paleontology and evolutionary biology

The conclusion that hyoid constrictor musculature has an important secondary role in jaw opening in *Atractosteus spatula* helps to explain how specialized jaw opening musculature repeatedly evolved from the muscles of hyobranchial and opercular control in multiple osteichthyan groups. The main jaw opening muscle in *Amia* and teleosts is the levator operculi (Lauder 1980a), which is a derived subdivision of the adductor operculi muscle (Lauder 1982) and, according to current phylogenies (Grande 2010), arose independently in *Amia* and teleosts. An independently derived levator operculi muscle with the potential to aid in jaw opening is also found in *Latimeria* (Lauder 1980b). Similarly, the specialized depressor mandibulae muscles of lepidosiren lungfish and tetrapods appear to be convergently evolved from the hyoid constrictor sheet in those groups (Bemis 1987). The repeated convergent evolution of specialized jaw muscles from muscles of hyobranchial and opercular control suggests a primitive, secondary jaw-opening role of these muscles among all osteichthyans, allowing selective pressures to act on increasingly specialized jaw-opening mechanisms in disparate groups. Comparative EMG work shows the adductor operculi is active in the earliest moments of jaw-opening in *Polypterus*, *Amia*, and *Lepisosteus*, whereas ventral hyoid musculature is active during jaw-opening for both

Amia and gar (Lauder 1980a). In constraining hyoid movements to strictly posterior retraction during jaw-opening, *A. spatula* demonstrates how hyoid constrictors may have functioned in this secondary capacity among basal osteichthyans prior to the evolution of specialized jaw-opening subdivisions.

Understanding *Atractosteus spatula* as a combined jaw-ram and suction feeding predator also helps to explain patterns of diversification among the closest extinct relatives of modern gars. With the shortest and widest jaws of modern gars (Grande 2010), *Atractosteus spatula* likely utilizes the most suction among an otherwise heavily jaw-ram adapted clade. However, among extinct gars, there are examples of extremely blunt-snouted lepisosteid gars, *Masillosteus* and *Cuneatus*, with durophagus and “micro” dentition respectively (Grande 2010) for which suction was probably the predominant mechanism of prey capture. The closely related obaichthid gars, *Dentilepisosteus* and *Obaichthys*, possessed elongate rostra with short jaws (Grande 2010), and appear to be convergently evolved with pivot-feeding syngnathiformes, which use an extreme form of jaw-ram followed by suction to capture prey (Longo et al. 2016). Within the specious ginglymodian radiation, the diversity of body types and jaw morphology implies a wide range of feeding strategies including durophagy, suction-feeding, non-predatory grazing, and detritophagy (Schaeffer 1967, Cavin 2010, Grande 2010). This diversity among fossil taxa, all more closely related to gars than any other modern taxon (Grande 2010), corroborate the findings of other researchers that showed there is often widespread diversity of forms within clades favoring jaw-ram, suction, or a combination of both (Longo et al. 2016, Cooper et al. 2017). This diversity would not be possible if not for the versatility of the plesiomorphic osteichthyan mechanism, demonstrated here by a “living fossil”, *A. spatula*.

3.6 – CONCLUSIONS

Through the use of high-speed videography, contrast enhanced μ CT, and manual manipulation, this study documents a surprisingly versatile feeding mechanism of *Atractosteus spatula* that is capable of prey capture through a combination of jaw-ram and suction feeding. Examination of high-speed videos show *A. spatula* uses a combination of lateral jaw movements, flat-plate suction, and delayed hyoid depression to capture prey. Manipulation of fresh specimens shows that expansion of the feeding apparatus is accomplished by an elaborate linkage mechanism that joins together movements of the jaws, palate, hyoid arch, and pectoral girdle. Although cranial expansion was thought to be limited in gars, *A. spatula* demonstrates flexibility between elements of the suspensorium, hyoid arch, mandibular arch, and pectoral girdle that enhances expansive capabilities of this platyrostral taxon. Detailed anatomical reconstructions show that modulation of cranial expansion during the feeding strike is accomplished through the use of plesiomorphic hyoid constrictor musculature which decouples the dual functions of the sternohyoideus – jaw opening and hyoid depression – and demonstrates a likely primitive secondary role for muscles of hyobranchial and opercular control in assisting jaw opening in osteichthyans. Although gars are traditionally considered ram-feeders that only use suction for prey processing, these findings show lepisosteid feeding kinematics and morphology have been heavily influenced by the need to maintain suction while elaborating a lateral snapping feeding mechanism.

CHAPTER 4 – RECONSTRUCTED CRANIAL KINEMATICS OF *TIKTAALIK ROSEAE*, A PRECURSOR OF TERRESTRIAL-STYLE FEEDING MECHANICS

4.1 – ABSTRACT

The evolution of terrestrial vertebrates was one of the most dramatic evolutionary transitions of vertebrate history, involving numerous changes to nearly every physiological system of tetrapodomorphs in order to colonize and adapt to a new environment. In order to fully shift to a terrestrial habitat, the feeding systems of tetrapodomorphs had to change to enable prey capture and processing in subaerial conditions. While aquatic vertebrates typically use suction in some form to capture and process prey in water, that feeding strategy is ineffective for use on land. Therefore, it is generally agreed by early tetrapod researchers that at some point in tetrapodomorph evolution, a suction-to-biting transition occurred. However, there is little to no consensus of when that transition happened, with some researchers claiming biting evolved early among aquatic tetrapodomorph fishes and others claiming the shift to biting occurred as a response to terrestrial pressures. Numerous studies of tetrapodomorph feeding attempt to isolate, compare, and correlate a handful of features of the tetrapodomorph fishes (e.g. lower jaw or sutural morphology) to specific feeding strategies, but far fewer have attempted to build an in-depth understanding of any single taxon's feeding system based on all available data. The numerous well-preserved and articulated specimens of *Tiktaalik roseae* provide a rare opportunity to reconstruct feeding of a tetrapodomorph fish immediately prior to the fin-to-limb, and the convergent features it shares with modern alligator gars (*Atractosteus spatula*) allow analogous aspects of its feeding anatomy to be understood in a functional context. Here, I present a detailed reconstruction of the feeding mechanism of *Tiktaalik roseae* that demonstrates a

transitional, hybrid (biting-suction) feeding mechanism similar to modern gars likely evolved among elpistostegid fishes. Despite evolving a dorsoventrally compressed and elongate snout that would normally restrict the ability of the feeding system to expand, *Tiktaalik* convergently evolved a cranial linkage system similar to *Atractosteus* that maintains the expansive capabilities of the feeding apparatus through intrasuspensorial mobility and a flexible joint between the cleithrum and anocleithrum of the pectoral girdle. Cranial expansion in gars is modulated by a plesiomorphic complement of hyoid constrictor musculature, which eventually give rise to the depressor mandibulae muscles of crown-group tetrapods. *Tiktaalik* lacks evidence for a functional depressor mandibulae muscle, but it is likely *Tiktaalik* used these plesiomorphic muscles in a manner similar to *Atractosteus* to modulate cranial movements and assist with jaw opening, thus paving the way for selective pressures in later tetrapods to subsequently evolve a true depressor mandibulae. Using a digital cranial linkage model and muscle reconstructions, this study demonstrates that the feeding system of *Tiktaalik* was capable of feeding kinematics similar to *Atractosteus*, which despite using a combination of both suction and biting to capture prey, is surprisingly similar to those used by modern terrestrial vertebrates. The convergent feeding system found in both gars and elpistostegids demonstrates how a terrestrial-style feeding system that decouples jaw movements and hyoid depression could have evolved in elpistostegid fishes for the purposes of prey capture in water but then be exapted for use on land.

Key words: intrasuspensorial mobility, depressor mandibulae, terrestrial-style feeding, convergent evolution, exaptation, water-to-land transition

4.2 – INTRODUCTION

Feeding across the water-to-land transition

The transition from water-to-land required drastic changes in nearly every physiological system of the earliest terrestrial vertebrates, with acquisition of prey being no exception. Water and air present vastly different physical demands for vertebrates feeding in either setting (Vogel 1994), and therefore amphibious vertebrates that are able to feed in both often employ drastically different kinematics depending on the medium (Heiss and De Volder 2016). A primary question that concerned early tetrapod researchers involves the question of how the earliest terrestrial vertebrates were able to adapt an aquatic feeding system for use on land. Aquatic vertebrates typically use suction when feeding underwater, but this feeding strategy is ineffective for use on land. Instead terrestrial vertebrates typically capture prey through some form of biting, and it is generally assumed that, at some point in the water-to-land transition, a transition from suction to biting based feeding also occurred (Markey and Marshall 2007). However, the timing of this transition is still in debate with some claiming tetrapodomorph fishes were well-adapted for biting (Johanson et al. 2003, Porro et al. 2015a) and others claiming the earliest terrestrial vertebrates may still have utilized a fair amount of suction (Heiss et al. 2013). Studies focused on lower jaw morphology suggest feeding strategies changed very little across the water-to-land transition (Ahlberg and Clack 1998, Anderson et al. 2013, Neenan et al. 2014), implying the extent of suction or biting used by the earliest terrestrial vertebrates was established at some point prior to the emergence of tetrapods. However, these studies do not present a clear hypothesis of how those lower jaws were being used (either for suction or biting). While the morphology is generally well-understood, the problem is that interpreting feeding morphology from a functional context requires a clear understanding of how that morphology was being used,

and, without any living examples of transitional tetrapodomorphs available, the focus of biomechanical studies turns to the study of modern analogs.

Modern analogs

Modern analogs, while not necessarily closely related to tetrapodomorphs, provide opportunities to study some aspects of their feeding mechanics due to the shared physical constraints facing vertebrate feeding systems. For instance, studies focused on kinematic differences between feeding in land and water may use salamanders that opportunistically or seasonally transition between both mediums (Heiss and De Vylder 2016). Studies interested in the use of aquatic feeding systems on land may focus on primarily aquatic actinopterygians that are capable of terrestrial excursions onto land for prey capture (Van Wassenbergh et al. 2006, Michel et al. 2015). With *Tiktaalik*, we have a rare opportunity to analyze feeding mechanics of a tetrapodomorph fish that lived immediately prior to the fin-to-limb transition. While some researchers believe *Tiktaalik* may have fed on land (Hohn-Schulte et al. 2013), *Tiktaalik* exhibits many features that suggest it was primarily or exclusively aquatic, and, therefore, an appropriate modern analog would be an aquatic taxon with platyrostral morphology. Suggested modern analogs for elpistostegids include lungfish, giant salamanders (Heiss et al. 2013), and crocodilians, but the feeding morphology of these taxa may not be representative of elpistostegid feeding morphology. Lungfish have palates that are fused to the skull bearing large durophagous tooth plates, but *Tiktaalik* has elongate jaws with an apparently mobile palate (Chapter 2). Giant salamanders have less consolidated braincases (Heiss et al. 2013), but their jaws are relatively short and parabolic, dissimilar to the elongate, unoccluded jaws of elpistostegids. Crocodilians have long unoccluded tooth rows, similar to elpistostegids, but crocodilians also evolved secondary palates that reinforce the snout to resist torsion and immobilize any palatal mobility

(Busbey 1995). Furthermore, in order to understand use of a feeding system during the preliminary stages of the water-to-land transition, it is also pertinent to use a modern analog whose ancestors never had a terrestrial stage. For these reasons, this study proposes to use a convergently evolved but distantly related actinopterygian species with a fish-like palate and crocodilian-like jaws, the alligator gar, *Atractosteus spatula*, as a potential modern analog for elpistostegids.

Convergent evolution of a gar-like feeding system

Cranial kinesis in limbed tetrapodomorphs is thought to have evolved from cranial kinesis of tetrapodomorph fishes (Thomson 1967, Iordansky 1990, Bolt and Lombard 2001); however, in the lead up to the evolution of limbed tetrapodomorphs, elpistostegids underwent a series of changes that are thought to have limited the expansive capabilities of the skull (Brazeau and Ahlberg 2006, Downs et al. 2008). The most prominent of these changes thought to limit cranial kinesis is the evolution of a platyrostral skull, which significantly alters the mechanisms of palatal mobility proposed for plesiomorphic osteolepidid and tristichopterid fishes (Thomson 1967). Alligator gars were recently recognized to have numerous specialized traits that maintain cranial kinesis despite similar evolution of an elongate rostrum, dorsoventrally compressed skull, and reduced hyomandibula (Chapter 3). Despite superficial similarities between alligator gars and elpistostegids (Fig. 4.1), it is uncertain if *Tiktaalik* shares analogous specialized features that would enable it to expand its skull in ways similar to *Atractosteus*. Therefore, the first aim of this study is to examine the feeding apparatus of both alligator gars and *Tiktaalik* for osteological correlates of cranial expansion that could indicate how cranial kinesis may have worked in a platyrostral tetrapodomorph. This aim requires the uses of computed tomography (CT) data from both alligator gars and *Tiktaalik* to assess aspects of the internal anatomy of both taxa.

Jaw opening mechanism in tetrapodomorph fishes

The jaw opening mechanism of tetrapodomorphs is not fully understood. The primary jaw opening musculature of non-mammalian, modern tetrapods consists of the anterior and posterior depressor mandibulae muscles, which are derived from the dorsal hyoid constrictor musculature of fish (Bemis 1987, Diogo 2008); however, there is uncertainty when this muscle evolved among sarcopterygians. It is absent in *Latimeria*, which uses the plesiomorphic, osteichthyan mechanical pathway of jaw opening, the sternohyoideus-mandibulohyoid ligament linkage (Lauder 1980b). Initially it was presumed that tetrapodomorph fishes had depressor mandibulae muscles on the basis that lepidosirenid lungfish possess a similar muscle that opens the jaws (Bemis and Lauder 1986). However, *Neoceratodus* lacks this muscle, and it is likely that the muscle in lepidosirenid lungfish is convergently evolved (Bemis 1987). This leaves the question open of when the depressor mandibulae evolved among tetrapodomorph fishes (Bemis 1986). Therefore, the second aim of this study is to examine the feeding apparatus of *Tiktaalik roseae* for evidence of either the plesiomorphic sternohyoideus-mandibulohyoid ligament based jaw-opening mechanism and/or a derived depressor mandibulae-based jaw-opening mechanism. This goal requires the use of CT data to examine the internal morphology of the best preserved lower jaws for muscle scars, as well as phylogenetic inferences of conserved muscle patterns found in both lungfish and cryptobranchid salamanders, in order to reconstruct the jaw opening mechanism of *Tiktaalik roseae*.

Transition from suction to biting

Central to the debate of when the suction-to-biting transition occurred is understanding how the feeding morphology of tetrapodomorphs may have been used. Previous studies have used osteological correlates of feeding, such as sutural morphology (Markey and Marshall 2007)

(Bolt 1974) or upper and lower jaw morphology (Anderson et al. 2013, Neenan et al. 2014), to categorize certain taxa as either suction feeders or biters. However, implicit in the argument that a transition from suction-to-biting occurred is the assumption that there would have been a time period when both feeding strategies were being used. On the basis of sutural morphology, *Tiktaalik* appears to have experienced compressive loads along the midline of the skull suggestive of biting (Chapter 2). Conversely, on the basis of mobile joints in the cheek and skull, *Tiktaalik* also appears to have a kinetic skull suggestive of some degree of suction generation (Chapter 2). We now know that alligator gars incorporate both lateral snapping and suction generation into their feeding strategy (Chapter 3), but it is by no means certain that similar kinematics were possible in *Tiktaalik*. Therefore, the third aim of this study is to determine if *Tiktaalik* was capable of the complex kinematics found in alligator gar, using a constrained linkage model of the feeding apparatus of *Tiktaalik roseae* superimposed on *Atractosteus* feeding kinematics. This model requires input of the osteological and musculature estimates determined from the previous two aims of this study, as well as feeding kinematics of *Atractosteus* determined from the previous chapter (Chapter 3).

4.3 – MATERIALS AND METHODS



Figure 4.1. Comparison of the rostral proportions of *Tiktaalik roseae* and *Atractosteus spatula*. Shown are the relative proportions of the skulls of *Tiktaalik roseae* (NUFV 110, left) and *Atractosteus spatula* (FMNH 17191, right). Both have large and robust hypobranchial apparatuses. White arrows correspond to the attachment point of the sternohyoideus musculature. While the overall geometry is similar, the jaw joint (jj) of *Atractosteus* is positioned anterior to the branchials (brs), whereas in *Tiktaalik* it is angled posteriorly and positioned lateral to the branchials. This has implications for the attachment of the mandibulohyoid ligament (mhl) to the lower jaws depending on how far posterior the ceratohyals (ch) extended. In this particular *Atractosteus* specimen, the lacrimomaxillae are removed.

4.3.1 – Convergent features between lepisosteids and elpistostegids

CT scanning of specimens

Extensive anatomical data from both *Tiktaalik roseae* and *Atractosteus spatula* were collected for the purpose of this study. In addition to the computed tomography datasets collected and analyzed in previous chapters, two additional CT scans of *Atractosteus spatula* were compared with features in *Tiktaalik*. First, an adult alligator gar skull (FMNH 119220D) was scanned at the GE Training Facility in Lewistown, PA using a GE Phoenix v|tome|x 240 kv/180kv scanner. This specimen was scanned at 190 kV and 280 μ A, with a voxel size of 106.436 μ m and a resolution of 9.395 pixels per mm.

An additional juvenile (3.5 years) alligator gar specimen was also scanned by the author at the UChicago PaleoCT scanning facility using a GE Phoenix v|tome|x 240 kv/180kv scanner. This specimen was scanned at 70 kV and 300 μ A, with a voxel size of 25 μ m and resolution of 40 pixels per mm.

Linkages in the feeding apparatus of Atractosteus

In order to assess whether or not *Tiktaalik* was capable of expansive kinematics similar to *Atractosteus spatula*, osteological correlates of *Atractosteus* cranial kinematics were identified from CT scans (Chapter 3). Expansion of the feeding apparatus of *Atractosteus* involves neurocranial elevation, jaw opening, hyoid retraction and rotation, pectoral girdle rotation, and suspensorial abduction (Chapter 3), and these movements required kinetic joints in least ten locations:

1. supracleithral-cleithral joint
2. quadrate-articular joint
3. hypohyal-hypohyal symphysis

4. mandibular symphysis
5. dermopalatine-vomerine joint
6. basipterygoid-metapterygoid joint
7. hyosymplectic-otic joint
8. ceratohyal-interhyal joint
9. interhyal-hyosymplectic joint
10. hyosymplectic-palatoquadrate joint

Three of these joints (the interhyal-hyosymplectic, ceratohyal-interhyal, and hyosymplectic-quadrate joints) involve one more cartilaginous elements that would not preserve in a fossil. However, the other joints, if present, can be identified and characterized from CT scans of *Tiktaalik roseae*. Each of these joints was identified in both contrast enhanced and non-contrast enhanced μ CT of *Atractosteus*, and then similar areas of flexion were identified in CT scans of *Tiktaalik roseae* (Fig. 4.2).

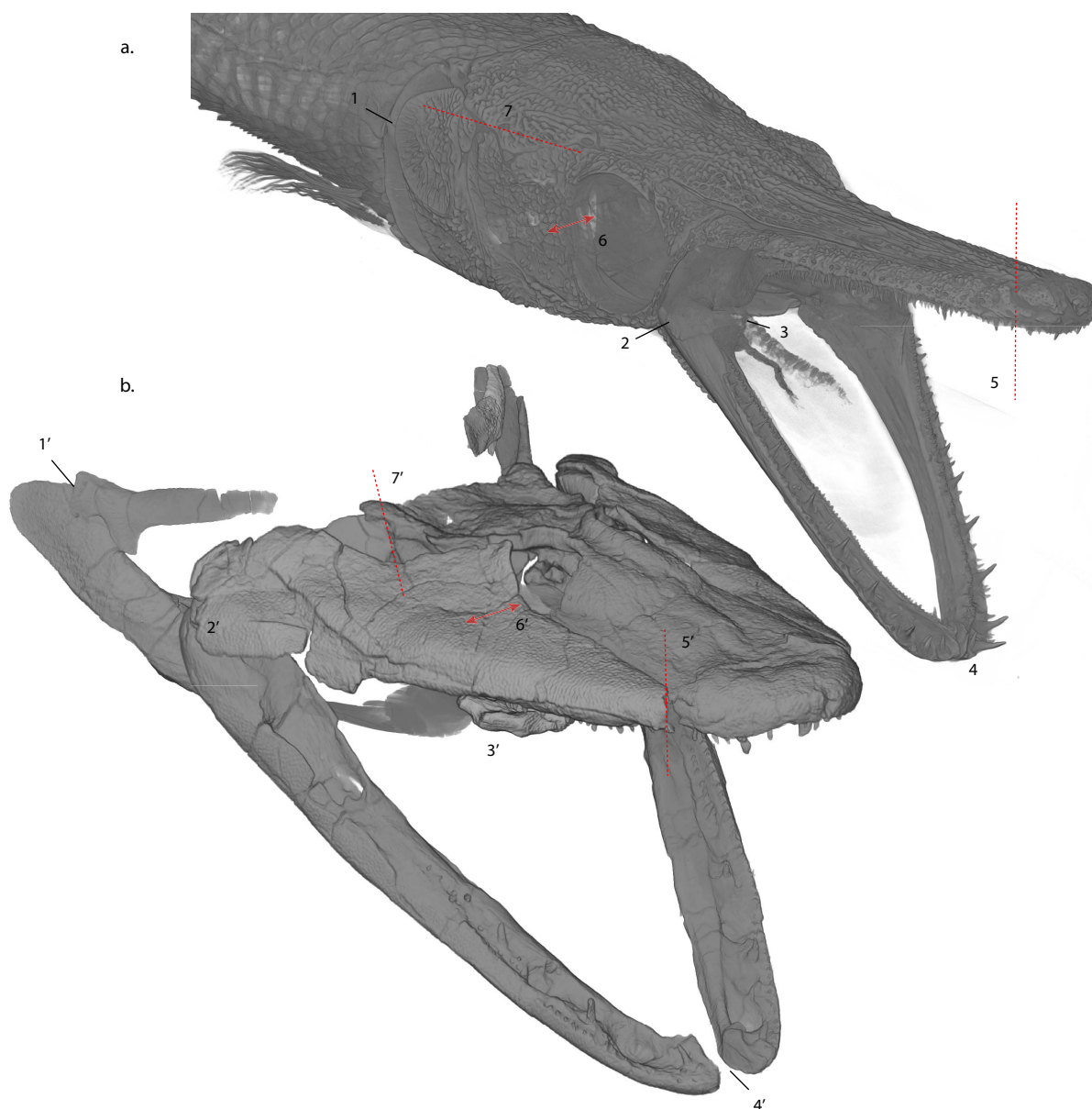


Figure 4.2. Positions of analogous joints in *Atractosteus spatula* and *Tiktaalik roseae*. Shown are analogous joints identified in *Atractosteus* (a) and *Tiktaalik* (b). (1) Supracleithral-cleithral joint. (2) Quadrate-articular joint. (3) Hypohyal-hypohyal symphysis. (4) Mandibular symphysis. (5) Dermopalatine-vomerine joint. (6) Basipterygoid-metapterygoid joint (internal to cheek). (7) Hyosymplectic-otic joint. Figures are not to scale.

4.3.2 – Phylogenetic bracketing of plesiomorphic feeding musculature

Conservative estimates of common hyoid constrictor musculature shared between gars, lungfish, tetrapodomorph fishes, and salamanders, were assumed to be present in *Tiktaalik* as well on the basis of an extant phylogenetic bracket (Witmer 1995). *Tiktaalik* likely possessed muscles derived from the embryonic dorsal mandibular constrictor, ventral hyoid constrictor, dorsal hyoid constrictor, and ventral hyoid constrictor, as well as hypobranchial and axial musculature plesiomorphic to all osteichthyans (Diogo 2008) (see table). No muscle found in tetrapods and outgroup taxa was presumed absent in *Tiktaalik*; however, specialized muscle subdivisions found only in tetrapods could not be assumed. Therefore, in cases where the derived (= tetrapod) condition was indeterminant (see table), the line of action and attachments points of those muscles were compared with the original function and attachments of the plesiomorphic (= osteichthyan) precursor. Due to the transitional nature of this fossil, it was important to keep in mind that specialized tetrapod muscles may have existed in an intermediate configuration in *Tiktaalik*.

Muscle attachments

Muscle attachments were based on documented cryptobranchid feeding musculature (Elwood and Cundall 1994, Kleinteich et al. 2014). The musculature for *Tiktaalik* was estimated using reported origins and insertions of those muscles. We assume the cryptobranchid configuration, because *Tiktaalik* is more closely related to salamanders than dipnoans. These muscles were then mapped onto dorsal, ventral, and medial cranial reconstructions.

Cryptobranchid salamanders were chosen as a template due to their plesiomorphic morphology among salamanders (Kleinteich et al. 2014). Using the extant phylogenetic bracket, we would assume that *Tiktaalik* shared a complement of muscles somewhere between lungfish

and tetrapods. Cryptobranchids are one of the most basal groups of salamanders in terms of morphology (Kleinteich et al. 2014). Since tetrapodomorph fishes are more closely related to salamanders than dipnoans (Clack 2012), for the purposes of this study, I assumed that shared musculature between lungfish and salamanders represents the primitive conditions shared by Dipnoi + Tetrapodomorpha.

Using the reconstructed cranial morphology for the feeding apparatus of NUFV 108 (C specimen) and 110 (E specimen) (Chapter 2), hyoid constrictor and jaw opening musculature was placed connecting to their reported cranial elements using *Cryptobranchus alleganiensis* as a template (Elwood and Cundall 1994) and lungfish (Bemis 1986) .

Table 4.1. Comparative osteichthyan feeding musculature and conditions inferred for *Tiktaalik*. Muscle homologies are based on literature for modern taxa: ¹(Wilga et al. 2000), ²(Diogo 2008), ³(Elwood and Cundall 1994), ⁴(Kleinteich et al. 2014), ⁵(Bemis 1987). Muscles shared between *Lepidosiren* and *Cryptobranchus* are presumed present in *Tiktaalik*. Muscles independently lost or specializations independently gained are considered indeterminant for *Tiktaalik*.

Muscle	<i>Atractosteus</i>	<i>Latimeria</i>	<i>Lepidosiren</i>	<i>Tiktaalik</i>	<i>Cryptobranchus</i>
Hypo-branchials	Sternohyoideus	Sternohyoideus	Rectus cervicis	Rectus cervicis	Rectus cervicis
	Absent*	Coraco-mandibularis ²	Geniothoracis ¹	Geniohyoideus? / geniothoracis?	Geniohyoideus
					Genioglossus?
					Hyoglossus?
Dorsal constrictor hyoideus	Adductor arcus palatini + Adductor hyomandibulae + Adductor operculi	Adductor arcus palatini + Adductor Hyomandibulae? + Adductor operculi + “Levator operculi” ⁵	“Depressor mandibulae” ² , Retractor mandibulae from middle constrictor sheet ⁵ + Constrictor operculi ²	Hyoid constrictor sheet merging with branchiohyoideus fibers and interhyoideus posterior fibers? / Constrictor operculi?	Depressor mandibulae anterior ²
			Levator hyoideus ²	Adductor arcus palatini + adductor hyomandibulae?	Depressor mandibulae posterior
Ventral constrictor hyoideus	Interhyoideus + Hyohyoideus	Interhyoideus	Interhyoideus (forming continuous sheet with constrictor operculi)	Interhyoideus anterior	Interhyoideus anterior
				Interhyoideus posterior/superficial hyoid constrictor	Interhyoideus posterior ⁴ / superficial hyoid constrictor ³
				Branchiohyoideus	Branchiohyoideus ⁴
Ventral mandibular constrictor	Inter-mandibularis	Inter-mandibularis anterior	Inter-mandibularis? ²	Intermandibularis anterior	Inter-mandibularis anterior
		Inter-mandibularis posterior		Intermandibularis posterior	Inter-mandibularis posterior
Dorsal mandibular constrictor	Dilatator operculi	Dilatator operculi	Dilatator operculi	?	?
	Levator arcus palatini	Levator arcus palatini	?	?	?
	Adductor mandibulae + subdivisions	Adductor mandibulae + subdivisions	Adductor mandibulae + subdivisions	Adductor mandibulae + subdivisions	Adductor mandibulae + subdivisions

4.3.3 – Constraining models of *Tiktaalik* feeding kinematics

Reconstructed anatomy of the skull of *Tiktaalik roseae* (NUFV 108) was used to form the basis of a cranial linkage model. This model was separated into the following component parts of the feeding apparatus based on the actual cranial components segmented from CT scans and

repositioned into life-like configurations that took into account deformation patterns of the particular specimen (Chapter 2):

- Neurocranium and dermatocranium
- Endochondral and dermal palate
- Lower jaws
- Dermal cheek
- Hyomandibula
- Basihyal and urohyal
- Cleithra and scapulocoracoid
- Anocleithrum
- Ceratobranchials (rigid link, approximate length)
- Sternohyoideus muscles (non-rigid link, approximate length)
- Connection between anocleithrum and back of the skull (rigid link, approximate length)

All manipulations of digitally segmented elements were done in Amira 6.5 (FEI).

Individually segmented elements can be rotated around specified axes of rotation relative to surrounding cranial elements, and the subsequent transformation can then be exported in the format of a four by four transformation matrix. In this way, each cranial element can be given a separate transformation matrix that defines its position at any given moment in a simulated feeding strike. Four phases were chosen to be modeled for the purposes of comparing with the four phases of the *Atractosteus* feeding strike: buccal expansion, pharyngeal expansion, opercular expansion, and rest (Chapter 3, Fig. 3.12). As a result, every element of the model had

to have a transformation matrix for each of the phases. By interpolating between any two transformation matrices, the Amira software is able to smoothly animate simultaneous movements of cranial elements and the model can be checked for intersecting elements or overextension of joints.

In order to constrain the model, particularly between elements of the skull, hyoid apparatus, and pectoral girdle, straight lines representing the soft tissue connection between the skull table and anocleithra, the cartilaginous ceratohyals, and the muscular sternohyoideus were applied to the model. The lines between the back-of-the-skull and anocleithra were kept at a set length, and neurocranial elevation was modeled as rotation of the cranium relative to an axis of rotation running through the anterior tips of the anocleithra (cpg, Fig. 4.11a-b). The lines representing the ceratohyals were also kept at fixed lengths (ch, Fig. 4.11a-c). Landmarks placed on the back of the jaws at the mandibulohyoid scar (Fig. 4.9) and on the anterolateral margins of the basihyal were moved in unison, and any rotation of the ceratohyals had to be centered on one of these landmarks. In contrast, the lines representing the sternohyoideus muscle were allowed to extend and contract slightly relative to their starting length. Landmarks placed midway along the length of the urohyal represented the sternohyoideus insertion, and landmarks on the anterior most edge of the scapulocoracoid represented its origin. The insertion of the sternohyoideus on the urohyal was not allowed to drop below the level of the origin or pass posterior to it, preventing unrealistic line of action of the muscle.

All other elements were able to move relative to surrounding elements, using gar kinematics as a template. A representative sequence of alligator gar feeding kinematics consisting of approximately 48° jaw opening, 10° neurocranial elevation, 47° hyoid depressions, 20° pectoral girdle rotation, and suspensorial abduction of 45% the width of the skull (Chapter 2)

was chosen for comparison with *Tiktaalik* cranial kinematics. These movements were superimposed over the cranial linkage model to the full extent that they could without disarticulating cranial elements, at which point no more rotation was applied and maximum values were recorded.

4.4 – RESULTS

4.4.1 – Assessment of a convergent cranial linkage system

Components of the feeding apparatus

The cranium of *Tiktaalik roseae* can be divided into several anatomical modules (i.e. the braincase, the palate, the cheek, the hyomandibula); however, the feeding system of osteichthyans incorporates several more elements that should be discussed here, including the lower jaws, the hypobranchial apparatus, and the pectoral girdle (Alexander 1970, Lauder 1980a). In gars these components are now understood to form a complex linkage that works to expand the feeding system during prey capture (Chapter 2). While apparent similarities between *Tiktaalik* and gars are the result of evolutionary convergence, and it is by no means certain that the feeding system of *Tiktaalik* is capable of expansion in the same way as gars, it is nevertheless possible to analyze similarities and differences of those joints between analogous cranial modules.

Shoulder

The shoulder girdle of *Tiktaalik* is notably separate from the back of the skull due to the loss of the extrascapulars (Daeschler et al. 2006, Shubin et al. 2006). In addition, the pectoral girdle itself shows sign of flexibility between its dermal elements. The anocleithrum and cleithrum are only loosely connected in the various specimens for which pectoral material is

known, and these elements share broad, overlapping, and smooth articular surfaces with each other. This implies that the joint between the anocleithrum and cleithrum may have been a flexible joint in life, similar to gars, allowing some additional degree of ventral rotation beyond that allowed by loss of the extrascapulars and supracleithrum (Fig. 4.5).

In gars, cleithral rotation occurs at the cleithral-supracleithral joint, and this rotation provides an important component of the linkage mechanism for cranial expansion. In rotating posteroventrally, the cleithrum drops the origin of the sternohyoideus ventrally and powerfully rotates the hyobranchial apparatus posteroventrally. In doing so, the feeding mechanism is able to expand ventrally below the ventral plane of the body.

Jaw joint and retroarticular process

The jaw joint of *Tiktaalik* faces posteriorly, and the retroarticular process does not extend far beyond the jaw joint. There is a clear scar along the back portion of the mandible (Fig. 4.9) that corresponds to a possible attachment point for the mandibulohyoid ligament identified in other tetrapodomorph fishes (Fox et al. 1995, Long et al. 1997, Ahlberg and Clack 1998). In CT scans, this scar corresponds to an elongate wedge of material between the surangular and articular that extends and tapers anteroventrally (Fig. 4.9). The mandibulohyoid ligament can be inferred in *Tiktaalik* due to its presence in salamanders (Elwood and Cundall 1994) and lungfish (Bemis 1987), and this ligament typically spans between the posterior ceratohyal and the back of the jaw. While the distal portion of the ceratohyal is unossified in *Tiktaalik*, this offers evidence that the hyoid arch likely extended as far posteriorly as the jaw joint and connected to the back of the lower jaw via the mandibulohyoid ligament.

The retroarticular process has a small indentation on the dorsal surface. While this has been interpreted as possibly an attachment point for a depressor mandibulae in tetrapodomorph

fishes (Jarvik 1980), it has also been reported in fossil coelacanth that likely lacked depressor mandibulae musculature (Friedman 2007). Alternatively, it has been proposed to be an articulation for the symplectic portion of the hyoid arch in other sarcopterygians (Friedman 2007), and its condition as an articular facet or muscle attachment in *Tiktaalik* is uncertain. Unlike the scar for the mandibulohyoid ligament, the underlying bone does not show any form of scarring that could indicate how this process may have been loaded if a muscle did attach to it (Fig. 4.9).

In *Atractosteus*, the mandibulohyoid ligament attaches to a small retroarticular process just below the jaw joint (Chapter 3). The jaw joint is even more posteriorly oriented in gars, because the jaw joint is anterior to the orbit in gars; however, the primary function of the mandibulohyoid ligament is to exert posterodorsal forces on the lower jaws via hyoid retraction. In either case, a jaw joint loaded due to posterodorsally oriented forces would likely be posteriorly facing.

Hyobranchial apparatus

The hyobranchial apparatus of *Tiktaalik* is large and robust. The hyobranchials are mostly ossified, and the basihyal bears a large tooth plate, similar to gars (Grande 2010) but unlike many aquatic salamanders (Deban and Wake 2000). The anterior ceratohyals are broad and taper posteriorly to an unossified distal margin. In life the ceratohyals likely extended to the distal portion of the hyomandibula, posterior to the jaw joint as suggested by the presence of a mandibulohyoid ligament scar, but this cannot be verified in the fossil itself. The presence of a symplectic is also uncertain except for the facet on the retroarticular process that is similar to the articular facet for the symplectic in coelacanth (Friedman 2007). In another elpistostegid, *Panderichthys*, the ossified operculum bears a groove on its inner surface thought to correspond

to the distal, unossified hyomandibula and symplectic (Brazeau and Ahlberg 2006), indicating that the hyoid arch extends posteriorly beyond the distal ossification extent in that closely related taxa.

The hypohyals connect to a large flat basihyal, which bears smooth articular surfaces (Downs et al. 2008). As a result, the hypohyals of *Tiktaalik* could likely adduct and abduct relative to each other at the midline, similar to the hypohyals of *Atractosteus* (Chapter 3) and *Cryptobranchus* (Elwood and Cundall 1994, Deban and Wake 2000).

Other branchial elements of *Tiktaalik* are well ossified and extend posterior to the jaw joint (Downs et al. 2008). Similar to *Acanthostega*, the ceratobranchials bear grooves interpreted for conveying blood vessels to the gills in early tetrapods (Coates and Clack 1991). It is possible that the mandibulohyoid ligament also continues to these anterior ceratobranchials, as in salamanders (Elwood and Cundall 1994).

Mandibular symphysial joint

The symphysis of *Tiktaalik* is smooth, short, and abutting. Similar to *Atractosteus*, it lacks distinct ridges or interdigitations between the mandibular ossifications and appears to allow intermandibular flexion (Fig. 4.8). While *Atractosteus spatula* possesses a short symphysis similar to *Tiktaalik*, other gar species in the genus *Lepisosteus* have an elongate mandibular symphysis (Grande 2010). In *Atractosteus*, this joint is filled with flexible fibrocartilage (Chapter 3) that allows some intermandibular flexibility. In *Atractosteus*, the intermandibular symphysis allows the jaws to flare laterally at the jaw joints relative to each other during suspensorial abduction.

Braincase

The braincases of *Atractosteus* and *Tiktaalik* possess several convergent features. Although plesiomorphic sarcopterygians have a partition in the neurocranium that separates the sphenethmoid from the otoccipital (Ahlberg et al. 1996), in *Tiktaalik* the partitions of the braincase show indications of being partially fused (Chapter 2). While this represents a large departure from earlier tetrapodomorph fishes (Thomson 1967), a single fused neurocranium is more similar to the condition in actinopterygians, including gar (Grande 2010). The sphenethmoid region of the braincases of both gars and *Tiktaalik* is extended anteriorly, along with the anterior articulation of the palate with the posterior wall of the nasal capsule (Fig. 4.3). The basiptyergoid processes of both taxa are enlarged relative to the plesiomorphic osteolepidid (Jarvik 1980, Clack 2012) and actinopterygian conditions (Wiley 1976, Grande 2010), providing increased articular surface area for the corresponding metapterygoid (Arratia and Schultze 1991, Clack 2012). The otoccipital regions of *Tiktaalik* (Daeschler et al. 2006, Downs et al. 2008) and gars (Grande 2010) are relatively short but retain clear articular surfaces for the hyomandibula (Fig. 4.3). Similarities of these features in the braincase are through evolutionary convergence as each lineage evolved elongate and platyrostral upper jaws.

Anterior connection of palate to the braincase

In *Tiktaalik*, the anterior connection of the palate to the braincase is formed by a small process of the dermopalatine that inserts above the vomer in a socket formed by the vomer ventrally and ethmoid dorsally (Chapter 2). Elsewhere, the entopterygoid abuts the braincase with a smooth articulation, that appears to permit movement between those elements. In various *Tiktaalik* specimens, the entopterygoids and corresponding lamina connected to the braincase are preserved in either closer articulation with the braincase or spread far away from it (Chapter

2), indicating the palate could move mediolaterally relative to the braincase. Lateral to the vomerine-palatal connection and the choana, the maxilla and premaxilla also have a loose connection between the dental arcades. In gars, an analogous overlap between the dermopalatine and vomer also exists and is tightly bound with dense, fibrous connective tissue (Fig. 4.6). Although firmly connected to the back of the nasal capsule, in gars, this connection enables slight mediolateral movements anteriorly, which translates to wide ranging mediolateral movements of the palatoquadrate posteriorly.

Posterior connection of palate to the braincase

In *Tiktaalik* the posterior articulation of the palate to the braincase consists of an ascending process of the metapterygoid (= epipterygoid) that fits into the suprapterygoid fossa (Chapter 2). Dorsal to the metapterygoid is an anterolateral projection of the prootic, which limits dorsal mobility of the palate. Ventral to the metapterygoid is a posterodorsal facing basiptyergoid process, which also limits ventral mobility of the palate. Lateral to the basiptyergoid process, in NUFV108 is a weakly ossified portion of the palate that fits around the rounded lateral portion of the basiptyergoid process (Chapter 2). While in tristichopterid fishes the suprapterygoid, prootic, and basiptyergoid processes are divergent (Jarvik 1980), in *Tiktaalik* these articulations all converge towards the same location on the lateral wall of the braincase due to dorsoventral compression of the skull (Chapter 2), implying a shift in the way the palate articulates with the braincase.

In gars, this articulation takes a very different morphology but with potentially analogous function. The basiptyergoid process is formed by a fusion of the prootic with the parasphenoid and provides a broad articular surface for mediolateral sliding (Chapter 3). Ventral mobility is limited by medial extension of the cheek, and dorsal mobility is limited by the orientation of the

basipterygoid joint as well as lateral extensions of the sphenoid cartilage. In the case of gars, mobility of the palate is limited to mediolateral sliding (Chapter 3), whereas in *Tiktaalik* the close proximity of the prootic and basipterygoid process similarly restricts movement of the palate to primarily mediolaterally sliding.

Connection of the hyomandibula to the braincase

In *Tiktaalik*, the hyomandibula articulates with the lateral commissure of the braincase at a posterior inclination, with the jaw joint positioned posterolaterally (Fig. 4.3 and 4.4). The inclination of the articular surface of the lateral commissure is primarily vertical with a slight dorsolateral angle. Rotation around this axis would result in primarily lateral abduction of the hyomandibula with some ventral rotation as well. In contrast, the gar hyomandibular articulation is horizontally suspended from the braincase with a slight anteromedial inclination (Fig. 4.3 and 4.4). This enables the gar hyomandibula to rotate dorsolaterally during suspensorial abduction. While the orientations of the hyomandibular articulations are completely orthogonal in these two taxa, the loose connections between the hyomandibular and palatoquadrate portions of the suspensorium suggest the articular axis of the hyomandibula does not dictate the rotational axis of the palatoquadrate.

Connection of palate to the hyomandibula

In both gars and *Tiktaalik* the connection of the palatoquadrate to the hyomandibula is loose and cartilaginous (in gars) or likely-cartilaginous (in *Tiktaalik*) (Fig. 4.4). In gars, the symplectic portion of the hyosymplectic cartilage underlies a posteroventral cartilaginous portion of the palatoquadrate, and at no point in ontogeny do the two portions of the suspensorium ever form a direct bone to bone contact (Arratia and Schultze 1991, Grande 2010). This connection allows the two portions of the suspensorium to twist relative to each other, enabling the palate to

slide laterally while the hyosymplectic rotates dorsolaterally. In *Tiktaalik*, the distal portion of the hyomandibula is unossified and extends posterolaterally alongside a grooved medial surface of the quadrate (Fig. 4.4). In *Panderichthys*, the ossified opercle similarly bears a groove suggestive of an unossified distal portion of the hyomandibula (Brazeau and Ahlberg 2006). The loose, cartilaginous connection between the two portions of the suspensorium in *Tiktaalik* may allow sliding to occur at their articulation, which would be necessary if both portions rotated laterally around separate rotational axes during suspensorial abduction (Fig. 4.3).

Dermal cheek and tooth row connections to the braincase

In *Tiktaalik*, the dermal cheek articulates with the braincase in two places, anterior to the orbit and posterior to the orbit. In both places the dermal cheek overlaps elements of the braincase in the form of a sliding scarf joint (Fig. 4.7). The lacrimal overlaps the prefrontal along the length of the rostrum all the way from the orbit to the divide in the dental arcade that separates the maxilla from the premaxilla (immediately lateral to the choana). Posteriorly, the postorbital overlaps a shelf formed by the intertemporal bone supported ventrally by the prootic process (Chapter 2). In both cases, the scarf joint formed by overlapping cranial elements slants ventrolaterally, implying the cheek could slide ventrolaterally at those articulations.

This is similar to the condition found in gars. In gars, the dermal skull roof overlaps bones of the cheek and palate anterior to the orbits (Fig. 4.7), primarily because the lacrimals in gars fuse with the maxilla to form the lacrimomaxilla which never overlay the shelves formed by the premaxilla and frontal bones. Instead, the cheek bones and associated musculature recede to just anterior to the orbit, leaving the ectopterygoid exposed in some places (Grande 2010).

Although the scarf joint is formed between different elements, it still allows mediolateral sliding between the cheek and palate along its length, from the break in the dental arcade between the

lacrimomaxilla and the premaxilla (as in *Tiktaalik*) to just anterior to the orbit. Posterior to the orbit, the cheek articulates with the braincase in the form of a simple hinge that enables the cheek to rotate dorsolaterally along with the hyomandibula (see above on different axes of hyomandibular rotation). In gars, the scarf joint that divides bones associated with a mobile palate and bones associated with a rigid braincase is not filled with dense connective tissue, allowing it to remain loose and mobile (Chapter 3).

Linkage mechanism of Tiktaalik

The feeding apparatus of *Tiktaalik* bears all the components of an expansive cranial linkage mechanism as seen in the alligator gar – neurocranial elevation, suspensorial abduction, jaw depression via hyoid retraction, hyoid depression via hyoid rotation, and pectoral girdle rotation (Chapter 3). Gars also maintain these components but elaborate them through specializations of their own. Neurocranial elevation lifts the cranial components away from hypobranchial elements, and similarly, cleithral rotation depresses hypobranchial elements relative to the neurocranium. The upper jaws and lower jaws are jointed to allow lateral abduction relative to the braincase, and the suspensorium is flexible to allow the hyomandibula and palatoquadrate to rotate on separate axes of rotation. Not only does *Tiktaalik* bear evidence of expansive cranial kinematics in its joint morphology, it also exhibits specialized analogous features for cranial expansion convergently evolved in gars (Figs. 4.2-4.8).

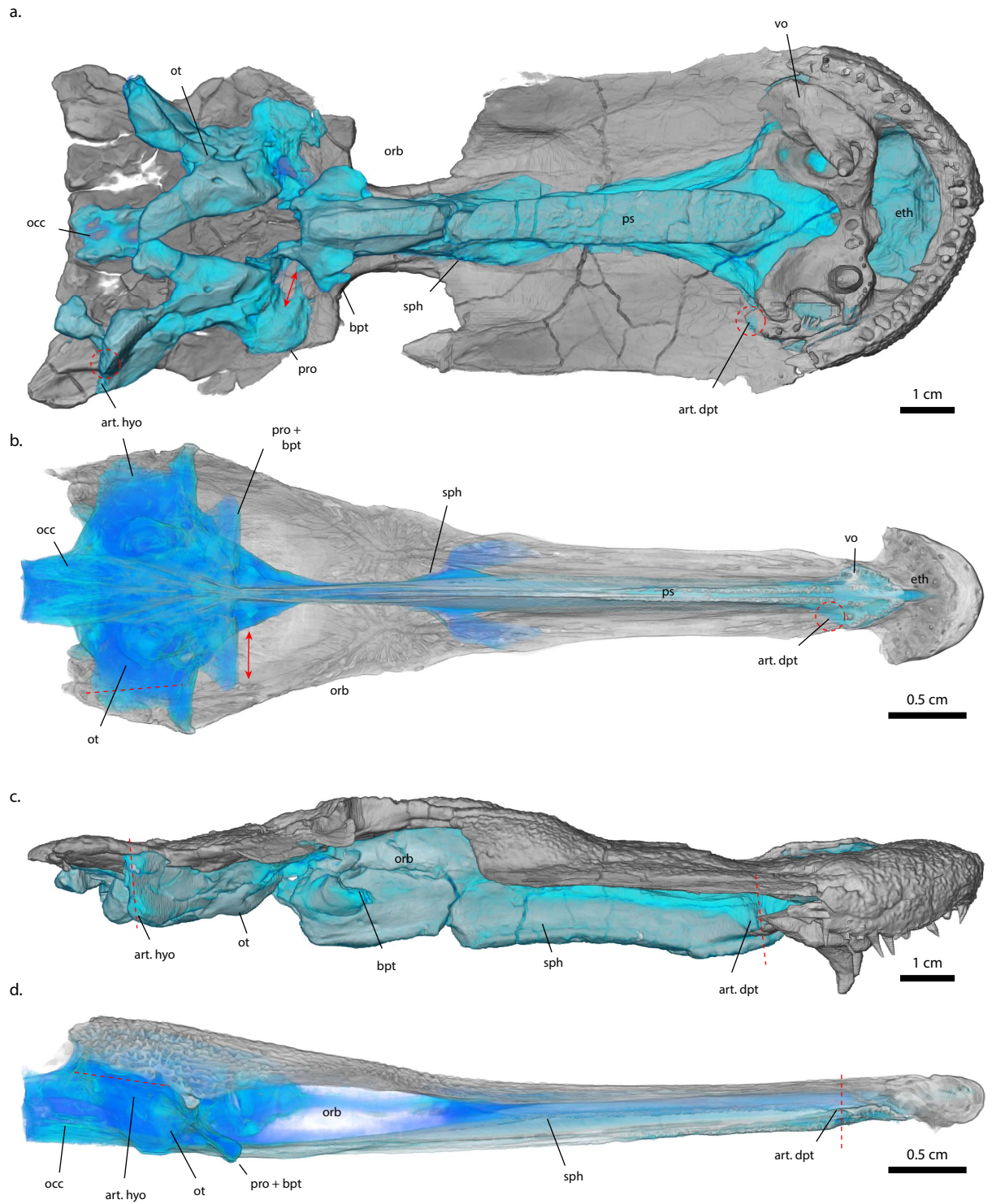


Figure 4.3. Comparison of the braincases of *Tiktaalik roseae* and *Atractosteus spatula*. Shown are similarities of the braincase of *Tiktaalik* (a+c) and *Atractosteus* (b+d) in ventral (a+b) and right lateral (c+d) views. Blue coloration indicates endochondral elements. Rostral

Figure 4.3, continued. elongation in both taxa is achieved by lengthening of the sphenethmoid (sph) region relative to the otoccipital (occ). Red dashed lines indicate articulations and proposed axes of rotation of suspensorial elements both within (straight line) and out of (circle) the field-of-view. Red arrows indicate a sliding articulation with the palate. The enlarged basipterygoid processes of both taxa are derived features of their respective lineages.

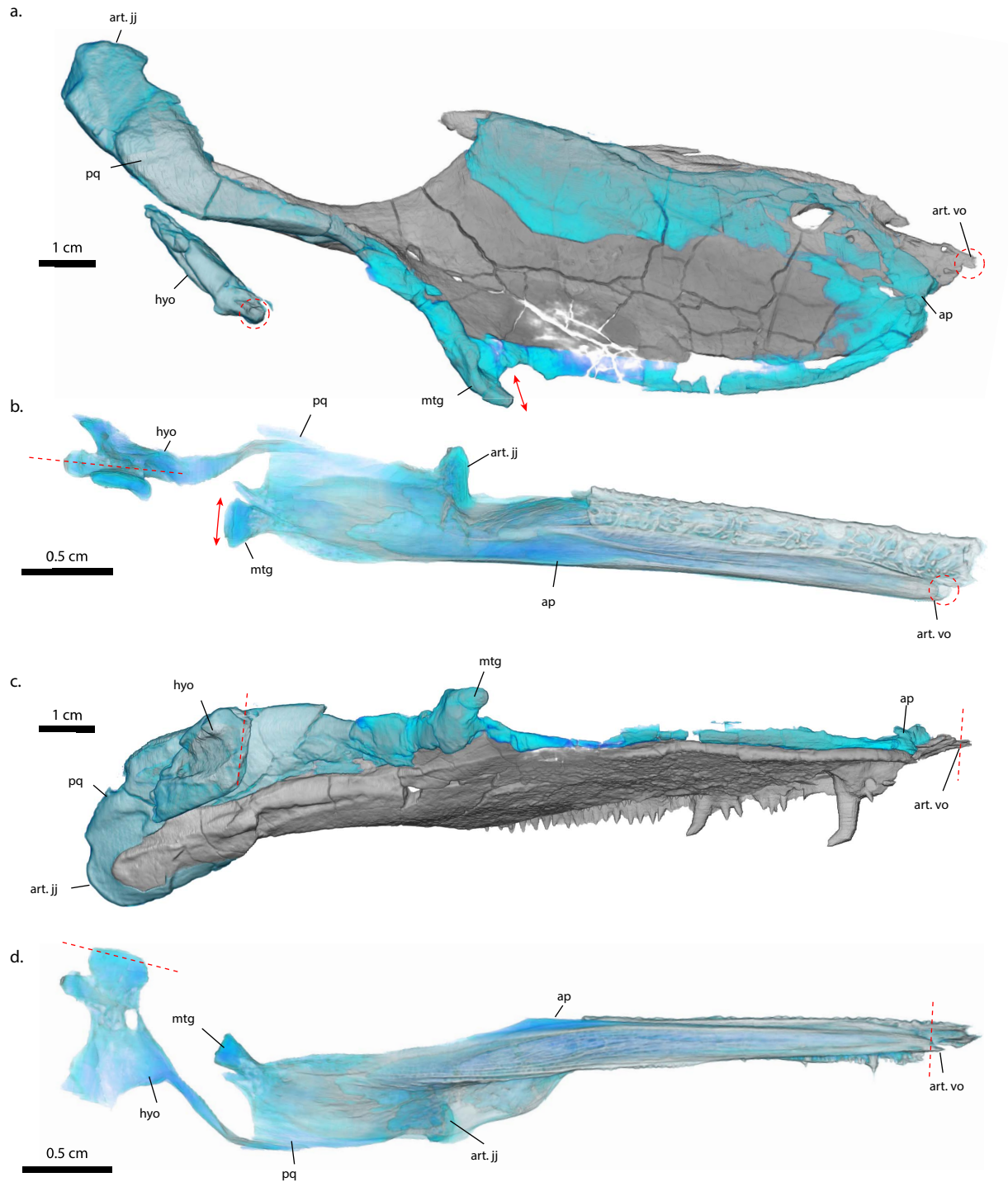


Figure 4.4. Comparison of the suspensorial elements of *Tiktaalik roseae* and *Atractosteus spatula*. Shown are similarities of the left suspensoria of *Tiktaalik* (a+c) and *Atractosteus* (b+d) in dorsal (a+b) and mesial (c+d) views. Blue coloration indicates endochondral elements. Red

Figure 4.4, continued. dashed lines indicate proposed axes of rotation of suspensorial elements both within (straight line) and out of (circle) the field-of-view. Red arrows indicate a sliding articulation with the braincase. Reduction of hyomandibular size relative to palatoquadrate is a derived trait found in both taxa relative to their respective evolutionary lineages, and development of a primarily cartilaginous contact between the hyomandibula and palatoquadrate is similarly derived.

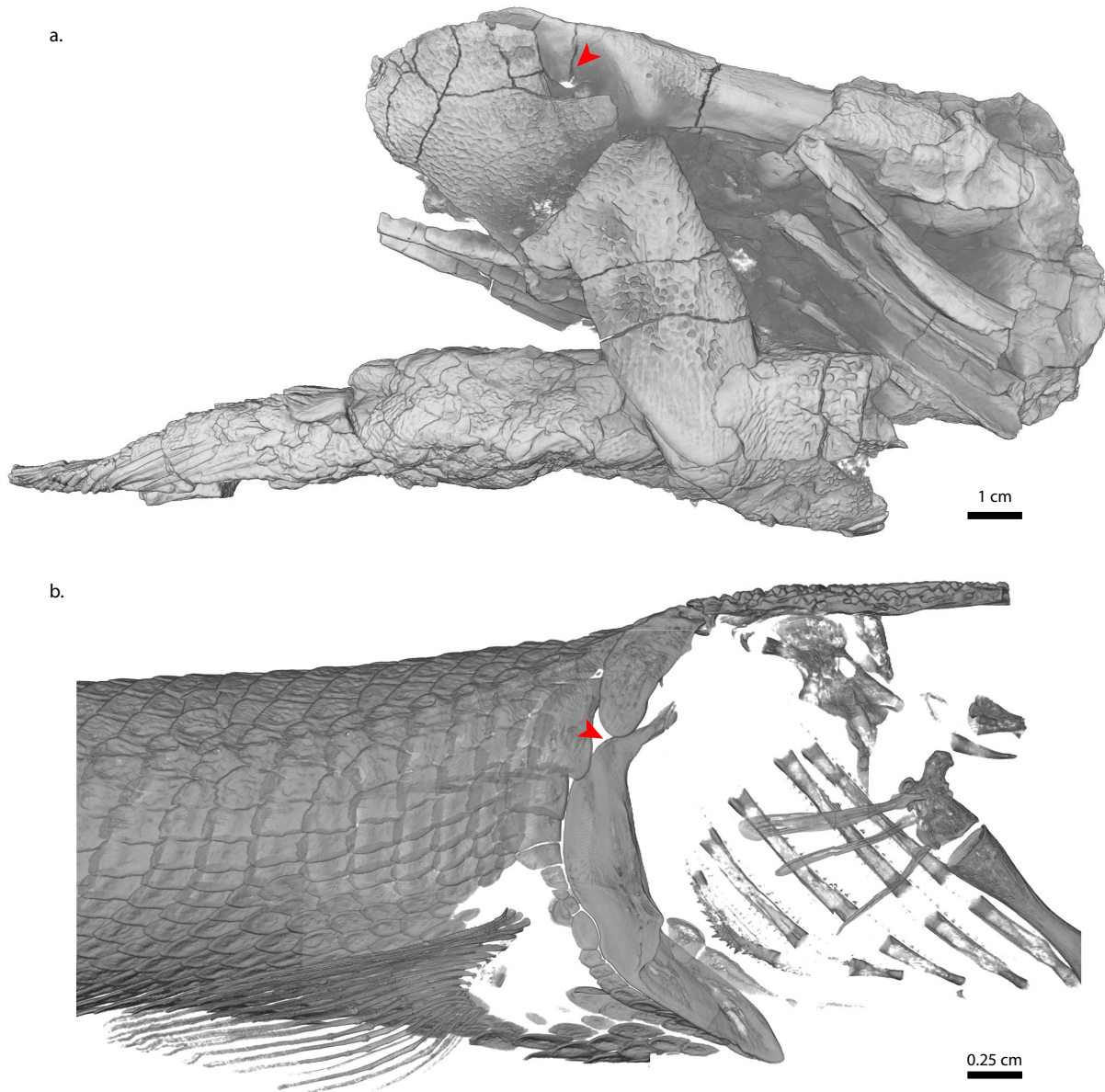


Figure 4.5. Comparison of the jointed pectoral girdles of *Tiktaalik roseae* and *Atractosteus spatula*. (a) The pectoral girdle of *Tiktaalik roseae* (NUFV 110). (b) The pectoral girdle of *Atractosteus spatula* (juvenile, same specimen used in Chapter 3). Red arrows indicate location of an analogous flexible joint between pectoral girdle elements: the supracleithral-anocleithral

Figure 4.5, continued. joint in *Tiktaalik* (a), and the cleithral-supracleithral joint in *Atractosteus* (b).

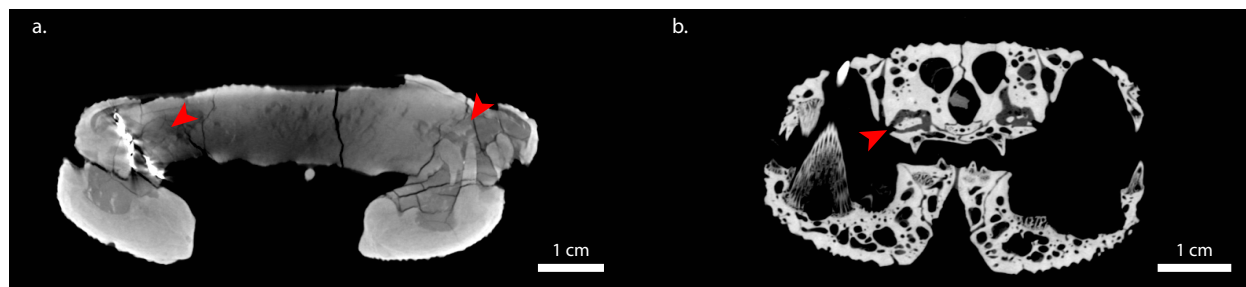


Figure 4.6. Comparison of the vomer-dermopalatine articulations of *Tiktaalik roseae* and *Atractosteus spatula*. Red arrows indicate where an anterior prong of the dermopalatine fits into a socket on the posterior wall of the nasal capsule immediately dorsal to the vomer for both (a) *Tiktaalik roseae* (NUFV 108) and (b) *Atractosteus spatula* (FMNH 119220D).

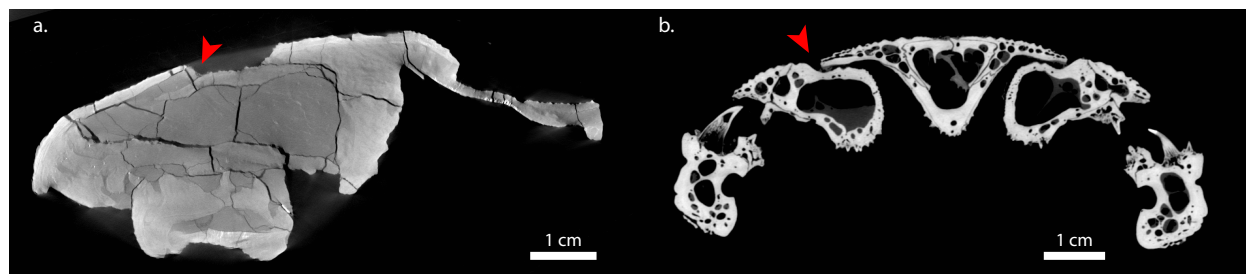


Figure 4.7. Comparison of the rostral scarf joints of *Tiktaalik roseae* and *Atractosteus spatula*. Red arrows indicate the exposed portion of the scarf joint between (a) the prefrontal-lacrimal in *Tiktaalik* (NUFV 110) and (b) the frontal-ectopterygoid in *Atractosteus* (FMNH 119220D). This joint is loose in filled in with matrix in all known specimens of *Tiktaalik*, unlike other beveled sutures found throughout the feeding apparatus (see Fig. 2.6 and 2.7). This joint is open and free of dense connective tissue in *Atractosteus* in comparison to other visible beveled sutures (see Fig. 3.4f).

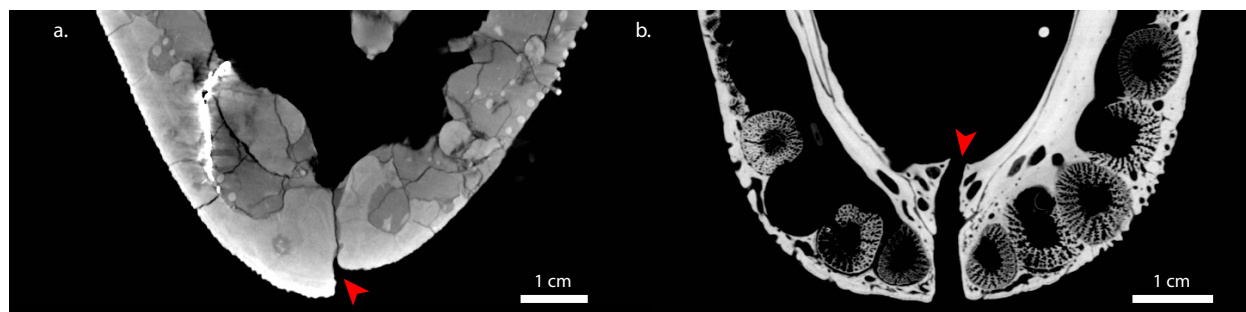


Figure 4.8. Comparison of the mandibular symphyses of *Tiktaalik roseae* and *Atractosteus spatula*. Red arrows indicate the mandibular symphysis of (a) *Tiktaalik roseae* (NUFV 108) and (b) *Atractosteus spatula* (FMNH 119220D). In both taxa, the articular surface is smooth, and, in

Figure 4.8, continued. *Atractosteus*, is filled with cartilage (Fig. 3.5). Evolution of plicidentine tooth structure is a derived trait of lepisosteid gars (Grande 2010) and a plesiomorphic condition for tetrapodomorphs (Warren and Turner 2006). *Atractosteus* has a short symphyseal region compared to other lepisosteid species of the *Lepisosteus* genus (Grande 2010).

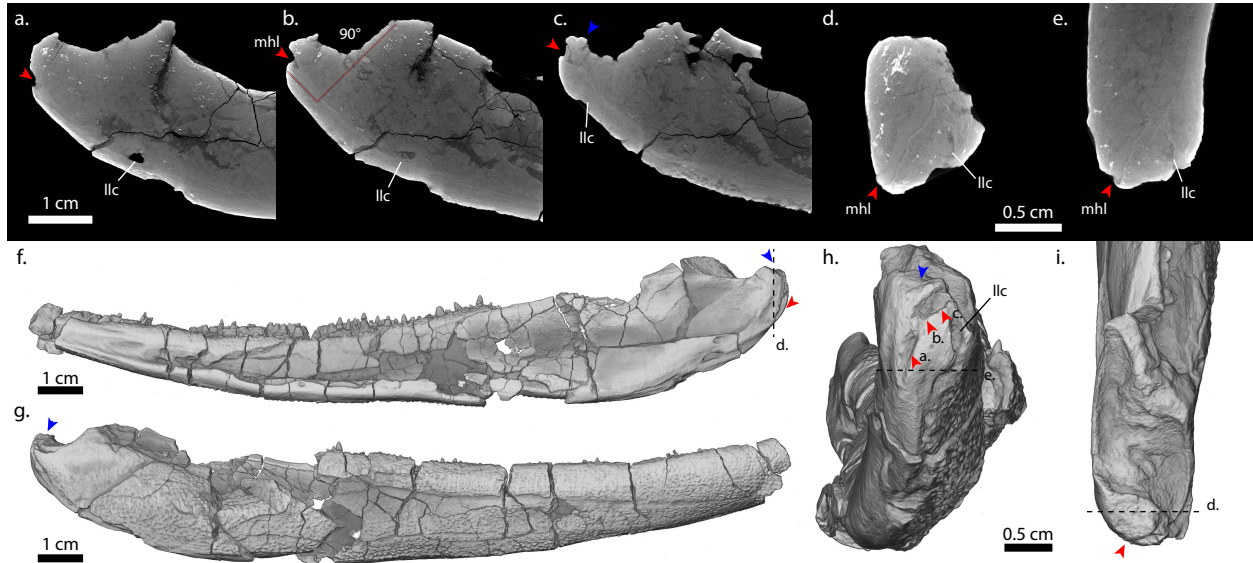


Figure 4.9. Evidence of soft tissue attachment to the posterior mandible of *Tiktaalik roseae*. Shown is the location of the mandibulohyoid ligament scar (red arrows) between the surangular and articular on the posterior medial surface of the right mandible of *Tiktaalik roseae* (NUFV 122). (a) Posterior medial portion of the scar; notice the internal ossification immediately interior to the scar that is wedge-shaped and posterodorsally oriented. (b) Medial portion of scar; notice the orthogonal (90°) orientation of the scar relative to the glenoid. (c) Dorsolateral portion of scar and retroarticular process; notice the contrasting lack of clear internal ossification on the retroarticular process (blue arrow) that could indicate the presence of a strong depressor mandibulae muscle. (d) Posterior view of the scar showing distinct separation from the lateral line canal (llc) from the mandibulohyoid ligament scar. (e) Dorsal view of the scar. (f) Medial external view of lower jaw. (g) Lateral external view of lower jaw. (h) Posterior external view showing positions of cross sections (red arrows). (i) Dorsal view of the glenoid; notice that the glenoid is posterior facing, as in other tetrapodomorph fishes but in contrast to limbed tetrapodomorphs (Ahlberg and Clack 1998)

4.4.2 – Estimation of cranial feeding musculature in *Tiktaalik roseae*

Hypobranchial musculature

The sternohyoideus (= rectus cervicis) of *Tiktaalik* likely spanned between the cleithra and the urohyal. The urohyal is a large, well-ossified bone in *Tiktaalik*, with a large ventral midline-ridge for attachment of the sternohyoideus muscles. At rest, the sternohyoideus would have been in the position to powerfully retract the hyoid, but, due to the dorsoventral compression of the skull, it would have had difficulty depressing the hyoid prior to pectoral girdle rotation due to the limited moment arm of the sternohyoideus around the presumed rotational axis of the ceratohyals.

Tiktaalik probably had a geniohyoideus muscle that spans between the chin and the fascia of the sternohyoideus (Fig. 4.10). Due to the dorsoventral compression of the skull and the elongate nature of the lower jaws, it is unlikely that the geniohyoideus would have been a powerful jaw opening muscle by itself. The displacement required to open the jaws around the jaw joint would have required significant posteroventral rotation of the hyoid, which the geniohyoideus would not have been capable of prior to rotation of the shoulder girdle. Due to the presence of a geniothoracis muscle in lungfish (Wilga et al. 2000), it is possible there was a direct connection between the jaws and the pectoral girdle (not figured), but this configuration would have the same issues in effecting jaw opening as a geniohyoideus muscle. Unless the cleithrum rotated significantly throughout jaw opening, a muscle spanning between the shoulder girdle and the chin would not be able to open the jaws very far because the lower jaws are so long.

Ventral hyoid constrictors

The ventral hyoid constrictor sheet of cryptobranchids consists of the intermandibularis anterior, intermandibularis posterior, interhyoideus anterior, interhyoideus posterior, and the superficial hyoid constrictor (Elwood and Cundall 1994, Kleinteich et al. 2014). While the intermandibularis muscles are derived from the mandibular arch (Diogo 2008), they are included here as part of the muscular sheet covering the ventral floor of the mouth. The intermandibularis anterior has no clear muscle attachment scar on the lower jaw of *Tiktaalik*, this muscle is small even in cryptobranchid salamanders (Kleinteich et al. 2014). The muscle may have been capable of weak adduction of the jaw joints towards the midline. The intermandibularis posterior, on the other hand has a very clear muscle scar found along the meckelian element along the lower jaw. This element has a curious ventral displacement the further posterior it reaches along the lower jaw. This muscle would have been a powerful adductor of the lower jaws towards the midline. The interhyoideus anterior would have been a powerful adductor of the ceratohyals, although due to lack of ossification of the posterior ceratohyals the attachment area of this muscle in *Tiktaalik* is unknown. In cryptobranchids, it spans between the ceratohyals and connects with a median raphe at the midline, intermingling fibers anteriorly with intermandibularis posterior (Kleinteich et al. 2014). Posteriorly, the interhyoideus posterior spans between the hyoid bars and the midline, and merges muscle fibers with the superficial hyoid constrictor (= hyohyoideus) posteriorly (Elwood and Cundall 1994). The superficial hyoid constrictor (= hyohyoideus) is a large flat muscle that joins at the midline and wraps around the lower jaws, reaching dorsally all the way to the dorsal midline posterior to the skull (Elwood and Cundall 1994). This muscle may have played an important role in constricting the opercular flap in *Tiktaalik*.

Dorsal hyoid constrictors

The dorsal hyoid constrictors are the developmental homologs of the depressor mandibulae musculature in tetrapods (Bemis 1986, 1987, Diogo 2008). In the plesiomorphic osteichthyan conditions, these muscles - the adductor arcus palatini, adductor hyomandibula, adductor operculi – span between the braincase and the palatoquadrate, hyomandibula, and operculum respectively (Lauder 1980a), but in tetrapods these muscles become the anterior and posterior depressor mandibulae. Depending on the plesiomorphic or derived muscle conditions among elpistostegid fishes, the jaw joint of *Tiktaalik* could have accommodated several different muscles attaching to it.

The depressor mandibulae anterior is a muscle that in cryptobranchids spans between the jaw joint and the squamosal bone (Elwood and Cundall 1994). In *Tiktaalik* the squamosal lies anteromedial to the jaw joint and is part of a mobile cheek separated from the braincase (Chapter 2). Any muscle that stretched between those two points would have had difficulty exerting muscle forces on the small retroarticular process of the lower jaws, because it would have to wrap around the posterior end of the quadrate. Since the squamosal is far removed from the braincase, the depressor mandibulae anterior may instead have operated similar to the dorsal margin of the opercular membrane. In its limited effective mechanical advantage for jaw opening, this muscle might have been a muscle that primarily constricted the opening of the gills posteriorly, particularly with the loss of the boney operculum. Among other elpistostegids that possessed boney opercles, such as *Panderichthys* (Brazeau and Ahlberg 2006), any muscle that lay in the configuration of a depressor mandibulae anterior would cover the medial surface of the operculum.

The depressor mandibulae posterior in cryptobranchids spans between the jaw joint and the lateral wall of the otic capsule (Elwood and Cundall 1994, Kleinteich et al. 2014). This muscle in *Tiktaalik* would have stretched from the retroarticular process of the lower jaw anteromedially to the lateral wall of the otic portion of the braincase (Fig. 4.10). Although, this line of action would have been a powerful medial adductor of the jaw joints, due to dorsoventral compression of the skull its line of action lies almost completely orthogonal to what would be expected for a depressor of the lower jaws (Fig. 4.11c). Instead of depressing the lower jaws posteroventrally, this muscle would have likely placed the jaw joints under medial adduction towards the midline. In this configuration, the muscle would have functioned much more like its homolog in osteichthyan fishes, the adductor arcus palatini (Bemis 1986, Diogo 2008).

Dorsal mandibular constrictors

Muscles of the mandibular arch include the anterior and posterior intermandibularis muscles (discussed with the ventral hyoid constrictors), the adductor mandibulae complex, the levator arcus palatini, and the dilatator operculi (Diogo 2008). The adductor chamber of *Tiktaalik* currently lies outside of the scope of this study, although there were probably at least three subdivisions of the adductor mandibulae (Bemis 1986, Diogo 2008). The levator arcus palatini is present in coelacanth (Millot and Anthony 1958, Diogo 2008) and has been proposed for tetrapodomorph fishes as well (Thomson 1967); however it is lost in lungfish and amphibians (Diogo 2008). If *Tiktaalik* had a mobile palate, it possible that it still retained a levator arcus palatini. The dilatator operculi on the other hand, was likely recently lost or repurposed in *Tiktaalik* due to the loss of the boney operculum (Daeschler et al. 2006)

Axial musculature

While axial musculature in *Tiktaalik* is assumed, it cannot be described in great detail due to posterior crushing of the skull. The fossa bridgei above the otic region of the braincase, well formed in *Eusthenopteron* (Jarvik 1980), appears to be crushed in *Tiktaalik*, leaving very little room for attachment of powerful neurocranial elevators. Nevertheless, *Tiktaalik* had a large basioccipital (Downs et al. 2008), around which neurocranial elevation could have occurred. Neurocranial elevation is an important part of feeding in osteichthyans and cryptobranchids, and therefore we can assume epaxial muscles played a large role in feeding in *Tiktaalik* as well, although the exact muscle topology cannot be estimated.

The scapulocoracoids of *Tiktaalik* were large and robust and likely could have supported powerful attachments for hypaxial muscles (Shubin et al. 2006). This is backed up by the presence of a mobile joint in the shoulder girdle that would have allowed retraction of the cleithra due to hypaxial retraction.

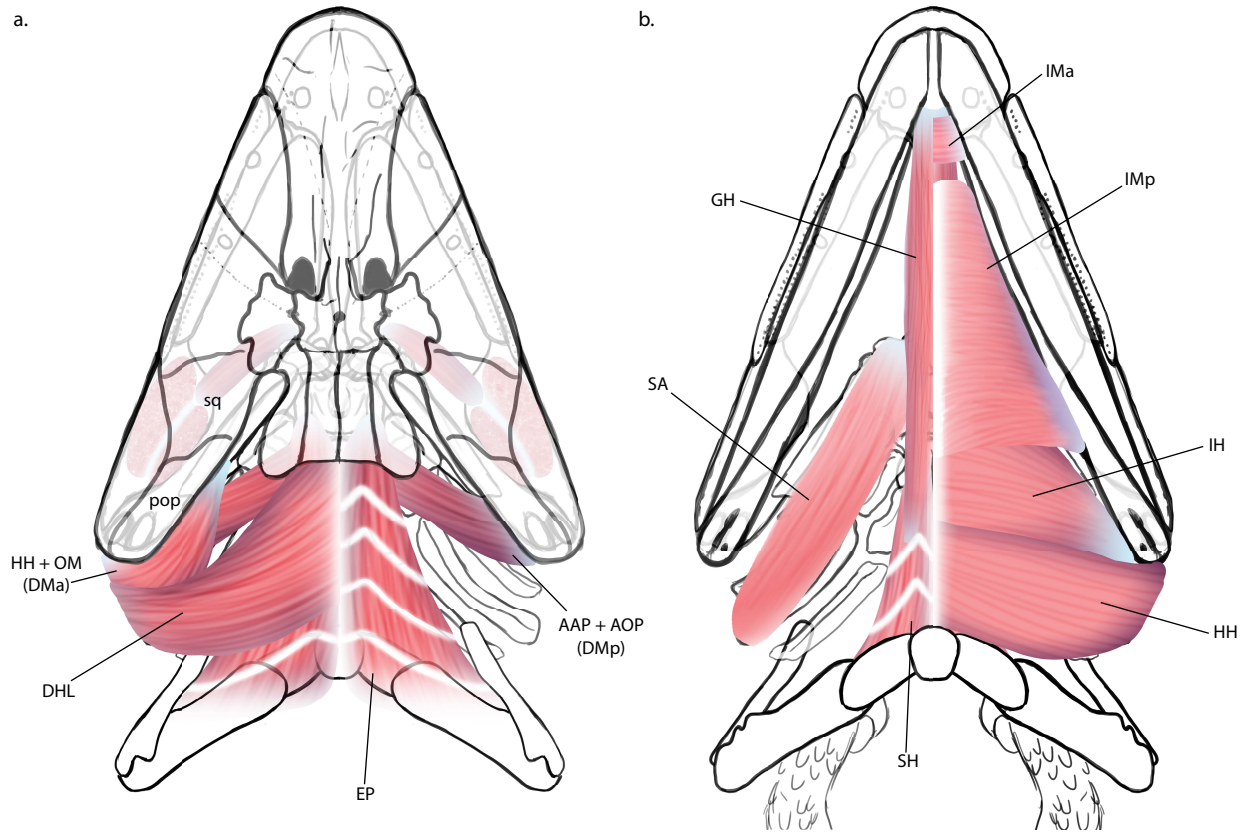


Figure 4.10. Proposed configuration of feeding musculature for *Tiktaalik roseae*.

Interpretation of (a) dorsal and (b) ventral muscle configurations based on homologous muscle configurations reported in cryptobranchid salamanders. The anterior depressor mandibulae (DMA) of salamanders spans between the retroarticular process of the lower jaw and the squamosal (sq), shown here as corresponding to the dorsal extent of hyohyoideus and opercular membrane (HH + OM) in *Tiktaalik*. The posterior depressor mandibulae of salamanders (DMp), spans between the retroarticular process of the lower jaw and the otic capsule and dorsal fascia, shown here as corresponding to the adductor arcus palatini (AAP) and adductor operculi (AOP) in *Tiktaalik*. Plesiomorphic osteichthyan terminology is used here for *Tiktaalik* due to the ineffective line of action for these muscles to directly open the lower jaws. In contrast, these muscles are still in position to effectively adduct the palate and hyoid arch. Other abbreviations: DHL (dorsal hyobranchial levators), EP (epaxials), GH (geniohyoideus), IH (interhyoideus), IMA (intermandibularis anterior), IMp (intermandibularis posterior), SA (subarcualis / branchiohyoideus), SH (sternohyoideus).

4.4.3 – Reconstructed feeding kinematics of *Tiktaalik roseae*

Assumptions required by this model

It is possible to manipulate the feeding apparatus of *Tiktaalik* into the four different phases of the gape cycle seen in *Atractosteus* feeding (Chapter 2), but some assumptions about the feeding system are necessary. First, the musculature and ligament reconstructions as well as evidence of a convergent flexible cranial linkage are taken into account (see results above). The following specializations are necessary for the *Tiktaalik* feeding system to share similar kinematics as a gar: a sliding articulation between the metapterygoid and basipterygoid, a sliding scarf joint between the cheek and braincase, separate rotations of the hyomandibula and palatoquadrate, and extensive rotation of the shoulder girdle at the anocleithral-cleithral joint. While this model does not assume the presence of effective jaw opening musculature, such as the depressor mandibulae anterior or posterior, it is possible that these muscles existed and jaw depression and hyoid depression were able to operate in a decoupled manner without the need for input by the hyoid constrictor musculature, as in gars. However, as evidenced by gars, modulation of the cranial linkage system into these various states requires nothing more than the plesiomorphic musculature found in osteichthyans (Chapter 2).

I. Buccal expansion:

In gars, buccal expansion is initiated by simultaneous neurocranial elevation and hyoid retraction. Assuming ventral hyoid constrictors are active early on in the feeding strike, as they are in gars, the hyoid is restricted from dropping below the level of the posterior lower jaws, and lateral rotation of the hyoid is restricted by the dorsal hyoid constrictors. Therefore, as the neurocranium of *Tiktaalik* elevates 10°, the hyoid and lower jaws elevate as well. However, hyoid elevation by 10° stretches the sternohyoideus away from the pectoral girdle. In order to

keep the sternohyoideus in contact with the pectoral girdle, the hyoid must retract relative to the lower jaws. This retracts the rigid bars used to simulate the cartilaginous ceratohyals (ch, Fig. 4.11). Due to the ceratohyal connection to the back of the lower jaw, hyoid retraction swings the lower jaws open (Fig. 4.13b). Jaw opening during neurocranial elevation without further shortening of sternohyoideus opens the jaws $\sim 31^\circ$, although this number could be higher depending on how much the sternohyoideus shortened in life. With the help of the hyoid constrictor sheath, no other specialized jaw-opening muscle other than the sternohyoideus are necessary to expand the buccal cavity prior to hyoid depression.

The hyoid apparatus of *Tiktaalik* is large, and space anterior to the pectoral girdle is limited (Fig. 4.12c). Since the mandibulohyoid ligament attaches close to the jaw joint, only slight retraction of the hyoid is necessary to fully open the jaws; however, even with these slight movements, the hyoid abuts the pectoral girdle. Without neurocranial elevation, significant retraction of the hyoid would impinge on the space likely occupied by the heart. If the mandibulohyoid ligament attached further away from the jaw joint, the sternohyoideus would have to contract by an unrealistic degree into the space dorsal to the interclavicle without the aid of pectoral girdle rotation.

While these cranial linkages are sufficient to open the lower jaws, it is possible that other muscles may assist in jaw opening as well. The geniohyoideus is reported to contribute to jaw opening in amphibians. However, in contrast to the mandibulohyoid ligament, this muscle inserts far from the center of rotation of the lower jaws, and as a result has extremely high mechanical advantage for jaw opening. The geniohyoideus would have to retract a significant distance to open the jaws only a few degrees (more about this in discussion section 2).

II. Pharyngeal expansion:

Pharyngeal expansion can begin with relaxation of the ventral hyoid constrictors and rotation of the pectoral girdle. In *Atractosteus*, the pectoral girdle is capable of rotating $\sim 20^\circ$. In *Tiktaalik*, with the hyoid no longer constrained against ventral rotation and the pectoral girdle rotating posteroventrally, the hyoid is capable of depressing 23° . While this number is smaller than the 47° reported for *Atractosteus*, further rotation of the pectoral girdle or hyoid would result in disarticulation of the pectoral girdle or depression of the hyoid below the origin of the sternohyoideus – an unlikely event.

Due to the close proximity of the line-of-action of the sternohyoideus to the center of rotation of the ceratohyals, the ability of the sternohyoideus to rotate the hyoid prior to pectoral girdle retraction is limited. Similar to the problem described for jaw opening, without significant pectoral girdle displacement, the sternohyoideus is only able to rotate the ceratohyals a few degrees by itself. As a result, pectoral girdle rotation is necessary to displace the hyoid far enough for the ceratohyals 23°

III. Opercular expansion:

Opercular expansion can begin with lateral abduction of the ceratohyal bars. In *Atractosteus*, relaxation of the dorsal hyoid constrictors and closure of the jaws protracts the mandibulohyoid ligament and posterior ceratohyals anteriorly. In *Tiktaalik*, similar closure of the lower jaws (from 30°) with the pectoral girdle rotated rotates the palates 4.64° at the dermopalatine-vomerine joint and produces a 12.4% lateral expansion of the jaw joints (Fig. 4.12b). While this is a smaller percentage than the 45% reported for *Atractosteus*, further abduction of the palate would result in disarticulation of the cheek from the prootic shelf. In

contrast to the 12.4% expansion of the jaws, however, this same rotation of 4.64° of the palate causes 22.12° rotation of the hyomandibula and expansion of the spiracular canal by 85%.

Lateral rotation of the palate necessitates lateral rotation of the hyomandibula as well. Since both suspensorial elements rotate on separate axes of rotation, the hyomandibular-otic articulation and the dermopalatine-vomer articulation, some sliding between the hyomandibula and palatoquadrate has to occur. This sliding articulation is supported by a groove on the medial surface of the palatoquadrate (Fig. 4.4c), which is present in osteolepidids as well (Thomson 1967). Separate movements of the hyomandibula and palatoquadrate produce greater lateral expansion of the feeding apparatus than would be the case with a single axis of rotation for both elements. Without separate rotation of the hyomandibula and palatoquadrate, the maximal dorsolateral rotation of the palate would be $\sim 20^\circ$ based on its suspension from the braincase (Chapter 2) resulting in $\sim 6\%$ expansion (i.e. $\cos 20^\circ$).

IV. Compression:

With suspensorial abduction and hyoid depression, the feeding apparatus is fully expanded by the time the jaws close. At this time the feeding system can return to its resting state by elevating and protracting the hyoid apparatus, presumably with the geniohyoideus muscle and ventral hyoid constrictors. The palate can return to its resting state using the adductor arcus palatini and adductor hyomandibulae. With the jaws closed and opercular and spiracular valve open, water is able to exit the feeding apparatus posteriorly (Fig. 4.13d), although it is possible water also exits the through the unoccluded tooth row anteriorly as well.

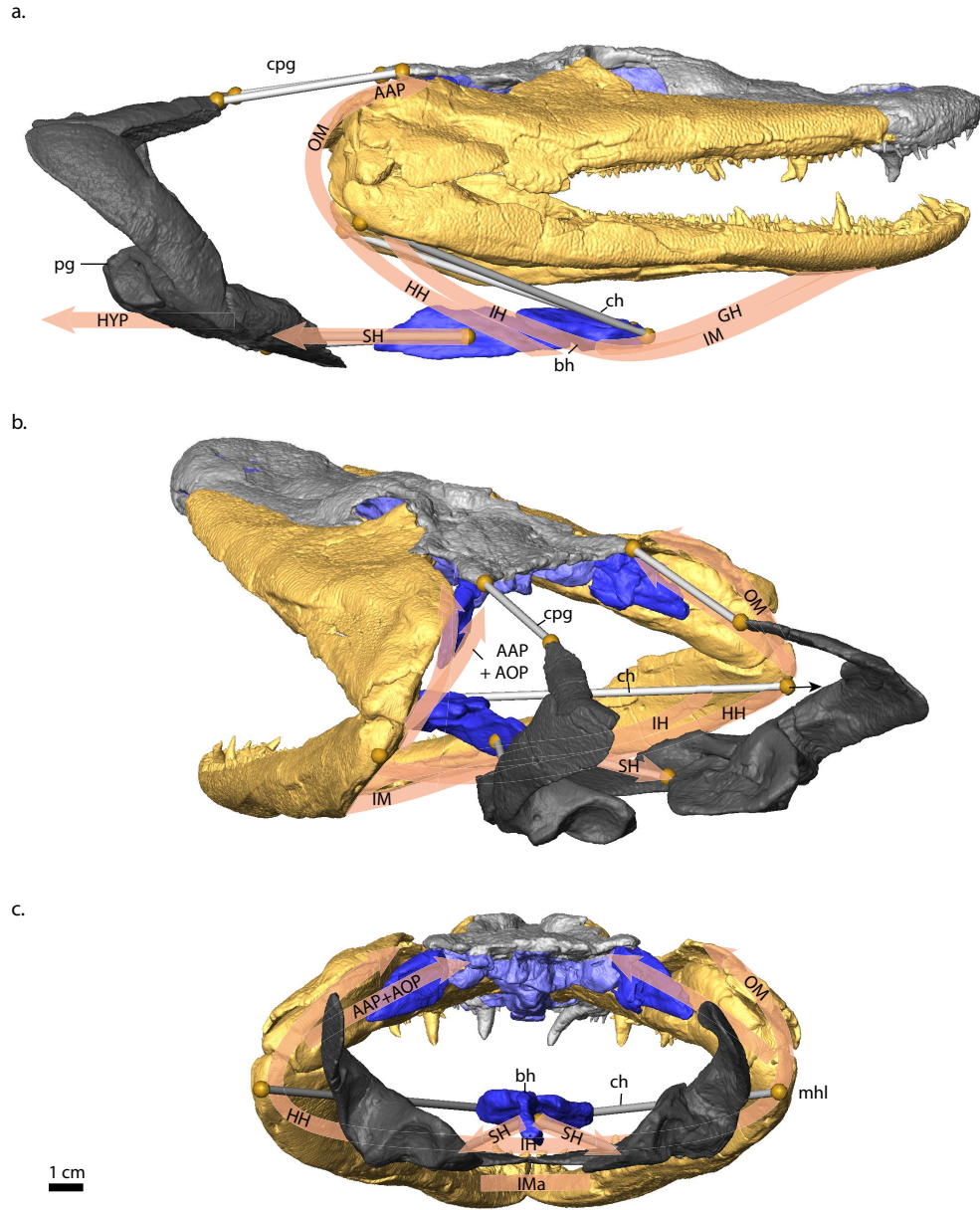


Figure 4.11. Cranial linkage system of *Tiktaalik roseae*. Shown is the proposed, reconstructed feeding system of *Tiktaalik roseae*, emphasizing the orientation and line of action of the depressor mandibulae precursors (OM, AAP, and AOP). (a) Lateral view showing the hyoid constrictors in a relaxed and expanded state to accommodate hyoid depression; notice the dorsal hyoid constrictor musculature must wrap around the back of the palate to reach the short retroarticular process. (b) Posterior oblique view showing jaw opening with the hyoid and sternohyoideus musculature surrounded by a sling of hyoid constrictor musculature; notice the depressor mandibulae precursors (OM, AAP, and AOP) are primarily oriented anteromedially (not dorsoposteriorly as would be necessary to open the jaws). (c) Posterior view showing a similar configuration of jaw opening muscles as in the previous view; notice the depressor

Figure 4.11, continued. mandibulae precursors (OM, AAP, and AOP) are well-positioned to adduct the suspensorium and recently-lost operculum. Abbreviations: AAP (adductor arcus palatini), AOP (adductor operculi), bh (basihyal), ch (rigid link representing the ceratohyal), cpg (rigid link representing connection between cranium and pectoral girdle), HH (hyohyoideus), HYP (hypaxials), IH (interhyoideus), IM (intermandibularis), IMa (anterior intermandibularis), mhl (mandibulohyoid ligament), OM (opercular membrane), pg (pectoral girdle), SH (sternohyoideus)

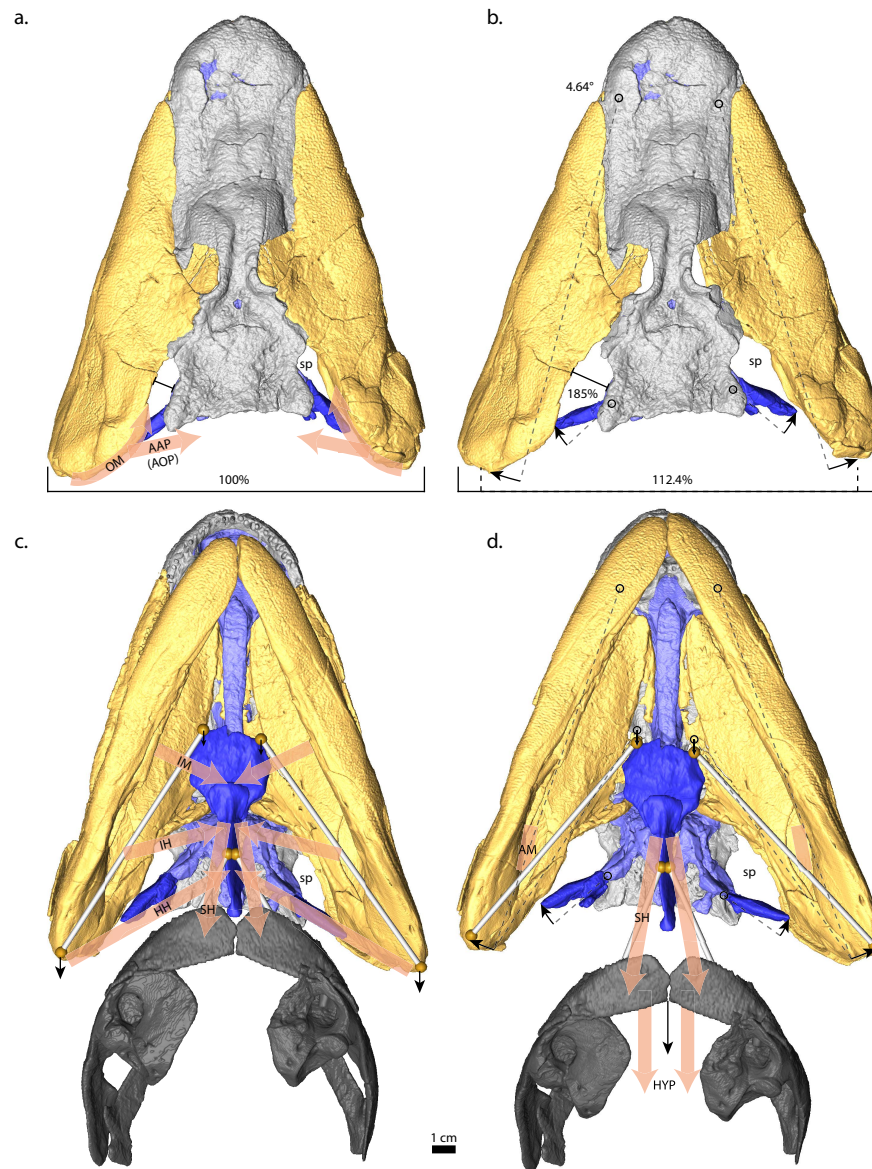


Figure 4.12. Proposed mechanism of suspensorial abduction in *Tiktaalik roseae*. Diagram showing the mechanism of suspensorial adduction (*a+c*) and suspensorial abduction (*b+d*) in *Tiktaalik roseae*. (*a*) Dorsal view showing the continuing role that depressor mandibulae precursors (AAP, AOP, and OM) have in adducting the suspensorium. (*b*) Dorsal view showing

Figure 4.12, continued. that abduction of the suspensorium involves separate axes of rotation for cheek and palate (yellow) and the hyomandibula (blue); notice, while the cranium only expands ~12% through these movements, the spiracle (sp) expands ~85%. (c) Ventral view showing suspensorial adduction can be maintained by ventral hyoid constrictors (IM, IH, and HH) while jaw opening is caused by hyoid retraction due to the sternohyoideus. (d) Ventral view showing lateral abduction of the ceratohyal bars due to retraction of the hyoid (blue), relaxation of hyoid constrictors, and protraction of the posterior ceratohyals; notice that some sliding of the hyomandibula relative to its connection with the palatoquadrate is necessary for lateral expansion of the feeding apparatus to occur. Black circles represent the axes of rotation of the palate (at the dermopalatine-vomer articulation) and hyomandibula (at its articulation with the lateral commissure). Black dashed lines show the initial starting positions of the suspensorium prior to abduction.

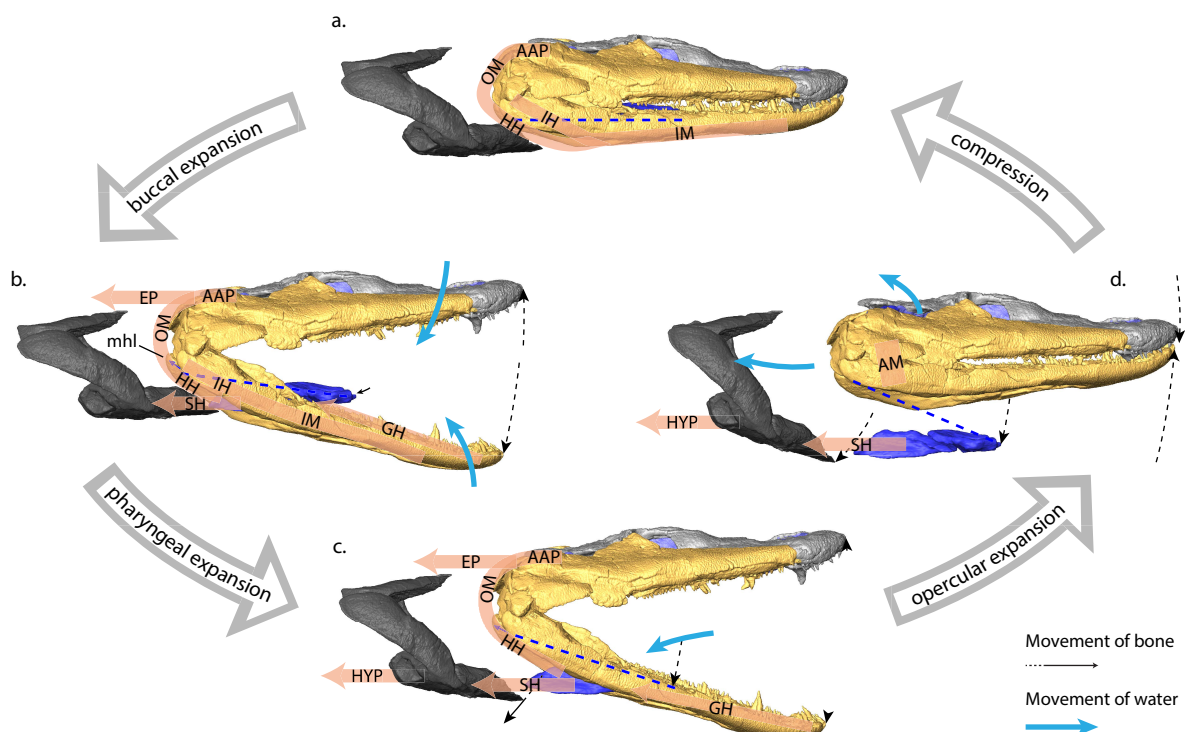


Figure 4.13. Reconstructed gape cycle and feeding kinematics of *Tiktaalik roseae*. The feeding apparatus of *Tiktaalik* is capable of successive expansions of the buccal, pharyngeal, and opercular cavities, modulated by hyoid constrictor musculature, which causes an anterior-to-posterior flow of water through the feeding apparatus (blue arrows) similar to feeding kinematics observed in *Atractosteus spatula* (Fig. 3.12). (a) At resting state, the ceratohyals (blue dashed line) and hyoid (blue) are in line with the pectoral girdle and are positioned within a sheath of hyoid constrictor musculature (IM, IH, HH, OM, AAP). (b) Buccal expansion is caused by retraction of the sternohyoideus, which retracts the mandibulohyoid ligament (dark blue arrow) and opens the lower jaws; notice that hyoid elevation is maintained by the ventral hyoid constrictor sheath (IM, IH, and HH) and suspensorial adduction is maintained by dorsal hyoid

Figure 4.13, continued. constrictors (AAP and OM) (see Fig. 4.11); (c) Pharyngeal expansion is caused by relaxation of the hyoid constrictors, allowing the hyoid (blue) to depress along with rotation of the pectoral girdle (dark grey). (d) Opercular expansion is caused by further rotation of the pectoral girdle (dark grey) by hypaxial musculature, while the jaws close due to the jaw adductors (AM) and the spiracle expands (Fig. 4.12). Notice that jaw closure rotates the posterior ceratohyals (blue dashed line) dorsolaterally, while pectoral girdle retraction rotates the anterior ceratohyals (blue dashed line) posteroventrally. Initial flow of water is caused by flat plate suction during jaw opening. Hyoid based suction can be delayed until the jaws have already opened due to activity of the hyoid constrictors. The geniohyoideus (GH) provides only limited jaw opening potential due to its shallow line-of-action and the extreme elongation the mandibles (high mechanical advantage but low displacement potential).

4.5 – DISCUSSION

4.5.1 – Maintenance of cranial expansion in a platyrostral system

The platyrostral skull of elpistostegids is a derived trait among tetrapodomorph fishes that coincides with rostral elongation of the skull and immobilization of the intracranial joint (Ahlberg et al. 1996, Brazeau and Ahlberg 2006, Daeschler et al. 2006). Elpistostegids evolved a platyrostral skull through a series of changes to the orientation of the palate, reduction of the hyomandibula, and lengthening of the sphenethmoid portion of the braincase (Ahlberg et al. 1996, Brazeau and Ahlberg 2006, Downs et al. 2008). While many of these changes were previously thought to reduce mobility of the skull and expansiveness of the feeding apparatus (Brazeau and Ahlberg 2006, Downs et al. 2008, Clack 2012), *Tiktaalik* possesses clear morphological features that indicate the palate and dermal cheek were still mobile relative to the braincase (Chapter 2). Furthermore, comparisons of cranial and pectoral girdle anatomy with alligator gars (Results, cranial linkage) have shown that *Tiktaalik* possessed all the features of an expansive cranial linkage system found in *Atractosteus spatula*, a platyrostral fish with the ability rapidly expand its feeding apparatus (Chapter 3). Two features in particular – pectoral

girdle rotation and intrasuspensorial mobility – enable *Tiktaalik roseae* to maintain an expansive feeding system.

While a platyrostral skull likely confers benefits to aquatic feeding vertebrates that capture prey with lateral snapping (Taylor 1987, Busbey 1995), among teleosts, widening of the skull reduces the overall contribution of suspensorial abduction to cranial expansion (Muller 1989) and increases the potential contribution of hyoid depression (Alexander 1970). However, the oblique angle of cranial muscles in a platyrostral skull also limits the effective mechanical advantage of those muscles (Busbey 1995), as well as the range of motion of the cranial elements they control (Alexander 1970, Adriaens and Verraes 1994). In the cranial linkage model of *Tiktaalik*, the posteroventral range of the hyoid apparatus is restricted to the ventral most excursion of the origin of the sternohyoideus (Fig. 4.11a). Additionally, due to large, robust hyobranchial apparatus of *Tiktaalik* and limited space anterior to the pectoral girdle (Fig. 4.12c), posteroventral movements of the hyoid are restricted to how much the pectoral girdle is also capable of retracting (Fig. 4.13d). These issues of hyobranchial geometry have been identified theoretically in fish skulls (Alexander 1970, Muller 1987) as well as shown to be the case in some dorsoventrally flattened catfish (Adriaens and Verraes 1994). Gars demonstrate how pectoral girdle rotation is able to mitigate some of these limitations by increasing the posteroventral range of motion of the hyoid (Chapter 3) and show how the mobile cleithral-anocleithral joint in *Tiktaalik* could help to increase the expansiveness of its platyrostral feeding system.

The other convergent feature found to increase the expansiveness of the skull in both *Atractosteus* and *Tiktaalik* is intrasuspensorial mobility. Both gars and elpistostegids have particularly loose connections between the hyomandibular and palatoquadrate portions of their

suspensorium (Arratia and Schultze 1991, Brazeau and Ahlberg 2006, Downs et al. 2008, Grande 2010). The cartilaginous connection between the hyomandibula and quadrate in both taxa enable the separate portions of the suspensorium to rotate around discrete axes of rotation (Chapter 3, Fig. 4.12b). While the suspensorium in most fish is fused between these elements (Arratia and Schultze 1991), constraining the suspensorium to rotate around a single axis (Lauder 1980a), several dorsoventrally compressed taxa (e.g. catfish) (Arratia 1990) and derived jaw-protruding specialists (Westneat and Wainwright 1989) are capable of rotating suspensorial elements relative to each other. Gars demonstrate how this trait is capable of maintaining cranial kinesis (Chapter 3) despite having a horizontal palate that should limit the lateral expansiveness of the skull (Muller 1989). While gars utilize intrasuspensorial mobility during feeding, it is its role in driving opercular expansion (Chapter 3) that is particularly interesting for *Tiktaalik*.

Fluid flow in aquatic taxa is important not only for feeding, but also respiration. As in *Acanthostega* (Coates and Clack 1991), *Tiktaalik* possesses grooved ceratobranchials indicative of gill respiration. However, *Tiktaalik* is the earliest tetrapodomorph that lacks a boney operculum (Daeschler et al. 2006). The effectiveness of opercular pumping may be diminished in the shift towards a platyrostral skull and loss of the operculum (Brazeau and Ahlberg 2006, Downs et al. 2008, Clack 2012), but the gills of *Tiktaalik* are nevertheless robust (Downs et al. 2008). By using a sliding basipterygoid-metapterygoid articulation of the palate, *Tiktaalik* is able to increase the lateral expansive range of the cheek (Fig. 4.12b) (see Results, opercular expansion), and likely would have still been able to pump water across its gills using suspensorial pumping (as observed for gars, Chapter 3). The method of suspensorial abduction described for gars and *Tiktaalik* is capable of expanding and contracting the opercular (post gill-bar) cavity regardless of positioning, size, or even existence of the operculum, and it is plausible

that the continued need for this hydrodynamic function in aquatic taxa prevented complete fusion of the palate to the braincase in platyrostral tetrapodomorphs.

In addition to expansion and contraction of the opercular cavity, suspensorial abduction in *Tiktaalik* also appears to affect the shape of the spiracular canal (Fig. 4.12b). Due to intrasuspensorial mobility between the hyomandibula and the palate, the spiracular canal widens by an estimated 85% during suspensorial abduction. As a result, water could be directed posteriorly through the gills or the spiracle during jaw closing (Fig. 4.13d) maintaining an anterior-to-posterior flow of water during feeding. This could have multiple benefits to a benthic fish and/or one living at the air-water interface. The spiracle in skates and rays enables them to draw water past the gills without taking in sediment from the benthos below (Brainerd and Ferry-Graham 2005). Conversely, the spiracle in *Polypterus* enables it to draw air in from the surface without fully emerging above water (Magid 1966). An increase in spiracular size is noted across the fin-to-limb transition (Brazeau and Ahlberg 2006, Clack 2007, Ahlberg et al. 2008) just as tetrapodomorphs begin to evolve platyrostral skulls.

Interestingly, many of the features that enable *Tiktaalik* to retain cranial expansion despite being platyrostral are important derived tetrapod traits thought to be related to the water-to-land transition. First, the loosened connection between the hyomandibula and the palatoquadrate enables intrasuspensorial mobility, but, as a result the hyomandibula eventually becomes further separated from the palatoquadrate and is incorporated into the hearing apparatus as the stapes (Clack 1994b). Whereas some intrasuspensorial mobility is implicit in models of cranial kinesis of osteolepidids with partitioned braincases (Thomson 1967), in those models the hyomandibula is an important integrating element of movements between separate regions of the braincase. With fusion of the braincase, that role is diminished (Thomson 1967, Brazeau and

Ahlberg 2006, Downs et al. 2008), and the basipterygoid-metapterygoid articulation of the braincase may have become enlarged to support and guide the movements of an newly independent palate, a transitional stage between the amphistylic suspensorial system of tetrapodomorph fishes and the autostylic suspensorial system of early tetrapods (Clack 1994b). The maintained cranial kinesis of *Tiktaalik* demonstrates this shift does not preclude palatal movements. Finally, the incorporation of pectoral girdle retraction as part of the system maintaining the expansive capabilities of the feeding apparatus could have widespread implications for the evolution of the limbed tetrapodomorph locomotory system. More work is needed to explore these implications further, because while each of these features enables aquatic suction to be maintained despite significant restructuring of the skull, they are also important derived tetrapodomorph traits that are eventually incorporated into the terrestrial tetrapod body plan.

4.5.2 – Jaw opening in *Tiktaalik* and insight into depressor mandibulae evolution

The unique cranial morphology of *Tiktaalik* provides a rare opportunity to examine the functional consequences of skull morphology on muscle function in a tetrapodomorph fish. Rapid changes to cranial morphology along the elpistostegid grade resulted in relatively extreme feeding morphology that would have significant functional consequences for any musculature attaching to it. Unlike the relatively general body plan of osteolepiforms (Ahlberg and Johanson 1998, Clack 2012), with ample attachment areas for musculature (Jarvik 1980) and mechanically advantageous lines-of-action for muscle function (Thomson 1967), the dorsoventrally flattened skull of *Tiktaalik* would have likely been subject to the same problems of limited attachment area and oblique muscle orientations faced by other platyrostral organisms (Busbey 1995). These

physical limitations are what enable us to make inferences of the details of the elpistostegid feeding system that would otherwise be impossible for less constrained morphologies.

While it is uncertain when depressor mandibulae musculature evolved along the tetrapod stem (Bemis 1987, Diogo 2008), *Tiktaalik* gives us clear insight into a stage of tetrapodomorph evolution where the depressor mandibulae muscles, if present, would have been limited in function. While the precursors of the depressor mandibulae muscles (suggested here as the adductor arcus palatini, and the dorsal extent of the hyohyoideus and opercular membrane, Fig. 4.10 and 4.11), likely existed in *Tiktaalik*, they probably still operated primarily as adductors of the palate and opercular flap due to their lines-of-action. These muscles have anteromedial orientations that would have been problematic for imparting posterodorsal muscle forces to the lower jaws (Fig. 4.11) but perfectly suited for their plesiomorphic roles of adducting the palate and opercular cavity. Furthermore, the lack of a retroarticular process with obvious scarring for a dorsally oriented muscle (Fig. 4.9) differentiates tetrapodomorph fishes from modern platyrostral taxa with comparatively large retroarticular processes (Busbey 1989, Heiss et al. 2013).

In contrast, gars demonstrate how a platyrostral fish with a small retroarticular process and plesiomorphic musculature is nevertheless able to use precursors of the depressor mandibulae to assist in jaw opening (Chapter 3). Hyoid constrictors are some of the earliest firing muscles during jaw opening in EMG studies of gars (Lauder 1980a), even though in *Atractosteus* their primary role in adducting the suspensorium after lateral flaring of the cheeks does not occur until after jaw closing (Chapter 3). Despite having no connection to the lower jaw, in restricting non-posterior movements of the hyoid, *Atractosteus* nevertheless uses the hyoid constrictors for use in jaw opening (Chapter 3). In contrast to *Atractosteus*, these muscles

in *Tiktaalik* likely attached close to the lower jaw, presumably on the medial surface of the quadrate or hyomandibula, as in rhizodonts and osteolepiforms (Brazeau and Jeffery 2008).

These findings suggest that *Tiktaalik* and earlier tetrapodomorph fishes may have relied on the plesiomorphic osteichthyan jaw opening mechanism. This system relies on the sternohyoideus as the primary jaw opening muscle, which imparts posterodorsal forces to the mandible via hyoid retraction by way of the mandibulohyoid ligament (Lauder 1980a, Wilga et al. 2000). Whereas there is little evidence for a functional depressor mandibulae in *Tiktaalik*, there are numerous indications of a robust sternohyoideus-based jaw opening mechanism in *Tiktaalik* and other tetrapodomorphs. First, the urohyal is a large, with ample insertion area for a powerful sternohyoideus muscle (Fig. 4.11). The jaw joint itself is posteriorly directed at the glenoid, similar to other tetrapodomorph fishes (Ahlberg and Clack 1998), suggesting that it is loaded with posteriorly directed forces rather than anteromedial forces (Fig. 4.9b). Additionally, in *Tiktaalik* the mandibulohyoid ligament scar is pronounced (Fig. 4.9) and corresponds to reports of similar scars in other tetrapodomorph fishes attributed to the mandibulohyoid ligament (Fox et al. 1995, Long et al. 1997, Ahlberg and Clack 1998, Zhu and Yu 2004)

While *Tiktaalik* may not have had specialized jaw opening musculature, it is possible that plesiomorphic hyoid constrictors nevertheless played an important role in jaw opening. Similar to gars (Chapter 3), by acting as a muscular sling through which the sternohyoideus is able to retract without rotating the hyoid, muscles such as the adductor arcus palatini, hyohyoideus, interhyoideus, and intermandibularis, assist the sternohyoideus to produce rapid and powerful jaw opening. Due to their attachment close to the lower jaws in *Tiktaalik* (but not in gars), these muscles may have gradually attained more of a direct role in jaw opening, and if so, there should be osteological correlates of that transition. The glenoid of the jaw joints eventually become

mores dorsally directed in limbed tetrapodomorphs (Ahlberg and Johanson 1998). With anterior advancement of the jaw joint, the origins of the depressor mandibulae (squamosal and lateral otic wall) eventually become more dorsally oriented to the jaw joint (Clack 2012). The crania of some tetrapodomorphs also tend to get more tall and narrow when compared with the particularly dorsoventrally compressed elpistostegids (Panchen 1985, Porro et al. 2015b). Furthermore, crown tetrapods eventually develop enlarged retroarticular processes (Witzmann and Schoch 2013) and tabular horns (another potential attachment site for the depressor mandibulae) (Panchen 1964) not found in tetrapodomorph fishes. Future applications of this work will be to apply quantitative methods to determine whether or not stem-tetrapods after the fin-to-limb transition possessed depressor mandibulae musculature, and it is likely that the most informative taxa for these future studies will be the most platyrostral ones.

4.5.3 – Evolution of terrestrial-style feeding kinematics

Through manipulation of the feeding mechanism of *Tiktaalik* and modeling its feeding apparatus as an expansive cranial linkage system, it is likely that *Tiktaalik* was capable of the same feeding kinematics as gars. While most osteichthyans are capable of cranial expansion from anterior-to-posterior (Lauder and Shaffer 1993), both gars and *Tiktaalik* underwent significant reconstruction of the feeding apparatus during convergent evolution of a platyrostral cranium that potentially limited that ability. Despite this restructuring of the feeding mechanism, each lineage maintained an expansive skull, presumably for hydrodynamic purposes. While it is not certain that *Tiktaalik* used an expansive feeding mechanism for the purposes of feeding, the strikingly convergent cranial proportions shared between *Atractosteus* and *Tiktaalik* suggests that, at the very least, these skulls shared similar hydrodynamic constraints when operating in

water (Vogel 1994). This allows us to discuss the feeding apparatus of *Tiktaalik* in terms of hydrodynamics using the feeding system of *Atractosteus* as a model.

The alligator gar has broad and elongate jaws that it uses to rapidly sweep through water to capture prey (Chapter 3). During jaw opening, these jaws act as broad flat plates that, while separating in water (Vogel 1994), draw water and prey towards the jaws while mitigating any bow wave caused by lateral sweeping (van Leeuwen and Muller 1984) (Chapter 3). During jaw opening and lateral sweeping, gars are able to keep the hyoid elevated (Chapter 3) through the use of hyoid constrictor muscles. This maintains a streamlined drag profile throughout lateral sweeping (Taylor 1987), but it also delays the onset of hyoid depression until the pharyngeal cavity is positioned closer to the prey. Effectiveness of suction is inversely proportional to the distance from mouth to the prey item (Wainwright et al. 2001), and by delaying hyoid depression, the effectiveness of hyoid based suction is enhanced. Finally, when the jaws begin to close, the suspensorium flares laterally, drawing water further posteriorly and allowing water displaced by the closing jaws to flow through the gills rather than the unoccluded tooth row (Chapter 3). In this way, the alligator gar utilizes the flow of water caused by its cranial kinematics to augment prey capture through rapid lateral snapping. While other physiological needs, such as maintaining suction for purposes of respiration, may be important factors for maintaining cranial kinesis in gars, *Atractosteus* nevertheless benefits from a synergistic combination of prey capture through biting and suction.

With similarly proportioned rostrum, jaws, and hyobranchial apparatus moving in similar ways as alligator gars, it is possible *Tiktaalik* also benefitted from similar hydrodynamic effects during feeding (Taylor 1987). *Tiktaalik* shares many convergent features with gars related to lateral snapping (see Results) and may have similarly captured prey through a combination of

suction and biting. While other factors, such as prey processing, gill respiration, or spiracular pumping may have been contributing factors in maintaining cranial kinesis in *Tiktaalik* (see discussion on maintained cranial expansion), it is the cranial kinematics possibly shared with gars for the purposes of feeding that allow us to make comparisons with other aquatic taxa.

Cryptobranchid salamanders are often compared to early tetrapods based on their primitive morphology, large size, and platyrostral skulls (Clack 2012, Heiss et al. 2013). While some are reported to use lateral strikes to capture prey (Elwood and Cundall 1994), they primarily capture prey using rapid expansion of the feeding apparatus (Heiss et al. 2013, Kleinteich et al. 2014). Expansion in cryptobranchids occurs from anterior to posterior, starting with rapid jaw opening caused by large depressor mandibulae musculature, followed by hyoid depression during jaw closing (Kleinteich et al. 2014). Due to their platyrostral jaws, jaw opening causes powerful flat plate suction which draws the prey inwards (Heiss et al. 2013); however, unlike most aquatic salamanders specialized in suction feeding, the cryptobranchids do not have open posterior gill slits that allow water to flow unidirectionally through the feeding apparatus (Deban and Wake 2000). Unidirectional suction feeding salamanders are significantly more effective at prey capture than ones unable to generate a unidirectional flow of water (Lauder and Shaffer 1986). As a result, delayed hyoid depression is an important aspect of cryptobranchid feeding, because pharyngeal cavity expansion during jaw closing enables water to be shunted posteriorly rather than forced back through the jaws (Deban and Wake 2000). Further specializations for suction feeding in cryptobranchids include large labial folds to occlude the gape, a flexible symphysis for directional control, cryptic coloration, and a smooth non-protrusible tongue (Elwood and Cundall 1994, Deban and Wake 2000, Heiss et al. 2013).

While gars and cryptobranchids use delayed hyoid depression during feeding in water, terrestrial tetrapods similarly use decoupled tongue and jaw movements to feed on land (Bramble and Wake 1985, Summers et al. 1998, Heiss and De Volder 2016). Similarities in kinematics of prey capture in cryptobranchids and terrestrial feeding salamanders have already been proposed on the pronounced decoupling of jaw and hyoid movements for the purposes of prey capture and prey processing (Deban and Wake 2000, Heiss et al. 2013), and it is believed that prey processing on land was the most difficult transition facing the earliest vertebrates feeding on land (Ashley-Ross et al. 2013). Terrestrial feeding tetrapods use coordinated but decoupled movements of the hyoid and jaws to control movements of the tongue for both prey capture and prey processing (Bramble and Wake 1985), and cryptobranchids do this as well for the purposes of prey capture using flat-plate suction and compensatory hyoid-based suction (Deban and Wake 2000, Heiss et al. 2013). However, what gars show us is that this same decoupling of hyoid and jaw movements is possible in an aquatic, biting-based taxon, with open gill slits and no specialized jaw opening musculature, such as *Tiktaalik*. By engaging in the same pattern of feeding kinematics as gar, it is possible *Tiktaalik* developed a terrestrial-style feeding cycle entirely in water (Fig. 4.13). While the functional purpose of these kinematics was not originally for use on land, it is possible that later taxa were able to coopt elpistostegid-style feeding kinematics when first attempting to process prey on land.

4.6 – CONCLUSIONS

The unique morphology of *Tiktaalik roseae* provides a rare opportunity to build an in-depth study of the feeding system of a tetrapodomorph fish that lived close to the fin-to-limb transition. The feeding apparatus of *Tiktaalik* shares many convergent features with gars, which

not only suggests similarities in terms of aspects of lepisosteid and elpistostegid feeding ecology but also provides insight into the limitations and constraints of the elpistostegid feeding morphology as well. By interpreting the elpistostegid grade as a distinct gar-like stage in stem-tetrapod evolution, we gain understanding of how some of the features of the terrestrial tetrapod feeding system evolved first in water. Many of the features previously thought to be elements of terrestrial feeding mechanics are actually features that evolved in tetrapodomorph fishes for the purposes of feeding in water.

Cranial expansion previously thought to be restricted in platyrostral taxa such as elpistostegids is shown to be maintained in *Tiktaalik* through independent axes of rotation of the hyomandibula and palatoquadrate (intrasuspensorial mobility) as well as the ability of the pectoral girdle to rotate posteroventrally. Gars demonstrate the use of these features in a feeding strike that combines elements of suction and biting to capture prey. While these features would likely have allowed *Tiktaalik* to generate suction during the feeding strike, these features would also have had implications for the respiratory and locomotory systems of early limbed tetrapodomorphs. In particular, function of the spiracular apparatus appears to have been enhanced by maintaining cranial kinesis.

While the precursors of specialized jaw opening muscles are integral to controlling palatal movements during feeding in fishes, gars show how those same muscles are also able to attain a secondary role in jaw opening. While the platyrostral morphology of *Tiktaalik* indicates these muscles still operated primarily as hyoid constrictors, muscle reconstructions and modeling of the feeding system of *Tiktaalik* show how the muscular precursors to the depressor mandibulae nevertheless could have played an important albeit indirect role in jaw opening,

subsequently enabling selective pressures to gradually enhance the jaw-opening role of the dorsal hyoid constrictors in early tetrapods.

Gars also demonstrate how terrestrial-style feeding kinematics can be an integral part of an aquatic feeding system that combines elements of both suction and biting to capture prey. The kinematics of decoupled hyoid depression and jaw opening in the gar feeding apparatus is directly comparable to those seen in terrestrial tetrapods but would have been possible in a tetrapodomorph fish such as *Tiktaalik* as well. Whereas decoupled jaw and hyoid movements would have allowed *Tiktaalik* to control the flow of water through the feeding apparatus, in early tetrapods the same decoupling of jaw and hyoid movements likely controlled movements of the tongue. While cryptobranchid salamanders also share kinematic patterns similar to those seen in *Atractosteus*, a gar-like stage in elpistostegids can explain how a terrestrial-style gape cycle can evolve prior to the evolution of specialized jaw opening musculature or the selective pressures of tongue control and subaerial feeding.

All these features demonstrate how a gar-like stage in tetrapodomorph evolution, such as that seen in *Tiktaalik roseae*, can simultaneously be adaptive for feeding in an aquatic context but also transitional for the derived features exhibited by later terrestrial tetrapods. As paralleled by the fin-to-limb transition, in which limbs evolved in water prior to a terrestrial stage, elpistostegids were also adapting features of enhanced suction generation, lateral snapping, and decoupled jaw-hyoid movements for the purposes of feeding in water that could subsequently be exapted for use on land by the earliest terrestrial vertebrates. By demonstrating that distantly related, non-tetrapodomorph fish such as gars are able to evolve many elements of a terrestrial-style feeding mechanism, this study shows that the evolutionary leap from water to land was made easier by incremental steps in water resulting in a terrestrial-style feeding mechanism.

CHAPTER 5 – CONCLUSIONS AND FUTURE DIRECTIONS

The benefits and applications of convergent evolution has been a persistent theme throughout each of the studies in this work. The morphological similarities shared between elpistostegids and lepisosteids are the result of millions of years of evolution that shaped their feeding systems into similar forms within their respective lineages. While superficial similarities that initially invited comparisons between these lineages, such as rostral proportions, could have been the result of mere coincidence, close examination of the feeding mechanisms of each group have revealed numerous, unexpected, analogous features suggestive of significant convergent use and selective pressures resulting from similar ecological niches. Gars were chosen as modern analogs in order to help interpret the feeding anatomy of *Tiktaalik roseae*; however, the process of examining shared features in *Atractosteus* uncovered some surprising aspects of alligator gar feeding as well. Evolutionary convergence is a powerful tool in biology and paleontology, because it enables a dialog between two taxa: the more we discovered about *Atractosteus*, the better we could interpret *Tiktaalik*, and vice versa. Elpistostegids apparently represented a very gar-like stage in the course of tetrapodomorph evolution, and it is possible that there is still much we could learn from the unique morphology of gars with direct applications to understanding the fin-to-limb and water-to-land transitions.

5.1 – FEEDING

Plicidentine tooth histology, where folds of dentine are arranged radially around the pulp cavity is a characteristic of fossil sarcopterygians, including the earliest terrestrial vertebrates, and a handful of amniote groups (Warren and Turner 2006, Maxwell et al. 2011). However, this

peculiar form of tooth structure has all but disappeared in modern taxa, except in varanid lizards, and gars (Warren and Turner 2006). Gars convergently evolved plicidentine tooth structure during the evolution of elongate jaws, and plicidentine is a synapomorphy that distinguishes lepisosteid gars from their sister clade, the obaichthyid gars (Grande 2010). Because this trait was convergently evolved in gars and is not a plesiomorphic holdover, future work on tetrapodomorph tooth evolution could benefit from studying the function of this particular form of teeth in gars. Finite element analysis (FEA) of plicidentine tooth structure in association with underlying bone morphology (see below) could be a fruitful avenue of research for understanding feeding morphology in tetrapodomorphs, particularly when compared with *in-vivo* studies among extant gars.

Plicidentine teeth form a particular tooth attachment with the underlying bone during development. This tooth attachment can be seen in empty tooth sockets of *Tiktaalik* as well as in gars (personal observation), and it is possible that convergent evolution of tooth replacement and attachment patterns in gars could provide valuable information for tooth development among extinct sarcopterygians for which that data is unavailable. In the course of CT scanning jaw material of *Tiktaalik roseae*, several instances were found of replacement teeth developing *in-situ* that could provide valuable data for tooth replacement studies among tetrapodomorphs. As *Lepisosteus oculatus* becomes increasingly used in evolutionary development studies, it may be possible to use gar teeth as a developmental model for early tetrapod tooth evolution.

Far more CT scans were collected during the course of this study than could be analyzed, and in particular lower jaw material was scanned for twelve of the nineteen known *Tiktaalik* specimens. These specimens represent a vast size range that could form the basis of an ontogenetic study of lower jaw development in a tetrapodomorph. Since lower jaws preserve

comparatively well in the tetrapodomorph fossil record (Ahlberg and Clack 1998), a study examining differences in lower jaws in a relatively well known taxa may provide valuable insight for taxa known from more fragmentary lower jaw material, such as *Elginerpeton* (Ahlberg 1995). Comparative FEA of tetrapodomorph lower jaws have already been proposed for *Acanthostega* and *Eusthenopteron* (Porro et al. 2015b, a), and *Tiktaalik* would form a natural extension of these studies in the future.

Furthermore, on the basis of this study, it seems probable that specialized depressor mandibulae evolved some time after the fin-to-limb transition. An additional fruitful avenue of research may be to examine the retroarticular processes of other tetrapodomorphs for evidence in a shift in way the mandible was loaded during feeding. The orientation of the jaw joint does undergo a shift among limbed tetrapodomorphs from posterior to dorsally facing (Ahlberg and Johanson 1998), which could indicate that shift coincided possibly with evolution of slightly taller skulls or posteriorly placed tabular horns (Panchen 1964, Howie 1969).

5.2 – RESPIRATION AND METABOLISM

Over the course of this study, the interplay of mechanisms of cranial expansion for the purposes of feeding and respiration were increasingly apparent. In *Tiktaalik* as well as in gars, it is possible that cranial expansion was maintained primarily for the purposes of respiration, with applications to feeding being of secondary function. However, until further study of the hydrodynamics of respiration in tetrapodomorphs is undertaken, that remains an untested hypothesis. *Polypterus* has functional spiracles, which it uses to inspire air (Graham et al. 2014). Future work in polypterids may benefit from modeling of the mechanisms of spiracular expansion similar to elpistostegids. Despite lacking functioning spiracles, gars are also capable

of gulping air from the surface of the water through expansion of their cranial apparatus (Rahn et al. 1971, Graham 1997). Complementary work in gars, may add to our understanding of early tetrapodomorph respiration due to their elongate, unoccluded tooth rows, platyrostral skulls, and large body sizes.

Intrasuspensorial mobility, found between the hyomandibular and palatoquadrate portions of the suspensorium in gars and elpistostegids, may have been more widespread than previously thought. The posteriorly inclined, “sub-holosteian” orientation of the suspensorium in basal actinopterygian (e.g. Redfieldiiformes) (Hutchinson 1973) and sarcopterygian fishes (Hitchcock 1995), likely had to use independent axes of rotation of suspensorial elements to laterally expand their opercular cavities. Taking flexibility between the hyomandibula and palatoquadrate into account in these taxa will likely improve models of these extinct fossil taxa for which suspensorial abduction was thought to be previously limited.

Furthermore, the role of air-breathing in an aquatic ambush predator, such as gars, could have interesting applications for tetrapodomorph research. Observing *Lepisosteus oculatus* in the lab, it was apparent that the air-breathing organ of gars could have numerous functions in addition to gas exchange (personal observation). After taking a gulp of air, a gar could remain perfectly still while in the presence of potential prey because gill movements either slowed or stopped altogether. Cryptic coloration, in combination with slowed fin movements, enabled the gar to approach unsuspecting prey, because the gar was able to reposition the orientation of its body in the water column, much like a submersible, presumably by shifting the volume of air along the length of its elongate lungs. Similar to gars, elpistostegids, had elongate bodies with the potential for cryptic reorientation of the body through gas volume redistribution.

Slowed gas exchange in suboptimal conditions may have been possible thanks to the role that extensive dermal sculpturing of tetrapodomorphs had in buffering metabolic acidosis (Janis et al. 2012, Witzmann and Brainerd 2017). The global atmospheric conditions during the fin-to-limb transition were likely lower in oxygen and higher in atmospheric carbon dioxide (Clack 2007). With extensive dermal sculpting, air-filled lungs, and an ability to survive in hypoxic and or hypercapnic water (Rahn et al. 1971), gars may provide a useful modern analog for studying the physiological functions of many of these features in tetrapodomorphs, which were likely large, ambush-predators, living in oxygen poor waters, with fish-like metabolic requirements.

5.3 – REPRODUCTION AND LOCOMOTION

Gars may provide insight into the reproductive strategies of tetrapodomorphs as well. During flooding events, adult alligator gars move out among the flooded vegetation to lay their eggs, and then, as flood waters recede, the young are concentrated into small ephemeral pools (Etnier and Starnes 1993, Buckmeier 2008). These pools remain isolated from the main river channel, where the young can feed on small fish and aquatic invertebrates in relative safety. This continues until floodwaters return and the young can return to the main population (Buckmeier 2008, Solomon et al. 2013), or, until the pools dry up completely, leaving the young gars to perish in mass die-offs. The use of an air-breathing organ may be essential for longevity in ephemeral pools.

The early limbed tetrapodomorph, *Acanthostega*, is known from mass-death assemblages where numerous juveniles died in large concentrated-numbers (Sanchez et al. 2016). While the authors suggest a school of *Acanthostega* may have swept into isolated pools by a flood where they subsequently died, on the basis of still unossified cartilage and lines-of-arrested-growth

(LAG lines), these individuals were likely subadult. Understanding gar reproduction, it is possible the young *Acanthostega* were gathered in those pools as part of the species reproductive strategy but were unable to escape during periods of long drought. The ability of tetrapodomorphs to extend lifespans in these situations could have been a driving factor in the acquisition of extensive dermal sculpting, spiracular breathing, and, possibly, weight-bearing limbs that could allow short excursions between bodies of water. New insight into the role that pectoral girdle retraction played in the feeding mechanism of tetrapodomorphs would likely have important implications for terrestrial locomotion as well, particularly as early tetrapodomorphs, like *Ichthyostega*, may have only been able to utilize limited crutching movements with the pectoral fins (Pierce et al. 2012).

LAG lines have been used in limbed tetrapodomorphs to determine periods of seasonality in the life-histories of *Acanthostega* (Sanchez et al. 2016), and a similar technique may be possible in *Tiktaalik* as well. While CT scanning pectoral elements of *Tiktaalik roseae*, distinct layers of dermal bone in the cleithrum appear to follow growth patterns similar to LAG lines. Further work will be needed to identify osteological correlates of LAG lines in the cleithra of modern fish, but if accurate, the potential to measure LAG lines in the cleithra of tetrapodomorphs, which tend to be better preserved in tetrapodomorphs than limb elements, would be an exciting new area of research.

5.4 – SKULL MECHANICS OF FOSSIL FISHES

Finally, the insight gained from modeling cranial kinematics in *Atractosteus spatula* and *Tiktaalik roseae* can be used to form the basis of feeding models in closely related taxa for each of their respective evolutionary lineages. Lepisosteiformes are a small subset of a once

widespread, taxonomically and morphologically diverse clade of non-teleosts actinopterygians, ginglymodians, that radiated during the Mesozoic (Cavin 2010, Grande 2010). The diversity of body types and jaw morphology within this radiation suggests a wide range of feeding strategies – including small-mouthed, suction-feeding semionotids (Schaeffer 1967, Cavin 2010), marine reef dwelling macrosemiids (Grande 2010), durophagous members of the paraphyletic ‘Lepidotes’ (Cavin 2010), and “cyprinid-like”, non-predatory grazers or detritivores forming the sister taxa to Lepisosteiformes (Cavin 2010). Without elongate jaws or jaw-protrusion, these close relatives of gars were probably strictly suction feeders, and a rigid covering of plesiomorphic, ganoid scales may have also limited their ability to pursue prey, like other body-ram predators (Webb et al. 1992, Porter and Motta 2004). Ginglymodians could have used the same plesiomorphic musculature as *Atractosteus spatula* to decouple jaw-opening from hyoid depression and modulate an anterior-to-posterior expansion of cranial elements for the purposes of suction feeding.

Similarly, the proposed cranial kinematics of *Tiktaalik roseae* presented here make clear hypotheses of the mobility and function of numerous bones of the feeding apparatus that can be tested in other taxa. While cranial kinesis was presumed for many limbed tetrapodomorphs and early tetrapods (Panchen 1964, Romer 1969, Beaumont 1977, Panchen 1985, Clack 1989, Iordansky 1990, Bolt and Lombard 2001), the mechanism and function of those kinematics remained elusive. By comparing the proposed mobility and functional morphology of *Tiktaalik*, with these other taxa, we can explore some of the functional consequences of morphological change to many of the cranial elements discussed here, including the hyomandibula, pterygoid, quadrate, dermopalatine, postorbital, lacrimal, hyoid apparatus, and cleithrum. Some of these explorations may amend the hypotheses of *Tiktaalik* feeding mechanics presented here, but it is

my hope that this detailed model of tetrapodomorph cranial kinematics will form the basis of many fruitful studies in the future.

REFERENCES:

- Adriaens, D., and W. Verraes. 1994. On the functional significance of the loss of the interhyal during ontogeny in *Clarias gariepinus* Burchell, 1822 (Teleostei: Siluroidei). *Belgian Journal of Zoology* **124**:139-155.
- Aerts, P. 1991. Hyoid morphology and movements relative to abducting forces during feeding in *Astatotilapia elegans* (Teleostei: Cichlidae). *Journal of Morphology* **208**:323-345.
- Ahlberg, P. E. 1995. *Elginerpeton pancheni* and the earliest tetrapod clade. *Nature* **373**:420.
- Ahlberg, P. E., and J. A. Clack. 1998. Lower jaws, lower tetrapods—a review based on the Devonian genus *Acanthostega*. *Earth and Environmental Science Transactions of the Royal Society of Edinburgh* **89**:11-46.
- Ahlberg, P. E., and J. A. Clack. 2006. Palaeontology - A firm step from water to land. *Nature* **440**:747-749.
- Ahlberg, P. E., J. A. Clack, and H. Blom. 2005. The axial skeleton of the Devonian tetrapod *Ichthyostega*. *Nature* **437**:137-140.
- Ahlberg, P. E., J. A. Clack, and E. Luksevics. 1996. Rapid braincase evolution between *Panderichthys* and the earliest tetrapods. *Nature* **381**:61-64.
- Ahlberg, P. E., J. A. Clack, E. Luksevics, H. Blom, and I. Zupins. 2008. *Ventastega curonica* and the origin of tetrapod morphology. *Nature* **453**:1199-1204.
- Ahlberg, P. E., and Z. Johanson. 1998. Osteolepiforms and the ancestry of tetrapods. *Nature* **395**:792-794.
- Ahlberg, P. E., E. Luksevics, and E. Mark-Kurik. 2000. A near-tetrapod from the Baltic Middle Devonian. *Palaeontology* **43**:533-548.
- Alexander, R. M. 1970. Mechanics of the feeding action of various teleost fishes. *Journal of Zoology* **162**:145-156.
- Allis, E. P. 1919. On certain Features of the Otic Region of the Chondrocranium of *Lepidosteus*, and Comparison with other Fishes and Higher Vertebrates. *Proceedings of the Zoological Society of London* **89**:245-266.
- Allis Jr, E. P. 1922. The cranial anatomy of *Polypterus*, with special reference to *Polypterus bichir*. *Journal of Anatomy* **56**:189.
- Anderson, P. S. L., M. Friedman, M. D. Brazeau, and E. J. Rayfield. 2011. Initial radiation of jaws demonstrated stability despite faunal and environmental change. *Nature* **476**:206-209.
- Anderson, P. S. L., M. Friedman, and M. Ruta. 2013. Late to the Table: Diversification of tetrapod mandibular biomechanics lagged behind the evolution of terrestriality. *Integrative and Comparative Biology*.

- Arratia, G. 1990. Development and diversity of the suspensorium of trichomycterids and comparison with loricarioids (Teleostei: Siluriformes). *Journal of Morphology* **205**:193-218.
- Arratia, G., and H.-P. Schultze. 1991. Palatoquadrate and its ossifications: Development and homology within osteichthyans. *Journal of Morphology* **208**:1-81.
- Ashley-Ross, M. A., S. T. Hsieh, A. C. Gibb, and R. W. Blob. 2013. Vertebrate land invasions—past, present, and future: an introduction to the symposium. *Integrative and Comparative Biology*:ict048.
- Askary, A., J. Smeeton, S. Paul, S. Schindler, I. Braasch, N. A. Ellis, J. Postlethwait, C. T. Miller, and J. G. Crump. 2016. Ancient origin of lubricated joints in bony vertebrates. *eLife* **5**:e16415.
- Beaumont, E. H. 1977. Cranial morphology of the Loxommatidae (Amphibia: Labyrinthodontia). *Philosophical Transactions of the Royal Society of London B: Biological Sciences* **280**:29-101.
- Bemis, W. E. 1986. Feeding Systems of Living Dipnoi: Anatomy and function. *Journal of Morphology* **190**:249-275.
- Bemis, W. E. 1987. Convergent evolution of jaw-opening muscles in lepidosirenid lungfishes and tetrapods. *Canadian Journal of Zoology* **65**:2814-2817.
- Bemis, W. E., and G. V. Lauder. 1986. Morphology and Function of the Feeding Apparatus of the Lungfish, *Lepidosiren paradoxa* (Dipnoi). *Journal of Morphology* **187**:81-108.
- Bolt, J. R. 1974. Evolution and Functional Interpretation of Some Suture Patterns in Paleozoic Labyrinthodont Amphibians and Other Lower Tetrapods. *Journal of Paleontology* **48**:434-458.
- Bolt, J. R., and R. E. Lombard. 2001. The mandible of the primitive tetrapod *Greererpeton*, and the early evolution of the tetrapod lower jaw. *Journal of Paleontology* **75**:1016-1042.
- Braasch, I., A. R. Gehrke, J. J. Smith, K. Kawasaki, T. Manousaki, J. Pasquier, A. Amores, T. Desvignes, P. Batzel, J. Catchen, A. M. Berlin, M. S. Campbell, D. Barrell, K. J. Martin, J. F. Mulley, V. Ravi, A. P. Lee, T. Nakamura, D. Chalopin, S. Fan, D. Weisel, C. Canestro, J. Sydes, F. E. G. Beaudry, Y. Sun, J. Hertel, M. J. Beam, M. Fasold, M. Ishiyama, J. Johnson, S. Kehr, M. Lara, J. H. Letaw, G. W. Litman, R. T. Litman, M. Mikami, T. Ota, N. R. Saha, L. Williams, P. F. Stadler, H. Wang, J. S. Taylor, Q. Fontenot, A. Ferrara, S. M. J. Searle, B. Aken, M. Yandell, I. Schneider, J. A. Yoder, J.-N. Volff, A. Meyer, C. T. Amemiya, B. Venkatesh, P. W. H. Holland, Y. Guiguen, J. Bobe, N. H. Shubin, F. Di Palma, J. Alföldi, K. Lindblad-Toh, and J. H. Postlethwait. 2016. The spotted gar genome illuminates vertebrate evolution and facilitates human-teleost comparisons. *Nat Genet* **48**:427-437.
- Brainerd, E. L., and L. A. Ferry-Graham. 2005. Mechanics of Respiratory Pumps. Pages 1-28 in E. S. Robert and V. L. George, editors. *Fish Physiology*. Academic Press.
- Bramble, D. M., and D. Wake. 1985. Feeding mechanisms of lower tetrapods. *Functional vertebrate morphology*:230-261.
- Brazeau, M. D., and P. E. Ahlberg. 2006. Tetrapod-like middle ear architecture in a Devonian fish. *Nature* **439**:318-321.

- Brazeau, M. D., and J. E. Jeffery. 2008. The hyomandibulae of rhizodontids (Sarcopterygii, stem-tetrapoda). *Journal of Morphology* **269**:654-665.
- Brito, P. M., J. Alvarado-Ortega, and F. J. Meunier. 2017. Earliest known lepisosteoid extends the range of anatomically modern gars to the Late Jurassic. *Scientific reports* **7**:17830.
- Bryant, H. N., A. Russell, and J. Thomason. 1995. Carnassial functioning in nimravid and felid sabertooths: theoretical basis and robustness of inferences. *Functional morphology in vertebrate paleontology*:116-135.
- Buckmeier, D. L. 2008. Life history and status of alligator gar *Atractosteus spatula*, with recommendations for management. TPWD Inland Fisheries Report, Heart of the Hills Fisheries Science Center.
- Busbey, A. B., III. 1989. Form and function of the feeding apparatus of *Alligator mississippiensis*. *Journal of Morphology* **202**:99-127.
- Busbey, A. B., III. 1995. The structural consequences of skull flattening in crocodilians. Pages 173–192 in J. J. Thomason, editor. *Functional morphology in vertebrate paleontology*. Cambridge University Press, Cambridge, UK.
- Camp, A. L., T. J. Roberts, and E. L. Brainerd. 2015. Swimming muscles power suction feeding in largemouth bass. *Proceedings of the National Academy of Sciences* **112**:8690-8695.
- Carroll, A. M., and P. C. Wainwright. 2003. Functional morphology of prey capture in the sturgeon, *Scaphirhynchus albus*. *Journal of Morphology* **256**:270-284.
- Cavin, L. 2010. Diversity of Mesozoic semionotiform fishes and the origin of gars (Lepisosteidae). *Naturwissenschaften* **97**:1035-1040.
- Cho, G., and D. Heath. 2000. Comparison of tricaine methanesulphonate (MS222) and clove oil anaesthesia effects on the physiology of juvenile chinook salmon *Oncorhynchus tshawytscha* (Walbaum). *Aquaculture research* **31**:537-546.
- Clack, J. A. 1989. Discovery of the earliest-known tetrapod stapes. *Nature* **342**:425-427.
- Clack, J. A. 1994a. *Acanthostega gunnari*, a Devonian tetrapod from Greenland: the snout, palate and ventral parts of the braincase, with a discussion of their significance. *Kommissionen for videnskabelige undersøgelser i Grønland*.
- Clack, J. A. 1994b. Earliest Known Tetrapod Braincase and the Evolution of the Stapes and Fenestra Ovalis. *Nature* **369**:392-394.
- Clack, J. A. 1998. The neurocranium of *Acanthostega gunnari* Jarvik and the evolution of the otic region in tetrapods. *Zoological Journal of the Linnean Society* **122**:61-97.
- Clack, J. A. 2001. The otoccipital region: origin, ontogeny and the fish-tetrapod transition. *Systematics Association Special Volume Series* **61**:392-405.

- Clack, J. A. 2002a. The dermal skull roof of *Acanthostega gunnari*, an early tetrapod from the Late Devonian. *Earth and Environmental Science Transactions of the Royal Society of Edinburgh* **93**:17-33.
- Clack, J. A. 2002b. An early tetrapod from 'Romer's Gap'. *Nature* **418**:72-76.
- Clack, J. A. 2007. Devonian climate change, breathing, and the origin of the tetrapod stem group. *Integrative and Comparative Biology* **47**:510-523.
- Clack, J. A. 2009. The Fin to Limb Transition: New Data, Interpretations, and Hypotheses from Paleontology and Developmental Biology. *Annual Review of Earth and Planetary Sciences* **37**:163-179.
- Clack, J. A. 2012. *Gaining ground: the origin and evolution of tetrapods*. Indiana University Press.
- Coates, M. I., and J. A. Clack. 1991. Fish-like gills and breathing in the earliest known tetrapod. *Nature* **352**:234-236.
- Coates, M. I., J. E. Jeffery, and M. Ruta. 2002. Fins to limbs: what the fossils say. *Evolution & development* **4**:390-401.
- Coates, M. I., M. Ruta, and M. Friedman. 2008. Ever Since Owen: Changing Perspectives on the Early Evolution of Tetrapods. *Annual Review of Ecology Evolution and Systematics* **39**:571-592.
- Cooper, W. J., C. B. Carter, A. J. Conith, A. N. Rice, and M. W. Westneat. 2017. The evolution of jaw protrusion mechanics is tightly coupled to benthic-pelagic divergence in damselfishes (Pomacentridae). *The Journal of Experimental Biology* **220**:652-666.
- Daeschler, E. B., N. H. Shubin, and F. A. Jenkins. 2006. A Devonian tetrapod-like fish and the evolution of the tetrapod body plan. *Nature* **440**:757-763.
- Damiani, R. J. 2001. Cranial anatomy of the giant Middle Triassic temnospondyl *Cherninia megarhina* and a review of feeding in mastodonsaurids.
- Darwin, C. 1859. *On the origin of species by means of natural selection*.
- Day, S. W., T. E. Higham, A. Y. Cheer, and P. C. Wainwright. 2005. Spatial and temporal patterns of water flow generated by suction-feeding bluegill sunfish *Lepomis macrochirus* resolved by Particle Image Velocimetry. *Journal of Experimental Biology* **208**:2661.
- Day, S. W., T. E. Higham, R. Holzman, and S. Van Wassenbergh. 2015. Morphology, kinematics, and dynamics: the mechanics of suction feeding in fishes. *Integrative and Comparative Biology* **55**:21-35.
- Deban, S. M., and D. B. Wake. 2000. Aquatic Feeding in Salamanders. Pages 65-94 in K. Schwenk, editor. *Feeding: Form, Function, and Evolution in Tetrapod Vertebrates*. Academic Press, San Diego.
- Diogo, R. 2008. Comparative anatomy, homologies and evolution of mandibular, hyoid and hypobranchial muscles of bony fish and tetrapods: a new insight. *Animal Biology* **58**:123-172.

- Downs, J. P., E. B. Daeschler, F. A. Jenkins, and N. H. Shubin. 2008. The cranial endoskeleton of *Tiktaalik roseae*. *Nature* **455**:925-929.
- Dutel, H., A. Herrel, G. Clément, and M. Herbin. 2013. A reevaluation of the anatomy of the jaw-closing system in the extant coelacanth *Latimeria chalumnae*. *Naturwissenschaften* **100**:1007-1022.
- Edgeworth, F. H. 1935. The cranial muscles of vertebrates. Cambridge University Press.
- Elwood, J. R. L., and D. Cundall. 1994. Morphology and behavior of the feeding apparatus in *Cryptobranchus alleganiensis* (Amphibia: Caudata). *Journal of Morphology* **220**:47-70.
- Etnier, D. A., and W. C. Starnes. 1993. The fishes of Tennessee. University of Tennessee Press.
- Ferry-Graham, L. A., P. C. Wainwright, C. D. Hulsey, and D. R. Bellwood. 2001. Evolution and mechanics of long jaws in butterflyfishes (Family Chaetodontidae). *Journal of Morphology* **248**:120-143.
- Fortuny, J., J. Marcé-Nogué, L. Gil, and À. Galobart. 2012. Skull Mechanics and the Evolutionary Patterns of the Otic Notch Closure in Capitosaur (Amphibia: Temnospondyli). *The Anatomical Record: Advances in Integrative Anatomy and Evolutionary Biology* **295**:1134-1146.
- Fox, R., K. Campbell, R. Barwick, and J. Long. 1995. A new osteolepiform fish from the lower Carboniferous Raymond Formation, Drummond Basin, Queensland. *Memoirs of the Queensland Museum* **38**:97-221.
- Friedman, M. 2007. *Styloichthys* as the oldest coelacanth: Implications for early osteichthyan interrelationships. *Journal of Systematic Palaeontology* **5**:289-343.
- Graham, Jeffrey B. 1997. Air-Breathing Fishes : Evolution, Diversity, and Adaptation. Academic Press, San Diego, CA.
- Graham, J. B., N. C. Wegner, L. A. Miller, C. J. Jew, N. C. Lai, R. M. Berquist, L. R. Frank, and J. A. Long. 2014. Spiracular air breathing in polypterid fishes and its implications for aerial respiration in stem tetrapods. *Nature Communications* **5**:3022.
- Grande, L. 2010. An Empirical Synthetic Pattern Study of Gars (Lepisosteiformes) and Closely Related Species, Based Mostly on Skeletal Anatomy: The Resurrection of Holostei. *American Society of Ichthyologists and Herpetologists Special Publication 6 supplementary issue of Copeia* **10**:i-x, 1-871.
- Haines, R. W. 1942. Eudiarthrodial joints in fishes. *Journal of Anatomy* **77**:12.
- Heiss, E., P. Aerts, and S. Van Wassenbergh. 2018. Aquatic–terrestrial transitions of feeding systems in vertebrates: a mechanical perspective. *The Journal of Experimental Biology* **221**.
- Heiss, E., and M. De Vylder. 2016. Dining dichotomy: aquatic and terrestrial prey capture behavior in the Himalayan newt *Tylotriton verrucosus*. *Biology Open* **5**:1500-1507.

- Heiss, E., N. Natchev, M. Gumpenberger, A. Weissenbacher, and S. Van Wassenbergh. 2013. Biomechanics and hydrodynamics of prey capture in the Chinese giant salamander reveal a high-performance jaw-powered suction feeding mechanism. *Journal of The Royal Society Interface* **10**.
- Hilton, E. J., P. Konstantinidis, N. K. Schnell, and C. B. Dillman. 2014. Identity of a Unique Cartilage in the Buccal Cavity of Gars (Neopterygii: Lepisosteiformes: Lepisosteidae). *Copeia* **2014**:50-55.
- Hitchcock, E. C. 1995. A functional interpretation of the anterior-most vertebrae and skull of *Eusthenopteron*. *Bulletin du Muséum national d'Histoire naturelle, 4ème série-section C—Sciences de la Terre, Paléontologie, Géologie, Minéralogie* **17**:269-285.
- Hohn-Schulte, B., H. Preuschoft, U. Witzel, and C. Distler-Hoffmann. 2013. Biomechanics and functional preconditions for terrestrial lifestyle in basal tetrapods, with special consideration of *Tiktaalik roseae*. *Historical Biology* **25**:167-181.
- Holzman, R., and P. C. Wainwright. 2009. How to surprise a copepod: Strike kinematics reduce hydrodynamic disturbance and increase stealth of suction-feeding fish. *Limnology and Oceanography* **54**:2201-2212.
- Howie, A. 1969. On a new capitosaurid labyrinthodont from East Africa. University of Cambridge.
- Hutchinson, P. 1973. A Revision of the Redfieldiiform and Perleidiform Fishes from the Triassic of Bekker's Kraal (South Africa) and Brookvale (New South Wales). British Museum.
- Iordansky, N. N. 1990. Evolution of cranial kinesis in lower tetrapods. *Netherlands Journal of Zoology* **40**:32-54.
- Janis, C. M., K. Devlin, D. E. Warren, and F. Witzmann. 2012. Dermal bone in early tetrapods: a palaeophysiological hypothesis of adaptation for terrestrial acidosis. *Proceedings of the Royal Society B: Biological Sciences* **279**:3035-3040.
- Jarvik, E. 1980. *Basic Structure and Evolution of Vertebrates*. Academic Press, New York, NY.
- Jarvik, E. 1996. The Devonian tetrapod *Ichthyostega*. *Lethaia* **29**:76-76.
- Johanson, Z., P. Ahlberg, and A. Ritchie. 2003. The braincase and palate of the tetrapodomorph sarcopterygian *Mandageria fairfaxi*: Morphological variability near the fish-tetrapod transition. *Palaeontology* **46**:271-293.
- Jollie, M. 1984. Development of Cranial and Pectoral Girdle Bones of *Lepisosteus* with a Note on Scales. *Copeia* **1984**:476-502.
- Kammerer, C. F., L. Grande, and M. W. Westneat. 2006. Comparative and developmental functional morphology of the jaws of living and fossil gars (Actinopterygii : Lepisosteidae). *Journal of Morphology* **267**:1017-1031.
- Kay, R. F., and M. Cartmill. 1977. Cranial morphology and adaptations of *Palaechthon nacimienti* and other Paromomyidae (Plesiadapoidea, ? Primates), with a description of a new genus and species. *Journal of Human Evolution* **6**:19-53.

- Kleinteich, T., J. Herzen, F. Beckmann, M. Matsui, and A. Haas. 2014. Anatomy, function, and evolution of jaw and hyobranchial muscles in cryptobranchoid salamander larvae. *Journal of Morphology* **275**:230-246.
- Konstantinidis, P., P. Warth, B. Naumann, B. Metscher, E. J. Hilton, and L. Olsson. 2015. The Developmental Pattern of the Musculature Associated with the Mandibular and Hyoid Arches in the Longnose Gar, *Lepisosteus osseus* (Actinopterygii, Ginglymodi, Lepisosteiformes). *Copeia* **103**:920-932.
- Lauder, G. 1985. Aquatic feeding in lower vertebrates. *Functional vertebrate morphology*:210-229.
- Lauder, G. V. 1980a. Evolution of the Feeding Mechanism in Primitive Actinopterygian Fishes: A Functional Anatomical Analysis of *Polypterus*, *Lepisosteus*, and *Amia*. *Journal of Morphology* **163**:283-317.
- Lauder, G. V. 1980b. The role of the hyoid apparatus in the feeding mechanism of the coelacanth *Latimeria chalumnae*. *Copeia*:1-9.
- Lauder, G. V. 1982. Patterns of Evolution in the Feeding Mechanism of Actinopterygian Fishes. *American Zoologist* **22**:275-285.
- Lauder, G. V. 1995. On the inference of function from structure. Pages 1-18 in J. J. Thomason, editor. *Functional morphology in vertebrate paleontology*. Cambridge University Press, Cambridge, UK.
- Lauder, G. V., and S. M. Norton. 1980. Asymmetrical Muscle Activity During Feeding in the Gar, *Lepisosteus Oculatus*. *The Journal of Experimental Biology* **84**:17-32.
- Lauder, G. V., and H. B. Shaffer. 1986. Functional design of the feeding mechanism in lower vertebrates: unidirectional and bidirectional flow systems in the tiger salamander. *Zoological Journal of the Linnean Society* **88**:277-290.
- Lauder, G. V., and H. B. Shaffer. 1993. Design of feeding systems in aquatic vertebrates: major patterns and their evolutionary interpretations. *The skull* **3**:113-149.
- Liem, K. F. 1978. Modulatory multiplicity in the functional repertoire of the feeding mechanism in cichlid fishes. I. Piscivores. *Journal of Morphology* **158**:323-360.
- Liem, K. F. 1980. Acquisition of energy by teleosts: adaptive mechanisms and evolutionary patterns. *Environmental physiology of fishes* **35**:299-334.
- Lombard, R., J. Bolt, and M. Carrano. 2006. The mandible of *Whatcheeria deltae*, an early tetrapod from the Late Mississippian of Iowa. *Amniote Paleobiology. Perspectives on the Evolution of Mammals, Birds, and Reptiles*:21-52.
- Long, J. A., R. E. Barwick, and K. S. W. Campbell. 1997. Osteology and functional morphology of the osteolepiform fish *Gogonasus andrewsae* Long, 1985, from the Upper Devonian Gogo Formation, Western Australia. *Western Australian Museum*.

- Longo, S. J., M. D. McGee, C. E. Oufiero, T. B. Waltzek, and P. C. Wainwright. 2016. Body ram, not suction, is the primary axis of suction-feeding diversity in spiny-rayed fishes. *Journal of Experimental Biology* **219**:119-128.
- MacIver, M. A., L. Schmitz, U. Mugan, T. D. Murphey, and C. D. Mobley. 2017. Massive increase in visual range preceded the origin of terrestrial vertebrates. *Proceedings of the National Academy of Sciences* **114**:E2375-E2384.
- Magid, A. M. A. 1966. Breathing and function of spiracles in *Polypterus senegalus*. *Animal Behaviour* **14**:530-533.
- Markey, M. J., and C. R. Marshall. 2007. Terrestrial-style feeding in a very early aquatic tetrapod is supported by evidence from experimental analysis of suture morphology. *Proceedings of the National Academy of Sciences of the United States of America* **104**:7134-7138.
- Maxwell, E. E., M. W. Caldwell, and D. O. Lamoureux. 2011. The structure and phylogenetic distribution of amniote plicidentine. *Journal of Vertebrate Paleontology* **31**:553-561.
- Michel, K. B., E. Heiss, P. Aerts, and S. Van Wassenbergh. 2015. A fish that uses its hydrodynamic tongue to feed on land. *Proceedings of the Royal Society of London B: Biological Sciences* **282**.
- Millot, J., and J. Anthony. 1958. *Anatomie de Latimeria chalumnae*, Tome 1: Squelette, muscles et formations de soutien. Paris: Centre National de la Recherche Scientifique.
- Muller, M. 1987. Optimization principles applied to the mechanism of neurocranium levation and mouth bottom depression in bony fishes (Halecostomi). *Journal of Theoretical Biology* **126**:343-368.
- Muller, M. 1989. A quantitative theory of expected volume changes of the mouth during feeding in teleost fishes. *Journal of Zoology* **217**:639-661.
- Muller, M., J. Osse, and J. Verhagen. 1982. A quantitative hydrodynamical model of suction feeding in fish. *Journal of Theoretical Biology* **95**:49-79.
- Nakamura, T., A. R. Gehrke, J. Lemberg, J. Szymaszek, and N. H. Shubin. 2016. Digits and fin rays share common developmental histories. *Nature*.
- Near, T. J., R. I. Eytan, A. Dornburg, K. L. Kuhn, J. A. Moore, M. P. Davis, P. C. Wainwright, M. Friedman, and W. L. Smith. 2012. Resolution of ray-finned fish phylogeny and timing of diversification. *Proceedings of the National Academy of Sciences* **109**:13698-13703.
- Neenan, J. M., M. Ruta, J. A. Clack, and E. J. Rayfield. 2014. Feeding biomechanics in *Acanthostega* and across the fish–tetrapod transition. *Proceedings of the Royal Society B: Biological Sciences* **281**:20132689.
- Niedzwiedzki, G., P. Szrek, K. Narkiewicz, M. Narkiewicz, and P. E. Ahlberg. 2010. Tetrapod trackways from the early Middle Devonian period of Poland. *Nature* **463**:43-48.
- Norton, S. F., and E. L. Brainerd. 1993. Convergence in the feeding mechanics of ecomorphologically similar species in the Centrarchidae and Cichlidae. *Journal of Experimental Biology* **176**:11-29.

- Olsen, A. M., and M. W. Westneat. 2015. StereoMorph: an R package for the collection of 3D landmarks and curves using a stereo camera set-up. *Methods in Ecology and Evolution* **6**:351-356.
- Panchen, A. 1985. On the amphibian *Crassigyrinus scoticus* Watson from the Carboniferous. *Phil. Trans. R. Soc. Lond. B* **309**:505-568.
- Panchen, A. L. 1964. The cranial anatomy of two Coal Measure anthracosaurs. *Philosophical Transactions of the Royal Society B: Biological Sciences* **247**:593-636.
- Pauwels, E., D. Van Loo, P. Cornillie, L. Brabant, and L. Van Hoorebeke. 2013. An exploratory study of contrast agents for soft tissue visualization by means of high resolution X-ray computed tomography imaging. *Journal of microscopy* **250**:21-31.
- Pierce, S. E., P. E. Ahlberg, J. R. Hutchinson, J. L. Molnar, S. Sanchez, P. Tafforeau, and J. A. Clack. 2013. Vertebral architecture in the earliest stem tetrapods. *Nature* **494**:226-229.
- Pierce, S. E., J. A. Clack, and J. R. Hutchinson. 2012. Three-dimensional limb joint mobility in the early tetrapod *Ichthyostega*. *Nature* **486**:523-526.
- Porro, L. B., E. J. Rayfield, and J. A. Clack. 2015a. Computed tomography, anatomical description and three-dimensional reconstruction of the lower jaw of *Eusthenopteron foordi* Whiteaves, 1881 from the Upper Devonian of Canada. *Palaeontology*:1-17.
- Porro, L. B., E. J. Rayfield, and J. A. Clack. 2015b. Descriptive Anatomy and Three-Dimensional Reconstruction of the Skull of the Early Tetrapod *Acanthostega gunnari* Jarvik, 1952. *PLoS ONE* **10**:e0118882.
- Porter, H. T., and P. J. Motta. 2004. A comparison of strike and prey capture kinematics of three species of piscivorous fishes: Florida gar (*Lepisosteus platyrhincus*), redbfin needlefish (*Strongylura notata*), and great barracuda (*Sphyraena barracuda*). *Marine Biology* **145**:989-1000.
- Rabosky, D. L., F. Santini, J. Eastman, S. A. Smith, B. Sidlauskas, J. Chang, and M. E. Alfaro. 2013. Rates of speciation and morphological evolution are correlated across the largest vertebrate radiation. *Nature Communications* **4**.
- Rahn, H., K. Rahn, B. Howell, C. Gans, and S. Tenney. 1971. Air breathing of the garfish (*Lepisosteus osseus*). *Respiration Physiology* **11**:285-307.
- Raney, E. C. 1942. Alligator gar feeds upon birds in Texas. *Copeia* **1942**:50-50.
- Rayfield, E. J., and A. C. Milner. 2008. Establishing a framework for archosaur cranial mechanics. *Paleobiology* **34**:494-515.
- Robertson, C. R., S. C. Zeug, and K. O. Winemiller. 2008. Associations between hydrological connectivity and resource partitioning among sympatric gar species (Lepisosteidae) in a Texas river and associated oxbows. *Ecology of Freshwater Fish* **17**:119-129.
- Romer, A. S. 1969. A temnospondylous labyrinthodont from the Lower Carboniferous. Cleveland Museum of Natural History.

- Rosen, D. E., P. L. Forey, B. G. Gardiner, and C. Patterson. 1981. Lungfishes, tetrapods, paleontology, and plesiomorphy. *Bulletin of the AMNH*; v. 167, article 4.
- Rudwick, M. J. S. 1964. The inference of function from structure in fossils. *The British Journal for the Philosophy of Science* **XV**:27-40.
- Sanchez, S., P. Tafforeau, J. A. Clack, and P. E. Ahlberg. 2016. Life history of the stem tetrapod *Acanthostega* revealed by synchrotron microtomography. *Nature* **advance online publication**.
- Sanford, C. P., and G. V. Lauder. 1989. Functional morphology of the “tongue-bite” in the osteoglossomorph fish *Notopterus*. *Journal of Morphology* **202**:379-408.
- Schaeffer, B. 1967. Late Triassic fishes from the western United States. *Bulletin of the AMNH*; v. 135, article 6.
- Schoch, R., and A. Milner. 2000. Stereospondyli. *Handbuch der Paläoherpetologie*, Teil 3B. Verlag Dr. Friedrich Pfeil, München.
- Schoch, R. R., and F. Witzmann. 2010. Bystrow’s Paradox – gills, fossils, and the fish-to-tetrapod transition. *Acta Zoologica*:1-15.
- Schultze, H. 1984. Juvenile Specimens of *Eusthenopteron foordi* Whiteaves, 1881 (Osteolepiform Rhipidistian, Pisces) from the Late Devonian of Miguasha, Quebec, Canada. *Journal of Vertebrate Paleontology* **4**:1-16.
- Schultze, H. 1996. The elpistostegid fish *Elpistostege*, the closest the Miguasha fauna comes to a tetrapod. *Devonian Fishes and Plants of Miguasha, Quebec, Canada*. Verlag Dr. Friedrich Pfeil, München:316-327.
- Schultze, H., and M. Arsenault. 1985. The panderichthyid fish *Elpistostege*: a close relative of tetrapods. *Palaeontology* **28**:293-309.
- Shubin, N. H., E. B. Daeschler, and F. A. Jenkins. 2006. The pectoral fin of *Tiktaalik roseae* and the origin of the tetrapod limb. *Nature* **440**:764-771.
- Smithson, T. R. 1982. The cranial morphology of *Greererpeton burkemorani* Romer (Amphibia: Temnospondyli). *Zoological Journal of the Linnean Society* **76**:29-90.
- Solomon, L. E., Q. E. Phelps, D. P. Herzog, C. J. Kennedy, and M. S. Taylor. 2013. Juvenile Alligator Gar Movement Patterns in a Disconnected Floodplain Habitat in Southeast Missouri. *American Midland Naturalist* **169**:336-344.
- Stössel, I. 1995. The discovery of a new Devonian tetrapod trackway in SW Ireland. *Journal of the Geological Society* **152**:407-413.
- Summers, A. P., K. F. Darouian, A. M. Richmond, and E. L. Brainerd. 1998. Kinematics of aquatic and terrestrial prey capture in *Terrapene carolina*, with implications for the evolution of feeding in cryptodire turtles. *Journal of Experimental Zoology* **281**:280-287.

- Taylor, M. A. 1987. How tetrapods feed in water: a functional analysis by paradigm. *Zoological Journal of the Linnean Society* **91**:171-195.
- Thomson, K. S. 1967. Mechanisms of intracranial kinetics in fossil rhipidistian fishes (Crossopterygii) and their relatives. *Journal of the Linnean Society of London, Zoology* **46**:223-253.
- van Leeuwen, J. L., and M. Muller. 1984. Optimum sucking techniques for predatory fish. *The Transactions of the Zoological Society of London* **37**:137-169.
- Van Wassenbergh, S., C. Bonte, and K. B. Michel. 2017. Terrestrial capture of prey by the reedfish, a model species for stem tetrapods. *Ecology and Evolution*:1-5.
- Van Wassenbergh, S., A. Herrel, D. Adriaens, F. Huysentruyt, S. Devaere, and P. Aerts. 2006. A catfish that can strike its prey on land. *Nature* **440**:881-881.
- Vogel, S. 1994. *Life in Moving Fluids: the physical biology of flow*. 2nd edition. Princeton University Press, Princeton, N.J.
- Vorobyeva, E., and H.-P. Schultze. 1991. Description and systematics of panderichthyid fishes with comments on their relationship to tetrapods. Origins of the higher groups of tetrapods: controversy and consensus **68**:109.
- Vorobyeva, E. I. 1980. Observations on two rhipidistian fishes from the Upper Devonian of Lode, Latvia. *Zoological Journal of the Linnean Society* **70**:191-201.
- Wainwright, P. C., L. A. Ferry-Graham, T. B. Waltzek, A. M. Carroll, C. D. Hulsey, and J. R. Grubich. 2001. Evaluating the use of ram and suction during prey capture by cichlid fishes. *Journal of Experimental Biology* **204**:3039-3051.
- Wainwright, P. C., M. D. McGee, S. J. Longo, and L. Patricia Hernandez. 2015. Origins, Innovations, and Diversification of Suction Feeding in Vertebrates. *Integrative and Comparative Biology* **55**:134-145.
- Wainwright, P. C., C. P. Sanford, S. M. Reilly, and G. V. Lauder. 1989. Evolution of motor patterns: aquatic feeding in salamanders and ray-finned fishes. *Brain, Behavior and Evolution* **34**:329-341.
- Wake, D. B. 1991. Homoplasy: the result of natural selection, or evidence of design limitations? *The American Naturalist* **138**:543-567.
- Waltzek, T. B., and P. C. Wainwright. 2003. Functional morphology of extreme jaw protrusion in Neotropical cichlids. *Journal of Morphology* **257**:96-106.
- Warren, A., and S. Turner. 2006. Tooth histology patterns in early tetrapods and the presence of 'dark dentine.'. *Transactions of the Royal Society of Edinburgh: Earth Sciences* **96**:113-130.
- Warren, J. W., and N. A. Wakefield. 1972. Trackways of Tetrapod Vertebrates from the Upper Devonian of Victoria, Australia. *Nature* **238**:469.
- Webb, P. W., D. H. Hardy, and V. L. Mehl. 1992. The effect of armored skin on the swimming of longnose gar, *Lepisosteus osseus*. *Canadian Journal of Zoology* **70**:1173-1179.

- Weishampel, D. B. 1995. Fossils, function, and phylogeny. Pages 34-54 in J. J. Thomason, editor. Functional morphology in vertebrate paleontology. Cambridge University Press, Cambridge, UK.
- Werth, A. J. 2006. Odontocete suction feeding: Experimental analysis of water flow and head shape. *Journal of Morphology* **267**:1415-1428.
- Westneat, M. W., and P. C. Wainwright. 1989. Feeding mechanism of *Epibulus insidiator* (Labridae; Teleostei): evolution of a novel functional system. *Journal of Morphology* **202**:129-150.
- Wiley, E. O. 1976. The phylogeny and biogeography of fossil and recent gars (Actinopterygii: Lepisosteidae). University of Kansas.
- Wilga, C. D., P. C. Wainwright, and P. J. Motta. 2000. Evolution of jaw depression mechanics in aquatic vertebrates: insights from Chondrichthyes. *Biological Journal of the Linnean Society* **71**:165-185.
- Witmer, L. M. 1995. The extant phylogenetic bracket and the importance of reconstructing soft tissues in fossils. Pages 19-33 in J. J. Thomason, editor. Functional morphology in vertebrate paleontology. Cambridge University Press, Cambridge, UK.
- Witzmann, F., and E. Brainerd. 2017. Modeling the physiology of the aquatic temnospondyl *Archegosaurus decheni* from the early Permian of Germany. *Mitteilungen aus dem Museum für Naturkunde in Berlin. Fossil Record* **20**:105.
- Witzmann, F., and R. R. Schoch. 2013. Reconstruction of cranial and hyobranchial muscles in the triassic temnospondyl *Gerrothorax* provides evidence for akinetic suction feeding. *Journal of Morphology* **274**:525-542.
- Witzmann, F., H. Scholz, J. Muller, and N. Kardjilov. 2010. Sculpture and vascularization of dermal bones, and the implications for the physiology of basal tetrapods. *Zoological Journal of the Linnean Society* **160**:302-340.
- Wright, J. J., S. R. David, and T. J. Near. 2012. Gene trees, species trees, and morphology converge on a similar phylogeny of living gars (Actinopterygii: Holostei: Lepisosteidae), an ancient clade of ray-finned fishes. *Molecular Phylogenetics and Evolution* **63**:848-856.
- Zhu, M., and X. Yu. 2004. Lower jaw character transitions among major sarcopterygian groups—a survey based on new materials from Yunnan, China. Recent advances in the origin and early radiation of vertebrates. Verlag Dr. Friedrich Pfeil, München:271-286.